CO_2 Reduction Strategies Through Proactive Removal and Utilization

by

Tae Hwan Lim

A dissertation submitted in partial fulfillment
of the requirements for the degree of
Doctor of Philosophy
(Mechanical Engineering)
in the University of Michigan
2022

Doctoral Committee:

Associate Professor Brian R. Ellis, Co-Chair
Professor Steven J. Skerlos, Co-Chair
Associate Professor Neil Dasgupta
Professor John E. Foster
Associate Professor Christian Lastoskie

Tae Hwan Lim

taelim@umich.edu

ORCID iD: 0000-0003-3764-2253

Dedication

For my parents, who have always encouraged me to pursue my passion.

Acknowledgements

It feels surreal that I am completing my Ph.D. in engineering – something I would have never imagined doing in my high school or even undergraduate years. I firmly believed that I would be continuously studying astrophysics, a subject of my passion since I was young. Things have changed. Things changed as I navigated and learned more about my own surroundings: the social structure we live in, the historical context behind the political struggles, and the environment we take for granted. Now that I look back, I am endlessly grateful for friends, colleagues, and mentors who have helped me successfully navigate this uncharted path.

One of the pivotal moments that motivated me to pursue a sustainability career is undoubtedly my involvement with Greenpeace, especially when I visited Fort McMurray to bear witness to the greater impact of Tar Sands on the environment and people. I sincerely thank Gabriel Gerow, Adam Conlin, and my fellow GOTs (all of you!) for making this adventure full of unforgettable memories and providing a strong motivation that led me here.

My Ph.D. journey was full of surprises and exciting learning experiences thanks to active yet diverse opportunities being offered at the University of Michigan. Even before the starting of my Ph.D., Susan Fancy at the Energy Institute, now at the Global CO_2 Initiative, has helped me jumpstart my career by supporting my conference participation and early start of my program. Susan – I sincerely thank you again for all your kind support! I enjoyed working as a student representative at the Rackham Student Government where I helped organize social events for fellow graduate students and start one of the early sustainability initiatives on campus. I would like to thank Climate Blue, especially Dr. Avik Basu for offering me an opportunity to participate in the 2018 United Nations Climate Change Conference that broadened my scope on climate change. I was very glad to team up with Brian Lezzi and Muhammad Abdullah and build an intercontinental, literally, sustainability community! I thank you guys for your initiatives and friendship. CO_2 Fast 2 Furious team – I would not forget the Patagonia case competition we participated in together, including hours-long creative discussions on how to reinvent a company considering strategies, technology, and marketing.

I sincerely thank my friends and colleagues in my co-advisor Prof. Ellis' group and committee Prof. Lastoskie's group – including Duo Zhang, Ellen Thompson, Anne Menefee, Jubilee Adeoye, and Christina Reynolds – who supported me in many different ways throughout my times at Michigan. Duo – I thank you tons for helping me get up to speed with understanding cement and concrete from the very basics! I would like to thank Zimu Yang and Nathaniel Wirgau at Professor Foster's lab for helping me set up the apparatus in the lab. I am indebted to Professor Benjamin Jorns who generously supported my experiment by loaning me a waveguide component that was essential for my experiments. Byungjun Lee helped validate my finite element model by supporting me with his expertise with infrared thermography – thank you! I would express my gratitude to my book club friends – and I just realized we never named our club – for suggesting eye-opening books and creating a pleasant and open environment for discussions for the last two years. Also, I cannot possibly forget to show my gratitude to Nicole Allen who has been the most genuine, fun, and supportive friend throughout my Ph.D. life.

I cannot possibly imagine my Ph.D. journey without my wonderful committee members: Neil – thank you always for providing valuable insights and bringing my attention back to the fundamentals; Christian – I have learned so much about how to control greenhouse gas with chemistry and chemical engineering by working with you; John – I cannot imagine my experimental work without your generous help. You were always eager to help whenever I needed help or had questions. I was able to push harder thanks to a positive and collaborative environment that you offered.

Lastly, to my two co-advisors, Steve and Brian – I cannot believe it's been already four years since I started working with you! I am sincerely grateful to have worked with you so closely both at professional and personal levels, and discuss every aspect of sustainability, design, and teaching together. You encouraged me to embrace my creativity and develop my own ideas which resulted in the experimental study of direct air capture. From the very beginning, you made sure I have all the support I needed, from the initial brainstorming to expanding the research coalition (Thank you, John!) and thinking about the next steps. What I learned by working with you is not limited to academic excellence; I learned the importance of thinking outside the box, how to mobilize consorted group efforts for greater goods, and the philosophy of prioritizing people above everything. I will be forever grateful for your kind mentorship!

Table of Contents

List of Tables

List of Figures

List of Appendices

Abstract

Limiting the global temperature rise within 1.5-2°C above the preindustrial era would require mass-scale CO_2 removal from the atmosphere. This dissertation explores novel strategies to lower the cost and accelerate the pace of removal by pioneering an alternative process for direct air capture (DAC) and innovative strategies to utilize CO_2 in the concrete industry with a combination of experiments and systems-level analyses.

First, the cost of using DAC as an industrial climate backstop by coupling it with geological sequestration is studied in the context of reducing CO_2 emissions from the U.S. electric sector. The least-cost optimization framework presents a clear picture that immediate and sustained mitigation needs to be prioritized; delaying undertaking mitigation measures beyond 2030 and relying on the backstop would cost an additional 580-2015 billion USD through 2050 compared to starting mitigation in 2020 and avoid using the backstop. However, still increasing global greenhouse gas emissions necessitates decreasing the heavy energy demand and cost of DAC. Sorbent regeneration experiments using microwaves revealed that meeting such requirements is possible. A substantial reduction of the regeneration time from over an hour to a matter of minutes was confirmed with the application of microwaves which can be used to decrease the cost of DAC through system downsizing. The lower temperature of the desorbed CO_2 gas (45-55°C) compared to that of the sorbents (>100°C) suggests a low-temperature desorption mechanism can be used to design a low-energy DAC system in the future.

The recovered CO_2 can be strategically utilized during the fabrication of cement and concrete products rather than being sequestered in the geosphere. The strength development of concrete induced by the added CO_2 enables an opportunity to magnify the overall CO_2 reduction while saving implementation costs through decreasing binder content. An assessment of the industry-wide application of such joint strategy reveals the significance of exploiting CO_2-induced property changes, not maximizing absorbed CO_2; over 10% of the emissions from the U.S. concrete manufacturing can be reduced through CO_2-enabled binder reduction, compared to 1% possible

through sequestration only. The saved material cost could fully mitigate the implementation costs of this strategy. Alternatively, CO_2 can be applied to an ultra-ductile material such as engineered cementitious composite (ECC) to mass-produce durable CO_2-embodying products using existing infrastructure. The environmental and economic benefits of CO_2-cured ECC-based railroad ties are evaluated against conventional concrete ties with a combined lifecycle framework and stochastic tie failure model that considers a wide range of tie failure patterns, replacement strategies, and resultant impacts on train operation. Despite the increased cost and carbon footprint (>50%) of an ECC tie, using ECC ties reduces the overall system cost by 25% and carbon footprint by 19% by requiring nearly 50% fewer ties over 100 years. The increased product longevity is the primary driver of the improvements, rather than the quantity of the CO_2 sequestered.

Altogether, this dissertation highlights the urgency for minimizing the reliance on carbon backstop and demonstrates how novel removal and utilization strategies can reduce the overall cost of CO_2 reduction; the virtue of proactive CO_2 utilization is complementing fossil mitigation now to minimize the gross scale of sequestration throughout the century, not maximizing sequestration in products. The findings of this work can serve as a groundwork to explore further proactive CO_2 removal and utilization opportunities to accelerate CO_2 reduction.

CHAPTER 1
Introduction

1.1 Climate Change and Negative Emissions

Recognizing the heavy physical, environmental, and socioeconomic risks of climate change and the anthropogenic origin of the issue, the Paris Agreement was adopted by 196 parties at the 2015 United Nations Climate Change Conference. The agreement set a long-term goal to limit global temperature rise to well below 2°C and pursue efforts to curb the increase to below 1.5°C above preindustrial levels. Achieving these goals would require limiting the total amount of greenhouse gases (GHG), 65% of which is CO_2 (The Intergovernmental Panel on Climate Change 2014), generated in the 21st century below a threshold called carbon budget which indicates the cumulative amount of GHG emissions humanity can emit and still have a chance to contain global temperature rise within certain limits. A recent study estimates that the remaining carbon budget is 230-440 billion tonnes of CO_2 ($GtCO_2$) from 2020 onwards for having a 67-50% chance of stabilizing the warming at or below 1.5°C (Damon Matthews *et al* 2021). If the current emissions rate of 40 $GtCO_2$/year were to be sustained, we expect to exceed the remaining carbon budget in 6-11 years, after which meeting the 1.5°C target becomes out of reach with conventional GHG reductions from fossil sources.

Given the extremely tight remaining carbon budget in combination with inadequate carbon mitigation efforts and pledges, removing excess CO_2 from the atmosphere is deemed essential to meet the 1.5°C or 2°C climate targets through mass-scale deployment of negative emissions technologies (NET) (Luderer *et al* 2018, Fuss *et al* 2018, National Academies of Sciences Engineering and Medicine 2019, Robiou du Pont *et al* 2016). The historic CO_2 emissions removed from the atmosphere, via a combination of physical, chemical, and biological processes, can be stored away from the natural carbon cycle to result in *negative* emissions that can be used to offset residual CO_2 emissions from fossil sources or global warming contribution from other GHGs such as methane, and can allow temporarily exceeding the carbon budget and still meeting the climate target (Fuss *et al* 2018, Luderer *et al* 2018). According to the extensive emissions pathway analysis

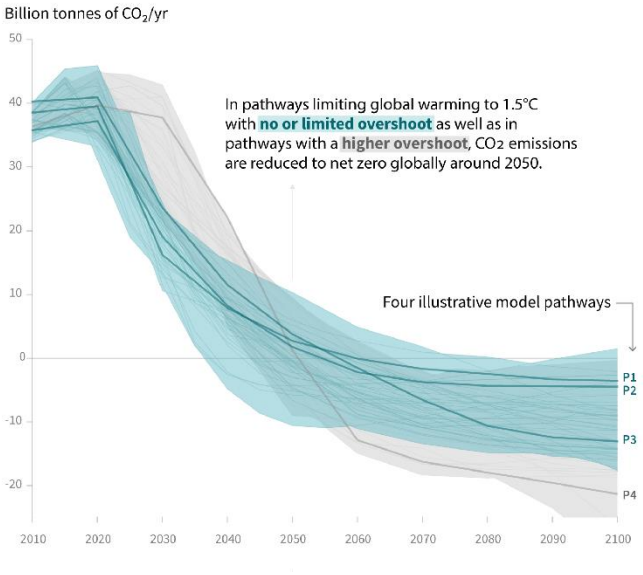

Figure 1.1. Emissions pathway from 2010 to 2100 compliant with 1.5°C climate target. From (Masson-Delmotte *et al* 2018)

made by Intergovernmental Panel on Climate Change (IPCC), nearly 90% of the scenarios compliant with 2°C warming and *all* scenarios meeting 1.5°C targets rely on the mass-scale deployment of NETs (Masson-Delmotte *et al* 2018, The Intergovernmental Panel on Climate Change 2014). While not all 2°C emissions pathways fundamentally rely on NETs, the scenarios that delay immediate mitigation measures similar to the current trajectories following a collection of national climate plans submitted by major economics essentially resemble 1.5°C scenarios; large-scale deployment of NET is necessary to meet the 2°C climate target. In all cases, IPCC studies find that approximately 100-1,000 $GtCO_2$ need to be cumulatively removed from the air across the 21st century. By 2100, up to 20 $GtCO_2$ need to be removed annually which is equivalent to nearly half of the current emissions rate as shown in Figure 1.1.

While carbon mitigation is generally defined as 'a human intervention to reduce the sources or enhance the sinks of GHG emissions' (The Intergovernmental Panel on Climate Change 2014), negative emissions introduce *reversed* anthropogenic carbon pathway and can be defined as human intervention to remove CO_2 emissions from the atmosphere (Minx *et al* 2018). When applied to the existing industrial landscape, this reversed carbon flow can be disaggregated into CO_2 recovery and end-use of CO_2, one of which application is geological sequestration. An alternative end-use of CO_2 includes utilization where CO_2 can be further utilized in industrial processes as a chemical feedstock, working fluid, solvent, or raw materials. In this work, we explore CO_2 recovery and

utilization/sequestration separately to elucidate unique challenges found in each of the strategies, and together to study its application in the existing technology ecosystem.

1.2 DIRECT AIR CAPTURE

One of the industrialized options to remove CO_2 from the atmosphere includes a process called direct air capture (DAC). The process of separating CO_2 from ambient air has been used since the 1940s as part of an essential life support system in submarines and spacecraft as well as to pre-treat air for cryogenic air separation or to produce fuels (Sanz-Pérez *et al* 2016, Keith *et al* 2018). Since the adoption of the idea for climate mitigation in 1999 (Lackner *et al* 1999), DAC has gradually accrued interests from fundamental research to commercial applications. DAC represents a cohort of technologies that directly extract CO_2 from air using engineered media and produce CO_2 in a range of concentrations. Typical processes involve sorbents or solvents that have a preferential chemical affinity to CO_2 to separate it from the air (Keith *et al* 2018, Wurzbacher *et al* 2016). The CO_2-rich sorbents or solvents can then be regenerated via chemical looping, humidity swing, or with temperature and/or pressure swing to produce a purified stream of CO_2. DAC can function as NET when the recovered CO_2 is sequestered in the geosphere or it can function as a source of CO_2 that has a negative carbon footprint for industrial activities.

At present, DAC is in its early stage of commercialization with 19 plants installed globally to capture about 11,000 tCO_2 each year (Carbon180 2021, IEA 2021). Scaling DAC to a climate-relevant giga-tonne capacity would pose significant scientific, technological, and socioeconomic challenges and uncertainties. For instance, the current cost estimates of CO_2 captured through the DAC process range greatly between \$30-\$1,000/tCO_2 depending on the choice of the capture process, capture media, and energy sources as well as the output CO_2 purity (Keith *et al* 2018, Socolow *et al* 2011, Sanz-Pérez *et al* 2016, Gertner 2019, Wilcox *et al* 2017). The most recent commercial DAC plant captures CO_2 reportedly at \$500-\$600/tCO_2 (Gertner 2019); this cost needs to fall below \$100/tCO_2 to become economically viable for mass-scale deployment (Lackner and Azarabadi 2021). The high resource and energy intensity of this process also means that substantial expansion and transformation of the existing industrial and energy infrastructure will be needed to accommodate DAC. A recent modeling study found that DAC can require up to 300 exajoules of electricity by 2100, which is over half the global demand today and nearly 25% of the projected global energy by the end of the 21st century (Realmonte *et al* 2019).

Therefore, this dissertation aims to advance our understanding of DAC regarding its process design, optimal implementation strategy, and techno-economic implications of its mass-scale implementation by addressing the following questions:

1. What are the systems-level implications of the large-scale deployment of DAC on existing industrial and energy infrastructure?
2. What framework can be used to assess the optimal deployment timing and scale of DAC to achieve a reduction target in conjunction with mitigation measures from fossil sources?
3. How can the DAC process design be improved to reduce its cost and energy demand?

1.3 Mineral Carbonation

The captured CO_2 can be sequestered in geological formations such as deep saline aquifers, unmineable coal seams, and basalt formation, to generate carbon offsets that are equivalent to carbon mitigated from reducing the use of fossil fuels. Alternatively, CO_2 can be further utilized in industrial applications. For instance, the cement and concrete industry provides a unique avenue to sequester CO_2 while producing high-value products. The high alkaline environment (pH > 13) of cement paste functions as a natural carbon sink through mineral carbonation. The gaseous CO_2 in ambient air dissolves into the alkaline porewater of the cement paste to produce carbonate ions (CO_3^{2-}), which subsequently reacts with calcium ions and precipitates the CO_2 as calcium carbonate ($CaCO_3$) (von Greve-Dierfeld *et al* 2020). (Xi *et al* 2016) found that close to 16.5 $GtCO_2$ was cumulatively sequestered in cement materials from 1930 to 2013 in this way and offset 43% of the CO_2 emitted during the production of cement over the same period, not accounting for the emissions generated from fossil fuels burned during the process. Increasing the natural carbon uptake in cement and concrete close to 100% at a reasonable timescale is challenged by slow carbonation kinetics due to low porosity and permeability of the material which limits CO_2 penetration into the interior volume. Also, promoting this weathering carbonation in the built environment can be detrimental to the structural integrity of the construction materials, as weathering carbonation can undermine the mechanical integrity of the binding matrix and can reduce pH of the cement porewater and compromise the passivation protection of the steel reinforcing bars that are an integral component of many modern concrete structures. These concerns are particularly critical with an increasing proportion of supplementary cementitious

materials (SCM) in the mixtures to reduce its GHG emissions, as the concretes designed with SCMs are more susceptible to these effects (von Greve-Dierfeld *et al* 2020).

However, carbonation can lead to enhancing the overall strength of the mixture when CO_2 is added during the fabrication process (Zhang *et al* 2017, Monkman *et al* 2018). The added CO_2 reacts with fresh concrete mixtures following a chemical pathway distinct from weathering carbonation and facilitates strength development of the mixture. The added CO_2 is precipitated during the process and becomes a permanent component of the binding matrix. Implementing this strategy worldwide is expected to sequester, and thus offset, 30-300 million tonnes of CO_2 (Parsons Brinckerhoff and Global CCS Institute 2011). This is close to 1-10% of the CO_2 emissions generated from cement production which highlights both challenges and opportunities for further carbon mitigation. The vast majority of the technology literature is based on carbonation curing that involves the reaction of CO_2 with freshly cast precast concrete products. This method of carbonation requires an elevated-to-pure CO_2 environment to expedite the reaction which currently limits its potential application to small precast products and is inadequate to use in a ready-mixed applications which constitute nearly 90% of the construction market (U.S. Geological Survey 2018). For ready-mixed applications, CO_2 can be added by reacting CO_2 with the recycled coarse aggregate that has uncarbonated cement paste or by adding CO_2 during the mixing stage. Similar to carbonation curing, CO_2 addition to ready-mixed applications also encounters significant challenges with scale. For instance, CO_2 storage is limited to about 0.15% by weight of cement when added during mixing (Monkman and MacDonald 2017), with an upper limit of the optimal dosage estimated to be 0.5% by weight (Monkman *et al* 2016). While the carbon offset potential in cement and concrete may be rather restricted, the total magnitude of CO_2 mitigation may be bigger. (Monkman and MacDonald 2017) reports that the magnitude of carbon mitigation can be amplified by more than 35 times when carbon-intensive Portland cement loading can be reduced by taking advantage of the strength development induced by added CO_2. Still, the lack of empirical data and variability of the process challenge the systematic assessment of employing such a strategy.

Therefore, this dissertation aims to expand our knowledge on the potential scale of CO_2 reduction and broader techno-economic implications of utilizing CO_2 in cement and concrete industry by investigating the following questions:

1. Under what conditions does added CO_2 improve the mechanical properties of the concrete products?
2. What framework can be used to optimize the concrete mixture designs that incorporate the added CO_2 considering changes in the material properties?
3. What would be the potential magnitude of net CO_2 reduction and implementation cost if CO_2 were to be added throughout the cement and concrete industry?
4. What is the lifecycle cost and net carbon reduction potential of mass-producing concrete products that sequester CO_2?

1.4 Dissertation Overview

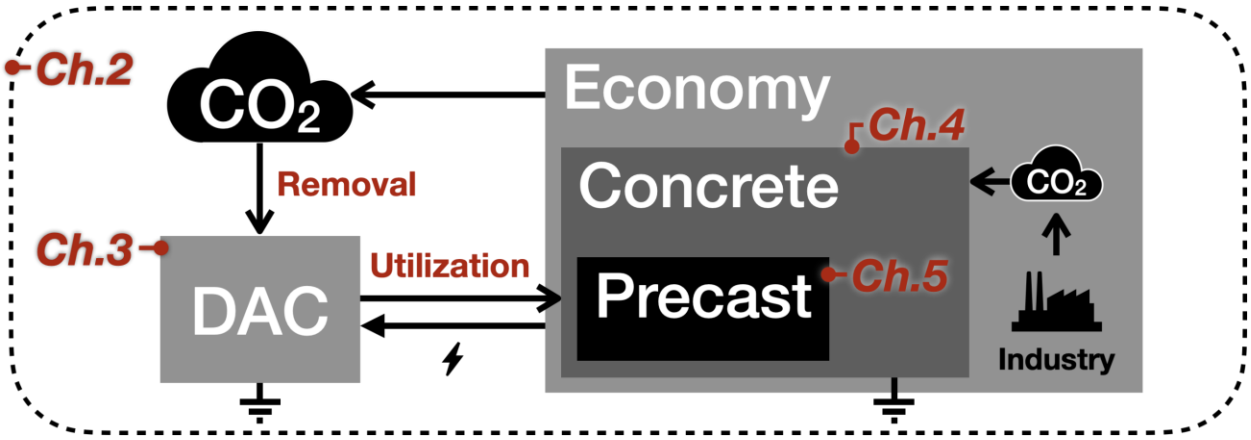

Figure 1.2. Overview of the carbon removal and utilization strategies analyzed in this dissertation

This dissertation explores and evaluates different technological pathways to remove CO_2 from the atmosphere and utilize it in the existing industrial ecosystem to promote net carbon reduction. Figure 1.2 illustrates carbon removal and utilization strategies analyzed in this work including using DAC as NET (Chapter 2), recovering CO_2 via microwave-based desorption (Chapter 3), utilizing CO_2 in cement and concrete fabrication (Chapter 4), and mass-producing CO_2-cured products (Chapter 5). Chapter 3 is based on experimental validation and the rest of the chapters assess systems-level, lifecycle benefits of potential carbon removal and utilization strategies. Chapter summaries are provided below.

Chapter 2 elucidates the role of NET in the overall carbon mitigation by studying the scale and cost of using DAC coupled with geological CO_2 storage in reducing 70% of the CO_2 emissions in the U.S. electric utility sector by 2050. Minimum-cost electricity generation and emissions trajectories are generated using a stock-and-flow-based optimization framework. We find that

purely economic-driven pathways will miss the 70% reduction target. Starting an immediate and sustained transition to low-carbon technologies before 2030 can meet the reduction target without needing DAC which is the most cost effective. Once the transition is delayed, DAC is required to meet the reduction target. However, delaying beyond 2035 would require so much DAC that meeting the target is economically infeasible. Each year of delay increases the overall cost of meeting the 70% reduction target by requiring increased DAC deployment, more rapid low-carbon transition, and expanding the gross electricity supply to power DAC. Each day of delay beyond 2020 costs nearly 100-345 million USD. Our results highlight the urgency of taking immediate and aggressive carbon mitigation measures.

The results of Chapter 2 highlights the high energy demand and cost of the DAC process as a major area for improvement. Based on this lesson, Chapter 3 experimentally explores the microwave-based sorbent regeneration technique as a low-energy, rapid CO_2 recovery strategy. About 5g of packed zeolite beads were saturated with industrial-grade CO_2 and were regenerated under vacuum (<10 Torr) with the application of a 2.45 GHz microwave supplied through a single-mode rectangular waveguide system. The CO_2 desorption rate and energy dissipated during regeneration were analyzed by studying mass transport of primary gas species and heat transfer processes during the experiments. The results show that dielectric heating via microwave application can shorten the regeneration time to below 30 minutes versus over an hour using conventional conduction-based regeneration. Approximately 40% of the adsorbed CO_2 was desorbed with 80 seconds of microwave application, with the rest desorbing slowly from sorbents near the outer edge of the packed structure over 20-30 minutes where temperature increase is lower. Our results confirm rapid CO_2 desorption process with microwave which could be used to substantially reduce the cost of the DAC system through downsizing. The lower temperature (45-55°C) of the desorbed CO_2 gas relative to the sorbent surface (>100°C) suggests that microwave may enable low-temperature desorption mechanism which calls for future research for validation.

The CO_2 removed from air or recovered from industrial processes can be further utilized to facilitate further CO_2 reduction, as opposed to offsetting emissions from fossil sources through sequestration. Chapter 4 evaluates the systems-level CO_2 reduction potential and associated cost of this alternative strategy when CO_2 is beneficially utilized in concrete fabrication while producing value-added goods. Past studies on CO_2 utilization in the concrete industry have primarily focused on maximizing CO_2 storage while focusing less on CO_2 avoidance made

possible by reducing binder use enabled added CO_2. Three technological approaches to add CO_2 are assessed: carbonation during curing, carbonation during mixing, or carbonation with recycled concrete aggregate. These techniques are evaluated for a cohort of concrete formulations representing the diverse mixture designs found in the U.S. ready-mixed and precast industries. Each formulation is optimized for reduced binder loading where the addition of CO_2 directly in the formulation recovers the lost compressive strength from the reduced binder. Our results show that over an order of magnitude more CO_2 can be avoided compared to sequestrating CO_2 alone when binder reduction is jointly implemented with CO_2 utilization. As a result, nearly 40% of the annual CO_2 emissions from the U.S. concrete industry could, in principle, be eliminated without relying on novel supplemental materials, alternative binders, or carbon capture and sequestration. The recently amended 45Q tax credit will not incentivize this strategy, as it only considers carbon sequestration. However, we find that the saved material cost from reduced binder use may provide a significant economic incentive to promote this joint strategy in practice. Hence, the real value of CO_2 utilization in concrete hinges on exploiting CO_2-induced property changes to yield additional emission reduction, not by maximizing absorbed CO_2. Thus, successful policy measures to facilitate CO_2 mitigation should focus on the overall scale of CO_2 reduction, including avoided emissions.

Precast concrete applications provide a mass-production route for CO_2-cured products. Chapter 5 estimates the lifecycle cost and environmental benefits of employing railway ties designed with added CO_2 in the U.S. rail infrastructure. Railway ties designed with ultra-ductile engineered cementitious composite (ECC) cured with CO_2 are evaluated against conventional prestressed concrete ties. The cradle-to-grave lifecycle model is combined with a use-phase stochastic model to evaluate systems-level cost and emissions of using concrete and ECC ties. A total of 400 uncertainty scenarios are generated with the stochastic model to evaluate a wide range of additional tie requirements during use, recurring tie replacement activities, and resultant train delays. We find that manufacturing and disposing of an ECC tie would increase both cost and greenhouse gas (GHG) emissions by over 60% relative to a concrete tie, largely due to the increased proportion of Portland cement. However, using ECC ties can result in an overall reduction in cost and GHG emissions as its expanded service life and durability would require a substantially fewer ties during use. We find that ECC ties can yield net GHG reduction once they last 25% longer than concrete ties. If ECC ties can last twice as long, the systems-level cost of

using ties can reduce by 23% while GHG emissions can reduce by 49%. The minimum sequestration requirement of 45Q would preclude ECC plants from benefiting from the incentive and even if it can, sequestration-based 45Q would only cover <10% of the increased manufacturing overhead. Our results highlight the need for policies to prioritize lifecycle GHG reduction to unlock the potentials of CO_2-based solutions.

REFERENCES

Carbon180 2021 The DAC MAPP Online: https://carbon180.org/dac-mapp

Damon Matthews H, Tokarska K B, Rogelj J, Smith C J, MacDougall A H, Haustein K, Mengis N, Sippel S, Forster P M and Knutti R 2021 An integrated approach to quantifying uncertainties in the remaining carbon budget *Commun. Earth Environ.* **2** 7 Online: http://dx.doi.org/10.1038/s43247-020-00064-9

Fuss S, Lamb W F, Callaghan M W, Hilaire J, Creutzig F, Amann T, Beringer T, de Oliveira Garcia W, Hartmann J, Khanna T, Luderer G, Nemet G F, Rogelj J, Smith P, Vicente J L V, Wilcox J, del Mar Zamora Dominguez M and Minx J C 2018 Negative emissions—Part 2: Costs, potentials and side effects *Environ. Res. Lett.* **13** 063002 Online: https://iopscience.iop.org/article/10.1088/1748-9326/aabf9f

Gertner J 2019 The Tiny Swiss Company That Thinks It Can Help Stop Climate Change Online: https://www.nytimes.com/2019/02/12/magazine/climeworks-business-climate-change.html

von Greve-Dierfeld S, Lothenbach B, Vollpracht A, Wu B, Huet B, Andrade C, Medina C, Thiel C, Gruyaert E, Vanoutrive H, Saéz del Bosque I F, Ignjatovic I, Elsen J, Provis J L, Scrivener K, Thienel K-C, Sideris K, Zajac M, Alderete N, Cizer Ö, Van den Heede P, Hooton R D, Kamali-Bernard S, Bernal S A, Zhao Z, Shi Z and De Belie N 2020 Understanding the carbonation of concrete with supplementary cementitious materials: a critical review by RILEM TC 281-CCC *Mater. Struct.* **53** 136 Online: https://link.springer.com/10.1617/s11527-020-01558-w

IEA 2021 Direct Air Capture Online: https://www.iea.org/reports/direct-air-capture

Keith D W, Holmes G, St. Angelo D and Heidel K 2018 A Process for Capturing CO_2 from the Atmosphere *Joule* **2** 1573–94 Online: https://linkinghub.elsevier.com/retrieve/pii/S2542435118302253

Lackner K S and Azarabadi H 2021 Buying down the Cost of Direct Air Capture *Ind. Eng. Chem. Res.* **60** 8196–208 Online: https://pubs.acs.org/doi/10.1021/acs.iecr.0c04839

Lackner K S, Ziock H-J and Grimes P 1999 *Carbon capture from air, is it an option?* (Los Alamos, NM: Los Alamos National Laboratory)

Luderer G, Vrontisi Z, Bertram C, Edelenbosch O Y, Pietzcker R C, Rogelj J, De Boer H S, Drouet L, Emmerling J, Fricko O, Fujimori S, Havlík P, Iyer G, Keramidas K, Kitous A, Pehl M, Krey V, Riahi K, Saveyn B, Tavoni M, Van Vuuren D P and Kriegler E 2018 Residual fossil CO_2 emissions in 1.5–2 °C pathways *Nat. Clim. Chang.* **8** 626–33 Online: http://www.nature.com/articles/s41558-018-0198-6

Masson-Delmotte V, Zhai P, Pörtner H-O H-O, Roberts D, Skea J, Shukla P R P R, Pirani A, Moufouma-Okia W, Péan C, Pidcock R, Connors S, Matthews J B R B R, Chen Y, Zhou X, Gomis M I M I, Lonnoy E, Maycock T, Tignor M and Waterfield T 2018 *IPCC, 2018: Summary for Policymakers. In: Global Warming of 1.5°C. An IPCC Special Report on the impacts of global warming of 1.5°C above pre-industrial levels and related global greenhouse gas emission pathways, in the context of strengthening the global* (Geneva) Online: https://www.ipcc.ch/site/assets/uploads/sites/2/2018/07/SR15_SPM_version_stand_alone_LR.pdf

Minx J C, Lamb W F, Callaghan M W, Fuss S, Hilaire J, Creutzig F, Amann T, Beringer T, de Oliveira Garcia W, Hartmann J, Khanna T, Lenzi D, Luderer G, Nemet G F, Rogelj J, Smith P, Vicente Vicente J L, Wilcox J and del Mar Zamora Dominguez M 2018 Negative emissions—Part 1: Research landscape and synthesis *Environ. Res. Lett.* **13** 063001 Online: https://iopscience.iop.org/article/10.1088/1748-9326/aabf9b

Monkman S, Kenward P A, Dipple G, MacDonald M and Raudsepp M 2018 Activation of cement hydration with carbon dioxide *J. Sustain. Cem. Mater.* **7** 160–81 Online: https://www.tandfonline.com/doi/full/10.1080/21650373.2018.1443854

Monkman S and MacDonald M 2017 On carbon dioxide utilization as a means to improve the sustainability of ready-mixed concrete *J. Clean. Prod.* **167** 365–75 Online: http://dx.doi.org/10.1016/j.jclepro.2017.08.194

Monkman S, Macdonald M and Hooton D 2016 Using CO_2 to reduce the carbon footprint of concrete *1st International Conference on Grand Challenges in Construction Materials* pp 1–8 Online: http://www.igcmat.com/papers/Monkman_igcmat_2016.pdf

National Academies of Sciences Engineering and Medicine 2019 *Negative Emissions Technologies and Reliable Sequestration* (Washington, D.C.: National Academies Press) Online: https://www.nap.edu/catalog/25259

Parsons Brinckerhoff and Global CCS Institute 2011 *Accelerating the update of CCS: Industrial Use of Captured Carbon Dioxide* Online: https://www.globalccsinstitute.com/archive/hub/publications/14026/accelerating-uptake-ccs-industrial-use-captured-carbon-dioxide.pdf

Realmonte G, Drouet L, Gambhir A, Glynn J, Hawkes A, Köberle A C and Tavoni M 2019 An inter-model assessment of the role of direct air capture in deep mitigation pathways *Nat. Commun.* **10** 3277 Online: http://dx.doi.org/10.1038/s41467-019-10842-5

Robiou du Pont Y, Jeffery M L, Gütschow J, Christoff P and Meinshausen M 2016 National contributions for decarbonizing the world economy in line with the G7 agreement *Environ.*

Res. Lett. **11** 054005 Online: https://iopscience.iop.org/article/10.1088/1748-9326/11/5/054005

Sanz-Pérez E S, Murdock C R, Didas S A and Jones C W 2016 Direct Capture of CO_2 from Ambient Air *Chem. Rev.* **116** 11840–76 Online: https://pubs.acs.org/doi/10.1021/acs.chemrev.6b00173

Socolow R, Desmond M, Aines R, Blackstock J, Bolland O, Kaarsberg T, Lewis N, Mazzotti M, Pfeffer A, Sawyer K, Siirola J, Smit B and Wilcox J 2011 Direct Air Capture of CO_2 with Chemicals Panel on Public Affairs *Am. Phys. Soc. - Panel Public Aff.* 100

The Intergovernmental Panel on Climate Change 2014 *Climate Change 2014: Mitigation of Climate Change. Summary for Policymakers and Technical Summary*

U.S. Geological Survey 2018 *Minerals Yearbook* Online: https://pubs.er.usgs.gov/publication/70048194

Wilcox J, Psarras P C and Liguori S 2017 Assessment of reasonable opportunities for direct air capture *Environ. Res. Lett.* **12** 065001 Online: http://stacks.iop.org/1748-9326/12/i=6/a=065001?key=crossref.8f905eab3cc9b6dbff082f94314ba4fa

Wurzbacher J A, Gebald C, Brunner S and Steinfeld A 2016 Heat and mass transfer of temperature–vacuum swing desorption for CO_2 capture from air *Chem. Eng. J.* **283** 1329–38 Online: http://dx.doi.org/10.1016/j.cej.2015.08.035

Xi F, Davis S J, Ciais P, Crawford-Brown D, Guan D, Pade C, Shi T, Syddall M, Lv J, Ji L, Bing L, Wang J, Wei W, Yang K-H, Lagerblad B, Galan I, Andrade C, Zhang Y and Liu Z 2016 Substantial global carbon uptake by cement carbonation *Nat. Geosci.* **9** 880–3 Online: http://www.nature.com/articles/ngeo2840

Zhang D, Ghouleh Z and Shao Y 2017 Review on carbonation curing of cement-based materials *J. CO_2 Util.* **21** 119–31 Online: https://doi.org/10.1016/j.jcou.2017.07.003

CHAPTER 2

Costs to Achieve Target Net Emissions Reductions in the U.S. Electric Sector Using Direct Air Capture

Reprinted from: Supekar S D, Lim T H and Skerlos S J 2019 Costs to achieve target net emissions reductions in the US electric sector using direct air capture *Environ. Res. Lett.* **14**
Note: Supekar S.D. and Lim T.H. contributed equally to first authorship

2.1 INTRODUCTION

Carbon dioxide removal from the atmosphere using "negative emission technologies" (NETs) using a combination of physical, chemical, or biological processes has been deemed essential to contain the increase in the average global temperature over pre-industrial times to 1.5 – 2 ºC (temperature anomaly) by the end of the century (Gasser *et al* 2015, Rogelj *et al* 2018). The criticality of NETs in achieving these climate targets given humanity's rapidly diminishing global carbon budget (Le Quéré *et al* 2016) has led to calls for more in-depth evaluations of individual NETs (Fuss *et al* 2016, Field and Mach 2017, van Vuuren *et al* 2017), particularly with regards to their scalability and systems-level impacts on the environment, economy, and society. The vast majority of published studies have focused on gigatonne-scale carbon dioxide removal approaches tied to biogeochemical and biogeophysical cycles such as bioenergy with carbon capture and sequestration and terrestrial carbon management (Minx *et al* 2018). There is also a growing research and commercial interest in the removal of atmospheric CO_2 through a process known as direct air capture, though the scalability and systems-level impacts of direct air capture (DAC) as a gigatonne-scale NET remain poorly understood according to a recent report prepared by the U.S. National Academies outlining research agendas for NETs (National Academies of Sciences, Engineering, and Medicine 2018).

In this paper we ask if, when, and to what extent could DAC, acting as a purely backstop measure, help achieve a 70% reduction in CO_2 emissions by 2050 relative to 2010. The 70% target corresponds to the greenhouse gas (GHG) emissions reduction stipulated in the IPCC's Fifth

Assessment Report (Pachauri *et al* 2015) for the resulting CO_2 concentration pathways to have a >66% likelihood to keep the temperature anomaly to 2 °C by 2100. This paper specifically focuses on the U.S. electricity generation sector, the emissions from which are responsible for about 30% (U.S. Environmental Protection Agency 2016) of U.S. GHG emissions and about 4% (World Resources Institute 2014) of the world's GHG emissions. The focus remains on CO_2 from fossil fuel combustion since it accounts for more than 98% (U.S. Environmental Protection Agency 2016) of the electric sector GHG emissions (CH_4, N_2O, and SF_6 comprise the rest).

Direct air capture here refers to the capture of atmospheric CO_2 using materials with preferential affinity for CO_2 over the other air gases, followed by storage/sequestration of the captured CO_2 (see Appendix A.1 for the DAC process considered in this paper). Since the seminal work on this technology in the 1990s (Lackner *et al* 1999) knowledge about the chemistry, engineering, and costs of DAC has advanced considerably (Minx *et al* 2018, Fuss *et al* 2018, Nemet *et al* 2018). (Sanz-Pérez *et al* 2016) provide a comprehensive review of the current state of the art in DAC technologies. Irrespective of the process chemistry employed for CO_2 capture from ambient air, DAC is an energy-consuming NET with heat and electricity requirements ranging between 7.6 – 15 GJ_{th}/tCO_2 (Boot-Handford *et al* 2014, Goeppert *et al* 2012) and 0.7 – 2.4 GJ_e/tCO_2, respectively (House *et al* 2009). CO_2 emissions from energy sources powering DAC plants will require major changes to the electric grid, which in turn will impact the optimal deployment of DAC plants, creating a recursive CO_2 feedback between DAC plants and their energy sources. This feedback between DAC plants and their energy sources greatly influences the systems-level private cost to society of achieving target emissions reductions. Appendix A.6 provides a detailed discussion and mathematical explanation of the recursive feedback.

Modeling these time-dependent systems-level interactions is foundational for evaluating the effectiveness of DAC as a viable large-scale NET. Table 2.1 summarizes major studies published on DAC, and shows that the vast majority of them explicitly or implicitly assume that energy sources powering DAC plants would be low-carbon or carbon-neutral. To the best of our knowledge, the major studies that address the dynamic nature of the DAC-energy supply interaction are by: (Chen and Tavoni 2013) who examine the global CO_2 removal potential using DAC through the year 2100 via the WITCH Integrated Assessment Model (IAM) (Bosetti *et al* 2006); (Kriegler *et al* 2013) who compare the potential of BECCS against DAC using the ReMIND

Table 2.1. Classification of the literature based on the system boundary scope of the analysis and carbon intensity assumptions of energy supply powering DAC plants. Note that some studies feature in multiple classifications.

Treatment of carbon intensity of energy sources powering DAC	Study
Explicit assumption of low-carbon/carbon neutral energy supply	(Baciocchi *et al* 2006)[a]; (Zhang *et al* 2017)[a]; (Lackner 2009)[a]; (Goldberg *et al* 2013)[a]; (Goldberg and Lackner 2015)[a]; (Geng *et al* 2016)[a]; (Sinha *et al* 2017)[a]; (Holmes and Keith 2012)[a]; (Keith *et al* 2018)[a]; (Smith *et al* 2016)[bce]; (Fuss *et al* 2016)[bce]; (Buck 2016)[bce]
Implicit assumption of low-carbon/carbon neutral energy supply based on timing of DAC deployment after 2050	(Socolow *et al* 2011)[a]; (House *et al* 2011)[a]; (Stolaroff *et al* 2008)[a]; (Parra *et al* 2017)[a]; (Zeman 2014)[a]; (Rockström *et al* 2017)[bce]; (Keith *et al* 2006)[bce]; (Fuss *et al* 2013)[bce]; (Marcucci *et al* 2017)[bce]
Cost and/or energy analysis leading to low-carbon/carbon neutral energy supply assumption	(House *et al* 2011)[a]; (Keith *et al* 2006)[a]; (Mazzotti *et al* 2013)[a]; (Kulkarni and Sholl 2012)[a]; (Zeman 2007)[a]; Zeman(Zeman 2014)[a]; (Simon *et al* 2011)[a]; (Pritchard et al 2015)[a]; (van der Giesen *et al* 2017)[a]; (National Academies of Sciences, Engineering, and Medicine 2018)[a]
Carbon intensity of electricity supply endogenously calculated in the model	(Chen and Tavoni 2013)[bce]; (Kriegler *et al* 2013)[bce]; (Wohland *et al* 2018)[bdf]; (Breyer et al 2019)[bdf]; (Creutzig *et al* 2019)[bce]; This study[bdf]

[a]Plant-level analysis; [b]Systems-level analysis; [c]Global scope; [d]Regional/sectoral scope; [e]Uses IAM; [f]Uses bottom-up model or some other simulation model

IAM (Leimbach *et al* 2010); (Creutzig *et al* 2019) who examine the collective deployment of DAC and BECCS globally through 2100; and (Wohland *et al* 2018) and (Breyer *et al* 2019) who respectively examine the potential for DAC powered by excess renewable generation in Europe and Maghreb region.

In this paper, we supplement this previous work by considering only the U.S. electric sector with an annual time resolution, and narrowly studying the potential role for DAC in CO_2 emissions reduction pathways leading up to 2050 using a non-IAM-based model.

Our overarching research question is: *should the U.S. electric sector rely on direct air capture to help achieve a 70% reduction target?* To address this question, this paper quantifies systems-level costs, deployment scale, and associated changes needed in the electric supply to accommodate DAC as a strategy for meeting CO_2 emissions targets within reasonable economic and practical bounds. Hence we intend to contribute to ongoing scientific dialogue on the prudence of deploying new low-carbon energy sources to power NETs as opposed to directing those resources to replace existing fossil fuel-based energy sources – a comparison that is deemed crucial to cost-effective climate change mitigation by the U.S. National Academies report on NETs (National Academies of Sciences, Engineering, and Medicine 2018).

Since the analysis is geared towards technological transformations pursuant to a sector-specific emissions goal, we follow guidance from (Ackerman *et al* 2009) and use an engineering-

based “least-cost” model (also known as a bottom-up model). Our use of this computationally simplified yet technologically rich representation allows us to supplement the IAM-based approach adopted by (Chen and Tavoni 2013) and (Kriegler *et al* 2013), as well as the stylized simulation model-based approach adopted by (Wohland *et al* 2018). It also allows us to analyze a large range of uncertainty scenarios that capture uncertainties in technology costs, fuel prices, emission factors, and electricity demand. We begin by briefly describing a previously published stock-and-flow model of the U.S. electric sector from which this work builds, and then focus on the addition of DAC to the model as required to answer our research question. Then we discuss key input data and assumptions employed in the analysis. Finally, we discuss the model results, limitations, and implications of our findings.

2.2 METHODOLOGY

The U.S. electric utilities sector (including combined heat and power units) is represented using the LETSACT model, which has been published previously (Supekar and Skerlos 2017). LETSACT is a linear programming optimization model that contains a stock-and-flow representation of U.S. electricity generating units (EGUs). It contains 13 generation technologies: pulverized coal and natural gas combined cycle with and without carbon capture and storage (CCS), gas turbine, petroleum, biomass, nuclear, conventional hydroelectric, on-shore wind, solar photovoltaic, solar thermal, and geothermal. The last six technologies on this list, along with coal and natural gas CCS, are referred to here as “low-carbon” EGU technologies.

The initial stock of EGUs as a function of EGU technology and age is populated using the U.S. EPA’s NEEDS database (U.S. Environmental Protection Agency 2015). Stocks are updated at 1-year intervals by changing EGU additions and retirements for each of the 13 technologies. Annual EGU additions, retirements, and stocks, collectively referred to as a “technology trajectory”, are decision variables in an optimization problem. The objective of the optimization problem is to minimize the net present value (NPV) of the total capital, operating, and retirement costs of EGUs over the analysis time horizon. The constraints include achieving electricity demand equal to supply, and a CO_2 emissions budget corresponding to a 70% reduction in emissions by 2050 relative to 2010. The CO_2 emissions budget is calculated as the area under the curve defined by a straight-line emission trajectory corresponding to the emissions reduction target (see Figure

A.5). We refer to this emissions target (approximately 50 $GtCO_2$) as the "70% reduction target" or the "2050 emissions budget".

Equations (2.1) –(2.4) describe the optimization problem formulation, where X^{new}, X^{ret}, and X^{stock} are the decision variables representing EGU additions, early retirements, and total stocks in MWh. The sets *N*, *T*, and *Y* contain EGU technologies, ages, years in the analysis time horizon, respectively. The model characterizes EGU costs and emissions on a per MWh generation basis. The coefficients c^{new}, c^{stock}, c^{ret} represent the unit costs of building and operating a MWh of new generation, retiring a MWh of existing generation, and operating a MWh of existing generation respectively. Similarly, e^{new} and e^{stock} represent the emissions per MWh of new and existing generation. The discount rate is given by *r*, which is assumed as 7% in this analysis. *E* is the emissions budget corresponding to the area under the straight-line emissions reduction trajectory, and *D* is the total non-DAC related electricity demand that is treated as exogenous.

$$\text{Minimize } f(X^{new}, X^{stock}, X^{ret}) = \sum_{k\in Y}\sum_{i\in N}\frac{c_{ik}^{new}X_{ik}^{new}}{(1+r)^{k-1}} + \sum_{k\in Y}\sum_{i\in N}\sum_{j\in T}\frac{c_{ijk}^{ret}X_{ijk}^{ret} + c_{ijk}^{stock}X_{ijk}^{stock}}{(1+r)^{k-1}} \quad (2.1)$$

Subject to

$$X_{ik}^{new}, X_{ijk}^{stock}, X_{ijk}^{ret} \geq 0 \;\forall\; i \in N, j \in T, k \in Y \quad (2.2)$$

$$\sum_{i\in N} X_{ik}^{new} + \sum_{i\in N}\sum_{j\in T} X_{ijk}^{stock} \geq D_k \;\forall\; k \in Y \quad (2.3)$$

$$\sum_{k\in Y}\sum_{i\in N} e_{ik}^{new}X_{ik}^{new} + \sum_{k\in Y}\sum_{i\in N}\sum_{j\in T} e_{ijk}^{stock}X_{ijk}^{stock} \leq E \quad (2.4)$$

Retirement in this analysis refers to the decommissioning of a unit of generation *prematurely* before its typical expected plant life. This "early retirement" could be an outcome of functional or economic obsolescence as a result of competing technologies or regulations. Early retirement is treated as separate from and in addition to the decommissioning of generation capacity at the end of its expected life. For instance, coal plants are built to typically serve for 60 years, and thus if the model chooses to decommission 1 MWh of coal generation after it reaches only 30 years of life, this would be treated as early retirement. The unit retirement cost (cret) is treated as the remaining capital liability, if any, on a unit of generation beyond its assumed financing period of 20 years. The retirement cost shown in equation (2.1) is therefore a function of both age and year of the EGU. Key details of the model in the context of this paper are provided in Appendix A.2. Additional information about the LETSACT model and its mathematical framework can be found in (Supekar and Skerlos 2017).

2.2.1 DAC representation in LETSACT

DAC plants are net consumers of heat and electricity and remove CO_2 from the atmosphere. This means that they add non-negative values to the right hand side of equations (2.3) and (2.4), which in turn affects decision variables on the left hand sides of those equations. To maintain the linearity of the model which is vital for minimizing computation time, we incorporate DAC into LETSACT by treating it as an EGU that consumes heat to produce *negative* useful power output and emit *negative* CO_2. To achieve this, we take energy and cost parameters reported in the literature (Keith *et al* 2018, Socolow *et al* 2011, Grant *et al* 2018) for a single aqueous alkaline sorbent-based DAC plant, and convert the parameters to a per MWh of electricity consumed basis.

For instance, the KOH + calcium caustic recovery loop-based DAC plant described by (Keith *et al* 2018) has a 1 Mt per year of CO_2 removal capacity, and requires 366 kWh of electricity and 5.25 GJ of heat per tonne of CO_2. This DAC plant would be equivalent to an EGU with –46.5 MW capacity (assuming a 90% capacity factor based on (Keith *et al* 2018)) that operates with a heat rate of about –13596 Btu/kWh as shown in equations (2.5) and (2.6). The 694 million USD capital cost and 26 and 18 USD/tCO_2 of O&M and transportation costs of the DAC plant are then converted to their equivalent EGU basis as shown in equations (2.7) and (2.8).

$$DAC^{EGU}_{Capacity} = \frac{-0.366\left(\frac{MWh}{tCO_2}\right) \times 10^6\left(\frac{tCO_2}{year}\right)}{365\left(\frac{days}{year}\right) \times 24\left(\frac{hours}{day}\right) \times 0.9} = -46.5\left(MW\right) \tag{2.5}$$

$$DAC^{EGU}_{HeatRate} = \frac{5.25\left(\frac{GJ}{tCO_2}\right) \times 947817\left(\frac{Btu}{GJ}\right)}{-366\left(\frac{kWh}{tCO_2}\right)} = -13596\left(\frac{Btu}{kWh}\right) \tag{2.6}$$

$$DAC^{EGU}_{CapCost} = \left|\frac{694\left(million\$\right)}{-46.5\left(MW\right)}\right| = 14925\left(\frac{\$}{kW}\right) \tag{2.7}$$

$$DAC^{EGU}_{O\&M+Transport} = \left|\frac{44\left(\frac{\$}{tCO_2}\right)}{-0.366\left(\frac{MWh}{tCO_2}\right)}\right| = 120.2\left(\frac{\$}{MWh}\right) \tag{2.8}$$

For every Mt of CO_2 by the DAC plant, 0.413 MtCO_2 is captured from natural gas combustion in the DAC plant's calciner as per the process described in the literature. We note that DAC costs and energy use are assumed to increase linearly with DAC deployement – that is, the costs and energy use of ten DAC plants with 1 MtCO_2 capacity is treated as equal to one DAC plant with 10 Mt CO_2 capacity. Thus, potential cost savings through economies of scale and energy savings through better thermal integration are not considered in this study.

In addition to ensuring structural consistency with the LETSACT framework, representation of DAC as an EGU captures the feedbacks between the DAC plants, the electric grid, and net CO_2 removal, and also quantifies the system-level costs associated with building and operating DAC plants together with the costs of EGU additions and retirements necessary for effective CO_2 removal. The capacity and timing of DAC deployment is thus determined in concert with changes in the electricity supply as required to stay within the CO_2 emissions budget at least cost. As such, the analysis views DAC with CO_2 storage as a measure that may act in conjunction with *preventive* and mitigation-based supply-side transformations to low-carbon/carbon-free EGUs.

2.2.2 Business-as-usual and climate action

We reference "business-as-usual" (BAU) when the LETSACT model is run *without* the emissions constraint given by eq. (2.4) to minimize the NPV of costs of meeting electricity demand. We reference the case *with* the emissions constraint as "climate action." By definition, climate action is a more aggressive CO_2 emissions timeline than BAU. Both BAU and climate action cases are subject to a constraint to emulate nation-wide implementation of the Renewable Portfolio Standard (RPS), which is imposed as an inequality constraint requiring at least 15% of the total generation to come from renewables by 2025. The difference in net present value of the cost difference between BAU and climate action, under identical input parameters, is defined as the "climate action cost."

The term "delayed climate action" is referenced when BAU continues beyond the model start year (2015). When climate action is delayed until a certain year, the model forces the BAU technology and emissions trajectory from 2015 to the year before the year in which climate action is initiated. The year in which climate action is initiated is called the "climate action year," and a set of climate action years is collectively to referred to as a "climate action timeframe." Table S5 provides a glossary of the terms introduced here and used throughout the rest of the paper, and Figure A.6 provides visual guidance for contextualizing the terminologies. The model treats 2050 emissions targets as infeasible *without* DAC and using preventive mitigation alone either when the primal-dual interior-point method used to solve the optimization problem returns an infeasible solution.

2.2.3 Uncertainty scenarios

Given large uncertainties in costs, emission characteristics, and demand over the analysis timeframe, we perform a sensitivity analysis by varying all key model inputs corresponding to technology and fuel costs, emissions, and demand at three levels – low, nominal, and high. The 3 parameter categories and 3 parameter levels give rise to $3^3 = 27$ scenarios for which least-cost EGU additions, retirements, stocks, emissions, and costs are calculated at each climate action year. As with EGU technologies, the sensitivity analysis includes uncertainties in DAC costs, emissions, energy demands at low, nominal, and high levels obtained from the literature. For each uncertainty scenario, we run the optimization model for all climate action years from 2015 – 2035. Single values expressed in the paper for quantities emanating from the 27 uncertainty scenarios reflect medians, and ranges reflect the first and ninth deciles, unless specified otherwise.

Appendix A.2 provides values and data sources for the uncertainty parameters. The appendix also contain links to result files containing costs, emissions, DAC deployment, EGU additions and retirements, and other important variables calculated for different uncertainty scenarios and climate action years as generated by the least-cost model. Links to codes used for the analysis and to generate these results are also included.

2.3 Results and Discussion

The model estimates that continued BAU emissions through 2050 would total 58 – 62 $GtCO_2$ as shown by the gray lines in Figure 2.1a. This is significantly higher than the 50 $GtCO_2$ budget. Despite falling short of the 2050 CO_2 reduction target, the model projects BAU emissions to follow a downward trend as shown in Figure 2.1b, with an estimated emissions reduction of 30 – 48% relative to 2010. This is because even without a 2050 emissions constraint, least-cost technology trajectories under BAU project that coal EGUs would be largely replaced with natural gas combined cycle EGUs, with the median fraction of total generation from coal falling to about 4% by 2050.

2.3.1 Preventive climate action

The analysis finds that initiating climate action within the next decade could still achieve 2050 CO_2 targets using prevetive mitigation alone, provided BAU emissions during any period of climate inaction follow the downward trend projected by the model. Without DAC (or other NETs), preventive climate action would thus be likely impossible if BAU emissions were allowed to continue beyond 2030. However, any delays in initiating timely preventive climate action

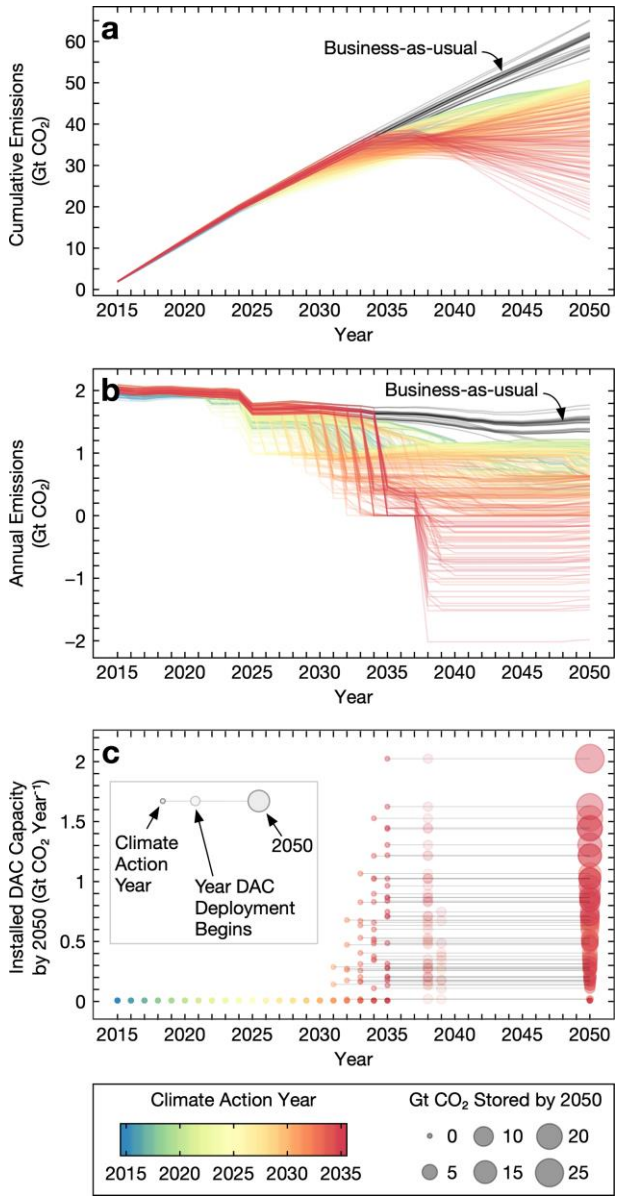

Figure 2.1. | a. Cumulative CO_2 emissions; b. annual CO_2 emissions; and c. DAC deployment under different climate action years. Each individual curve or data point represents a single uncertainty scenario. Segments in c indicate the delay between start of climate action and actual deployment of DAC plants.

starting in 2020 will result in progressively higher costs, as shown in Figure 2.2a in which the distribution of the total climate action costs through 2050 across various uncertainty scenarios is plotted as a function of the climate action year. For instance, delays in initiating climate action increase the median climate action cost through 2050 from about 135 billion USD for climate action year 2020 to 175 billion USD and 320 billion USD for climate action years 2025 and 2030, respectively.

The higher cost of delays relative to climate action starting in 2020 result from higher retirement of fossil fuel-based EGUs to compensate for excess BAU emissions. Figure 2.2b shows

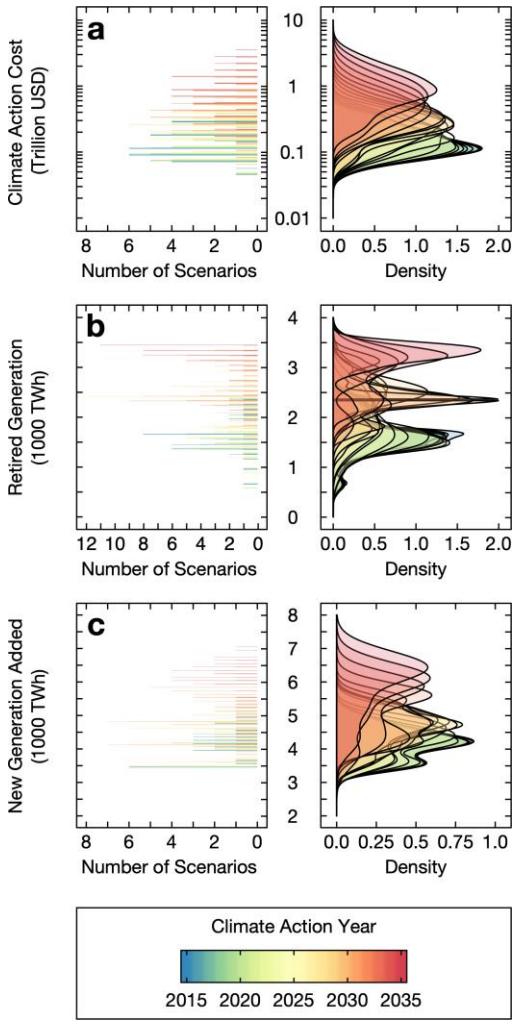

Figure 2.2. | a. Climate action cost; b. total generation retired early through 2050; and c. total new generation added through 2050 as a function of climate action year. Approximated Gaussian density distribution for each quantity in the left panels in a – c is shown in their respective right panels.

EGU retirements through 2050 increasing with delays in climate action. Total (median) EGU retirements through 2050 increase from 1570 TWh for climate action year 2020 to 1830 TWh for climate action year 2025 (16% increase), and 2350 TWh for climate action year 2030 (50% increase). New generation added to compensate for the higher retirements and meet the overall electricity demand accounts for the largest fraction of the increase in climate action costs. Median total EGU additions through 2050 increase from 4190 TWh for climate action year 2020 to 4275 TWh for climate action year 2025 (2% increase), and 4780 TWh for climate action year 2030 (14% increase). Figure 2.2c shows the distribution of EGU additions through 2050 as a function of climate action year.

2.3.2 DAC-based climate action

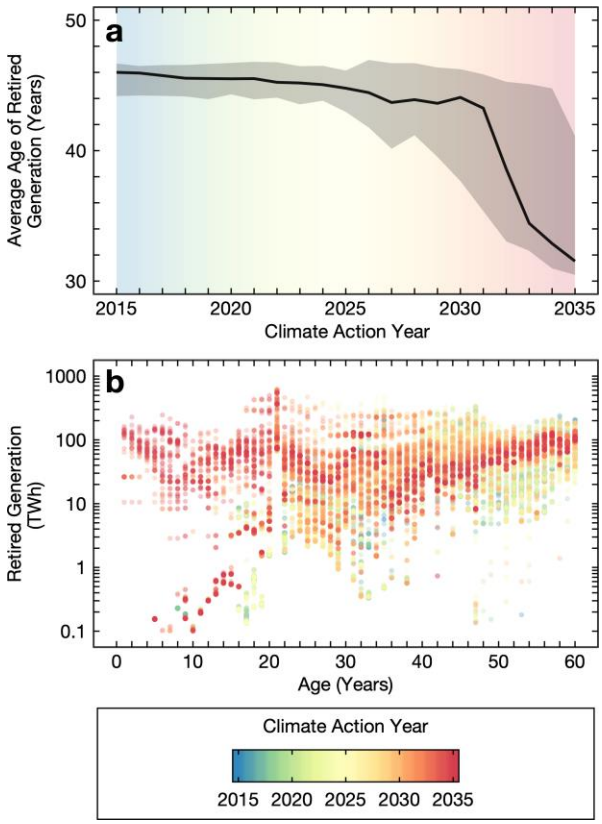

Figure 2.3. | a. Generation-weighted average age of retired EGUs as a function of climate action year, where solid line represents the median, and bands represent first and ninth decile values across uncertainty scenarios; and b. retired generation as a function of EGU age for all uncertainty scenarios.

Although DAC is available to be deployed at any time, the least-cost model prefers preventive mitigation over DAC unless preventive mitigation alone without NETs becomes infeasible. This confirms the premise of this study that DAC would serve as a backstop technology option towards achieving climate targets. The model shows that about 7% of the uncertainty scenarios would require DAC starting in climate action year 2031 as shown in Figure 2.1c. This fraction rises to 80% of the uncertainty scenarios by climate action year 2035. The median DAC capacity installed by 2050 under DAC-based climate action increases from 0.2 $GtCO_2$/year in climate action year 2031 to 0.8 $GtCO_2$/year in climate action year 2035. The median CO_2 storage through 2050, indicated by the bubble sizes in Figure 2.1c, is estimated to be 2.5 $GtCO_2$ for climate action year 2031, and 9.9 $GtCO_2$ for climate action year 2035. These values include CO_2 captured from the DAC plant calciner. The total CO_2 storage potential in the US is estimated to be between 413 and 448 Gt (see section A.4.2 for more on this estimate) according to a recent NETL study (Grant et al 2017). It is therefore unlikely that CO_2 storage for DAC would exceed the total CO_2 storage capacity.

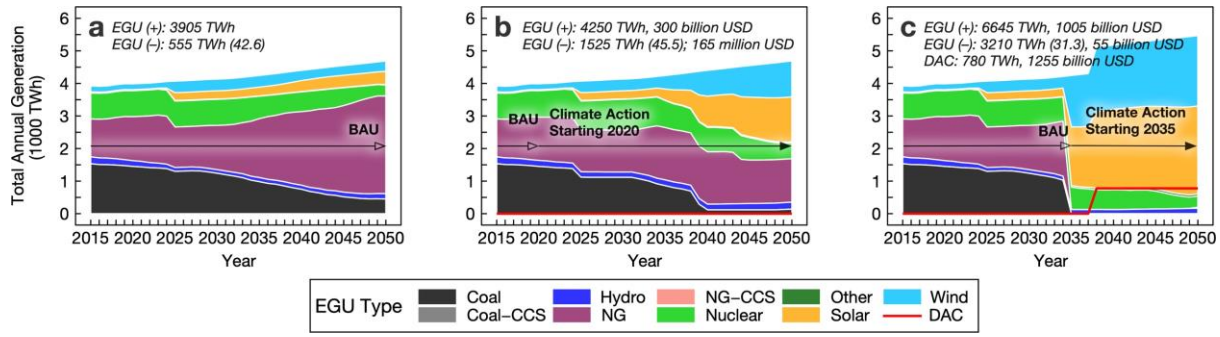

Figure 2.4. | Least-cost technology trajectories under a. BAU; b. climate action starting in 2020; and c. climate action starting in 2035. Values shown for a single uncertainty scenario. EGU additions are retirements through 2050 are marked by EGU (+) and EGU (–), respectively. Costs in b and c are relative to BAU, and cost of EGU additions relative to BAU include any savings in fuel and operating costs. Values in parentheses next to EGU (–) indicate the average age of retired generation.

Figure 2.1b and c further show that DAC deployment would be preceded by a brief period during which emissions fall significantly. Median emissions intensity of the electricity supply before DAC is deployed is found to be about 25 $kgCO_2/MWh$, although the 90^{th} percentile value is as high as 93 $kgCO_2/MWh$. For reference, the average emissions intensity of utility-scale electricity supply in 2017 was about 460 $kgCO_2/MWh$ (U.S. Energy Information Administration 2018). The emissions drop is achieved by retiring most of the remaining fossil fuel EGUs in the fleet and replacing them with low-carbon EGUs to minimize the cost of offsetting further CO_2 emissions from energy sources powering the DAC plants.

Not only is the total EGU retirement under DAC-based climate action considerably higher than preventive mitigation-based climate action as shown in Figure 2.2c, but the average age of retired EGUs is considerably lower in DAC-based climate action as shown in Figure 2.3a. In fact, Figure 2.3b shows that DAC-based climate action would lead to the early retirement of several of the same EGUs as preventive climate action – only sooner and in greater numbers supplemented by the retirement of much younger EGUs as clearly seen in the peak around age 21 – immediately after the capital liability of plants is paid off by age 20. Figure A.7 illustrates this phenomenon for a single uncertainty scenario to provide clarity on this crucial point. In other words, we find that *in order for DAC-based climate action to cost-effectively achieve 2050 emission targets, the EGU turnover expected under timely preventive climate action cannot be avoided*. Rather, deferring this EGU turnover would hasten what would otherwise have been be a more gradual turnover under timely preventive climate action, and the private costs to society would balloon.

Figure 2.4 illustrates EGU turnover for a specific scenario. It shows how timely preventive action would lead to a relatively gradual reduction in coal generation and eventual phase out before

2040. Emissions prevented from coal EGUs, together with considerable deployment of renewable EGUs would in fact allow the operation of significantly more efficient natural gas EGUs without CCS and still meet the 2050 CO_2 budget, as shown in Figure 2.4b. However, continued BAU emissions from delays in climate action would quickly require much higher emissions reduction rates. This could lead to phase out of coal *earlier* while also *limiting* the amount of natural gas generation possible, as shown in Figure 2.4c. These observations also hold true for the uncertainty scenarios that rely on NG-CCS and renewables for low-carbon electricity (roughly 25% of all uncertainty scenarios feature natural gas EGUs with CCS; see Figure A.8 for an example of one such technology trajectory).

The hastened turnover under delayed DAC-based climate action would significantly increase costs as shown in Figure 2.2a. The median climate action cost for DAC-based climate action starting 2035 is found to be 1005 billion USD through 2050. Comparing this to the median cost of climate action without DAC starting in 2020 discussed earlier, 135 billion USD, we find that DAC-based climate action will be costlier by an order of magnitude or more, and the higher costs would be deferred to future generations.

DAC-based climate action would also draw a considerable amount of electricity from utilities. The median electricity demand for powering DAC plants is estimated to be 5% of the total electricity supply by 2050, although this demand could be as high as 15% of the total supply if a DAC capacity of more than 2 $GtCO_2$/year is deployed. Further, every tonne of CO_2 captured also requires 5.25 – 8.1 GJ of heat, which means that every 0.1 Gt CO_2/year of DAC capacity installed would create an annual heat energy demand of about 0.5 – 0.75 quadrillion Btus (quads) in addition to the electricity demand. For context, the total natural gas use for electric power in the U.S. in 2018 was estimated to be about 10.75 quads (U.S. Energy Information Administration 2019). If this heat is provided by natural gas, as has been assumed in this study based on available process data in the literature, DAC would also create a significant demand for non-renewable energy. To mitigate this, alternate sources of high-temperature heat for the DAC process such as biomass-dervied fuels and electrofuels warrant exploration from the standpoint of process compatibility, overall energy balance, and system-level impacts.

The impact of discount rate on the results was examined by running the model with a 4% and 10% discount rate. When the future is discounted at a lower rate of 4%, the model places greater emphasis on preventive mitigation without DAC through higher EGU early retirement and

replacement with low-carbon EGUs than the 7% case. The resulting BAU emissions are lower, and therefore DAC deployment is lower than the 7% case. The reverse trend is seen when the future is discounted at a higher rate of 10%. BAU emissions are found to be higher in the 10% case than the 7% case, and therefore DAC deployment is higher and is needed earlier than the 7% case. Results for these and discount rates are provided in Appendix A.10.1.

2.3.3 Model limitations

The model used in the study does not pose constraints on the rate of turnover of EGUs. Other potentially important factors excluded from the analysis include "outgassing" of CO_2 from the oceans (Tokarska and Zickfeld 2015); emissions from the construction of DAC plants (de Jonge *et al* 2019) and additional EGUs; and non-CO_2 GHG emissions from the electricity generation, transmission, and distribution systems. Any of these factors could effectively reduce the available equivalent CO_2 budget through 2050. To compensate for a reduced CO_2 budget, significantly higher rates of CO_2 removal than those estimated in this study would be needed, which in turn would need even greater numbers of EGU retirements and additions – a non-linear feedback loop which has been shown in this study to have a non-linear effect on costs.

On the other hand, the model estimates that the median coal and natural gas use would be significantly lower compared to BAU (see Figure A.9), which would lead to substantially lower upstream emissions from fuel supply chains (such as fugitive methane emissions) that are excluded from the analysis and can increase the equivalent CO_2 budget. While quantification of the impacts of these factors on the CO_2 budget falls outside the scope of the analysis, we ran the model under two additional emission targets – 60% by 2050 and 80% by 2050 – to understand the sensitivity of the results and conclusions to this parameter. The results show that for a CO_2 reduction target of 60% by 2050, DAC may be needed in about 20% of the uncertainty scenarios by climate action year 2035. The installed DAC capacity in this case is also found to be lower than the 70% reduction case as would be expected for a lower emission target. For the 80% reduction target, DAC may be needed as early as 2028 and at much higher installed capacity, with more than 50% of the uncertainty scenarios requiring DAC to achieve the emission target by climate action year 2031. Results from these additional emission targets are provided in Appendix A.10.2.

Climate action costs could be higher if lost revenues are included in the valuation of EGUs retired early as suggested by some (Pomykacz and Olmsted 2014). Additionally, the effects on the

system capital and operating cost from inclusion of factors such as spinning reserves, ancillary services, energy storage, and transmission constraints that may be captured by a dispatch and unit commitment model are not modeled in this study. Costs associated with expanding the transmission and distribution network to support the high penetration of low-carbon EGUs are also excluded. As pointed out by studies in the literature (Kroposki 2017, Heuberger and Mac Dowell 2018), these factors could significantly increase the climate action costs of DAC-based interventions. On the other hand, as found by (Wohland *et al* 2018), there may also exist synergies within the electric dispatch system whereby DAC could in fact reduce curtailment of renewables and thus decrease overall system costs compared to values estimated in this study. A systematic inclusion of these factors into the least-cost model used in this study would be undertaken as part of the future work on DAC-based climate action.

2.4 CONCLUSIONS

This analysis finds that continued BAU emissions beyond 2030 would neccessitate coupling preventive mitigation with 0.2 – 1.4 $GtCO_2$/year of DAC or similar NET as a backstop technology measure to offset historic emissions in order to achieve a 70% reduction in CO_2 emissions by 2050. This is despite a somewhat optimistic decline in emissions projected under BAU by the least-cost model used in the analysis. Any DAC-based climate action would involve the retirement of many of the same fossil fuel-based EGUs that would be retired under preventive climate action starting now, and necessitate additional retirement of newer and more efficient natural gas-based EGUs (without carbon capture). To compensate for such extensive early retirement of EGUs and meet projected electricity demand, significantly more new low-carbon EGUs would need to be deployed in addition to building DAC plants.

The key conclusions of the study that – (1) DAC is far from a substitute for preventive climate action since EGU turnover expected under preventive climate action would be a pre-requisite for effective CO_2 removal with DAC, and (2) although modest CO_2 removal rates could be achieved with DAC, preventive mitigation would be less expensive, would afford a more gradual turnover of fossil fuel-based EGUs, and require significantly fewer low-carbon EGUs to achieve the 2050 CO_2 budget – remain robust to the uncertainties surrounding costs, electricity demand, and other factors examined in this analysis.

REFERENCES

Ackerman F, DeCanio S J, Howarth R B and Sheeran K 2009 Limitations of integrated assessment models of climate change *Clim. Change* **95** 297–315

Boot-Handford M E, Abanades J C, Anthony E J, Blunt M J, Brandani S, Mac Dowell N, Fernández J R, Ferrari M-C, Gross R, Hallett J P, Haszeldine R S, Heptonstall P, Lyngfelt A, Makuch Z, Mangano E, Porter R T J, Pourkashanian M, Rochelle G T, Shah N, Yao J G and Fennell P S 2014 Carbon capture and storage update *Energy Env. Sci* **7** 130–89

Bosetti V, Carraro C, Galeotti M, Massetti E and Tavoni M 2006 WITCH - A World Induced Technical Change Hybrid Model *SSRN Electron. J.* **93** 2873–86

Breyer C, Fasihi M and Aghahosseini A 2019 Carbon dioxide direct air capture for effective climate change mitigation based on renewable electricity: a new type of energy system sector coupling *Mitig. Adapt. Strateg. Glob. Change* Online: http://link.springer.com/10.1007/s11027-019-9847-y

Chen C and Tavoni M 2013 Direct air capture of CO_2 and climate stabilization: A model based assessment *Clim. Change* **118** 59–72

Creutzig F, Breyer C, Hilaire J, Minx J, Peters G P and Socolow R 2019 The mutual dependence of negative emission technologies and energy systems *Energy Environ. Sci.* **12** 1805–17

Field C B and Mach K J 2017 Rightsizing carbon dioxide removal *Science* **356** 706–7

Fuss S, Jones C D, Kraxner F, Peters G P, Smith P, Tavoni M, van Vuuren D P, Canadell J G, Jackson R B, Milne J, Moreira J R, Nakicenovic N, Sharifi A and Yamagata Y 2016 Research priorities for negative emissions *Environ. Res. Lett.* **11** 115007

Fuss S, Lamb W F, Callaghan M W, Hilaire J, Creutzig F, Amann T, Beringer T, de Oliveira Garcia W, Hartmann J, Khanna T, Luderer G, Nemet G F, Rogelj J, Smith P, Vicente J L V, Wilcox J, del Mar Zamora Dominguez M and Minx J C 2018 Negative emissions—Part 2: Costs, potentials and side effects *Environ. Res. Lett.* **13** 063002

Gasser T, Guivarch C, Tachiiri K, Jones C D and Ciais P 2015 Negative emissions physically needed to keep global warming below 2 °C *Nat. Commun.* **6** Online: http://www.nature.com/articles/ncomms8958

Goeppert A, Czaun M, Surya Prakash G K and Olah G A 2012 Air as the renewable carbon source of the future: an overview of CO_2 capture from the atmosphere *Energy Environ. Sci.* **5** 7833

Grant T, Guinan A, Shih C Y, Lin S, Vikara D, Morgan D and Remson D 2018 Comparative analysis of transport and storage options from a CO_2 source perspective *Int. J. Greenh. Gas Control* **72** 175–91

Grant T, Morgan D and Gerdes K 2017 Carbon Dioxide Transport and Storage Costs in NETL Studies Quality Guidelines for Energy System Studies (Pittsburgh, PA: NETL) (https://netl.doe.gov/energy-analysis/details?id=1027)

Heuberger C F and Mac Dowell N 2018 Real-World Challenges with a Rapid Transition to 100% Renewable Power Systems *Joule* **2** 367–70

House K Z, Harvey C F, Aziz M J and Schrag D P 2009 The energy penalty of post-combustion CO_2 capture & storage and its implications for retrofitting the U.S. installed base *Energy Environ. Sci.* **2** 193

de Jonge M M J, Daemen J, Loriaux J M, Steinmann Z J N and Huijbregts M A J 2019 Life cycle carbon efficiency of Direct Air Capture systems with strong hydroxide sorbents *Int. J. Greenh. Gas Control* **80** 25–31

Keith D W, Holmes G, St. Angelo D and Heidel K 2018 A Process for Capturing CO_2 from the Atmosphere *Joule* **2** 1573–94

Kriegler E, Edenhofer O, Reuster L, Luderer G and Klein D 2013 Is atmospheric carbon dioxide removal a game changer for climate change mitigation? *Clim. Change* **118** 45–57

Kroposki B 2017 Integrating high levels of variable renewable energy into electric power systems *J. Mod. Power Syst. Clean Energy* **5** 831–7

Lackner K S, Ziock H-J and Grimes P 1999 *Carbon capture from air, is it an option?* (Los Alamos, NM: Los Alamos National Laboratory)

Le Quéré C, Andrew R M, Canadell J G, Sitch S, Korsbakken J I, Peters G P, Manning A C, Boden T A, Tans P P, Houghton R A, Keeling R F, Alin S, Andrews O D, Anthoni P, Barbero L, Bopp L, Chevallier F, Chini L P, Ciais P, Currie K, Delire C, Doney S C, Friedlingstein P, Gkritzalis T, Harris I, Hauck J, Haverd V, Hoppema M, Klein Goldewijk K, Jain A K, Kato E, Körtzinger A, Landschützer P, Lefèvre N, Lenton A, Lienert S, Lombardozzi D, Melton J R, Metzl N, Millero F, Monteiro P M S, Munro D R, Nabel J E M S, Nakaoka S, O'Brien K, Olsen A, Omar A M, Ono T, Pierrot D, Poulter B, Rödenbeck C, Salisbury J, Schuster U, Schwinger J, Séférian R, Skjelvan I, Stocker B D, Sutton A J, Takahashi T, Tian H, Tilbrook B, van der Laan-Luijkx I T, van der Werf G R, Viovy N, Walker A P, Wiltshire A J and Zaehle S 2016 Global Carbon Budget 2016 *Earth Syst. Sci. Data* **8** 605–49

Leimbach M, Bauer N, Baumstark L and Edenhofer O 2010 Mitigation costs in a globalized world: Climate policy analysis with REMIND-R *Environ. Model. Assess.* **15** 155–73

Minx J C, Lamb W F, Callaghan M W, Fuss S, Hilaire J, Creutzig F, Amann T, Beringer T, de Oliveira Garcia W, Hartmann J, Khanna T, Lenzi D, Luderer G, Nemet G F, Rogelj J, Smith P, Vicente Vicente J L, Wilcox J and del Mar Zamora Dominguez M 2018 Negative emissions—Part 1: Research landscape and synthesis *Environ. Res. Lett.* **13** 063001

National Academies of Sciences, Engineering, and Medicine 2018 *Negative Emissions Technologies and Reliable Sequestration: A Research Agenda* (Washington, D.C.: National Academies Press) Online: https://www.nap.edu/catalog/25259

Nemet G F, Callaghan M W, Creutzig F, Fuss S, Hartmann J, Hilaire J, Lamb W F, Minx J C, Rogers S and Smith P 2018 Negative emissions—Part 3: Innovation and upscaling *Environ. Res. Lett.* **13** 063003

Pachauri R K, Mayer L and Intergovernmental Panel on Climate Change 2015 *Climate change 2014: synthesis report* (Geneva, Switzerland: Intergovernmental Panel on Climate Change)

Pomykacz M and Olmsted C 2014 The Appraisal of Power Plants *Apprais. J.* **2014** 216–30

Rogelj J, Popp A, Calvin K V, Luderer G, Emmerling J, Gernaat D, Fujimori S, Strefler J, Hasegawa T, Marangoni G, Krey V, Kriegler E, Riahi K, van Vuuren D P, Doelman J, Drouet L, Edmonds J, Fricko O, Harmsen M, Havlík P, Humpenöder F, Stehfest E and Tavoni M 2018 Scenarios towards limiting global mean temperature increase below 1.5 °C *Nat. Clim. Change* **8** 325–32

Sanz-Pérez E S, Murdock C R, Didas S A and Jones C W 2016 Direct Capture of CO_2 from Ambient Air *Chem. Rev.* **116** 11840–76

Socolow R, Desmond M, Aines R, Blackstock J, Bolland O, Kaarsberg T, Lewis N, Mazzotti M, Pfeffer A, Sawyer K, Siirola J, Smit B and Wilcox J 2011 Direct Air Capture of CO_2 with Chemicals Panel on Public Affairs *Am. Phys. Soc. - Panel Public Aff.* 100

Supekar S D and Skerlos S J 2017 Analysis of Costs and Time Frame for Reducing CO_2 Emissions by 70% in the U.S. Auto and Energy Sectors by 2050 *Environ. Sci. Technol.* **51** 10932–42

Tokarska K B and Zickfeld K 2015 The effectiveness of net negative carbon dioxide emissions in reversing anthropogenic climate change *Environ. Res. Lett.* **10**

U.S. Energy Information Administration 2019 *Annual Energy Outlook 2019* (Washington, DC) Online: https://www.eia.gov/outlooks/aeo/data/browser/#/?id=2-AEO2019&cases=ref2019&sourcekey=0

U.S. Energy Information Administration 2018 *Electric Power Annual 2017* (Washington, DC) Online: https://www.eia.gov/electricity/annual/pdf/epa.pdf

U.S. Environmental Protection Agency 2016 *Inventory of U.S. Greenhouse Gas Emissions and Sinks 1990 – 2014* (Washington, DC) Online: https://www.epa.gov/ghgemissions/inventory-us-greenhouse-gas-emissions-and-sinks

U.S. Environmental Protection Agency 2015 *National Electric Energy Data System (NEEDS) v.5.14* (Washington, DC)

van Vuuren D P, Hof A F, van Sluisveld M A E and Riahi K 2017 Open discussion of negative emissions is urgently needed *Nat. Energy* **2** 902–4

Wohland J, Witthaut D and Schleussner C-F 2018 Negative Emission Potential of Direct Air Capture Powered by Renewable Excess Electricity in Europe *Earths Future* **6** 1380–4

World Resources Institute 2014 CAIT - Country Greenhouse Gas Emissions Data Online: https://www.wri.org/resources/data-sets/cait-country-greenhouse-gas-emissions-data

CHAPTER 3

Experimental Evaluation of Accelerated CO_2 Desorption Using Microwaves

LIST OF SYMBOLS

t	Time [s]
ω	Angular frequency of electromagnetic wave [Hz]
ε_0	Permittivity of free space [F/m]
ε_{r}	Relative permittivity of a material [1]
$\varepsilon_r^{"}$	Imaginary part of the relative complex dielectric permittivity [1]
$\vec{E}$	Electric field of the electromagnetic wave [V/m]
P_0	Ambient pressure [Pa]
P_x	Partial pressure of species x (CO_2, air, argon) [Pa]
P_{tot}	Total pressure inside chamber [Pa]
$\hat{P}_x$	Partial pressure of species x leaked into the chamber [Pa]
$\underline{P}$	Average pressure inside pipes that connect the chamber and the vacuum pump [Pa]
$\hat{P}_{CO_2}$	Partial pressure of desorbed CO_2 [Pa]
C_v, C_i, C_m	Conductance of pipes at viscous, intermediate, and molecular regime based on Knudsen number [m^3/s]
J	Scaling factor that relates conductance at intermediate flow regime when the molecular conductance is taken as 1 [1]
S_0	Pumping speed [m^3/hour]
V	Chamber volume [m^3]
V_z	Volume of zeolite sorbent [m^3]
M_x	Molecular weight of species x [g/mol]
R_0	Ideal gas constant [J/K-mol]
T_x	Temperature of species x [K]
T_z, T_a, T_g, T_w, T_m	Temperature of zeolite, adsorbed CO_2, desorbed CO_2 gas, waveguide, and mica cage [K]
$T_{0,x}$	Reference temperature of species x [K]
D	Effective diameter of pipes [m]
L	Effective length of pipes [m]
μ_x	Coefficient of viscosity of species x [poise]
$\mu_{0,x}$	Coefficient of viscosity of species x at reference temperature [poise]
c_x	Sutherland's constant of species x at reference temperature [K]
n_x	Mole of gas species x [mol]
$\dot{q}_d$	Dissipated microwave power density [W/m^3]
$\dot{Q}_d$	Microwave power dissipated during CO_2 desorption [W]
$\dot{Q}_i, \dot{Q}_r, \dot{Q}_t, \dot{Q}_{rr}$	Incident, reflected, transmitted, and re-reflected microwave power [W]

$\dot{Q}_l$	Leaked power to the environment [W]
$\dot{Q}_z$	Power used to heat zeolite sorbents [W]
$\dot{Q}_{CO_2}$	Power used to heat adsorbed CO_2 [W]
$\dot{Q}_{\Delta H}$	Power used to overcome enthalpy of CO_2 desorption [W]
$\dot{Q}_g$	Power used to heat gases [W]
$\dot{Q}_{hl}$	Power lost to environment via conduction and radiation [W]
$\dot{Q}_c$	Power lost through conduction [W]
$\dot{Q}_r$	Power lost through radiation [W]
$\dot{Q}_{wg}$	Power used to heat waveguide [W]
m_z, m_a, m_g, m_w, m_m	Mass of zeolite, adsorbed CO_2, desorbed CO_2 gas, waveguide, and mica cage [kg]
$C_{p,z}, C_{p,a}, C_{p,w}, C_{p,m}$	Specific heat capacity of zeolite, adsorbed CO_2, desorbed CO_2 gas, and mica cage [J/g-K]
ΔH	Heat of adsorption of CO_2 [kJ/mol]
σ_{SB}	Stefan-Boltzmann constant [W/m^2-T^4]
ε	Surface emissivity [1]
μ_r	Relative permeability of a material [1]
k_0	Wave number in vacuum [rad/m]
σ_e	Electrical conductivity [S/m]
ρ	Density [kg/m^3]
k	Thermal conductivity []
G	Surface irradiation [W/m^2]
n	Refractive index [1]
η	Efficiency of the vacuum pump [1]
γ	Specific heat ratio [1]

3.1 INTRODUCTION

The industrial removal of excess CO_2 from the atmosphere is deemed essential to limit the average global temperature rise within 1.5-2°C above pre-industrial levels consistent with the Paris Agreement (Gasser *et al* 2015, Rogelj *et al* 2018, Masson-Delmotte *et al* 2018). Close to 90% of the emissions pathways leading to 2°C of warming and *all* scenarios compatible with 1.5°C of warming require large-scale deployment of negative emissions technologies (NET) by the end of this century (EASAC 2018, Masson-Delmotte *et al* 2018, Intergovernmental Panel on Climate Change 2014). It is estimated that between 10 and 40 billion tonnes of CO_2 ($GtCO_2$) need to be removed annually by 2100 (Intergovernmental Panel on Climate Change 2014, Marcucci and Panos 2017), a scale comparable with the 36.8 $GtCO_2$ that we emit today (Friedlingstein *et al* 2019).

One of the industrialized NETs includes sorbent-based direct air capture (DAC), which can produce a purified stream of CO_2 from atmospheric air – or from other dilute sources – using

adsorbents that have a preferential affinity for CO_2 over other gases. The current cost of DAC, which is expected to be around $300 per tonne of CO_2 based on kilotonne scale pilot plants, needs to reduce drastically to achieve mass-scale utilization. In 2018, around 20-23 million tonnes of CO_2 recovered from diverse industrial processes were traded in a global market at about $19 per tonne which highlight the challenges in scalability and economics that DAC needs to overcome to function as NET (Parsons Brinckerhoff and Global CCS Institute 2011, Greenwood n.d.).

The high cost of DAC can be significantly attributed to the regeneration process where CO_2-rich sorbents are heated to around 100°C under vacuum. The current conduction-based heat transfer process consumes about 8-11 times more energy than the enthalpy of desorption of the capturing media, which is the theoretical minimum energy for regeneration, totaling 80% of the system energy (Wurzbacher *et al* 2016). Conduction based regeneration is somewhat slow (on the order of hours), and hence requiring oversized regeneration systems, due to non-uniform heating profiles and maximum temperature limits (around 100°C) to avoid thermal degradation. Further, capital expenditures to procure sorbents needed to operate the system can constitute 80% of the system cost of DAC (National Academies of Sciences Engineering and Medicine 2019). Current efforts to improve the regeneration process include using steam purging to either substitute or supplement conductive heat transfer (Gebald *et al* 2019, Sinha *et al* 2017).

Microwaves can also be used to induce a fast, lower-temperature mechanism that can reduce the cost and energy of the regeneration. Such benefits have been demonstrated in a number of adsorbent regeneration studies using microwave that involved a diverse set of adsorbent-adsorbate pairs with a wide range of microwave absorption capacities (Meier *et al* 2009, Turner *et al* 2000, Coss and Cha 2000, Polaert *et al* 2010, Chronopoulos *et al* 2014, Webley and Zhang 2014, Cherbański and Molga 2009, Falciglia *et al* 2018). Microwave can reduce the overall energy demand by 1) promoting gas desorption at a lower bulk temperature through selective heating near sorption sites (Vallee and Conner 2006) and 2) shortening processing time with an accelerated heating rate (Jones *et al* 2002, Falciglia *et al* 2018).

Such analysis involving CO_2 as an adsorbate is missing at present, but two studies have demonstrated the possibility of microwave-induced CO_2 desorption from sorbents (Chronopoulos *et al* 2014, Webley and Zhang 2014). Chronopoulos found that desorbing CO_2 from activated carbon can be made four times as fast as heating sorbents with a furnace. Webley showed that a

short pulse (~20s) of microwave can be used to supplement pressure swing CO_2 desorption from zeolite 13x and reduce electricity demand for pumping.

Based on these initial studies, we aim to further validate microwave-based CO_2 desorption process for DAC application regarding the 1) possibility of near-complete desorption of CO_2 from sorbents, 2) degree of processing time reduction, and 3) energy demand of the process considering system inefficiencies. We desorb CO_2 from packed zeolite 13x beads using a lab-scale apparatus that emulates setup of a typical commercial-scale microwave system. We investigate minimum-energy microwave operation to heat sorbents, considering the heating duration and temperature uniformity. CO_2 desorption rate and the total amount of the desorbed CO_2 were quantified by measuring mass changes of the sorbents and studying mass transport of the major gaseous species throughout the experiments. The bulk heating profile and uniformity of the sorbents were analyzed with an infrared (IR) thermography and a built finite element model (FEM) to study energy consumption of the process. We compare the processing time and energy demand during microwave-induced regeneration with the conduction-based reference study to assess the technical feasibility of using microwave for DAC application.

3.2 METHOD.

3.2.1 Adsorbent selection and setup

Commercial zeolite 13X beads (4-8 mesh) were supplied from Sigma-Aldrich. Zeolite 13X was selected for its relatively high CO_2 selectivity and microwave absorption. Single-component CO_2 adsorption isotherm of the zeolite beads was measured with a Micrometrics ASAP 2050 Pressure Sorption Analyzer at pressure ranges between 0.03-760 Torr and at two temperature points (25 and 90°C) (Figure S3.1). About 4 mmol/g of CO_2 is adsorbed by zeolite at standard temperature and pressure, which is close to the lower end of the 4.2-6.0 mmol/g range found by past studies (Son *et al* 2018, Morales-Ospino *et al* 2020, Wilson and Tezel 2020, Cheung *et al* 2012, Wang *et al* 2013). The lower value found in this study might be an artifact of a higher binder content of the purchased sorbent. The CO_2 adsorption capacity decreases at elevated temperatures which enable temperature-driven regeneration.

Dielectric heating is governed by the material permittivity using Equation (3.1). It is suggested that microwave is preferentially absorbed by charge-neutralizing cations (e.g. Na^+) as well as surface silanol groups of the zeolite which promote CO_2 binding (Ohgushi *et al* 2001, Turner *et al*

2000, Webley and Zhang 2014). Resultant selective heating near CO_2 binding sites could lead to an energy-efficient regeneration process. Published permittivity data of the zeolite with a low level of adsorbed water (2%) is assumed to represent the permittivity of the purchased zeolite.

$$\dot{q}_d = \frac{\omega}{2}\varepsilon_0\varepsilon_r^{"}|\vec{E}|^2 \tag{3.1}$$

3.2.2 Experimental setup and procedures of CO_2 desorption

The CO_2 desorption experiments were performed at the Plasma Science and Technology Laboratory at the University of Michigan. The system used in this investigation comprised of a single-mode (TE_{10} dominant) rectangular waveguide microwave applicator fitted with a vacuum-compatible cylindrical reaction chamber containing zeolite beads packed into a planar volume. The attached auxiliary pumping and gas injection system enables in-situ sorbent outgassing, CO_2 adsorption, and desorption (Figure 3.1). This setup is essentially a miniaturized version of a potential commercial-scale design where a larger, thin sorbent panel can be treated with microwave in a uniform fashion – either with horn antenna or with a slotted waveguide. This design shares characteristics with an industrial setup where shaped foodstuffs are conveyed into single or multi-mode microwave cavities for processing (Resurreccion *et al* 2013). A microwave at 2.45 GHz was generated with a magnetron controlled by an adjustable power supply (Richardson SM745, maximum output power 1.9kW). A three-port isolator (National Instruments, maximum power 3kW) was used to protect the magnetron from reflected power. A three-stub tuner was used to manually adjust and match the impedance of the microwave to that of the load to maximize the electromagnetic coupling of the system. The incident microwave was concentrated at the tapered portion of the rectangular waveguide (Sairem, surfaguide) where the chamber containing zeolite structure was placed through a top opening. The surfaguide was installed with two bi-directional couplers on both ends to measure incident and reflected microwave to and from sorbent as well as transmitted and re-reflected microwave power. Microwave power measurements were made with two sets of HP power meters (435B) and sensors (8481A) as well as two

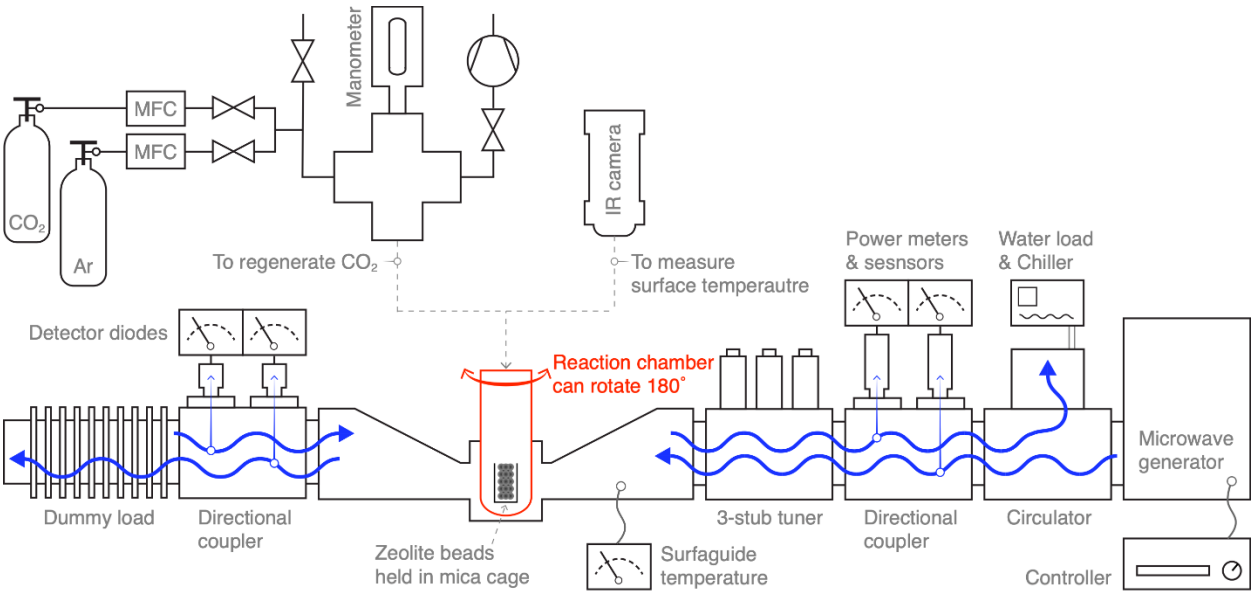

Figure 3.1. The experimental setup comprises single-mode microwave applicator, packed zeolites inside reaction chamber, and auxiliary system that controls gas flows and pressure inside the chamber. Analytical balance is not shown in this diagram.

microwave detector diodes (S-TEAM, DM211), all of which were calibrated prior to use in experiments. A custom-made reaction chamber was built from microwave-transparent Pyrex that made a vacuum seal with an auxiliary system via an o-ring and a clamp. Packed zeolite beads were configured into a packed, planar form with a perforated mica cage allowing for gas diffusion and microwave penetration. Flexible bellows used for vacuum connections permitted 180° rotation of the reaction chamber under vacuum to alternate the incidence of microwave on zeolite. Industrial grade CO_2 and argon gas was introduced at a known flow rate via mass flow controllers (MKS P4B). A dual-stage rotary vane pump (Edwards, E2 1.5) was used to create a vacuum. The pressure inside the chamber was measured with a capacitance manometer throughout the experiments (MKS Baratron 627C).

Each CO_2 desorption experiment employed approximately 5 grams of new zeolite samples and followed a three-step process of outgassing, CO_2 adsorption, and desorption. Mass changes of the sorbents between outgassing, CO_2 adsorption, and desorption steps were measured by temporarily disconnecting the chamber from the system and measuring its mass using an analytical balance (Mettler Toledo AT201). The chamber was backfilled with argon and sealed during detachments to avoid possible contamination. Mass changes between each of the steps quantify the absolute amount of CO_2 adsorbed and desorbed during the experiments.

During outgassing, zeolites were heated above 150°C with 84W of microwave under vacuum (<10 Torr) for 80-120 minutes. The outgassing was considered complete when the chamber pressure stabilized below 0.1 Torr, close to the ultimate pressure measured with the absence of sorbent. The mass of the chamber is measured once the chamber cools down to ambient level. Upon reinstallation of the chamber, pressure is lowered to 0.1 Torr and CO_2 gas is introduced using a mass flow controller (MFC). An excess amount of CO_2 is injected to fully saturate surface binding sites. CO_2 adsorption was considered complete when the pressure drop from CO_2 adsorption was overridden by air leakage, leading to a pressure rise. Complete CO_2 adsorption typically took 65-100 minutes. The mass of the chamber containing CO_2-rich sorbents was recorded. Desorption is initiated by evacuating the chamber with the vacuum pump running at full capacity. The microwave source was powered on after 30 seconds when chamber pressure was reduced to nearly 1,000 Pa, 1% of the ambient level. Total chamber pressure is recorded throughout microwave application. Desorption was deemed complete typically after 30-55 minutes of microwave input when the chamber pressure stabilized near 0.1 Torr. Upon completion, the mass of the chamber that contains regenerated sorbent was measured.

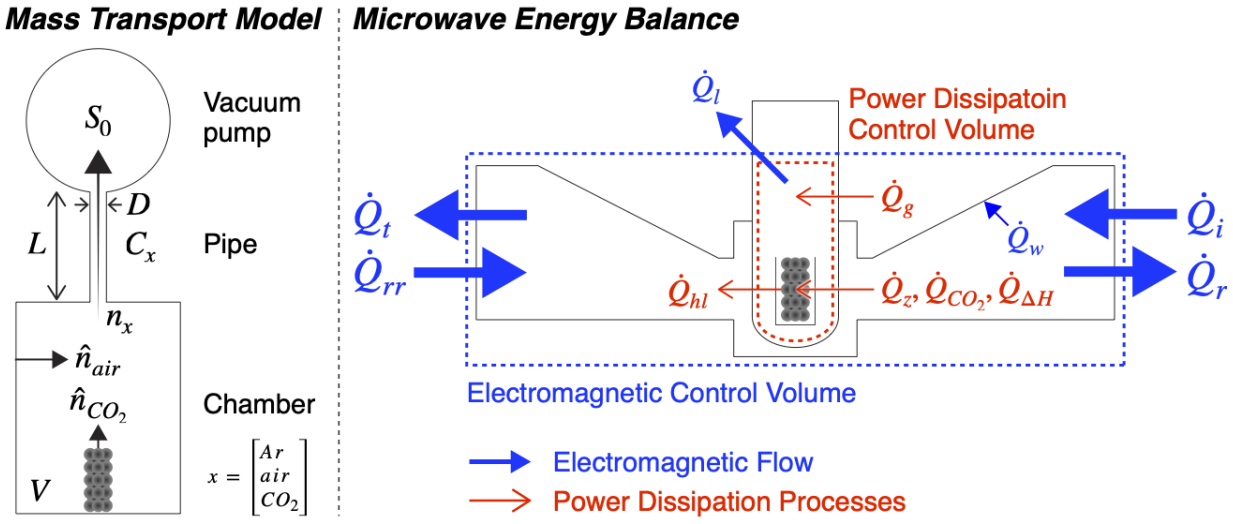

Figure 3.2. (a) Gas phase mass transport and (b) microwave power dissipation models used in this study.

3.2.3 Mass transport and energy balance of the system

During regeneration, gas transport of the desorbed CO_2 as well as residual air and argon gases can be calculated using a simplified geometry depicted in Figure 3.2a, where the zeolite-containing chamber is connected to the vacuum pump with a single pipe. The CO_2 desorption rate can be

derived from the measured total chamber pressure by considering gas-specific conductance, temperature, and leakage rate using equation (3.2)-(3.9) (Roth 2012, White 2006). Viscous and intermediate flow regimes are accounted for when calculating the conductance of the gases. The 'hat' notation denotes quantities produced inside the chamber, including the desorbed CO_2 from zeolite and the leaked-in air. Importantly, this gas transport model accounts for the *accumulation* of the desorbed CO_2 inside the chamber due to the limited pipe conductance. The gas temperature is estimated by finding the value that matches the total amount of the desorbed CO_2 from equation (3.8)-(3.9) with the mass change of the chamber before and after the desorption. The temperature of air and argon inside the chamber was assumed to be at an ambient level initially and then would equilibrate with that of CO_2 upon the onset of microwave-induced regeneration due to fast gas diffusion in the vacuum (Wurzbacher et al 2016). Further details on the gas transport model including parameters represented in Figure 3.2a and procedures to calculate desorption rate are provided in Appendix B.1.

$$\frac{dP_x}{dt} = -\frac{C_{x,i}S_0}{V\left(C_{x,i}+S_0\right)}P_x + \frac{d\hat{P}_x}{dt} \tag{3.2}$$

$$C_{x,v} = \frac{\pi}{128\eta_x}\frac{D^4}{L}\bar{P} \tag{3.3}$$

$$C_{x,m} = 3.81\sqrt{\frac{T_x}{M_x}}\frac{D^3}{L} \tag{3.4}$$

$$C_{x,i} = C_{x,m}J_x \tag{3.5}$$

$$J_x = \frac{C_{x,v}}{C_{x,m}} + \frac{1+\sqrt{\frac{M_x}{R_0T_x}}\cdot\frac{DP_{tot}}{\mu_x}}{1+1.24\sqrt{\frac{M_x}{R_0T_x}}\cdot\frac{DP_{tot}}{\mu_x}} \tag{3.6}$$

$$\mu_x = \mu_{0,x}\frac{T_{0,x}+c_x}{T_x+c_x}\left(\frac{T_x}{T_{0,x}}\right)^{\frac{3}{2}} \tag{3.7}$$

$$\frac{d\hat{P}_{CO_2}}{dt} = \frac{dP_{CO_2}}{dt} + \frac{C_{CO_2}S_0}{V(C_{CO_2}+S_0)}P_{CO_2} \tag{3.8}$$

$$n_x = \frac{P_xV}{R_0T_x} \tag{3.9}$$

Microwave power dissipated during CO_2 desorption (3.10) was estimated by aggregating power used to heat materials and overcome the enthalpy barrier, and power lost through heat

transfer (equation (3.12)-(3.16)). Figure 3.2b illustrates the system boundary and power dissipation terms included in the power analysis. The gas desorption rate and temperature derived from the gas transport analysis were used. The heating rate of the materials and heat lost via conduction and radiation were estimated using a combination of surrogate surface temperature measurement with an IR thermometer (FLIR A325) and a 3-D finite element model (FEM) based on COMSOL software packages. The FEM calculates dielectric heating of packed sorbents and associated heat transfer under vacuum using a simplified geometry involving zeolites, mica cage, reaction chamber, and Surfaguide. Finally, the leaked power ($\dot{Q}$) is calculated by comparing (3.10) and (3.11) which balance microwaves inside and outside of the system boundary. Further details on the FEM are available in Appendix B.2.

$$\dot{Q}_d = \dot{Q}_z + \dot{Q}_{CO_2} + \dot{Q}_{\Delta H} + \dot{Q}_g + \dot{Q}_{hl} \tag{3.10}$$

$$\dot{Q}_d = \dot{Q}_i - \dot{Q}_r - \dot{Q}_t + \dot{Q}_{rr} - \dot{Q}_l - \dot{Q}_{wg} \tag{3.11}$$

$$\dot{Q}_z = m_z C_{p,z} \frac{dT_z}{dt} \tag{3.12}$$

$$\dot{Q}_{CO_2} = m_a C_{p,a} \frac{dT_a}{dt} \tag{3.13}$$

$$\dot{Q}_{\Delta H} = \dot{m}_g \Delta H \tag{3.14}$$

$$\dot{Q}_g = \dot{m}_g C_{p,g} \Delta T_g \tag{3.15}$$

$$\dot{Q}_{hl} = m_m C_{p,m} \frac{dT_m}{dt} + \varepsilon \sigma_{SB} A (T_2^4 - T_1^4) \tag{3.16}$$

$$\dot{Q}_{wg} = m_w C_{p,w} \frac{dT_w}{dt} \tag{3.17}$$

3.3 Results and Discussion

3.3.1 Regeneration duration and energy consumption with microwaves

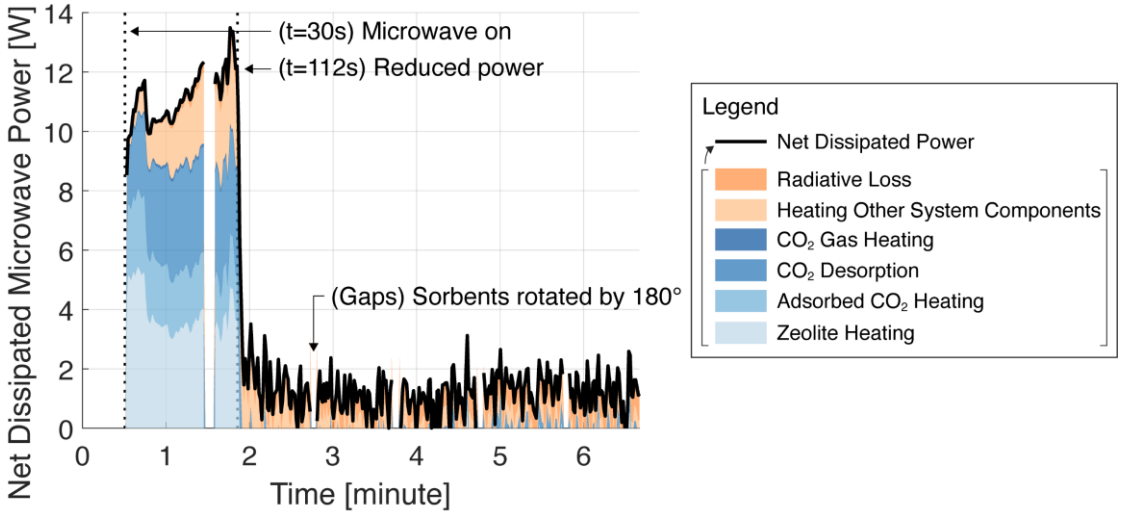

Figure 3.3. Net microwave power dissipated through different energy processes, including heating materials, desorbing CO_2, heat lost to the environment, and leaked power. Effective processing power indicates microwave power used to induce CO_2 desorption, including heat loss terms.

The CO_2 desorption experiment was carried out with 5g of zeolite beads packed in a 1cm-thick mica cage following the 3-step process described in the methods. Microwave power was dynamically changed from 216W to 55W while alternating its incidence direction approximately every minute. This process successfully heated zeolites to about 135°C in just over a minute and maintained the temperature throughout the experiment (see Appendix B.2.3-B.2.4 for details).

The power analysis reveals that only about 5% of the incident microwave power was dissipated to induce CO_2 desorption and associated heat transfer processes. The 95% of the power did not contribute to sorbent regeneration due to the 1) impedance mismatching that caused nearly 37% and 27% of the microwaves to be reflected from and transmitted through zeolites respectively, and 2) inefficient shielding that leaked 31% of the power to the environment. This significant system inefficiency can be improved with a combination of appropriate applicator design and sorbent setup. For instance, microwave application efficiency of commercial/industrial microwave processors typically exceeds 90%. But improving the system efficiency is not further investigated in this work. Instead, this analysis focuses on the expected energy demand of the microwave-based desorption process when system efficiency is improved. This is done by estimating the dissipated

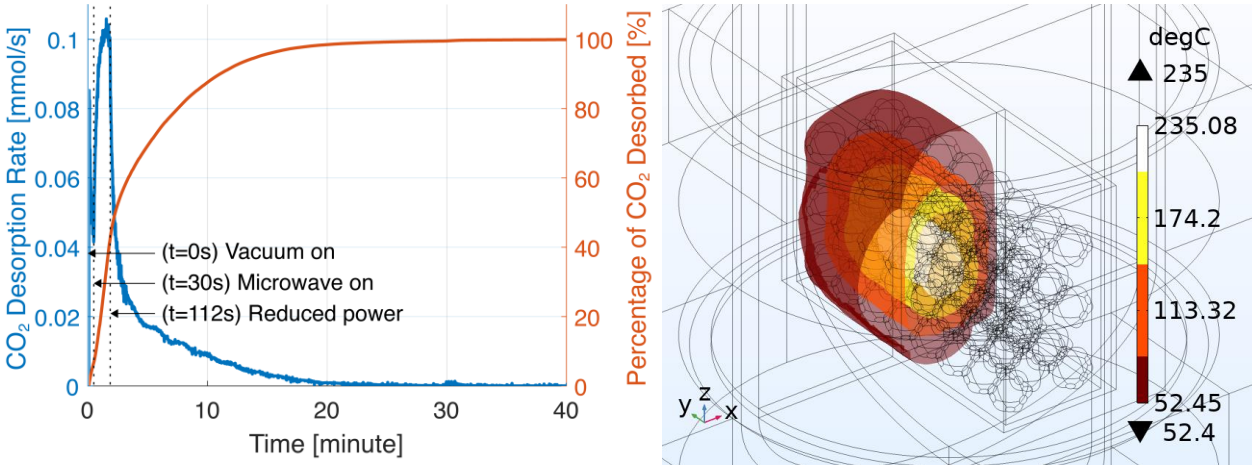

Figure 3.4. (a) Calculated molar percentage of CO_2, air, and argon gas during microwave application, (b) simulated isothermal contour of the packed sorbent structure after a minute of microwave input

power when desorbing CO_2 by aggregating primary energy processes (equation (3.10)-(3.17)) outlined in the method section.

As a result, we conclude that about 11W and 1.5W of microwave power is dissipated by the system to desorb CO_2 during and after the rapid heating as shown in Figure 3.3. During rapid heating, majority of the dissipated microwave energy was used to heat zeolite (35%), heat adsorbed CO_2 (18%), and desorb CO_2 (29%). Heat lost to the adjacent environment through conductive and radiative transfer increases over time as the zeolites are heated with microwaves. Once the microwave power is reduced after rapid heating, the temperature of the zeolites remains at a relatively constant level; the dissipated microwave power is primarily used to compensate for the energy lost through conduction and radiation while desorbing the rest of the CO_2. Radiative heat loss becomes a predominant power dissipation process after a few minutes of microwave application.

The mass change of the packed zeolites before and after microwave application indicates 4.1 mmol/g of cyclic capacity which is consistent with the separate CO_2 adsorption estimation made with ASAP 2050, confirming near-complete adsorption and desorption of CO_2 during the experiment. The aggregate quantity of the desorbed CO_2 calculated with the mass transport model (Figure 3.4a) matches this value, considering elevated temperature – estimated to be between 45-55°C – of the exiting gas due to the thermal regeneration process. The estimated temperature of the effluent gas using the mass transport model is in good agreement with the measurement made by Webley (Webley and Zhang 2014), where the temperature of the exiting CO_2 upon microwave-induced regeneration inside a multi-mode cavity was found to be elevated by 40°C.

The lower temperature of the desorbed CO_2 gas (45-55°C) compared to the sorbent surface (>100°C) suggests that microwaves induce low-temperature desorption driven by a selective heating process, which is inherently more energy-efficient than conventional bulk heating-based desorption. This observation is consistent with past findings where microwaves selectively heated adsorbate-adsorbent binding sites instead of bulk material (Meier *et al* 2009, Turner *et al* 2000, Coss and Cha 2000, Polaert *et al* 2010, Chronopoulos *et al* 2014, Webley and Zhang 2014, Cherbański and Molga 2009, Falciglia *et al* 2018). While confirming this selective process is outside of the scope of this study, our findings warrant further investigations into this energy-efficient CO_2 desorption process induced by microwave energy.

The application of microwave energy accelerates CO_2 desorption as illustrated in Figure 3.4a, which shows a dominant portion of the adsorbed CO_2 is desorbed within a few minutes. Approximately 42% of the adsorbed CO_2 is desorbed in 82 seconds using 11W of average microwave power. Heating analysis with FEM suggests that most of the desorbed CO_2 originates from the hot interior core, whose peak temperature reached above 200°C (Figure 3.4b). Desorbing the rest of the CO_2 takes a progressively longer time and hence increases the overall energy consumption. Compared to 42% of the adsorbed CO_2 desorbed in 82 seconds, desorbing 80% and 99% of the adsorbed CO_2 requires total of 450 and 1,380 seconds of microwave input, respectively. Heating analysis suggests that this is due to the slower desorption kinetics near the outer edge of the sorbent structure where the temperature is lower (<100°C) as shown in Figure 3.4b. This trend is also confirmed with the IR measurements.

The elongated processing time caused by non-uniform heating can significantly impact the overall energy demand and purity of the recovered CO_2. Considering 4.1 mmol/g of the cyclic working capacity of zeolite, close to 2.4 GJ/tCO_2 of energy is used to desorb 42% of the CO_2 in the initial rapid heating phase. However, desorbing 99% of the CO_2 can require nearly 4 GJ/tCO_2 due a longer microwave application requirement. At the same time, the lengthened processing time negatively impacts the purity of the recovered CO_2 due to air leaked into the system during regeneration. The leaked-in air diluted and limited the purity of the recovered CO_2 under 90% (Figure B.4). The CO_2 purity continuously decreased with prolonged treatment. Since some level of leakage is unavoidable in any vacuum system, expedited regeneration through a more uniform heating can help minimize dilution and the overall energy demand of the regeneration process.

The shortened regeneration time could result in a systems-level cost savings through system-downsizing. It is anticipated that 80% of the system cost of the future, industrial-scale DAC would be spent to procure sorbents throughout system lifetime (National Academies of Sciences Engineering and Medicine 2019). Therefore, for instance, a 50% reduction in regeneration duration of an example DAC plant that operates on one hour of CO_2 adsorption followed by one hour of regeneration can increase its throughput by 33%. This can lead to 26% of the system-wise cost savings by requiring 33% less sorbents when other cost parameters are little changed. Reducing regeneration duration down to 10 minutes, from 60 minutes, could lead to a 57% cost reduction of a DAC plant. Ultimately, fully utilizing such benefits would require process optimization that considers cost and operational constraints. However, this simplified example highlights that further system-wide studies of microwave regeneration are warranted.

3.3.2 Comparison of microwave-based regeneration with conduction-based system

The microwave energy demand estimated in this study can be compared to the past sorbent and DAC literatures considering 1) different levels of sorbent working capacity and 2) disparate enthalpy of desorption of the sorbent materials. First, microwave energy demand at lower working capacities can be estimated by linearly scaling energy used to cause regeneration – including adsorbed CO_2 heating, enthalpy of desorption, and heating desorbed CO_2 gas – as well as the mass of the desorbed CO_2 using a ratio of the new capacity and 4.1 mmol/g. This linear approximation is supported by relatively consistent adsorption energy distribution of zeolite over a range of CO_2 loading. Gaseous species adsorb on zeolite surface by forming a monolayer (Son *et al* 2018); multi-layer adsorption that can show disparate heat of adsorption at higher loadings is prohibited. Also, while the heat of adsorption is expected to generally increase with decreasing CO_2 loading, the deviation remains relatively small except for at extremely low CO_2 loadings. The heat of adsorption of the zeolite employed in this study was found to be stable at around 35 kJ/mol at 40-60% of the maximum loading at standard temperature and pressure (Reynolds 2019). The heat of adsorption is found to be elevated to about 37 kJ/mol at 20% of the maximum loading. Thus, reasonable estimations can be made with linear approximation.

The processing duration and energy demand of the microwave-induced CO_2 desorption can be compared to a reference conduction-based temperature-vacuum swing system. Wurzbacher estimated that CO_2 recovery from amine-functionalized sorbents by supplying heat under vacuum

via conduction needed 11.2-14.5 GJ/tCO_2 of thermal energy over the duration of two hours with 0.32-0.65 mmol/g of CO_2 working capacity (Wurzbacher *et al* 2012). Compared to the heat of desorption of the sorbent, approximately 8.2-10.7 more energy was needed to desorb CO_2. Using microwaves, desorbing 99% of the adsorbed CO_2 from zeolite took 22.7 minutes while requiring 17 GJ/tCO_2 of energy based on linearly extrapolating the calculated energy data at 0.5 mmol/g of working capacity. Close to 20 times more energy was needed to desorb CO_2 using microwaves compared to the heat of CO_2 desorption (38 kJ/mol) at this reduced working capacity. This suggests that microwave-based regeneration could significantly shorten the processing time by four-fold compared to the conventional conduction-based system but at a higher energy consumption. The higher estimated energy demand is believed to have been caused by an overheating of zeolite to beyond 200°C while a moderate temperature below 150°C is sufficient to induce CO_2 desorption (Morales-Ospino *et al* 2020).

A supplementary experiment was carried out where the peak top surface temperature is maintained at close to 120°C, instead of 150°C to test if the energy demand can be lowered. The processing time to desorb 99% of the adsorbed CO_2 took 30.8 minutes while energy demand was reduced to 8.4 GJ/tCO_2 or 9.7 times the heat of desorption. Regeneration duration was 26% of the conduction reference while expending a lower amount of energy. Past studies have demonstrated CO_2 desorption from zeolite at temperatures as low as 60°C albeit at slower kinetics through conduction-based heating (Wilson and Tezel 2020, Morales-Ospino *et al* 2020). The low temperature of the desorbed CO_2 gas (45-55°C) observed in this study further supports the hypothesis that microwaves can be used to induce CO_2 desorption at even lower temperature. Thus, further energy reduction is anticipated when microwaves are used to heat zeolite to 100°C or lower, and such regions warrant future investigation to reduce system cycle time and energy consumption in balance.

3.4 Summary and Conclusions

In this study, we experimentally demonstrated that rapid, near-complete desorption of the adsorbed CO_2 is possible with microwaves. Approximately 5g of packed zeolite 13x sorbents were heated above 135°C in about a minute of microwave application under vacuum (<10 Torr). A mass transport model suggested that about 40% of the adsorbed CO_2 was desorbed in this short period. Desorbing the rest of the CO_2 required a progressively longer time due to the lower temperature

increase at the outer edge of the packed structure. Overall, desorbing 99% of the adsorbed CO_2 took between 22 and 30 minutes, a significant improvement from over an hour required by the conventional conduction-based regeneration. Our results suggest that the regeneration duration can be further reduced to a matter of minutes by improving heating uniformity. The shortened regeneration duration, in turn, increases system throughput which can promote system downsizing that can significantly improve the economics of the CO_2 recovery system. We estimated the possible range of energy demand when the observed system inefficiencies of the current apparatus were improved. Our results suggest that microwave-based CO_2 desorption could require a similar level of energy to the conventional conduction-based regeneration when sorbent overheating can be minimized. A sensitivity test shows that concurrent reduction of processing time and energy demand with microwaves is possible if the system inefficiencies can be minimized. Our results also highlight the importance of inducing uniform heating and avoiding overheating of the sorbents; the development of such a microwave-based system would enable reducing both energy demand and cost of the DAC system without relying on novel sorbent materials. Based on these results, additional research around alternative means of CO_2 desorption, such as using microwaves, is warranted to better understand, and hopefully accelerate, the development of mass-scale carbon-based infrastructure.

REFERENCES

Cherbański R and Molga E 2009 Intensification of desorption processes by use of microwaves-An overview of possible applications and industrial perspectives *Chem. Eng. Process. Process Intensif.* **48** 48–58

Cheung O, Liu Q, Bacsik Z and Hedin N 2012 Silicoaluminophosphates as CO_2 sorbents *Microporous Mesoporous Mater.* **156** 90–6 Online: http://dx.doi.org/10.1016/j.micromeso.2012.02.003

Chronopoulos T, Fernandez-Diez Y, Maroto-Valer M M, Ocone R and Reay D A 2014 CO_2 desorption via microwave heating for post-combustion carbon capture *Microporous Mesoporous Mater.* **197** 288–90 Online: http://dx.doi.org/10.1016/j.micromeso.2014.06.032

Coss P M and Cha C Y 2000 Microwave regeneration of activated carbon used for removal of solvents from vented air *J. Air Waste Manag. Assoc.* **50** 529–35

EASAC 2018 *Negative emission technologies: What role in meeting Paris Agreement targets?* Online: https://easac.eu/fileadmin/PDF_s/reports_statements/Negative_Carbon/EASAC_Report_on_Negative_Emission_Technologies.pdf

Falciglia P P, Roccaro P, Bonanno L, De Guidi G, Vagliasindi F G A and Romano S 2018 A review on the microwave heating as a sustainable technique for environmental remediation/detoxification applications *Renew. Sustain. Energy Rev.* **95** 147–70 Online: https://doi.org/10.1016/j.rser.2018.07.031

Friedlingstein P, Jones M W, O'Sullivan M, Andrew R M, Hauck J, Peters G P, Peters W, Pongratz J, Sitch S, Le Quéré C, Bakker D C E, Canadell J G, Ciais P, Jackson R B, Anthoni P, Barbero L, Bastos A, Bastrikov V, Becker M, Bopp L, Buitenhuis E, Chandra N, Chevallier F, Chini L P, Currie K I, Feely R A, Gehlen M, Gilfillan D, Gkritzalis T, Goll D S, Gruber N, Gutekunst S, Harris I, Haverd V, Houghton R A, Hurtt G, Ilyina T, Jain A K, Joetzjer E, Kaplan J O, Kato E, Klein Goldewijk K, Korsbakken J I, Landschützer P, Lauvset S K, Lefèvre N, Lenton A, Lienert S, Lombardozzi D, Marland G, McGuire P C, Melton J R, Metzl N, Munro D R, Nabel J E M S, Nakaoka S-I, Neill C, Omar A M, Ono T, Peregon A, Pierrot D, Poulter B, Rehder G, Resplandy L, Robertson E, Rödenbeck C, Séférian R, Schwinger J, Smith N, Tans P P, Tian H, Tilbrook B, Tubiello F N, van der Werf G R, Wiltshire A J and Zaehle S 2019 Global Carbon Budget 2019 *Earth Syst. Sci. Data* **11** 1783–838 Online: https://essd.copernicus.org/articles/11/1783/2019/

Gasser T, Guivarch C, Tachiiri K, Jones C D and Ciais P 2015 Negative emissions physically needed to keep global warming below 2 °C *Nat. Commun.* **6** 7958 Online: http://www.nature.com/doifinder/10.1038/ncomms8958

Gebald C, Repond N and Wurzbacher A 2019 Steam assisted vacuum desorption process for carbon dioxide capture

Greenwood A Market outlook: Europe CO_2 shortage highlights critical uses Online: https://www.icis.com/explore/resources/news/2018/07/19/10243175/market-outlook-europe-CO_2-shortage-highlights-critical-uses/

Intergovernmental Panel on Climate Change 2014 *Climate Change 2014: Synthesis Report. Contribution of Working Groups I, II and III to the Fifth Assessment Report of the Intergovernmental Panel on Climate Change* (Geneva)

Jones D A, Lelyveld T P, Mavrofidis S D, Kingman S W and Miles N J 2002 Microwave heating applications in environmental engineering - A review *Resour. Conserv. Recycl.* **34** 75–90

Marcucci A and Panos E 2017 The road to achieving the long-term Paris targets : energy transition and the role of direct air capture 181–93

Masson-Delmotte V, Zhai P, Pörtner H-O H-O, Roberts D, Skea J, Shukla P R P R, Pirani A, Moufouma-Okia W, Péan C, Pidcock R, Connors S, Matthews J B R B R, Chen Y, Zhou X, Gomis M I M I, Lonnoy E, Maycock T, Tignor M and Waterfield T 2018 *IPCC, 2018: Summary for Policymakers. In: Global Warming of 1.5°C. An IPCC Special Report on the impacts of global warming of 1.5°C above pre-industrial levels and related global greenhouse gas emission pathways, in the context of strengthening the global* (Geneva) Online: https://www.ipcc.ch/site/assets/uploads/sites/2/2018/07/SR15_SPM_version_stand_alone_LR.pdf

Meier M, Turner M, Vallee S, Conner W C, Lee K H and Yngvesson K S 2009 Microwave regeneration of zeolites in a 1 meter colum *AIChE J.* **55** 1906–13

Morales-Ospino R, Santiago R G, Siqueira R M, de Azevedo D C S and Bastos-Neto M 2020 Assessment of CO_2 desorption from 13X zeolite for a prospective TSA process *Adsorption* **26** 813–24 Online: https://doi.org/10.1007/s10450-019-00192-5

National Academies of Sciences Engineering and Medicine 2019 *Negative Emissions Technologies and Reliable Sequestration* (Washington, D.C.: National Academies Press) Online: https://www.nap.edu/catalog/25259

Ohgushi T, Komarneni S and Bhalla A S 2001 Mechanism of microwave heating of zeolite A *J. Porous Mater.* **8** 23–35

Parsons Brinckerhoff and Global CCS Institute 2011 *Accelerating the update of CCS: Industrial Use of Captured Carbon Dioxide* Online: https://www.globalccsinstitute.com/archive/hub/publications/14026/accelerating-uptake-ccs-industrial-use-captured-carbon-dioxide.pdf

Polaert I, Estel L, Huyghe R and Thomas M 2010 Adsorbents regeneration under microwave irradiation for dehydration and volatile organic compounds gas treatment *Chem. Eng. J.* **162** 941–8 Online: http://dx.doi.org/10.1016/j.cej.2010.06.047

Resurreccion F P, Tang J, Pedrow P, Cavalieri R, Liu F and Tang Z 2013 Development of a computer simulation model for processing food in a microwave assisted thermal sterilization (MATS) system *J. Food Eng.* **118** 406–16 Online: http://dx.doi.org/10.1016/j.jfoodeng.2013.04.021

Reynolds C 2019 *Decarbonizing Freight Transport: Mobile Carbon Capture from Heavy-Duty Vehicles* Online: http://hdl.handle.net/2027.42/151521

Rogelj J, Popp A, Calvin K V., Luderer G, Emmerling J, Gernaat D, Fujimori S, Strefler J, Hasegawa T, Marangoni G, Krey V, Kriegler E, Riahi K, van Vuuren D P, Doelman J, Drouet L, Edmonds J, Fricko O, Harmsen M, Havlík P, Humpenöder F, Stehfest E and Tavoni M 2018 Scenarios towards limiting global mean temperature increase below 1.5 °C *Nat. Clim. Chang.*

Roth A 2012 *Vacuum Technology* (North Holland)

Sinha A, Darunte L A, Jones C W, Realff M J and Kawajiri Y 2017 Systems Design and Economic Analysis of Direct Air Capture of CO_2 through Temperature Vacuum Swing Adsorption Using MIL-101(Cr)-PEI-800 and mmen-Mg2(dobpdc) MOF Adsorbents *Ind. Eng. Chem. Res.* **56** 750–64 Online: http://pubs.acs.org/doi/abs/10.1021/acs.iecr.6b03887

Son K N, Cmarik G E, Knox J C, Weibel J A and Garimella S V. 2018 Measurement and Prediction of the Heat of Adsorption and Equilibrium Concentration of CO_2 on Zeolite 13X *J. Chem. Eng. Data* **63** 1663–74 Online: https://pubs.acs.org/doi/10.1021/acs.jced.8b00019

Turner M D, Laurence R L, Conner W C and Yngvesson K S 2000 Microwave radiation's influence on sorption and competitive sorption in zeolites *AIChE J.* **46** 758–68

Vallee S J and Conner W C 2006 Microwaves and Sorption on Oxides: A Surface Temperature Investigation *J. Phys. Chem. B* **110** 15459–70 Online: https://pubs.acs.org/doi/10.1021/jp061679h

Wang L, Yang Y, Shen W, Kong X, Li P, Yu J and Rodrigues A E 2013 CO_2 capture from flue gas in an existing coal-fired power plant by two successive pilot-scale VPSA units *Ind. Eng. Chem. Res.* **52** 7947–55

Webley P A and Zhang J 2014 Microwave assisted vacuum regeneration for CO_2 capture from wet flue gas *Adsorption* **20** 201–10

White F 2006 *Viscous Fluid Flow* (McGraw-Hill)

Wilson S M W and Tezel F H 2020 Direct Dry Air Capture of CO_2 Using VTSA with Faujasite Zeolites *Ind. Eng. Chem. Res.* **59** 8783–94

Wurzbacher J A, Gebald C, Brunner S and Steinfeld A 2016 Heat and mass transfer of temperature–vacuum swing desorption for CO_2 capture from air *Chem. Eng. J.* **283** 1329–38 Online: http://dx.doi.org/10.1016/j.cej.2015.08.035

Wurzbacher J A, Gebald C, Piatkowski N and Steinfeld A 2012 Concurrent Separation of CO_2 and H 2 O from Air by a Temperature-Vacuum Swing Adsorption/Desorption Cycle *Environ. Sci. Technol.* **46** 9191–8 Online: https://pubs.acs.org/doi/10.1021/es301953k

CHAPTER 4

Mitigating CO_2 Emissions of Concrete Manufacturing through CO_2-Enabled Binder Reduction

Reprinted from: Lim T, Ellis B R and Skerlos S J 2019 Mitigating CO_2 emissions of concrete manufacturing through CO_2-enabled binder reduction *Environ. Res. Lett.* **14** 114014 Online: http://iopscience.iop.org/article/10.1088/1748-9326/ab466e

4.1 INTRODUCTION

A recent report from the Intergovernmental Panel on Climate Change regarding climate-related impacts of global warming of 1.5ºC above pre-industrial levels, found that global CO_2 emissions need to drop below zero starting mid-century (Masson-Delmotte *et al* 2018). The concrete industry is one of the major obstacles to achieving a net negative economy; with a current CO_2 reduction target limited to only reaching 25% below current levels by 2050 (International Energy Agency 2018). Today, global annual concrete consumption stands at 10 billion m^3, or 25 billion tonnes, which makes it the most utilized engineered material around the world (Miller *et al* 2016, Petek Gursel *et al* 2014). Despite the need to reduce global CO_2 emissions, concrete consumption is expected to increase by 12-23% by 2050 compared to 2014 (International Energy Agency 2018).

Reducing CO_2 emissions from concrete is challenged by the CO_2 emitted during the production of Ordinary Portland Cement (OPC), a main binder of concrete. Cement production alone represents about 85% of the CO_2 emissions from concrete manufacturing (Miller *et al* 2016) and contributes around 7% of global CO_2 emissions (International Energy Agency 2018, Andrew 2018) today. Approximately 60-70% of this CO_2 is generated during limestone decomposition, also known as the calcination process, and thus cannot be mitigated by transitioning to a low-carbon energy supply chain. Therefore, efforts to curb CO_2 emissions from concrete fabrication have focused on substituting clinker-rich OPC with supplementary cementitious materials (SCMs), which are usually repurposed industrial byproducts providing similar mechanical

properties to OPC. There is widespread agreement in the literature that incorporation of SCM offers one of the largest CO_2 mitigation opportunities until other options, such as carbon capture and sequestration (CCS) or alternative binders, become commercially viable (International Energy Agency 2018, Cement Sustainability Initiative and European Cement Research Academy 2017, World Business Council for Sustainable Development 2015, Neuhoff *et al* 2014, Müller and Harnisch 2008, Mineral Products Association 2013, CEMBUREAU 2013, Miller *et al* 2016, Benhelal *et al* 2013, Schneider *et al* 2011, International Energy Agency 2017, Scrivener 2016). However, expanded use of SCM is unlikely to meet long-term CO_2 reduction goals in the concrete industry. The most common SCMs include fly ash (FA) and granulated ground blast furnace slag (GGBS), which are already being utilized near to their maximum potentials (Miller 2018). In the U.S., the utilization of GGBS has been supply-limited for decades (U.S. Geological Survey 2018, Miller 2018). The utilization rate of FA in U.S. concrete reached 64% in 2017 and can potentially increase in the short-term due to growing demand and regulations that require reclamation of land-filled FA (American Coal Ash Association 2018). However, its long-term growth potential is in question due to reductions in coal-combustion electricity production (International Energy Agency 2018, Damineli and John 2012, Gursel *et al* 2016, Miller 2018) and the high demand of FA coming from numerous applications, including soil amendment and structural fill (Yao *et al* 2015). The nonhomogeneous quality of FA that depends on a number of factors including the parent coal, plant operations, and post-combustion processes can further limit its use as a SCM.

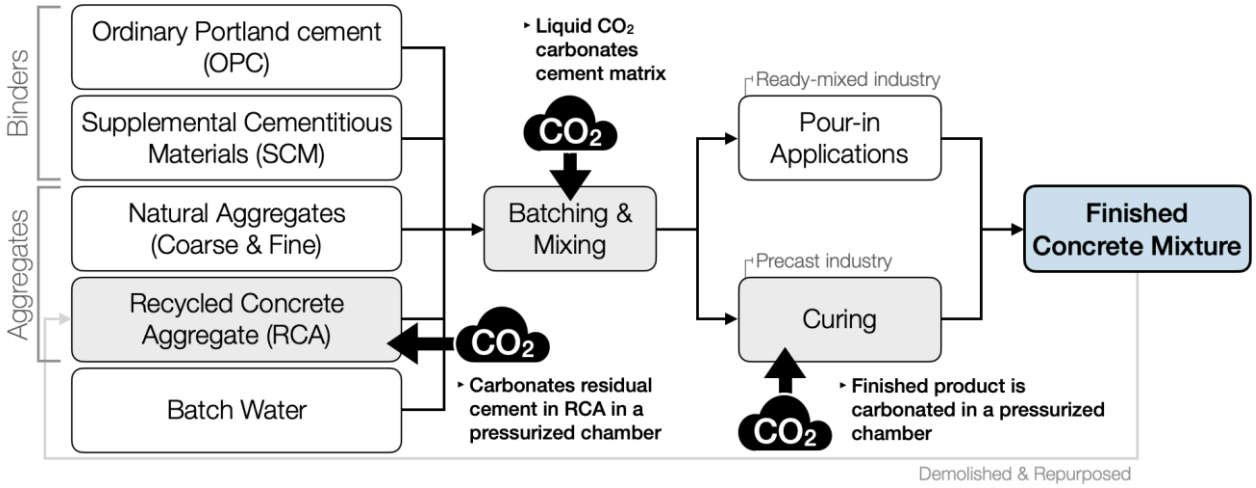

Figure 4.1. Flow diagram of concrete mixture formulation. CO_2 can be utilized and permanently sequestered in RCA, during batching & mixing, or during the curing process. Chemical admixtures typically comprise less than 1% of the total mass of concrete and thus are excluded from this study (see Appendix C.1).

Expected supply limitations of FA and GGBS in the near future are encouraging researchers to explore additional options; other minerals and waste materials can be used as SCM (Siddique and Naik 2004, Jani and Hogland 2014, Aprianti *et al* 2015, Batayneh *et al* 2007, Van der Zee and Zeman 2016, Ramezanianpour *et al* 2009, Tennis *et al* 2011); optimized low-clinker system can be used as a binder (Scrivener *et al* 2018); clinker-free geopolymer can replace OPC (Duxson *et al* 2007); self-healing concrete can mitigate CO_2 emissions from repair events (Tittelboom and Belie 2013, Li and Herbert 2012); and ductile engineered composites can reduce lifecycle CO_2 emission with an extended service life (Keoleian *et al* 2005, Lepech *et al* 2008). Another area of active research includes so-called "CO_2 utilization" in concrete where concrete is formulated with added CO_2 either in its constituents before casting, during batching and mixing, or in finished products. Three main CO_2 utilization strategies in concrete formulation can be found in the literature as shown in Figure 4.1, including carbonation curing (Rostami *et al* 2012, Shi *et al* 2016, Zhang *et al* 2016), carbonation during mixing (Monkman and MacDonald 2016, 2017, Monkman *et al* 2015, 2016), and carbonation with recycled concrete aggregate (RCA) (Xuan *et al* 2016). Thus far, the majority of studies on CO_2 utilization in concrete exclusively explored mitigation opportunities through sequestration using carbonation curing (Cement Sustainability Initiative and European Cement Research Academy 2017, FERNANDEZ BERTOS *et al* 2004, Ghoshal and Zeman 2010, Hasanbeigi *et al* 2012, Parsons Brinckerhoff and Global CCS Institute 2011, Jang *et al* 2016). By implementing this strategy worldwide, it is estimated that about 30-300 million tonnes (Mt) of CO_2 could be sequestered globally in the future (Parsons Brinckerhoff and Global CCS Institute 2011), which is close to 1-10% of CO_2 emitted from manufacturing cement (Andrew 2018).

A review of the literature indicates that most of the state-of-the-art research on CO_2 utilization has failed to consider the systems-level design optimization of concrete mixtures achievable with embodied CO_2. When CO_2 is introduced to freshly cast concrete or into its constituents prior to casting, the introduced CO_2 either becomes part of the binding matrix or improves the mechanical properties of the constituents, resulting in increased overall concrete strength. Hence the same level of compressive strength can be achieved with a lower amount of binder, resulting in a significant decrease of CO_2 emissions. Indeed, the effectiveness of this strategy was shown in a recent case study when CO_2 was added during mixing, where the overall scale of CO_2 mitigation

was magnified by 35 times compared to sequestration alone (Monkman and MacDonald 2017). In this work, we conduct a more comprehensive assessment of this strategy.

CO_2 utilization alone may not be an economical option for reducing CO_2 emissions in concrete compared to other alternatives, even when it is financially supported by tax credits such as 45Q that reward sequestered CO_2. However, the saved material cost associated with reduced binder could help promote CO_2 utilization in a cost-competitive manner. For instance, the cost of abating one tonne of CO_2 emissions through diverse management and technological interventions, including on-site CCS in cement plants, has been estimated to cost between $5-$450 (Kajaste and Hurme 2016). However, offsetting one tonne of CO_2 by implementing carbonation curing could incur additional costs between $350-$750 (National Energy Technology Laboratory 2013). Given that the cost of manufacturing binders, especially OPC, constitutes over half of the total cost of concrete mixtures, the additional cost incurred by CO_2 utilization can potentially be mitigated if there is concomitant reduction in the use of binder materials. In this case, the concrete formulated with added CO_2 and reduced binder loading could be cost-competitive with conventional concrete.

In this study we assess the potential scale of net CO_2 reduction and net cost savings achievable by employing the combined strategy of reducing binder and utilizing CO_2 in concrete formulations. This study is conducted at the national level, utilizing a set of concrete mixtures that represents the diversity of formulations used in the U.S. Compressive strength measured at 28 days are used as a primary technical criterion for all mixtures. We evaluate three CO_2 utilization strategies – including carbonation curing, carbonation during mixing, and addition of carbonated RCA – by employing each of them in combination with reduced binder at a time. We examine the overall CO_2 reduction potential of the combined strategy against direct CO_2 sequestration as a result of utilizing CO_2 alone. The financial incentive of reducing binder loading is compared with the tax incentive associated with the 45Q tax credit as amended in the FUTURE Act bill.

4.2 METHODS

Our national CO_2 footprint and material cost assessments of concrete manufacturing in the U.S. are conducted at a mixture level, using a set of mixtures that collectively represents the industry. Figure 4.2 summarizes the derivation process of a CO_2-amended mixture from a conventional mixture and how the collection of mixtures is used to emulate the U.S. concrete industry. Here, concrete mixtures are plotted in terms of compressive strength and binder intensity,

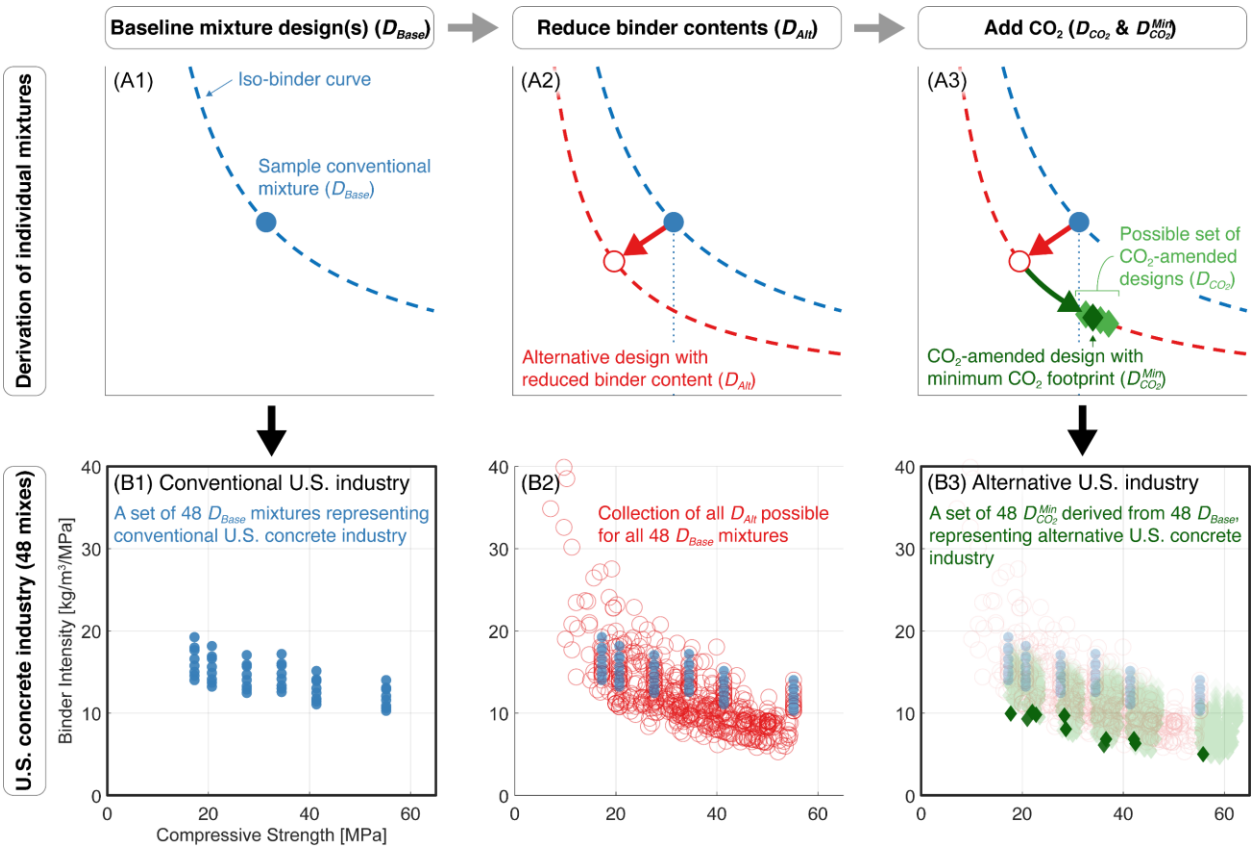

Figure 4.2. Derivation of CO_2-amended mixture designs ($D_{CO_2}^{Min}$) from conventional designs (D_{Base}). The conventional U.S. concrete industry is represented by a set of 48 D_{Base} mixtures, while the alternative U.S. concrete industry that utilizes CO_2 at its full capacity is emulated by a set of 48 $D_{CO_2}^{Min}$ mixtures. Three such alternative U.S. industry are produced by applying one of the CO_2 utilization strategies at a time.

which is defined by normalizing total binder content in a mixture with its compressive strength as shown below. In this study, binders may include OPC, FA, GGBS, silica fume, metakaolin, and natural pozzolans that contain volcanic ash and shale ash. Limestone may also be used to substitute binders as a filler.

$$binder\ intensity = \frac{total\ binder\ [kg/m^3]}{compressive\ strength\ [MPa]}$$

To start, we use a cohort of 48 baseline mixture designs (D_{Base}) to represent the diversity of mixtures currently employed in the U.S. This cohort of 48 D_{Base} designs are based on benchmark mixtures reported by the National Ready-Mixed Concrete Association (NRMCA) (National Ready Mixed Concrete Association 2016) and are displayed in Figure 4.2 (B1). The 48 D_{Base} mixtures, each weighted with its national production volume (National Ready Mixed Concrete Association 2016, Van Oss 2018), closely emulate the conventional U.S. concrete industry as shown in Table 4.1. For each of these D_{Base} mixtures, we formulate a set of alternative designs (D_{Alt}) that have

lower binder content and reduced compressive strength than the original D_{Base}. This is done by finding such mixtures from a list of 696 validated concrete mixtures compiled from 32 published reports and papers (details are available in Appendix C.12). Figure 4.2 (A2) shows an example of a possible D_{Alt}. Since each D_{Alt} has lost a fraction of its compressive strength relative to its original D_{Base}, each D_{Alt} is then formulated with added CO_2 to recover its lost compressive strength. The addition of CO_2 provides a boost in compressive strength to each D_{Alt}, yielding a new set of mixture designs that we call D_{CO_2}, whose compressive strength is equal to or surpasses that of D_{Base}, as shown in Figure 4.2 (A3). From the set of D_{CO_2} mixtures derived from each of the 48 D_{Base} mixture designs, the one that features the lowest net CO_2 footprint–considering both the effects of reducing binder (avoiding CO_2 emissions in the formulation) and adding CO_2 (by absorbing CO_2 content in the formulation)–is called $D_{CO_2}^{Min}$. Since we employ one CO_2 utilization method at a time, we generate three sets of $D_{CO_2}^{Min}$, each containing 48 mixtures that replace 48 D_{Base} mixtures when CO_2 is added during mixing, curing, or during the recycling of concrete aggregate. Each of these sets of 48 $D_{CO_2}^{Min}$ mixtures, each substituting its D_{Base} counterpart without compromising strength, represents the diversity of possible alternatives and thus simulates the alternative U.S. concrete industry optimized for reduced binder use enabled by the inclusion of CO_2 in its formulation. Further details of this step-wise approach are provided in section C.2.

CO_2 footprint and material cost of each of the D_{Base} and $D_{CO_2}^{Min}$ mixtures are then calculated by aggregating constituent-level values. This includes CO_2 emitted and cost incurred from manufacturing of each constituent, transporting it to concrete plants and preparing them as a final product – mixed concrete for ready-mixed application or finished precast products. We assumed industrial grade (purity ≥ 99.5%) liquid byproduct CO_2 from ethanol, ammonia, or hydrogen plants would be used for the CO_2 utilization processes. The additional CO_2 emitted and cost incurred

Table 4.1. Comparison of the built cohort and the U.S. concrete industry using national averaged mixture compositions and distributions in terms of compressive strength. C.Agg. and F.Agg. represent coarse and fine natural aggregate, respectively.

	Average Constituent Loading [kg/m^3]					Compressive Strength Distribution [MPa]		
	OPC	FA	GGBS	C.Agg.	F.Agg.	≤24	>24 & ≤34.5	>34.5
Cohort (D_{Base})	319.5	60.7	14.1	936.5	793.8	49.5%	44.7%	5.8%
U.S. Reference(National Ready Mixed Concrete Association 2016)	271	51	12	979	839	49%	45%	6%

during purifying, liquefying and transporting byproduct CO_2 to concrete plants as well as from applying CO_2 treatment to concrete were included in our calculation (El-Hassan and Shao 2014, Shao 2014, Parsons Brinckerhoff and Global CCS Institute 2011, Supekar and Skerlos 2014). The CO_2 emitted and material cost incurred nationally from manufacturing concrete in the U.S. can then be estimate by summing CO_2 footprint and material cost of each of the 48 mixtures weighted by its national production volume. Thus, the net CO_2 mitigation and material cost savings achievable for each of the three CO_2 utilization strategies are determined by assessing the changes in total CO_2 footprint and material cost of the 48 $D_{CO_2}^{Min}$ mixtures compared to those of the original 48 D_{Base} mixtures. The assumptions, data sources, and calculations applied are available in section C.3-C.4.

With this approach, we investigate three possible mitigation cases to address existing uncertainties on available concrete mixture designs. The assumptions and procedures outlined above define an alternative U.S. concrete industry that utilizes CO_2 to create reduced binder formulations at full scale. Since this case does not consider future supply restrictions of FA and GGBS, the resulting CO_2 mitigation potential is likely an overestimation. Therefore, the calculations here represent a "high mitigation case" that could be achieved with a novel SCM that does not compromise compressive strength of concrete and therefore can replace high proportions of binders without additional CO_2 emissions. We then create what we consider to be a more realistic mitigation case that accounts for future supply restriction of FA and GGBS and use this as our "nominal mitigation case". This case is generated by recreating three sets of $D_{CO_2}^{Min}$ mixtures using each of the CO_2 utilization strategies following the same procedure as above but when deriving D_{Alt}, we only use mixtures that have equal or less FA or GGBS content than D_{Base} for D_{Alt}. Lastly, we present a "low mitigation case" which represents a limiting scenario where only commercial mixture designs that are being used today are available in the future without further improvement. This design-restricted scenario can be emulated by reproducing three sets of $D_{CO_2}^{Min}$ mixtures as we only allow conventional D_{Base} mixtures to serve as D_{Alt} mixtures. The opportunity to reduce binder loading is then highly constrained. Consequently, we generate nine results by evaluating three CO_2 utilization strategies in three levels of mitigation cases.

Many input variables and data used in this study were also found with a range of uncertainty in the literature. These variables included the annual concrete consumption rate in the U.S., the CO_2 emissions and costs associated with manufacturing each constituent, and the maximum

market penetration rate attainable for each of the CO_2 utilization strategies. Three uncertainty levels were allowed for each of these four parameters, generating 81 uncertainty cases. These 81 cases can be applied to the nine results created above to generate 729 results. Since results generated with 81 uncertainty cases show consistent trends, we only report median results in the following section for clarity. The results generated with the full spectrum of uncertainty cases are presented in section C.6.

4.3 Results and Discussion

If reduced binder loading is jointly employed with CO_2 sequestration throughout the concrete industry, the potential scale of atmospheric CO_2 reduction increases by over an order of magnitude compared to partially offsetting the emissions solely through CO_2 sequestration in the concrete. Figure 4.3 shows that the amount of CO_2 emissions that can be offset solely through sequestration (horizontal dotted lines) is limited to about 1.09-1. 23% of current CO_2 emissions from the U.S. concrete industry if CO_2 is added during mixing or in RCA. With respect to the possibility of reducing binder to its maximal potential in the nominal mitigation case, the industry-wide CO_2 mitigation potential increases to about 31-38% of the emissions when CO_2 is added in RCA or during mixing. Considering that approximately 75.5 Mt of CO_2 are annually emitted from concrete manufacturing in the U.S., this translates into about 23.3-28.5 Mt of mitigated CO_2 where over 98% of which are avoided CO_2 emissions from reduced binder use (see Appendix C.7 for further information). Compared to CO_2 offset through sequestration, this represents a 25x-35x increase in

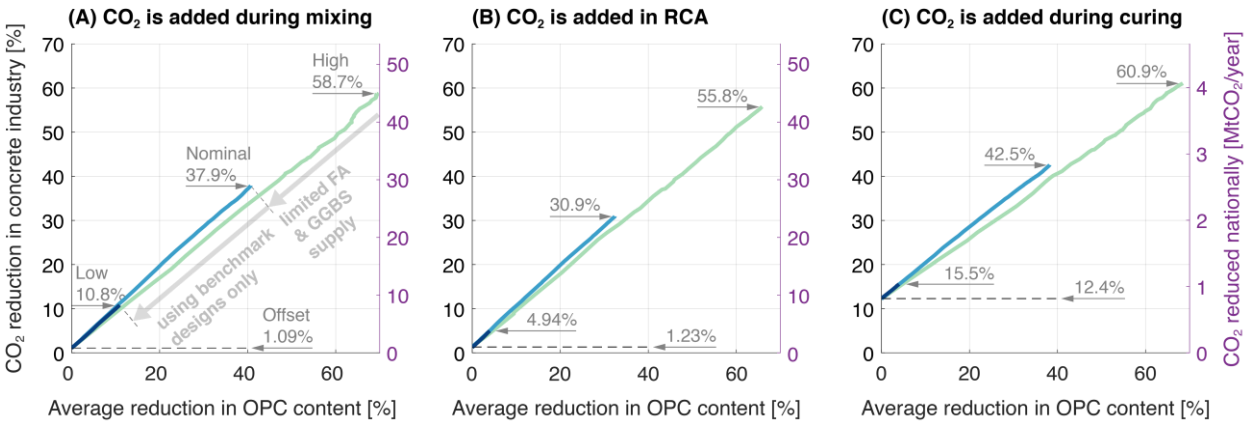

Figure 4.3. The overall CO_2 mitigation achievable by implementing combined strategy of reducing binder and adding CO_2 in concrete formulation (A) during mixing, (B) in RCA, or (C) through curing. The displayed values indicate the largest CO_2 mitigation achievable for each mitigation case. Only median results are presented here. A full set of results including uncertainty bounds are provided in appendix C.6.

mitigated CO_2 emissions. Although more CO_2 is sequestered in carbonation curing per volume of treated concrete, the total potential to reduce industry-wide CO_2 emissions is relatively low (about 4% of total industry emissions), as this approach is limited to the precast industry. The potential scale of CO_2 reduction when carbonation curing is employed would likely be smaller considering that carbonation curing can only treat the volume of concrete near the surface and the actual precast products tend to have a larger volume than previously studied lab samples.

The differences between low, nominal, and high mitigation cases mainly result from assumptions around the capacity to reduce OPC content from mixtures in each case, which is primarily determined by the abundance and diversity of the SCM available to replace OPC. For instance, the high mitigation case assumes it is possible to increase the use of GGBS by about 6-8 times compared to the current level, which reduces OPC consumption by over 60% when CO_2 is added during mixing or in RCA. Consequently, the mitigation potential can expand up to 54 times compared to the CO_2 reduction achievable with direct sequestration alone. However, when the incorporation rate of GGBS is constrained below the current level in the nominal case, OPC is reduced primarily by expanding the use of limestone, which is a trend consistent with observations in previous literature (Miller *et al* 2018, International Energy Agency 2018). In the nominal cases shown in Figure 4.3, about 11-19% of limestone by mass of OPC is included in mixtures when CO_2 is added during curing or mixing–which is comparable or higher than the typical incorporation rate of up to 15% and made possible by CO_2-induced compressive strength enhancement (Yoneyama 2013, Tennis *et al* 2011). As a result, about 32-41% of OPC is replaced. It is the adverse impact on compressive strength from dilution that prevents further replacement of OPC with limestone, limiting additional binder reduction. When the available mixture design for D_{Alt} is further restricted to existing benchmark designs in the low mitigation case, limestone is no longer available and mitigation potential is further constrained. But even in this restricted case, CO_2 mitigation potential may increase by nearly an order of magnitude compared to partially offsetting emissions through CO_2 sequestration alone if reducing binder is considered.

Theoretically, the three CO_2 utilization technologies investigated in this study can be jointly implemented to maximize CO_2 mitigation as they target different components of concrete. For instance, He et al. found a compound boost in compressive strength when CO_2 was added during mixing and also during curing (He *et al* 2017). The compound effect may prove important in the future when optimizing concrete formulations. However, few experimental studies to date have

investigated non-linear interactions between carbonated components and their impact on compressive strength. Therefore, joint application of multiple CO_2 utilization techniques was not considered here and the presented results are based on implementing one CO_2 utilization technique at a time.

In the nominal mitigation cases, maximal OPC reductions range from 32-41%. Since OPC comprises nearly 50% of the material cost, this results in a total cost reduction of 18% or $3.6 billion across the U.S. if CO_2 were added universally during mixing or in RCA (Figure 4.4). Cost reduction is limited to 1.5% or $300 million when carbonation curing is implemented nationwide. In Figure 4.4, these cost savings are superimposed with the cost uncertainty of CO_2 utilization, which includes both the cost of byproduct CO_2 and the cost of carbonation treatments. The byproduct CO_2 is assumed to cost between $34/t$CO_2$ and $69/t$CO_2$ and the cost of CO_2 utilization processes ranges between $10/t$CO_2$ and $2,000/t$CO_2$ (see Appendix C.3.2-C.3.3 for details). The upper end of the cost uncertainty reflects non-optimized cases and thus the realistic cost is expected to be closer to the lower end of the spectrum. The cost incurred by utilizing CO_2 nationally is then estimated by multiplying these CO_2-normalized cost bounds with the total amount of CO_2 sequestered in concrete throughout the industry. The yellow bounds in Figure 4.4 depict the range of cost of utilizing CO_2 nationally.

We find that the saved material cost could fully mitigate the additional cost of CO_2 utilization without external financial support if OPC content in concrete is reduced by either over 5% when CO_2 is added in RCA or beyond 16% when CO_2 is injected during mixing. In these cases, the

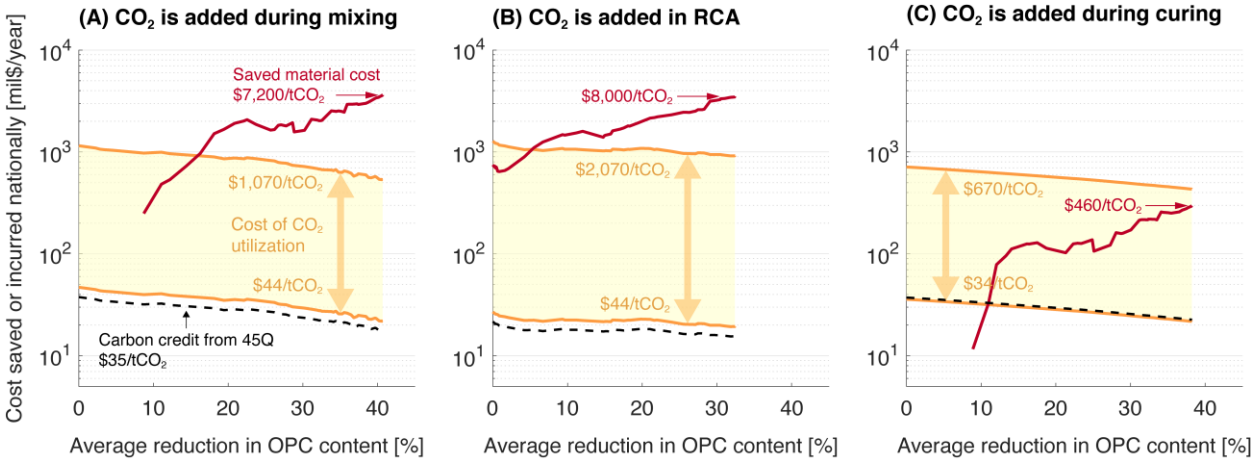

Figure 4.4. Material cost saved and additional cost incurred by implementing the combined strategies when CO_2 is added (A) during mixing, (B) in RCA, or (C) through curing. The displayed values indicate the costs normalized by sequestered CO_2. The dotted lines indicate carbon credit available from amended 45Q.

resulting $D_{CO_2}^{Min}$ mixtures would have the same cost as their D_{Base} counterparts. Figure 4.4 shows that if OPC use can be reduced further, the saved cost (red curve) clearly rises above the cost uncertainty of CO_2 utilization (yellow range) and there is a strong possibility that the $D_{CO_2}^{Min}$ mixtures cost less than their D_{Base} counterparts. For instance, when CO_2 is added during mixing or in RCA with maximal OPC reduction, over \$7,000 is saved per tonne of CO_2 sequestered. This is more than enough to mitigate the additional cost incurred by utilizing CO_2, which can range between \$34 and \$2,070 per tonne of CO_2 utilized (Figure 4.4). If the saved cost is contained within the cost uncertainty – as in the case of carbonation curing, or when CO_2 is added during mixing or in RCA with a low degree of OPC reduction – additional support might be needed to make $D_{CO_2}^{Min}$ mixtures cost-competitive. As an example, $D_{CO_2}^{Min}$ mixtures prepared with carbonation curing would require up to \$210/tCO_2 of carbon credit to cost the same as its D_{Base} counterparts when its OPC reduction is maximized to about 38% (Figure 4.4 C).

In the U.S., the amended 45Q provides up to \$35 of tax credit for every tonne of CO_2 sequestered in as a result of beneficial use. The applicable tax credit for concrete products will be lower if CO_2 is sourced from external entities as the credit needs to be split between concrete manufacturers and CO_2 capture facilities, the recipient of the credit under 45Q. However, the minimum sequestration requirement of 25,000 tCO_2 per year may bar many concrete manufacturers from participating in 45Q. The concrete industry is comprised of highly distributed small-scale operators to accommodate local demands; the average market share of a typical ready-mixed and precast facility is approximately 0.018% and 0.093%, respectively (National Ready Mixed Concrete Association 2018, Connor 2018). As shown in Figure 4.5 A, the amount of CO_2 that can be sequestered in concrete by a single concrete facility significantly falls short of the minimum sequestration requirement even when all of its concrete is fabricated with added CO_2. Instead, all concrete mixtures produced by a leading manufacturer may need to be formulated with added CO_2 across all its facilities in the U.S. to be eligible for 45Q. An example of a leading ready-mixed company shown in Figure 4.5 B operates 335 locations in the U.S. with a market share of 4.7% in ready-mixed industry (National Ready Mixed Concrete Association 2018). An example precast leader has 77 locations in the U.S. with a market share of 9.1% in precast industry (Connor 2018). Such a high initial eligibility criterion may defeat the purpose of 45Q to foster the implementation of emerging CO_2 technologies. Additionally, the sequestration-based mechanism of 45Q does not incentivize binder reduction since the reduced CO_2 emissions from avoided binder

use are not applicable for the credit. As a result, 45Q may distract industry attention away from CO_2 utilization methods that do not sequester a high proportion of CO_2, such as CO_2 addition during mixing or in RCA, even though such techniques have a much higher net carbon mitigation potential. This disproportional incentive is also shown in Figure 4.5; it is relatively easier to meet the eligibility criterion of 45Q with carbonation curing than with other CO_2 utilization methods. Hence, a more comprehensive incentive system should encourage binder reduction strategies to be coupled with CO_2 addition. Such a mechanism could promote material cost savings while driving aggressive CO_2 emission reductions.

Although this analysis is based on a simplified technical criterion of 28-day compressive strength and with a primary focus in the U.S., the main findings that more efficient use of OPC provides significant CO_2 reduction opportunity and that added CO_2 can catalyze further OPC reduction would be valid for the global concrete industry. To show this, the results generated with randomly selected D_{Base} mixtures from the database indeed show a consistent trend with the results created with the original 48 D_{Base} mixtures (section C.8). But other parameters excluded in this analysis such as workability, set time, permeability, early compressive strength and compressive strength measured at a longer period beyond 28 days need to be considered when selecting alternative mixtures for practical purposes. The specific requirement for fresh or hardened concrete properties, and potential synergies and tradeoffs between added CO_2 and constituents could influence the final mixture choices.(Zhang *et al* 2016, Monkman and MacDonald 2017)

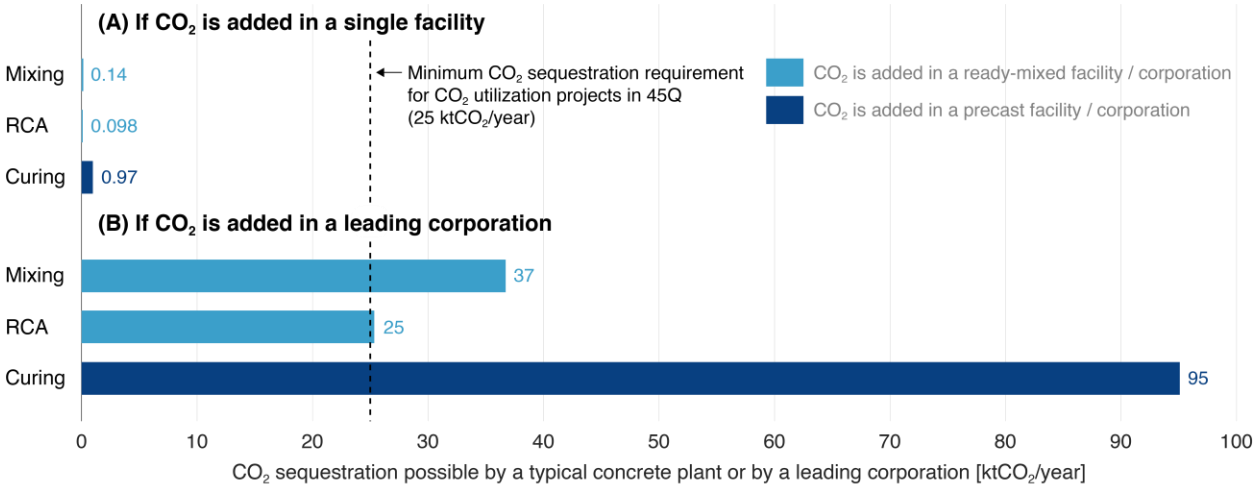

Figure 4.5. Comparison of the minimum eligibility requirement for 45Q and CO_2 sequestration possible by implementing one of the three CO_2 utilization technologies in concrete. The calculated values are based on the nominal mitigation case when OPC content is minimized.

Future studies on CO_2 utilization in concrete need to assess the impact of added CO_2 on ductility and tensile strength, which dictates long-term durability and lifecycle CO_2 footprint of concrete rather than compressive strength; past efforts to strengthen concrete structures by increasing their compressive strength has led to premature deterioration in recent decades.(Mehta and Burrows 2001) This is because increasing compressive strength tends to make concrete more vulnerable to cracking,(Mehta and Burrows 2001) and the ingress of external detrimental species along the cracks ultimately deteriorates structural integrity. The resulting additional repair events and reduced service life can substantially increase the life cycle CO_2 emissions and cost of concrete. For instance, comparative studies on a bridge deck showed nearly 30% reduction in life cycle CO_2 emissions and cost when brittle concrete was replaced with engineered cementitious composite (ECC) that has enhanced ductility by several orders of magnitude.(Kendall *et al* 2008, Keoleian *et al* 2005) If the added CO_2 in ECC can be used to reduce OPC content without compromising its ductility, additional CO_2 emission may be mitigated. But the review of existing literature shows lack of experimental data beyond compressive strength; among the 696 collected mixtures used in this study, only about 9% were measured for tensile strength and none were tested for ductility; none of the carbonated mixtures were evaluated for their impacts on tensile strength or ductility. This lack of data highlights both challenges and future opportunities for CO_2 utilization.

4.4 CONCLUSION

Despite the recent interest in devising an actionable and climate-compatible CO_2 reduction roadmap in concrete industry, the combined strategy of reduced binder use and CO_2 utilization has not been recognized enough a highly desirable option (Energy Transitions Commission 2018, International Energy Agency 2018, 2017). This is a critical concern as the global implementation of the combined strategy would enable gigatonne-scale CO_2 emissions reduction without relying on novel SCMs, alternative binders, or CCS. For instance, if the nominal mitigation potentials determined in this study were scaled to a global level, roughly 930 to 1,100 Mt of annual CO_2 emissions from the concrete industry could be mitigated by incorporating CO_2 in concrete formulation during mixing or in RCA. If carbonation curing were applied worldwide, about 110 Mt of CO_2 emissions could be mitigated. Comparatively speaking, only about 32-41 Mt of CO_2 could be mitigated globally solely through direct sequestration. Therefore, we find that the

combined strategy of binder reduction and CO_2 utilization could provide economically viable, aggressive CO_2 reduction pathways that can help advance the concrete industry toward carbon neutrality.

Data Availability

The data that supports the findings of this study are provided in the supplementary material of this article. The corresponding codes and input file as well as output results presented in this article are openly available at the online repository at https://umich.box.com/s/jpae59stixbjlkf6y2lqol4jpmshkd5d.

References

American Coal Ash Association 2018 *Coal Ash Recycling Reaches Record 64 Percent Amid Shifting Production and Use Patterns* Online: https://www.acaa-usa.org/Portals/9/Files/PDFs/Coal-Ash-Production-and-Use-2017.pdf

Andrew R M 2018 Global CO_2 emissions from cement production *Earth Syst. Sci. Data* **10** 195–217 Online: https://www.earth-syst-sci-data.net/10/195/2018/

Aprianti E, Shafigh P, Bahri S and Farahani J N 2015 Supplementary cementitious materials origin from agricultural wastes – A review *Constr. Build. Mater.* **74** 176–87 Online: http://dx.doi.org/10.1016/j.conbuildmat.2014.10.010

Batayneh M, Marie I and Asi I 2007 Use of selected waste materials in concrete mixes *Waste Manag.* **27** 1870–6 Online: https://linkinghub.elsevier.com/retrieve/pii/S0956053X06002601

Benhelal E, Zahedi G, Shamsaei E and Bahadori A 2013 Global strategies and potentials to curb CO_2 emissions in cement industry *J. Clean. Prod.* **51** 142–61 Online: http://dx.doi.org/10.1016/j.jclepro.2012.10.049

CEMBUREAU 2013 *The role of cement in the 2050 low-carbon economy* (Brussels) Online: https://lowcarboneconomy.cembureau.eu/wp-content/uploads/2018/09/cembureau-full-report.pdf

Cement Sustainability Initiative and European Cement Research Academy 2017 *Development of State of the Art-Techniques in Cement Manufacturing: Trying to Look Ahead* Online: https://docs.wbcsd.org/2017/06/CSI_ECRA_Technology_Papers_2017.pdf

Connor C O 2018 *IBISWorld Industry Report 32739 Precast Concrete Manufacturing in the US*

Damineli B L and John V M 2012 Developing Low CO_2 Concretes: Is Clinker Replacement Sufficient? The Need of Cement Use Efficiency Improvement *Key Eng. Mater.* **517** 342–51 Online: http://www.scientific.net/KEM.517.342

Duxson P, Fernandez-Jimenez J, Provis J L, Lukey G C, Palomo A and van Deventer J S J 2007 Geopolymer technology : the current state of the art 2917–33

El-Hassan H and Shao Y 2014 Carbon Storage through Concrete Block Carbonation *J. Clean Energy Technol.* **2** 287–91 Online: http://www.jocet.org/index.php?m=content&c=index&a=show&catid=34&id=414

Energy Transitions Commission 2018 *Mission Possible: Reaching Net-Zero Carbon Emissions From Harder-To-Abate Sectors By Mid-Century* Online: http://www.energy-transitions.org/mission-possible

FERNANDEZ BERTOS M, SIMONS S, HILLS C and CAREY P 2004 A review of accelerated carbonation technology in the treatment of cement-based materials and sequestration of CO_2 *J. Hazard. Mater.* **112** 193–205 Online: https://linkinghub.elsevier.com/retrieve/pii/S0304389404002675

Ghoshal S and Zeman F 2010 Carbon dioxide (CO_2) capture and storage technology in the cement and concrete industry *Developments and Innovation in Carbon Dioxide (CO_2) Capture and Storage Technology* vol 1 (Elsevier) pp 469–91 Online: http://www.sciencedirect.com/science/article/pii/B9781845695330500163

Gursel A P, Maryman H and Ostertag C 2016 A life-cycle approach to environmental, mechanical, and durability properties of "green" concrete mixes with rice husk ash *J. Clean. Prod.* **112** 823–36 Online: http://dx.doi.org/10.1016/j.jclepro.2015.06.029

Hasanbeigi A, Price L and Lin E 2012 Emerging energy-efficiency and CO_2 emission-reduction technologies for cement and concrete production: A technical review *Renew. Sustain. Energy Rev.* **16** 6220–38 Online: http://dx.doi.org/10.1016/j.rser.2012.07.019

He Z, Li Z and Shao Y 2017 Effect of Carbonation Mixing on CO_2 Uptake and Strength Gain in Concrete *J. Mater. Civ. Eng.* **29** 04017176 Online: http://ascelibrary.org/doi/10.1061/%28ASCE%29MT.1943-5533.0002031

International Energy Agency 2017 Energy Technology Perspectives 2017 443 Online: http://www.iea.org/etp/publications/%0Ahttp://www.oecd-ilibrary.org/energy/energy-technology-perspectives-2017_energy_tech-2017-en

International Energy Agency 2018 *Technology Roadmap - Low-Carbon transition in the Cement Industry* Online: https://webstore.iea.org/technology-roadmap-low-carbon-transition-in-the-cement-industry

Jang J G, Kim G M, Kim H J and Lee H K 2016 Review on recent advances in CO_2 utilization and sequestration technologies in cement-based materials *Constr. Build. Mater.* **127** 762–73 Online: http://dx.doi.org/10.1016/j.conbuildmat.2016.10.017

Jani Y and Hogland W 2014 Waste glass in the production of cement and concrete – A review *J. Environ. Chem. Eng.* **2** 1767–75 Online: http://dx.doi.org/10.1016/j.jece.2014.03.016

Kajaste R and Hurme M 2016 Cement industry greenhouse gas emissions – management options and abatement cost *J. Clean. Prod.* **112** 4041–52 Online: http://dx.doi.org/10.1016/j.jclepro.2015.07.055

Kendall A, Keoleian G A and Helfand G E 2008 Integrated Life-Cycle Assessment and Life-Cycle Cost Analysis Model for Concrete Bridge Deck Applications *J. Infrastruct. Syst.* **14** 214–22 Online: http://ascelibrary.org/doi/10.1061/%28ASCE%291076-0342%282008%2914%3A3%28214%29

Keoleian G A, Kendall A, Dettling J E, Smith V M, Chandler R F, Lepech M D and Li V C 2005 Life Cycle Modeling of Concrete Bridge Design: Comparison of Engineered Cementitious Composite Link Slabs and Conventional Steel Expansion Joints *J. Infrastruct. Syst.* **11** 51–60 Online: http://ascelibrary.org/doi/10.1061/%28ASCE%291076-0342%282005%2911%3A1%2851%29

Lepech M D, Li V C, Robertson R E and Keoleian G A 2008 Design of green engineered cementitious composites for improved sustainability *ACI Mater. J.* **105** 567–75

Li V C and Herbert E 2012 Robust Self-Healing Concrete for Sustainable Infrastructure *J. Adv. Concr. Technol.* **10** 207–18 Online: http://jlc.jst.go.jp/DN/JST.JSTAGE/jact/10.207?lang=en&from=CrossRef&type=abstract

Masson-Delmotte V, Zhai P, Pörtner H-O H-O, Roberts D, Skea J, Shukla P R P R, Pirani A, Moufouma-Okia W, Péan C, Pidcock R, Connors S, Matthews J B R B R, Chen Y, Zhou X, Gomis M I M I, Lonnoy E, Maycock T, Tignor M and Waterfield T 2018 *IPCC, 2018: Summary for Policymakers. In: Global Warming of 1.5°C. An IPCC Special Report on the impacts of global warming of 1.5°C above pre-industrial levels and related global greenhouse gas emission pathways, in the context of strengthening the global* (Geneva) Online: https://www.ipcc.ch/site/assets/uploads/sites/2/2018/07/SR15_SPM_version_stand_alone_LR.pdf

Mehta B Y P K and Burrows R W 2001 Building durable structures in the 21st century *Concr. Int.* **23** 57–63 Online: http://citeseerx.ist.psu.edu/viewdoc/download?doi=10.1.1.475.5570&rep=rep1&type=pdf

Miller S A 2018 Supplementary cementitious materials to mitigate greenhouse gas emissions from concrete: can there be too much of a good thing? *J. Clean. Prod.* **178** 587–98 Online: https://doi.org/10.1016/j.jclepro.2018.01.008

Miller S A, Horvath A and Monteiro P J M 2016 Readily implementable techniques can cut annual CO_2 emissions from the production of concrete by over 20% *Environ. Res. Lett.* **11** 074029 Online: https://iopscience.iop.org/article/10.1088/1748-9326/11/7/074029

Miller S A, John V M, Pacca S A and Horvath A 2018 Carbon dioxide reduction potential in the global cement industry by 2050 *Cem. Concr. Res.* **114** 115–24 Online: http://dx.doi.org/10.1016/j.cemconres.2017.08.026

Mineral Products Association 2013 *MPA 2050 strategy Plan* (London) Online: https://mineralproducts.org/documents/MPA_Cement_2050_Strategy.pdf

Monkman S and MacDonald M 2016 Carbon dioxide upcycling into industrially produced concrete blocks *Constr. Build. Mater.* **124** 127–32 Online: http://dx.doi.org/10.1016/j.conbuildmat.2016.07.046

Monkman S and MacDonald M 2017 On carbon dioxide utilization as a means to improve the sustainability of ready-mixed concrete *J. Clean. Prod.* **167** 365–75 Online: http://dx.doi.org/10.1016/j.jclepro.2017.08.194

Monkman S, Macdonald M and Hooton D 2016 Using CO_2 to reduce the carbon footprint of concrete *1st International Conference on Grand Challenges in Construction Materials* pp 1–8 Online: http://www.igcmat.com/papers/Monkman_igcmat_2016.pdf

Monkman S, MacDonald M and Hooton D 2015 Using Carbon Dioxide as a Beneficial Admixture in Ready-Mixed Concrete *NRMCA 2015 International Concrete Sustainability Conference* Online: https://www.emcoblock.com/pdf/divisions/bay-ready-mix/SMonkman-NRMCA-ICSC-2015-draft-150414.pdf

Müller N and Harnisch J 2008 *A blueprint for a climate friendly cement industry* (Gland) Online: http://d2ouvy59p0dg6k.cloudfront.net/downloads/english_report_lr_pdf.pdf

National Energy Technology Laboratory 2013 *Novel CO_2 Utilization Concepts: Working Paper* Online: https://www.netl.doe.gov/energy-analysis/details?id=783

National Ready Mixed Concrete Association 2016 *NRMCA Member National and Regional Life Cycle Assessment Benchmark (Industry Average) Report – Version 2 . 0* Online: https://www.nrmca.org/sustainability/EPDProgram/Downloads/NRMCA_Benchmark_Report_-_October_14_2014_web.pdf

National Ready Mixed Concrete Association 2018 U.S. Ready Mixed Concrete Production Statistics Online: https://www.nrmca.org/concrete/data.asp

Neuhoff K, Acworth W, Ancygier A, Branger F, Christmas I, Haussner M, Ismer R, van Rooij A, Sartor O, Sato M and Schopp A 2014 *Carbon Control and Competitiveness Post 2020: The Cement Report* Online: http://climatestrategies.org/wp-content/uploads/2014/02/climate-strategies-cement-report-final.pdf

Van Oss H G 2018 *2015 Minerals Yearbook - Cement* Online: https://prd-wret.s3-us-west-2.amazonaws.com/assets/palladium/production/atoms/files/myb1-2015-cemen.pdf

Parsons Brinckerhoff and Global CCS Institute 2011 *Accelerating the update of CCS: Industrial Use of Captured Carbon Dioxide* Online: https://www.globalccsinstitute.com/archive/hub/publications/14026/accelerating-uptake-ccs-industrial-use-captured-carbon-dioxide.pdf

Petek Gursel A, Masanet E, Horvath A and Stadel A 2014 Life-cycle inventory analysis of concrete production: A critical review *Cem. Concr. Compos.* **51** 38–48 Online: http://dx.doi.org/10.1016/j.cemconcomp.2014.03.005

Ramezanianpour A A, Ghiasvand E, Nickseresht I, Mahdikhani M and Moodi F 2009 Influence of various amounts of limestone powder on performance of Portland limestone cement concretes *Cem. Concr. Compos.* **31** 715–20 Online: http://dx.doi.org/10.1016/j.cemconcomp.2009.08.003

Rostami V, Shao Y, Boyd A J and He Z 2012 Microstructure of cement paste subject to early carbonation curing *Cem. Concr. Res.* **42** 186–93 Online: http://dx.doi.org/10.1016/j.cemconres.2011.09.010

Schneider M, Romer M, Tschudin M and Bolio H 2011 Sustainable cement production—present and future *Cem. Concr. Res.* **41** 642–50 Online: https://linkinghub.elsevier.com/retrieve/pii/S0008884611000950

Scrivener K L 2016 Eco-efficient cements : Potential economically viable solutions for a low-CO_2 cement-based materials industry .

Scrivener K, Martirena F, Bishnoi S and Maity S 2018 Calcined clay limestone cements (LC3) *Cem. Concr. Res.* **114** 49–56 Online: https://doi.org/10.1016/j.cemconres.2017.08.017

Shao Y 2014 *Beneficial Use of Carbon Dioxide in Precast Concrete Production* Online: https://www.osti.gov/servlets/purl/1155035

Shi C, Li Y, Zhang J, Li W, Chong L and Xie Z 2016 Performance enhancement of recycled concrete aggregate – A review *J. Clean. Prod.* **112** 466–72 Online: http://dx.doi.org/10.1016/j.jclepro.2015.08.057

Siddique R and Naik T R 2004 Properties of concrete containing scrap-tire rubber – an overview *Waste Manag.* **24** 563–9 Online: https://linkinghub.elsevier.com/retrieve/pii/S0956053X04000212

Supekar S D and Skerlos S J 2014 Market-Driven Emissions from Recovery of Carbon Dioxide Gas *Environ. Sci. Technol.* **48** 14615–23 Online: https://pubs.acs.org/sharingguidelines

Tennis P D, Thomas M D a and Weiss W J 2011 *State-of-the-Art Report on Use of Limestone in Cements at Levels of up to 15%* Online: http://www2.cement.org/pdf_files/sn3148.pdf

Tittelboom K Van and Belie N De 2013 *Self-Healing in Cementitious Materials—A Review*

U.S. Geological Survey 2018 *Mineral Commodity Summaries* Online: https://s3-us-west-2.amazonaws.com/prd-wret/assets/palladium/production/mineral-pubs/mcs/mcs2018.pdf

World Business Council for Sustainable Development 2015 *Low Carbon Technology Partnerships initiative (LCTPi) - Cement: full report* (New York) Online: https://docs.wbcsd.org/2015/11/LCTPi-Cement-Report.pdf

Xuan D, Zhan B and Poon C S 2016 Assessment of mechanical properties of concrete incorporating carbonated recycled concrete aggregates *Cem. Concr. Compos.* **65** 67–74 Online: http://dx.doi.org/10.1016/j.cemconcomp.2015.10.018

Yao Z T, Ji X S, Sarker P K, Tang J H, Ge L Q, Xia M S and Xi Y Q 2015 A comprehensive review on the applications of coal fly ash *Earth-Science Rev.* **141** 105–21 Online: https://linkinghub.elsevier.com/retrieve/pii/S0012825214002219

Yoneyama J 2013 Robust filtering for sampled-data fuzzy systems *Fuzzy Sets Syst.* **217** 110–29 Online: http://www.researchgate.net/publication/242297652_Portland-Limestone_Cement_State-of-the-Art_Report_and_Gap_Analysis_For_CSA_A_3000/file/9c9605293cabf99b5f.pdf%5Cnhttp://www.bcrmca.ca/media/CSA A3000.pdf

Van der Zee S and Zeman F 2016 Production of carbon negative precipitated calcium carbonate from waste concrete *Can. J. Chem. Eng.* **94** 2153–9 Online: http://doi.wiley.com/10.1002/cjce.22619

Zhang D, Cai X and Shao Y 2016 Carbonation Curing of Precast Fly Ash Concrete *J. Mater. Civ. Eng.* **28** 04016127 Online: http://ascelibrary.org/doi/10.1061/%28ASCE%29MT.1943-5533.0001649

CHAPTER 5

Lifecycle Cost and Emissions Benefits of Using Railway Ties Fabricated with Ductile Cementitious Composites and Carbonation Curing

5.1 INTRODUCTION

Decarbonizing the cement and concrete industry is an important milestone to achieve a net carbon-neutral economy. Today, cement is responsible for about 7% of the global CO_2 emissions, and consumption of concrete is expected to continuously increase toward 2050 (International Energy Agency 2018, 2020). In the US alone, the construction sector expects to add 121 billion square feet of buildings by 2050 (Portland Cement Association 2021b) and the recent $1 trillion investment plan on infrastructure through the Infrastructure Investment and Jobs Act will create further demands.

In 2021, industrial associations in cement and concrete published roadmaps to reach net carbon neutrality by 2050 without relying on offsets (Portland Cement Association 2021b, Global Cement and Concrete Association 2021). Carbon capture, utilization, and storage (CCUS) are promoted as one of the central pillars of the roadmaps that mitigate 36% of the emissions, along with other solutions such as alternative binding materials, energy efficiency, and optimized mixture design and use. Mineral carbonation, one of the CCUS options, provides an attractive avenue to permanently store CO_2 on a climate-relevant scale while producing value-added products. The inherent alkalinity of concrete (pH >13) provides an attractive thermodynamically favorable carbon sink through mineral precipitation. When applied in a controlled manner, the added CO_2 can become part of the binding matrix or improve the mechanical properties of the mixture to enhance the overall strength of the concrete. (Lim *et al* 2019) found that if the strength improvement facilitated by CO_2 can be coupled with binder reduction, both the cost and emissions associated with manufacturing concrete products can be substantially reduced. While the CO_2 mitigation potential in the US concrete industry may be limited to about 1% of its annual emissions by CO_2 storage alone, simultaneously reducing binder loading in the mixture can avoid nearly 40%

of the annual emissions. If CO_2 can be globally added throughout the concrete industry, (Lim *et al* 2019) anticipates that approximately a giga-ton of CO_2 emissions can be mitigated each year without relying on novel materials, supplementary materials, or fossil-based carbon capture and sequestration.

Mass-produced precast concrete products provide one attractive near-term avenue to beneficially utilize and store CO_2. Examples of precast concrete products include railway ties, pipes, and panels, as well as structural elements used in bridges and culverts. In this study, we explore CO_2 utilization and sequestration in railway ties. Traditionally, railway tracks across the U.S. were constructed using wood ties. Since the 1970s, major railroads in the U.S. have been upgrading rail infrastructure by replacing wood ties with concrete ties to provide high-speed passenger services, to enable high-tonnage freight operations, to accommodate higher traffic volume, and to cope with the difficulties of finding quality woods. For instance, Amtrak – which owns or maintains 2,408 miles of tracks in the U.S. – started upgrading the heavily congested Northeast Corridor (NEC) with concrete ties in 1978 and currently plans to eventually replace all wood ties with concrete ties in the future and is annually investing close to $39 million for the program (Amtrak 2021, 2019b).

However, past lifecycle assessment (LCA) studies on wood and concrete ties thus far show mixed results. Concrete ties are expected to have a longer service life of about 45 years compared to 30 years for wood ties. Due to its extended service life, (Crawford 2009) found that lifecycle greenhouse gas (GHG) emissions from using concrete ties can be 17-54% of the emissions generated from using wood ties for the same period. (Milford and Allwood 2010) compared concrete ties with hardwood and softwood ties and found concrete ties emit lower GHG emissions during manufacturing and disposal. On the contrary, (Bolin and Smith 2013) showed that using concrete ties can increase GHG emissions by 5.8 times compared to using wood ties. A study conducted by (Werner *et al* 2009) reports that wood ties made with oak or beech are nearly carbon-neutral throughout their lifetime and thus emit significantly less GHG than the concrete alternative. A recent analysis by (Rempelos *et al* 2020) reported mixed results; softwood ties emitted the least amount of GHG at low traffic loads whereas concrete ties exhibited the least amount of GHG emissions at high traffic conditions.

Moreover, historic replacement data of concrete ties suggest that the service life and durability of concrete ties in the track can significantly deviate from engineering assumptions that formed

the basis of the past studies and purchase decisions by railroads. One of the major premises of the concrete tie adoption was its superior durability that leads to little premature failure (<4%) before its design service life (Sullivan 1983). Similarly, nearly *all* LCA and train operations studies assumed that concrete ties only need to be replaced once during its use (Lovett *et al* 2015, Bolin and Smith 2013, Rempelos *et al* 2020, Crawford 2009, Milford and Allwood 2010, Werner *et al* 2009). However, catastrophic failures have led to premature replacement of at least 31% of the 10 million concrete ties surveyed in the U.S. since the 1970s (Railway Tie Association 2010, Anon 1991, Amtrak 2019b, 2012, Cloutier 2014). In some cases, the entire cohort of concrete ties installed in the track needed to be replaced within 10 years of installation. Prominent premature failure of concrete ties was also observed in the U.K. where about 31-52 percent of the concrete ties were replaced before reaching 50 percent of their design life (Rempelos *et al* 2020).

Prematurely failed ties can induce non-linear economic and environmental impacts through replacement activities and train delays, none of which were accounted for in the past studies due to their simplified assumptions on concrete tie failure and replacement. Typical tie replacement involves a track laying system (TLS) where a purpose-built train can efficiently replace all ties in the affected track section at about $910 per tie (Northeast Corridor Commission 2018, 2019, Amtrak 2020, Northeast Corridor Commission 2021, 2020). Alternatively, individual ties can be replaced without affecting adjacent ties via spot removal at $2,940/tie. These values considerably deviate from the typical purchasing cost of a concrete tie around $100, which was used to represent the replacement cost of a concrete tie in the past studies. Also, tie replacements determine the total number of ties eventually needed to support the track as TLS replaces all – both good and bad – ties in the application length. If failed ties are left on the track due to overloaded maintenance, trains need to reduce speed when passing the affected zone (as known as slow order) to ensure safe operation (Federal Railroad Administration n.d., Office of Railroad Safety 2018, Cloutier 2014). While not all slow orders are caused by faulty ties, slow order was found to be one of the leading causes of train delays (Federal Railroad Administration 2012) and operational loss (Amtrak 2019a).

As a result of the considerably higher systems-level cost of using concrete ties observed by the users and ambiguity on its environmental benefits, the use of concrete ties is largely limited in a niche market. According to a recent tie survey conducted by (Smith 2019) that represented 85%

of the reported tie purchases made in the U.S. in 2018, concrete ties represented less than 5% of the annual tie market with diminishing market shares.

Thus, we re-visit the lifecycle cost and environmental impacts of using concrete ties considering systems-level impacts from tie replacement and slow orders and compare it with a novel tie designed with engineered cementitious composite (ECC) cured with added CO_2. ECC is a fiber-reinforced composite material (2 vol%) that suppresses the occurrence of fracture failure, a primary failure mechanism of concrete, including concrete ties. Due to their extreme tensile ductility, nearly 500 times that of conventional concrete (Li 2008), ECC ties can be designed without prestressing elements which have facilitated premature failure of concrete ties (Mayville A *et al* 2014). The elimination of prestressing elements also expands the scale of CO_2 storage in ECC as ECC is no longer required to maintain strong alkalinity to chemically protect steel against corrosion as conventional concrete does. At the same time, ECC-based products are expected to be more durable and have an extended lifetime that can have an environmental benefit. A case study of a bridge link slab designed with ECC showed reductions of 40% in life cycle energy consumption and 33% in greenhouse gas emissions considering the extended service life of the link slab as well as reduced maintenance events and construction-related traffic congestion (Keoleian *et al* 2005).

This study aims to provide comprehensive systems-level environmental and economic impacts when implementing CO_2-cured ECC ties relative to prestressed concrete ties. The analysis is based on maintaining 1km of track section over 100 years with either prestressed concrete or ECC ties. First, we modeled manufacturing and end-of-life processes for each of the ties considering the cost premium and added environmental emissions of ECC tie relative to that of concrete ties. Second, the systems-level environmental and economic profile of using ties are assessed with a stochastic use-phase model that evaluates the stochastic failure of ties over use, recurring tie replacements based on renewal strategy, and concomitant impacts from altered train operations. The stochastic model is based on Monte Carlo simulation that studies a wide range of uncertainty scenarios and considers tie longevity, temporal and spatial spread of the failed ties on the track, tie replacement strategies, and resulting slow orders of the trains when replacement capacity is overloaded. The use-phase model informs the ultimate number of ties needed to maintain the track considering necessary stochastic tie replacement and additional cost and emissions incurred from train delays. The detailed manufacturing process and cost modeling are

performed in conjunction with a techno-economic assessment guideline by the Global CO_2 Initiative (Zimmerman *et al* 2020). The lifecycle environmental impact is estimated by applying developed lifecycle inventories to the systems-level results.

5.2 METHODS

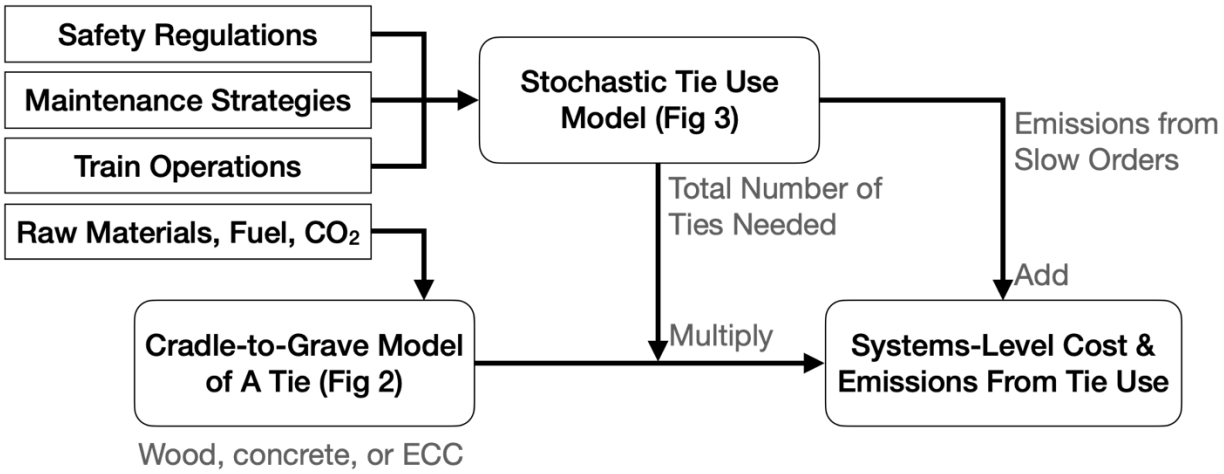

Figure 5.1. Overall model structure to estimate systems-level environmental footprint of using concrete and ECC ties

The analysis presented here is based on providing rail support for train transits in a 1-km length of track in the U.S. for 100 years following the safety standard set forth by FRA and Amtrak (Federal Railroad Administration n.d., Office of Railroad Safety 2018, Cloutier 2014). Figure 5.1 shows the overall structure of the analysis that combines the cradle-to-grave model of a tie (Figure 5.2) – designed with either concrete or ECC – with a stochastic use-phase model (Figure 5.3) which assesses the overall systems-level impact of using ties, including recurring tie replacements and concomitant train delays.

5.2.1 Cradle-to-grave model of concrete and ECC ties

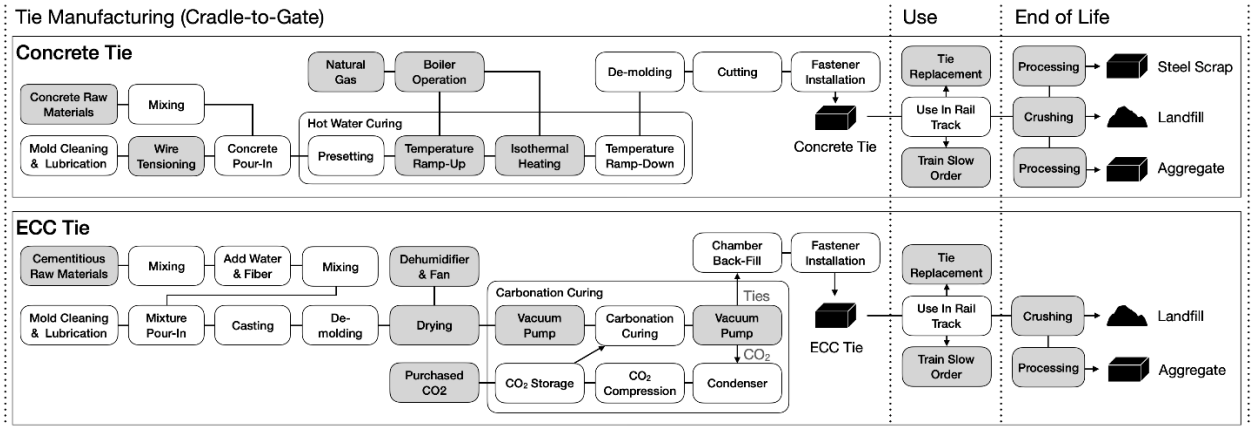

Figure 5.2. Cradle-to-grave model of concrete and ECC tie manufacturing and end of life treatment. Use phase processes are separately estimated using a stochastic model

Major manufacturing and end-of-life processes considered in this analysis are illustrated in Figure 5.2. Our concrete tie manufacturing model is largely based on the industrial configuration published by (H.J. Grimbergen b.v. 2007). The plant outputs 250,000 ties annually through 24/7/365 operation from eight long-line production beds each fabricating 80 ties per day. Prestressing elements consist of 28 individual wires (OD 5.32mm), each of which is tensioned to 34 kN prior to concrete molding. After two hours of casting, ties are cured with hot water following the temperature profile recommended by (Precast/Prestressed Concrete Institute 2021). Based on the typical curing setup and configuration used in this study, 3.9 m^3 of natural gas and 0.45 kWh of electricity is used on average to cure one tie using an industrial boiler, accounting for the extra energy needed to heat steel forms, energy lost to the environment, and system efficiency (Personal communication 2021). The eight production beds are operated in a staggered manner to ensure the continuous operation of a natural gas boiler that supplies hot water for curing. Upon curing, which takes about 20 hours, prestressing wires are de-tensioned and ties are demolded for storage.

ECC is a novel material with limited but growing commercial applications in construction. ECC tie manufacturing processes are largely based on the model concrete tie facility with replacement of conventional curing with carbonation curing. The representative ECC tie plant outputs 180,000 ties annually from 12 production lines using 720 tie molds operated in a staggered fashion to maximize equipment utilization. The ECC mixture is cast in molds for 20 hours in an ambient environment. Upon demolding, the ties are transported to a drying room equipped with an industrial fan and a dehumidifier to partially remove pore water for 30 hours to facilitate CO_2 uptake in the subsequent carbonation curing (Zhang *et al* 2021). Fan-drying is typically used for lab-scale experiments. For industrial ECC production, we conservatively assumed that both fans and industrial dehumidifiers would be needed. The dried ECC ties are then reacted with CO_2 inside carbonation chambers under mile pressure (5 bars) for 50 hours. Data gathered when fabricating a sample ECC tie were used to represent industrial processes. Carbonation chambers are based on commercial autoclaves for masonry units retrofitted for CO_2 application. While producing an ECC tie requires 100 hours, four times longer than producing a concrete tie, reduction in production rate can be minimized by curtailing equipment downtime throughout multiple production lines. A total of four tie molds, drying rooms, and six carbonation chambers each sized to treat 180 ties at a time are employed for manufacturing. As a result, the ECC plant output is reduced by 28% compared

to concrete tie manufacturing. Pressurized CO_2 supply lines and vacuum pumps are employed during carbonation curing to minimize CO_2 loss during treatment. A range of CO_2 supply chain options is considered for ECC including byproduct CO_2 supplied from an ethanol plant and CO_2 recovered on-site using direct air capture (DAC).

Based on the modeled processes, the manufacturing cost of a concrete and ECC tie is calculated by considering the cost of raw materials, labor, as well as capital and operational expenditures (Zimmerman *et al* 2020). The cost premium of ECC tie manufacturing compared to producing wood or concrete ties is calculated to assess its economic feasibility. The estimated manufacturing cost of ties does not represent the total manufacturing cost as not all processes are included for evaluation. Further details on modeling assumptions and data sources are provided in Appendix D.1.

5.2.2 Cradle-to-grave LCA models

The cradle-to-grave LCA models account for primary processes (grey boxes in Figure 5.2) unique to using each of the tie types for comparative analysis. Thus, these LCA results do not cover the complete environmental impacts of a tie. Use phase includes emissions from tie replacement events, both TLS and spot treatment, and additional fuel and electricity demand from altered train operation due to slow orders. After their useful life of approximately 30 years, 1.1% of the ties are reused by the railroad, 27% of wood ties are reused for non-structural purposes, and 66% are used for energy recovery through combustion while the rest and landfilled (Smith 2019). Concrete ties can be either landfilled or further processed to extract reinforcing steel and converted into coarse aggregates. It is assumed that about 59% of the rebar is recovered as scrap metal (AISI and SMA 2021) and 60% of concrete is converted into coarse aggregates (Nagataki *et al* 2004). Similar to concrete, ECC ties are assumed to be recycled as coarse aggregates at the same rate. Lifecycle inventory data were obtained from Ecoinvent 3 database (Wernet *et al* 2016). Transport distance of each of the raw materials was based on national average values reported by (National Ready Mixed Concrete Association 2016) when available. PVA fiber is represented by processed polyethylene as in (Keoleian *et al* 2005). Industry average or product-level lifecycle impact results of OPC, rebar, and chemical admixtures were imported from published environmental product declarations (Portland Cement Association 2021a, Commercial Metals 2015, European Federation

of Concrete Admixtures Associations Ltd. (EFCA) 2015, 2020). Table D.2 summarizes the environmental impact of tie manufacturing and disposal.

5.2.3 Stochastic tie replacement during use phase

The stochastic model evaluates direct and indirect costs and emissions generated during the use of ties after their initial installation. The analysis is performed using a straight, zero-grade track of 100 km over 100 years. The expanded track length is used to adequately capture the magnitude of train delays that can stretch to tens of kilometers. The installed ties are evaluated, replaced, and train operations are adjusted accordingly each month. Failure of the installed ties is estimated with the Weibull distribution. In each month, the age of the ties is evaluated, assigned with a grade, and replaced with new ties either with spot replacement or TLS according to the predefined replacement rules and capacities. If any of the failed ties cannot be replaced in a given month, trains reduce speed around the affected section according to the safety standard. Ties that are either nearing the end of life or failed are prioritized for replacement. In the end, the model estimates the total number of the failed ties, ties that were replaced via spot treatment or TLS, hours of train delays, and additional fuel and electricity consumed during altered operation. The resultant cost and emissions are normalized to 1km of the track section. Figure 5.3 summarizes the structure of the stochastic model. A total of 400 Monte Carlo iterations were used to derive results, where key parameters on tie failure, tie replacement, and train operations were varied within a finite range to produce a range of results. Each iteration generates a pair of results, one for concrete and the other for ECC ties, where parameters pertaining to tie replacement and train operation are kept the same for both ties. This allows us to systematically assess the relative, consequential impact of using different ties. The list of the parameters used in the stochastic model and their ranges are provided in Table D.4.

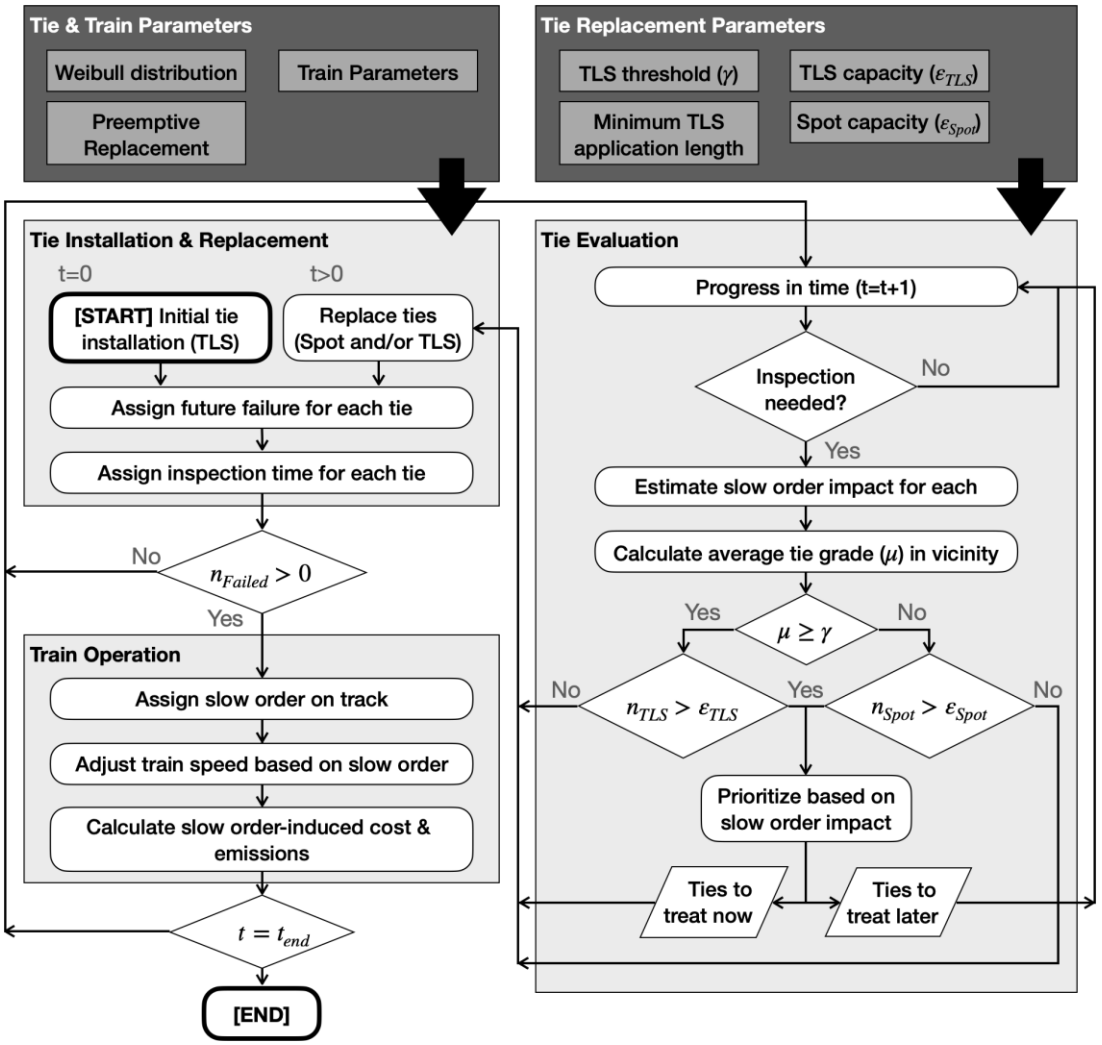

Figure 5.3. The overall structure of the use-phase stochastic tie replacement and train operation model

While past studies (Crawford 2009, Bolin and Smith 2013, Rempelos *et al* 2020, Lovett *et al* 2015) have assumed few concrete ties would prematurely fail before their service life, historic replacement data of about 11 million concrete ties installed in the U.S. since 1978 show a significant history of premature failure (Railway Tie Association 2010, Anon 1991, Amtrak 2019b, 2012, Cloutier 2014). Figure 5.4 illustrates the historic failure data of concrete ties (red circles) reported by major freight and passenger railroads in North America. Millions of ties have catastrophically failed and needed to be replaced sooner than design service life, in some cases as soon as within a few years since installation. One million ties installed by Amtrak between 1978-1982 that are anticipating retirement without experiencing catastrophic failures are indicated with a green circle.

The stochastic failure of ties over time is estimated with Weibull distribution that is defined with age (t), the average service life of a tie (μ), as well as scaling (λ) and shape (k) parameters

(5.1). Weibull parameters are derived from the historical replacement data of about 127,500 wood ties (MacLEAN 1957) and are adjusted to reflect the expanded service life of concrete and ECC ties. We assume that concrete ties can last between 40-60 years. An extended range of 40-100 years is used to model ECC ties. The simulated ranges of cumulative failure rate for concrete and ECC ties are shown in Figure 5.4(a). The established ranges roughly overlap with the observed failure pattern at lower ranges.

$$\frac{k}{\mu\lambda}\left(\frac{t}{\mu\lambda}\right)^{k-1} e^{\left(\frac{t}{\mu\lambda}\right)^{k}}, t \geq 0 \qquad (5.1)$$

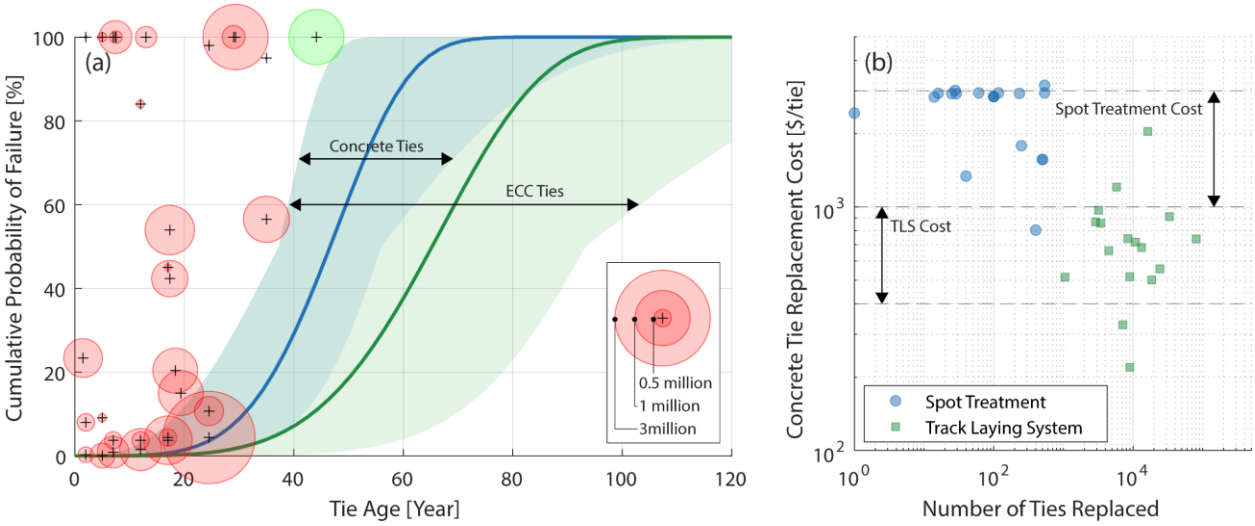

Figure 5.4. (a) Replacement history of concrete ties and the range of failure distribution for concrete and ECC ties, (b) per tie concrete tie replacement observed by Amtrak using TLS or spot treatment. Dashed lines show lower and upper bound used in this study

At the starting year (t=0), the 100-km of track section is installed with new ties, either concrete or ECC, using TLS. Major railroads, including Amtrak, assign a *grade* to each tie to keep track of the condition of the ties over time. The *grade* starts with one upon installation and increases to five when it eventually fails and can no longer retain the distance between the rail tracks required for safe train transit (Cloutier 2014). The defective ties need to be replaced within a month to avoid slower train transit (*slow order*) as mandated by FRA and railroads (Office of Railroad Safety 2018). In the model, linearly increasing function from zero (new installation) to one (failure) is assigned to each tie where the timing of failure is determined by the Weibull function.

The failed ties can be replaced either with spot treatment or TLS. While the decision rule of choosing between spot replacement and TLS can govern the total amount of ties needed and thus the overall economic and environmental profiles of using ties, little information is available. In the

model, the average grade of the ties adjacent to the failed or failing ties is used as a guiding rule. If the average grade exceeds a threshold value that is predefined at the starting of the iteration, all ties within a small section surrounding the failed or failing ties are replaced with TLS; otherwise, only the degraded ties are spot replaced. The newly installed ties follow the same Weibull failure function.

Degrading ties can be preemptively replaced prior to failure to accommodate limited replacement capacity, track availability, and backlogged maintenances. In our model, degraded ties can be replaced 0-6 years prior to failure (Amtrak 2019b) by controlling the degradation threshold at each iteration. Once the grade of a tie exceeds the degradation threshold, it is treated for replacement each month along with the failed ties. While the failed ties cause slow order if untreated, the degraded ties do not induce slow order. All in all, the Monte Carlo model simulates a wide range of tie replacement rules and strategies, from preemptively spot-replacing ties that are nearing failure to minimize slow order, to allowing certain levels of slow orders in order to mass-replace many failed ties efficiently.

The cost of concrete tie replacement is represented to be between $400-$1,000/tie for spot treatment and between $1,000-$3,000/tie for TLS based on recent replacement data of 684,000 concrete ties as shown in Figure 5.4(b) (Northeast Corridor Commission 2018, 2019, Amtrak 2020, Northeast Corridor Commission 2021, 2020). For ECC tie replacement, the cost ranges of concrete tie replacement were modified to reflect the cost premium of ECC tie manufacturing. As a result, the cost of ECC tie replacement with TLS and spot treatment is between $450-1125/tie, and $1015-3050/tie, respectively.

In each Monte Carlo iteration, a representative electric passenger train operates on the track with a predefined daily number of commutes. If the track is free of defective ties, trains are assumed to operate at a maximum allowed speed (MAS) as determined by FRA (Federal Railroad Administration n.d., Office of Railroad Safety 2018). The presence of defective ties will force trains to reduce speed, as low as 10 miles per hour when passing the affected zones. The length of the affected zone and the magnitude of speed reduction are determined by the spatial distribution of the failed ties and follow the regulations set forth by Amtrak and FRA (Federal Railroad Administration n.d., Office of Railroad Safety 2018, Cloutier 2014). While passing the slow-ordered zones, trains need to decelerate to pass the zone at a safe speed then accelerate to recover the MAS. The speed profile is calculated accounting for the tractive effort, traveling speed, and

mass of the trains (National Academies of Sciences Engineering and Medicine 2015). Additional electricity needed for train acceleration is calculated assuming the motors operate at their maximum capacity during the additional phase of the acceleration, which provides an upper bound of the slow-order related cost and emissions. The cost of delay includes ownership and operational cost of the train cars, additional expenditures related to fuel and labor, and lading. Delay cost of the passenger trains also accounts for the cost of additional time of travel Transportation (U.S. Department of Transportation 2016).

5.2.4 Systems-level economic and environmental impact from tie use

The stochastic model generates distributions of 1) how many total numbers of ties are ultimately required to service the track and 2) how many hours of train delays have occurred with associated cost and emissions from altered train operation, considering a wide range of variables and strategies available. The estimated total number of ties is multiplied by the lifecycle cost and emissions associated with manufacturing and disposing of concrete or ECC ties that were estimated in the cradle-to-grave model to yield systems-level cost and emissions directly related to using ties. Cost and emissions associated with the altered train operation include additional diesel fuel or electricity consumed as well as labor, overhead, and delay cost of the transport and passenger. These indirect costs and emissions are added to the tie-related values to result in systems-level costs and emissions of using ties. Lifecycle environmental impacts are assessed with global warming potential (GWP), ozone depletion potential (ODP), acidification potential (AP), and eutrophication potential (EP).

5.3 RESULTS AND DISCUSSION

5.3.1 Economic and environmental profile of tie manufacturing and disposal

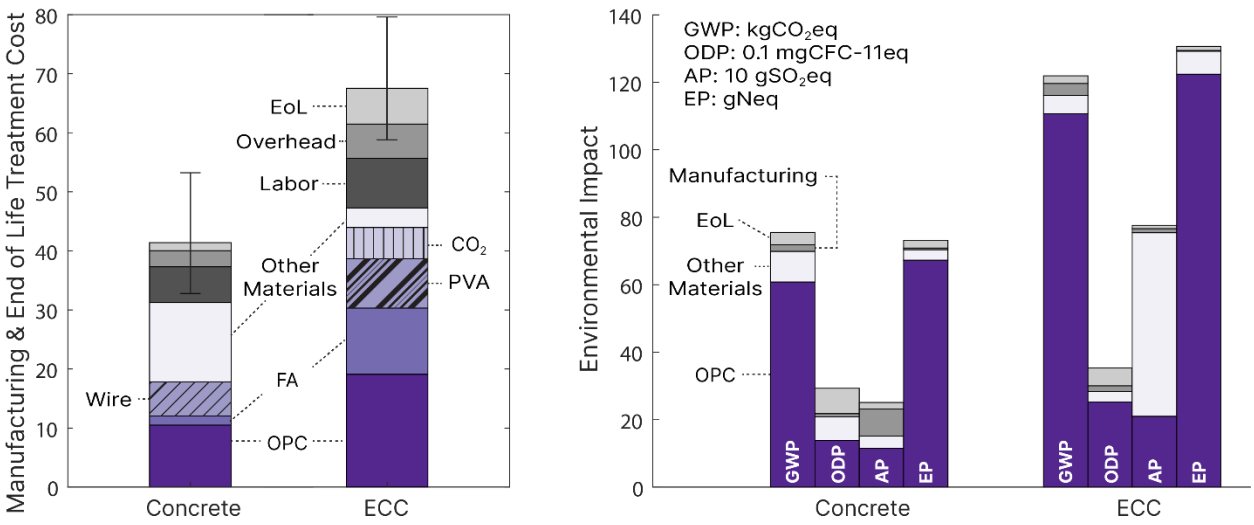

Figure 5.5. Economic and environmental comparison of using a concrete or an ECC tie based on manufacturing and end of life treatment

Figure 5.5 summarizes the cost and environmental impact of manufacturing and disposing of concrete and ECC ties fabricated with added CO_2. Based on the primary materials, equipment, and processes considered, the manufacturing cost of a concrete tie is estimated to be around $40/tie which is lower than the current market cost of around $100/tie. Nearly 78% of the cost is spent on purchasing raw materials. OPC, HRWR, and prestressing wire are collectively responsible for 80% of the material cost. Wage and manufacturing overhead account for about 15% and 7%, respectively. Manufacturing an ECC tie costs nearly $61.5, about 54% more expensive than a concrete counterpart. The cost of raw material rose by 51%, driven by increased use of OPC, FA, and inclusion of PVA fiber. The cost of manufacturing overhead is increased by 112% considering capital expenditure and electricity needed for carbonation curing.

For both concrete and ECC ties, their cradle-to-gate environmental impact is mostly driven by OPC. For instance, the contribution from OPC to GWP comprises over 80% and 90% of the cradle-to-gate emissions for a concrete and ECC tie, respectively. For GWP, ODP, and EP, the cradle-to-gate environmental impacts of an ECC tie increased by 20-78% compared to a concrete tie. The AP impact increased by 200% which is mostly associated with electricity used during recovering CO_2 from ammonia or ethanol plants. GWP contribution from the added CO_2 is less than 2% in ECC manufacturing.

Incorporating CO_2 recovered from air into an ECC tie can reduce its GWP but would not be enough to lower it to or below the GWP of a concrete tie. We assume that CO_2 recovered from the air can be supplied via a first-of-a-kind industrial-scale DAC at $600/tCO2 that has a negative carbon footprint at -0.41 $kgCO_2eq$ of GWP per kg of captured CO_2 (Deutz and Bardow 2021).

Incorporating air-supplied CO_2 would increase the cost fraction of CO_2 in manufacturing from 8.6% to 11% while reducing 6.7 kg CO_2eq of GWP from ECC. With this 5.5% of reduction in GWP, the carbon footprint of ECC is at 115 kgCO_2eq/tie which is still 53% higher than that of a concrete tie. Even in a future scenario when DAC is entirely powered by wind and DAC-supplied CO_2 has a GWP of -0.95 kgCO_2eq/kg, the GWP of an ECC tie would be 44% higher than that of a concrete tie. The increased proportion of OPC in ECC, by over 80% than concrete, and the limited fraction of OPC available for carbonation, about 10 wt%, limits GWP reduction potential with added CO_2. Thus, strategies that can further reduce the mass of OPC in ECC, such as increased inclusion of supplementary cementitious materials or utilizing CO_2-enabled binder reduction (Lim *et al* 2019) can be prioritized to facilitate additional CO_2 reduction.

While significantly improved tensile strength and ductility of ECC as well as the elimination of the prestressing element are expected to provide an expanded service life for ECC ties, this is yet to be validated through field studies. A past study of using ECC as a bridge link slab (Keoleian *et al* 2005) assumed doubling of product life with ECC and found a significant reduction in environmental impact compared to conventional design, which is implicitly uncertain and needs future validation. The studied ECC-based bridge deck link slab was installed in southeast Michigan, the USA in 2005. Thus far, the installed ECC link slab shows little sign of traditional wear after nearly 15 years in use (University of Michigan n.d.). Based on our cradle-to-grave economic and environmental impact analysis, an ECC tie needs to last about 60% longer than a concrete tie to be economically and environmentally – based on GWP – competitive, respectively, which is less than 100% increase in service life assumed in the bridge link slab study. But ultimately, testing ECC ties in a real environment should be part of priorities of future work.

5.3.2 Systems-level economic and environmental impact

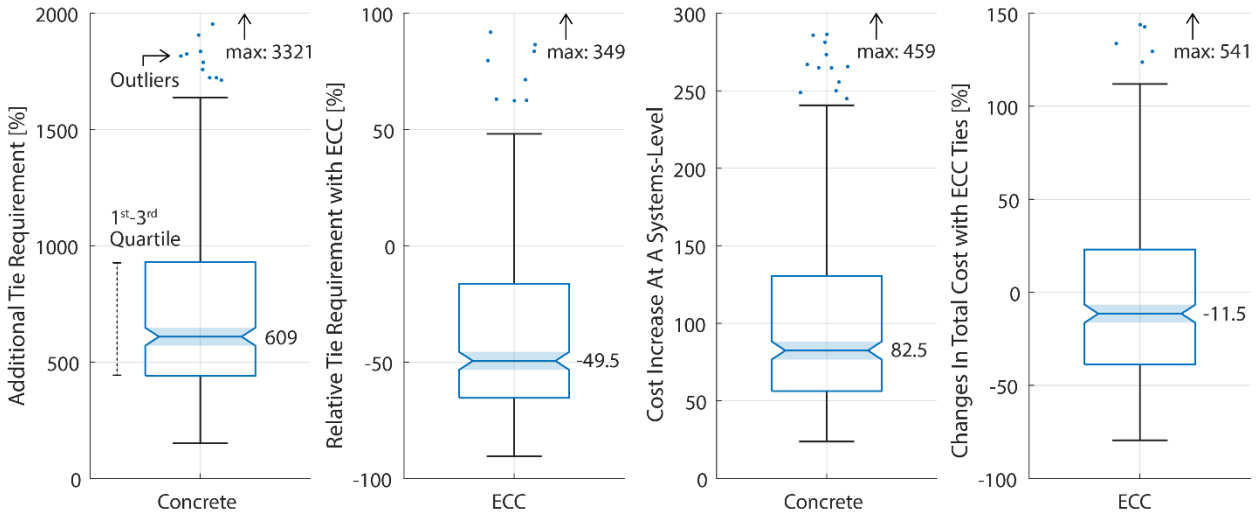

Figure 5.6. Systems-level impact from use-phase shows (a) additional concrete ties needed throughout lifecycle relative to what's initially needed, (b) reduction in total tie requirements when switching to ECC ties, (c) systems-level cost increase when using concrete ties, and (d) lifecycle cost reduction when switching to ECC ties

However, the inclusion of stochastic replacement of ties and possible train delays provides a substantially different economic and environmental outlook of using ties (Figure 5.6). If the track is constructed with ideal concrete ties that do not prematurely fail until the end of design life as assumed in *all* past studies (Crawford 2009, Bolin and Smith 2013, Rempelos *et al* 2020), a total of 2-3x the number of ties needed to build the track is needed over 100 years. But when the stochastic tie failure is accounted for, the total number of ties needed increases by nearly six times using the median value. When ECC ties are used, the total number of ties needed over 100 years decreases by 50% compared to using concrete ties.

The cost of using ECC ties can be lower than using concrete ties when direct and indirect costs incurred during the use phase are accounted for. The initial tie-related construction cost of a 1km rail track using concrete ties is estimated to be around 0.76-1.7 million USD. If the concrete ties behave ideally, 5-16% more cost would be incurred throughout 100 years of use from tie replacement based on a 5% annual discount rate. However, accounting for the systems-level impact increases these values to nearly 82% due to extra ties and delays in train transit. Switching concrete ties with ECC results in an overall cost reduction by 11% at the systems level, although manufacturing and disposing of an ECC tie is 63% more expensive than a concrete tie.

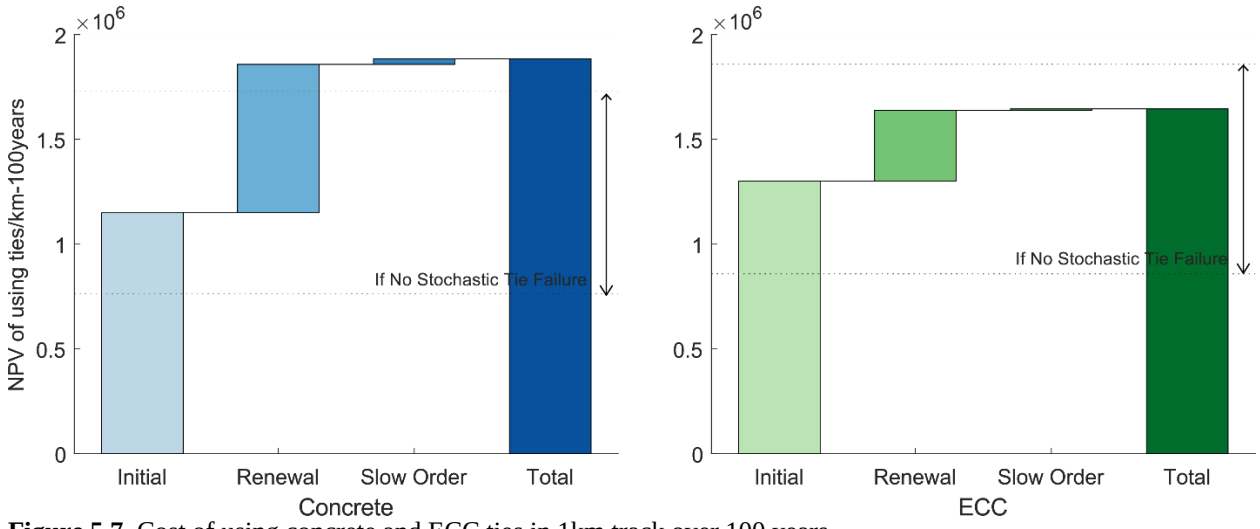

Figure 5.7. Cost of using concrete and ECC ties in 1km track over 100 years

The primary drivers of lifecycle cost increase when using ties include recurring tie replacement activities and train delays. Figure 5.7 presents the inventory of lifecycle cost of using concrete and ECC ties in terms of the cost of initial tie installation, recurring stochastic tie replacement events, and train delays. Each of these categories is represented with a median value taken from the 400 Monte Carlo iterations to highlight the relative contributions. Here, the initial tie installation cost involves the cost of tie purchasing as well as the overhead cost of TLS such as capital and operational expenditures and labor. Tie replacement after initial installation can be performed in a combination of spot treatment and TLS according to the strategies employed in each of the uncertainty scenarios. While the initial installation cost is higher for ECC ties, decreases in the total number of ties needed and the resultant train delays during use make the systems-level cost of using ECC ties about 24% lower than that of using concrete ties. While there exist extreme cases where delay-related cost overwhelms the systems-level cost, recurring tie replacement cost is the dominant contributor to the systems-level cost based on median values.

While the cost contributions of tie replacement and train delay were less than that of the initial tie replacement, they can drive up the lifecycle cost when suboptimal tie replacement strategies are implemented. These inadequate strategies commonly feature at least one of the following patterns: 1) an excess number of ties are used due to a heavy reliance on TLS that prematurely replace a substantial number of non-defective ties, 2) trains are significantly delayed by backlogged replacements due to a combination of limited replacement capacity and a narrow temporal window for tie replacement just before its failure. In an extreme case, the entire track length was renewed with concrete ties 33 times after the initial installation. In another case, the

delay-related cost can overwhelm (77%) the total system-level cost. The lifecycle cost of using ties can rise significantly as a result, as shown in the distribution in Figure 5.6. In these cases, the cost of tie renewal or slow order can increase up to nearly three times the cost of initial tie installation and dominate the systems-level cost.

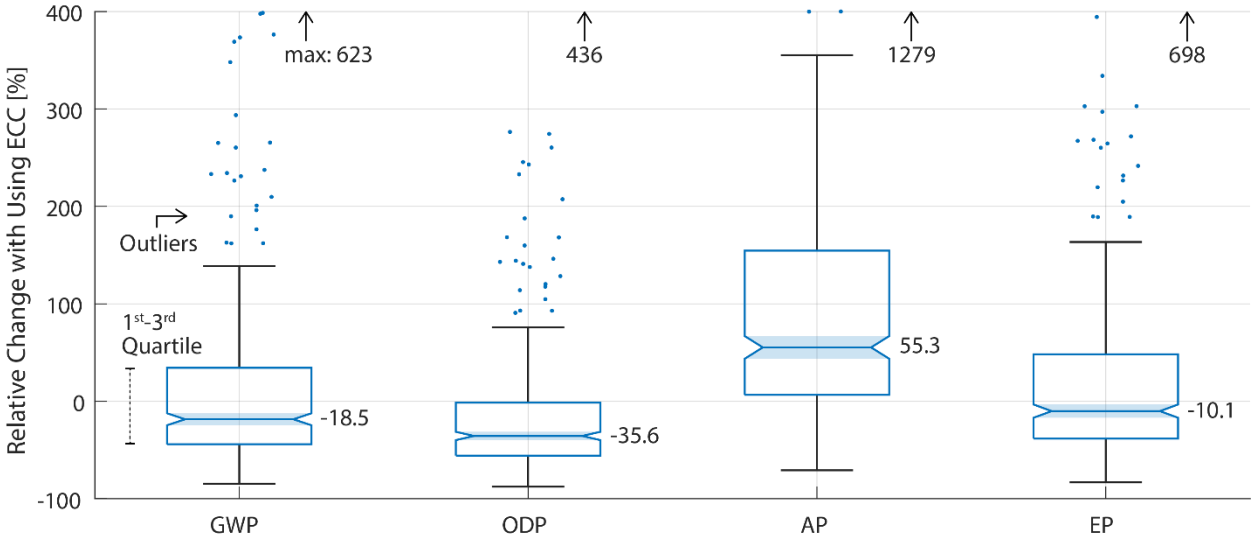

Figure 5.8. Relative changes in lifecycle GWP, ODP, AP, and EP when switching from using concrete to ECC ties

The expanded scope of the systems-level analysis also provides a substantially different environmental perspective of using ties. Compared to the emissions associated with the initial tie installation, the overall emissions from tie use over 100 years increases by nearly seven-fold in all environmental impact parameters considered due to recurring tie replacements and train delays. While the lifecycle environmental impact from manufacturing and disposing of an ECC tie is generally higher than a concrete tie by 20-78%, or by 200% for AP, switching to ECC ties results in an overall decrease in lifecycle environmental footprints over 100 years as shown in Figure 5.8. For instance, the GWP is decreased by 18% based on the median, driven by a reduced total number of ties used over 100 years; switching to ECC ties results in a 49% reduction in the total ties needed to maintain the track.

5.3.3 Probability of yielding net economic and environmental benefits with ECC ties

While switching to ECC ties results in net reductions in lifecycle cost and emissions at median cases, the lifecycle cost and/or emissions increased in many simulated scenarios. Based on 400 Monte Carlo iterations, using ECC ties has a 61% probability of reducing lifecycle GHG emissions and a 61% chance of reducing lifecycle cost relative to using concrete ties. The rather limited magnitude of GWP reduction and the likelihood to reduce GWP with ECC is associated with

increased GHG emissions during the manufacturing and disposal of an ECC tie, which is 62% higher than that of a concrete tie.

Note that this analysis assumes that ECC ties have a 40% longer service life on average relative to concrete ties which is yet to be validated through field studies. To further explore the uncertainties related to the longevity of ECC ties, we adjusted the upper bound of its service life and generated another sets of Monte Carlo results using the same replacement and train parameters. We found that the average service life of ECC ties needs to be at least 25% longer than that of concrete ties to induce net GWP reductions at median distribution. At this longevity level, total GWP was reduced with ECC in 50% of the iterations. Increasing the average longevity of ECC ties to twice as long as concrete ties increase both the magnitude (from 18 to 49%) and probability (from 61 to 70%) of net GWP reduction with ECC. If the mean service life of ECC increased from 40% to 100% longer than concrete ties, the systems-level cost of using ECC ties further reduces from -11% to -23% at median distribution. The primary driver of improvement in both systems-level cost and emissions is a reduction in the total number of ties needed; the decrease in the number of ties needed was further reduced from -49% to -68% at the median.

The rather moderate level of further cost reductions with increasing longevity is in part influenced by the annual discount rate (r). Reducing r from 5% to 0% results in a 4-6x increase in the systems-level cost of using concrete and ECC ties, which illustrates the significance and magnitude of the tie replacement and train delays that occur in the future. Thus, the systems-level cost reduction with ECC can be magnified with low r, as most longevity-related benefits occur in the future. At r = 0% discount rate, median cost savings with ECC ties when they last twice as long is -65%, rather than -23% when r = 5%. The percentage of iterations where ECC ties yield net cost reduction further increases from 70% to 82% at the same time.

To capitalize on the systems-level cost and emissions reductions that are spread out in the future, ECC ties first need to overcome the initial cost barrier of manufacturing. In the US, section 45Q tax credit can provide up to $35 per tonne of CO_2 sequestered for industrial CO_2 utilization projects that are not for enhanced oil recovery. Our model ECC facility can sequester 2,160 tCO_2 by producing about 180,000 ties each year. The 45Q would provide up to $0.4 of credit per ECC tie, which can cover less than 10% of the increased manufacturing overhead when producing ECC ties, not accounting for the increased cost of raw materials. The minimum eligibility requirement of sequestering 25 ktCO_2 each year further challenges the effectiveness of 45Q; meeting minimum

eligibility would require scaling up the model ECC facility by more than an order of magnitude. Multiple bills have been introduced after the 2018 amendment of 45Q to eliminate the eligibility threshold and to expand the scale of financial incentives (Clean Air Task Force 2021). Many bills aim to increase the credit to industrial sequestration up to $85/tCO2. However, even with this increase, the ECC plant would only receive $1/tie which can cover less than 20% of the increased overhead cost. Compensating for the increased overhead cost of producing ECC solely through sequestration-based incentives would require close to $450 of credit per tonne of CO_2 sequestered, which is more than two times higher than the highest credit being proposed.

5.3.4 Conclusions

In this study, we systematically compared the lifecycle cost and emissions of using CO_2-cured railway ties designed with ECC in comparison to conventional concrete ties. The cradle-to-grave lifecycle model is combined with a stochastic use-phase model of concrete and ECC ties that generates a set of uncertainty results based on a wide range of assumptions on tie failure, tie replacement strategies, and capacities, as well as impacts on train operation. We find that the cost and GWP associated with manufacturing and disposing of an ECC tie increases by 63% and 62% relative to a concrete tie, respectively, which is largely driven by the increased proportion of Portland cement used in ECC ties. The incorporation of air-captured CO_2 can partially offset (11%) the increased GWP of an ECC tie but it would still be 44% higher than a concrete tie. However, we find that using ECC ties results in net reductions in lifecycle cost and environmental impacts due to a substantially lower number of ties being needed throughout the product lifecycle. ECC ties can result in net GWP reduction once its service life is 25% greater than concrete ties. If ECC ties can last twice as long, the systems-level cost of using ties can reduce by 23% with a 5% discount rate while GWP reduces by 49%. Upgrading all ties in NEC with ECC would sequester a total of 47 ktCO_2 over 100 years while annually reducing 1 ktCO_2 compared to using concrete ties. The practical scale of CO_2 reduction maybe higher when increased ridership from reduced train delays is accounted for, which is outside the scope of this study. The minimum sequestration requirement of 45Q would preclude ECC plants from benefiting from the incentive and even if it can, sequestration-based 45Q would only cover <10% of the increased manufacturing overhead. Our results highlight the need for policies to prioritize lifecycle GHG reduction, including both stored and avoided emissions, to unlock the potentials of CO_2-based solutions.

5.4 REFERENCES

AISI and SMA 2021 *Determination of Steel Recycling Rates in the United States*

Amtrak 2019a *Amtrak. 2019. Train Operations- Better Estimates Needed of the Financial Impacts of Poor On-Time Performance*

Amtrak 2020 *Five-Year Plans - Service and Asset Line Plans | FY 2021-2026*

Amtrak 2021 *General and Legislative Annual Report & Fiscal Year 2019 Grant Request* Online: https://www.amtrak.com/content/dam/projects/dotcom/english/public/documents/corporate/reports/Amtrak-General-Legislative-Annual-Report-FY2019-Grant-Request.pdf

Amtrak 2019b *Infrastructure Asset Line Plan FY20-24* Online: https://www.amtrak.com/content/dam/projects/dotcom/english/public/documents/corporate/businessplanning/Amtrak-Infrastructure-Asset-Line-Plan-FY20-24.pdf

Amtrak 2012 *Report on Concrete Ties on Amtrak's NEC* Online: https://downloads.regulations.gov/FRA-2011-0027-0017/attachment_1.pdf

Anon 1991 *In Re Lone Star Ind. Concrete Rr Cross Ties Lit.* Online: https://law.justia.com/cases/federal/district-courts/FSupp/776/206/2340316/

Bolin C A and Smith S T 2013 Life Cycle Assessment of Creosote-Treated Wooden Railroad Crossties in the US with Comparisons to Concrete and Plastic Composite Railroad Crossties *J. Transp. Technol.* **03** 149–61 Online: http://www.scirp.org/journal/doi.aspx?DOI=10.4236/jtts.2013.32015

Clean Air Task Force 2021 Scaling Up Climate Ambition: Carbon Capture, Removal, and Storage Priorities in the 117th Congress Online: https://www.catf.us/2021/05/scaling-up-climate-ambition-carbon-capture-removal-and-storage-priorities-in-the-117th-congress/

Cloutier A 2014 Concrete Ties - The Amtrak Experience

Commercial Metals 2015 *Environmental Product Declaration - Concrete Reinforcing Steel* Online: https://www.astm.org/CERTIFICATION/DOCS/253.EPD_for_Concrete_Reinforcing_Steel.pdf

Crawford R H 2009 Greenhouse Gas Emissions Embodied in Reinforced Concrete and Timber Railway Sleepers *Environ. Sci. Technol.* **43** 3885–90 Online: https://pubs.acs.org/doi/10.1021/es8023836

Deutz S and Bardow A 2021 Life-cycle assessment of an industrial direct air capture process based on temperature–vacuum swing adsorption *Nat. Energy* **6** 203–13 Online: http://www.nature.com/articles/s41560-020-00771-9

European Federation of Concrete Admixtures Associations Ltd. (EFCA) 2020 Concrete admixtures – Air entrainers

European Federation of Concrete Admixtures Associations Ltd. (EFCA) 2015 *Environmental Product Declaration: Concrete admixtures – Plasticisers and Superplasticisers*

Federal Railroad Administration 2012 *Analysis of the Causes of Amtrak Train Delays*

Federal Railroad Administration Track and Rail and Infrastructure Integrity Compliance Manual: Volume II - Track Safety Standards, Chapter 1 Track safety Standards Classes 1 through 5

Global Cement and Concrete Association 2021 *Roadmap for Net Zero Concrete* Online: https://gccassociation.org/concretefuture/wp-content/uploads/2021/10/GCCA-Concrete-Future-Roadmap.pdf

H.J. Grimbergen b.v. 2007 L. B. Foster successfully introduces Long-line Production Technology to manufacture CXT ® Concrete Ties 290–3 Online: https://www.grimbergen.nl/wp-content/uploads/2016/02/Foster_0207_en.pdf

International Energy Agency 2020 *Energy Technology Perspectives 2020* (OECD) Online: https://www.oecd-ilibrary.org/energy/energy-technology-perspectives-2020_ab43a9a5-en

International Energy Agency 2018 *Technology Roadmap - Low-Carbon transition in the Cement Industry* Online: https://webstore.iea.org/technology-roadmap-low-carbon-transition-in-the-cement-industry

Keoleian G A, Kendall A, Dettling J E, Smith V M, Chandler R F, Lepech M D and Li V C 2005 Life Cycle Modeling of Concrete Bridge Design: Comparison of Engineered Cementitious Composite Link Slabs and Conventional Steel Expansion Joints *J. Infrastruct. Syst.* **11** 51–60 Online: http://ascelibrary.org/doi/10.1061/%28ASCE%291076-0342%282005%2911%3A1%2851%29

Li V C 2008 Engineered cementitious composite (ecc): Material, structural, and durability performance *Concrete Construction Engineering Handbook, Second Edition* pp 1001–48

Lim T, Ellis B R and Skerlos S J 2019 Mitigating CO_2 emissions of concrete manufacturing through CO 2 -enabled binder reduction *Environ. Res. Lett.* **14** 114014 Online: http://iopscience.iop.org/article/10.1088/1748-9326/ab466e

Lovett A H, Dick C T, Ruppert C and Barkan C P L 2015 Cost and Delay of Railroad Timber and Concrete Crosstie Maintenance and Replacement *Transp. Res. Rec. J. Transp. Res. Board* **2476** 37–44 Online: http://journals.sagepub.com/doi/10.3141/2476-06

MacLEAN J D 1957 *Percentage Renewals and Average Life of Railway Ties*

Mayville A R, Jiang L and Sherman M 2014 Performance Evaluation of Concrete Railroad Ties on the Northeast Corridor 171p Online: http://www.fra.dot.gov/Elib/Document/3610%5Cnhttps://trid.trb.org/view/1304992

Milford R L and Allwood J M 2010 Assessing the CO_2 impact of current and future rail track in the UK *Transp. Res. Part D Transp. Environ.* **15** 61–72 Online: http://dx.doi.org/10.1016/j.trd.2009.09.003

Nagataki S, Gokce A, Saeki T and Hisada M 2004 Assessment of recycling process induced damage sensitivity of recycled concrete aggregates *Cem. Concr. Res.* **34** 965–71 Online: https://linkinghub.elsevier.com/retrieve/pii/S0008884603004046

National Academies of Sciences Engineering and Medicine 2015 *Technical Document and User Guide for the Multi-Modal Passenger Simulation Model for Comparing Passenger Rail Energy Consumption with Competing Modes* (Washington, D.C.: Transportation Research Board) Online: http://www.nap.edu/catalog/22080

National Ready Mixed Concrete Association 2016 *NRMCA Member National and Regional Life Cycle Assessment Benchmark (Industry Average) Report – Version 2 . 0* Online: https://www.nrmca.org/sustainability/EPDProgram/Downloads/NRMCA_Benchmark_Report_-_October_14_2014_web.pdf

Northeast Corridor Commission 2020 Northeast Corridor Annual Report : Operations and Infrastructure Fiscal Year 2019

Northeast Corridor Commission 2021 Northeast Corridor Annual Report : Operations and Infrastructure Fiscal Year 2020

Northeast Corridor Commission 2018 Northeast Corridor One-Year Implementation Plan Fiscal Year 2018

Northeast Corridor Commission 2019 Northeast Corridor One-Year Implementation Plan Fiscal Year 2019

Office of Railroad Safety 2018 *Track and Rail and Infrastructure Integrity Compliance Manual: Volume II - Chapter 2 - Track Safety Standards Classes 6 through 9* Online: https://railroads.dot.gov/elibrary/track-and-rail-and-infrastructure-integrity-compliance-manual-volume-ii-chapter-1-0

Personal communication 2021 Sioux Corporation

Portland Cement Association 2021a *Environmental Product Declaration - Portland Cement*

Portland Cement Association 2021b *Roadmap to Carbon Neutrality* Online: www.cement.org

Precast/Prestressed Concrete Institute 2021 *Manual for Quality Control for Plants and Production of Structural Precast Concrete Products, 5th Edition (MNL-116-21)* (Precast/Prestressed Concrete Institute)

Railway Tie Association 2010 *Assessment of Concrete Tie Life on U.S. Freight Railroads* Online: http://www.rta.org/assets/docs/TieReports/tie report 12.pdf%0Ahttp://www.rta.org/tiereports

Rempelos G, Preston J and Blainey S 2020 A carbon footprint analysis of railway sleepers in the United Kingdom *Transp. Res. Part D Transp. Environ.* **81** 102285 Online: https://doi.org/10.1016/j.trd.2020.102285

Smith S T 2019 2018 Railroad Tie Survey *J. Transp. Technol.* **09** 276–86 Online: http://www.scirp.org/journal/doi.aspx?DOI=10.4236/jtts.2019.93017

Sullivan D F 1983 Rationale and Technology Used By Amtrak To Select Concrete Ties for Use in Northeast Corridor *Transp. Res. Rec.* 1–6

U.S. Department of Transportation 2016 Revised Departmental Guidance on Valuation of Travel Time in Economic Analysis Online: https://www.transportation.gov/office-policy/transportation-policy/revised-departmental-guidance-valuation-travel-time-economic

University of Michigan Bendable Concrete Utilized on a Bridge Deck Online: https://www.urbanlab.umich.edu/project/bendable-concrete-utilized-on-a-bridge-deck-engineered-cementitious-composite-or-ecc/

Werner F, Richter K, Holz A, Dübendorf E, Levering M, Vuilleumier M-A, Infrastruktur S, Sven-Dirk Richtberg B, Dummer J, Arlt O, Wülknitz GmbH I, Peter Nowaczyk W and Schrägle R 2009 Life cycle assessment (LCA) of railway sleepers Comparison of railway sleepers made from concrete, steel, beech wood and oak wood 7 Online: http://www.vhn.org/pdf/LCA-biels-samenv.pdf

Wernet G, Bauer C, Steubing B, Reinhard J, Moreno-Ruiz E and Weidema B 2016 The ecoinvent database version 3 (part I): overview and methodology *Int. J. Life Cycle Assess.* **21** 1218–30 Online: http://link.springer.com/10.1007/s11367-016-1087-8

Zhang D, Ellis B R, Jaworska B, Hu W-H and Li V C 2021 Carbonation curing for precast Engineered Cementitious Composites *Constr. Build. Mater.* **313** 125502 Online: https://doi.org/10.1016/j.conbuildmat.2021.125502

Zimmerman A, Müller L and Wang Y 2020 *Techno-Economic Assessment & Life Cycle Assessment Guidelines for CO_2 Utilization (Version 1.1)* Online: http://hdl.handle.net/2027.42/162573

CHAPTER 6
Conclusions

6.1 Dissertation Summary and Implications

Carbon removal from the atmosphere is increasingly regarded as an irreplaceable strategy to limit global temperature rise below 2°C or 1.5°C relative to the preindustrial era as set forth in the Paris Agreement. Making carbon removal available at a required giga-tonne scale and integrating recovered CO_2 into the existing energy and industrial infrastructure in an optimal fashion is contingent on overcoming scientific, technological, and social-economic challenges in a timely manner. This dissertation aims to advance our knowledge of the role of carbon removal and utilization in the overall carbon reduction scheme, not only in terms of providing negative emissions but also in enabling other strategies that can facilitate further CO_2 reductions. Our results highlight both the opportunities and further research directions to advance DAC process and to maximize net CO_2 reduction by utilizing CO_2 in the existing industry.

The results from Chapter 2 highlight the criticality of undertaking immediate, sustained carbon mitigation measures to minimize the overall cost of meeting climate targets. Delays in initiating deep decarbonization will require supplementing carbon mitigation from fossil sources with carbon removal whose scale and cost are determined by the magnitude of delay. According to Chapter 2, compensating for the delay-induced excess CO_2 emissions with NET would be costly; each day of delay starting 2020 incurs an additional 100-345 million USD to meet 70% reduction goals in the U.S. electric sector. This delay cost accounts for the installation cost of DAC plants as well as cost to transition into low-carbon technologies, prematurely retiring young natural gas generators, and expanding the overall electricity generation capacity to power DAC plants. In the U.S. electricity sector alone, meeting the CO_2 reduction target became infeasible once mitigation measures were delayed more than 15 years due to ballooning costs. Our findings are supported by a recent global-level assessment of using DAC to meet 1.5°C or 2°C climate targets (Realmonte *et al* 2019) where global CO_2 emissions need to peak by 2035 to meet the climate

goals and that high energy demand from DAC would entail a substantial transformation of the global energy infrastructure. However, the global CO_2 emissions are estimated to continuously increase in the near term (Robiou du Pont *et al* 2016), which is a suboptimal, risky route that would evidently rely on large-scale deployment of NETs to meet climate targets.

Thus, optimizing the carbon removal process (Chapter 3) and exploring strategies to maximize carbon reduction via removal (Chapter 4-Chapter 5) will be critical. In Chapter 3, we experimentally verified one alternative mechanism to recover CO_2 from sorbent in the DAC process using a microwave. A combination of experimental measurement and simulation calculations show that microwave application may reduce the overall processing time of CO_2 desorption from approximately an hour to a matter of minutes. The increased throughput has a potential to substantially reduce the overall system cost of DAC through downsizing, which motivates future techno-economic analysis (TEA) of such a configuration. The low observed temperature (45-55°C) of the desorbed CO_2 gas suggests that microwave induces low-temperature desorption mechanism driven by a selective heating process which is inherently more energy-efficient than conventional bulk heating mechanism. This observation is consistent with the findings of the past studies on microwave-based sorbent regeneration where microwave selectively heat adsorbate-adsorbent binding sites (Meier *et al* 2009, Turner *et al* 2000, Coss and Cha 2000, Polaert *et al* 2010, Chronopoulos *et al* 2014, Webley and Zhang 2014, Cherbański and Molga 2009, Falciglia *et al* 2018). Future research can focus on validating the selective process and low energy mechanism using an alternative experimental configuration that generates more uniform heating. Also, techno-economic assessment can study systems-level implications on cost and energy demand of the DAC system when the rapid regeneration process with microwave can be used to downsize the system. Such a high-throughput, reduced-size system may accelerate the implementation of DAC as capital cost related to sorbent is expected to dominate the overall system cost in the future (National Academies of Sciences Engineering and Medicine 2019).

The cement and concrete industry provide a unique avenue to sequester CO_2 to generate additional CO_2 reduction (Chapter 4) and to mass-produce CO_2-cured products (Chapter 5). Results of Chapter 4 show that CO_2-induced property changes of the material can be used to substantially increase the magnitude of the net CO_2 reduction. Direct sequestration alone could offset close to 1% of the CO_2 emitted during the manufacturing of concrete. However, over an order of magnitude more CO_2 can be avoided when binder reduction enabled by CO_2-induced

strength development can be jointly implemented with CO_2 sequestration; the net CO_2 reduction can increase to nearly 40% of the annual CO_2 emissions from the U.S. concrete industry without relying on novel materials or carbon capture and sequestration. We estimate that roughly a gigatonne of CO_2 emissions can be reduced by globally implementing this strategy, which is almost a third of the emissions originating from cement and concrete production today. This alternative CO_2 utilization and sequestration strategy can potentially provide an alternative to NETs that are based on the offset. However, further research is required to reduce uncertainties to generate more accurate insights on reduction potentials.

Precast applications provide near-term opportunities to mass-produce CO_2-cured products. In Chapter 5, lifecycle assessment coupled with stochastic use-phase model showed that railway ties designed with CO_2-cured ECC can yield net reductions in cost and GHG emissions relative to conventional prestressed concrete counterparts. The level of economic and environmental benefits is determined by the degree of service life expansion which is yet to be validated in the field. A point of reference can be provided by a case study where a bridge link slab designed with ECC was installed in Michigan, USA in 2005. Thus far, the installed ECC link slab shows little sign of traditional wear after nearly 15 years in use (University of Michigan n.d.). (Keoleian *et al* 2005) found a significant reduction in environmental impact based on the doubling of the life of the ECC structure. If the ECC tie can last twice as long, as suggested by (Keoleian *et al* 2005), net GHG emissions can be reduced by 49% throughout the product lifecycle including consequential emissions from altered train operations. Based on 40% of longevity improvement with ECC, upgrading all ties in NEC with ECC would sequester a total of 47 $ktCO_2$ over 100 years while annually reducing 1 $ktCO_2$ compared to using concrete ties. Field tests can provide further evidence on the service life of ECC rail tie and thus its lifecycle economic and environmental benefits.

The real value of CO_2 utilization and sequestration in cement and concrete hinges on reducing potential reliance on NET through 1) complementing ongoing fossil fuel mitigation now, and 2) decreasing recalcitrant CO_2 emissions from cement production, rather than its absolute scale of sequestration. As shown in Chapter 4, the global application of CO_2 utilization throughout the concrete industry is expected to sequester 32-41 $MtCO_2$ each year, which is orders of magnitude smaller than up to 20 $GtCO_2$ that needs to be annually sequestered in the geosphere by 2100. CO_2 utilization in cement and concrete, however, can be implemented now to supplement urgently

needed immediate CO_2 reduction that can substantially decrease the overall cost of meeting the reduction target (Chapter 2). The near-term CO_2 utilization strategy such as CO_2-embodying railway tie production (Chapter 5) can thus create lasting economic and environmental benefits despite its small sequestration potential in an absolute scale. At the same time, CO_2 utilization provides an alternative strategy to reduce recalcitrant emissions generated during cement production, especially when CO_2 is creatively utilized to further reduce emissions as highlighted in Chapter 4. The associated cost saving opportunities can further accelerate early and expanded adaptation of these novel strategies that can maximize economic and environmental benefits.

The recent, and ongoing, pandemic caused by Coronavirus disease 2019 (COVID-19) has generated an unprecedented impact on GHG emissions. The global GHG emissions in 2020 dropped by nearly 7% relative to 2019 driven by severe perturbation in human activities (Friedlingstein *et al* 2020). This level of reduction is aligned with the mitigation pathway compatible with meeting the 1.5°C goal (Matthews *et al* 2020). However, this record GHG reduction is deemed temporary as the global emissions are rapidly rebounding back to the pre-COVID level (Friedlingstein *et al* 2020). While this highlights the magnitude of carbon inertia the global society needs to overcome, this also opens opportunities to accelerate carbon reduction measures. Until the end of August 2020, 12.2 trillion USD of stimuli packages were amassed globally in response to COVID (Andrijevic *et al* 2020). The same paper finds that additional net investment to support low-carbon transformation at the same period is a mere 0.2% of the announced stimuli, suggesting opportunities to support climate-positive post-COVID recovery. This dissertation supports the inclusion of a bold and robust framework to support nascent carbon removal and utilization technologies and applications to align the recovery plans with the climate goals.

The analyses of this work highlight the needs to base policy with the lifecycle CO_2 reduction benefits, including avoided CO_2. In the U.S., the existing 45Q tax credit was amended in 2018 to provide a tax incentive for carbon capture and sequestration projects across industry, which is regarded as one of the most comprehensive financial inventive to date. The incentive provided by 45Q is based on the quantity of CO_2 sequestered; the current system provides up to $35 for CO_2 storage in industrial applications that are not enhanced oil recovery (Jones and Sherlock 2020). While this sequestration-based policy provides clear financial initiatives for emerging CCUS projects, we find that its sequestration basis neglects avoided CO_2, whose reduction potentials

could be an order of magnitude larger than sequestration alone (Chapter 4), and the minimum eligibility requirement risk excluding many prominent CO_2 sequestration projects. For instance, an ECC plant that annually manufactures 180,000 rail ties (Chapter 5) can store 2,160 tCO_2, which is an order of magnitude smaller than the minimum requirement of 25 $ktCO_2$. Even when this eligibility requirement is lifted and the incentive expanded to provide \$85/tCO_2 as proposed by policy advocacies (Clean Air Task Force 2021), the provided incentive (\$1/tie) can cover less than 20% of the additional manufacturing overhead incurred compared to producing conventional concrete ties. These shortfalls further extend to carbonation during mixing or carbonation of recycled concrete aggregates that can offer much higher CO_2 reduction (Chapter 4); the amount of CO_2 sequestered by typical concrete plants though these techniques are anticipated to be less than 0.15 $ktCO_2$. Our results make it clear that appropriate policy needs to consider avoided CO_2 to incentivize maximizing the overall carbon reduction. Systems-level consideration and lifecycle assessment are indispensable tools for successfully evaluate and promote CO_2 mitigation, especially when the beneficial use of CO_2 unlocks additional carbon reduction whose magnitude could be larger than the offset provided by stored CO_2.

Between 2020 and 2021, the first open solicitation for carbon removal was made by Microsoft and Stripe. Microsoft aims to remove all of its emissions – current, and past – by 2050 since its foundation in 1975. To avoid solutions with low reliability and permanence and to support *high-quality* solutions that are measurable, reliable, and generate net removal, the proposals focusing on CO_2 avoidance – roughly 25% of the received projects – were rejected (Joppa *et al* 2021). This rule may be used to differentiate geosphere-based solutions from biosphere-centric projects. But this rule will need further refinement before it can be applied to the coupled CO_2 storage and binder reduction strategy explored in this work; CO_2 is permanently stored at a measurable quantity, yet the primary CO_2 mitigation occurs through avoided emissions from binder reduction. The ambiguity in the current rule permits both rejection of the strategy based on the reliance on avoidance and support of the strategy considering the permanence and the scale of the carbon reduction. The timely resolution of these key questions could accelerate the development of a range of CO_2 removal, utilization, and sequestration strategies that are rapidly gaining academic and entrepreneurial interests. Defining and delineating the quality of CO_2 removal based on the permanence, uncertainties, quantifiability, side effects, co-benefits, and potential scale would

require consolidated efforts amongst academia and industry which would be crucial in advancing promising carbon removal solutions in a timely manner.

6.2 Future Research Directions

6.2.1 Advancing microwave-based CO_2 recovery

While this work validated the rapid CO_2 recovery process with microwave, the energy demand of the process and its systems-level implication need further exploration. One of the challenges identified in our experiments was impedance matching of sorbent load with microwave source; the configuration utilized in our experiment was only able to utilize about 5% of the incident energy to induce CO_2 desorption. The leakage of microwave further complicated accurate characterization of energy dissipated during the process. These challenges, however, are not inherently impossible to overcome. Microwave has been widely used in industrial settings, such as food processing, to substantially reduce the overall energy demand of the system relative to the conventional heating method. The efficiency of these commercial, industrial-scale systems typically exceeds 90%. Another major challenge includes heating uniformity. The applicator used in this work created a strong temperature gradient across the packed sorbent that overheated core while underheating sorbents near the outer edge. Uniform heating can prevent excess energy demand while shortening the process by avoiding prolonged microwave application for underheated regions. The new designs can also consider the joint application of microwave and conductive heat transfer where microwave can be used to heat the interior of the sorbent volume whereas the outer surface can be heated through conduction. Such a design may be able to exploit the benefits of both processes to further reduce energy demand and processing time of the CO_2 recovery process. High-frequency electromagnetic modeling tools can be used to design and test different configurations with high accuracy, but ultimately experimental validation would be needed to prove the simulation and advance the design.

6.2.2 Techno-economic and lifecycle assessment of novel DAC process

TEA and LCA can shed light on the potential systems-level benefits and challenges of the novel microwave-based desorption process as well as its overall environmental impact. A recent review of the NETs suggest that the system cost of the n^{th}-of-a-kind mature DAC system in the future would be largely composed of capital expenditures to procure sorbents (80%) considering

the typical service life of sorbents of 0.25-5 years (National Academies of Sciences Engineering and Medicine 2019). This suggests that the system downsizing enabled by a rapid regeneration process with microwave may induce substantial cost reduction of the DAC system. For instance, reducing regeneration duration from an hour to 20 minutes can reduce the overall CO_2 recovery cycle time by a third which enables recovery of the CO_2 using 34% fewer sorbent materials. The future TEA and LCA studies can be designed to address the following questions to advance our knowledge on DAC process and assess market potentials of the microwave-based CO_2 recovery techniques:

1. What is the practical range of the increased throughput based on the achievable range of processing time?
2. What level of system efficiency is needed for a microwave-based system to economically compete with the conventional DAC design?
3. What are the tradeoffs between maximizing system efficiency and minimizing processing time?
4. What are the technological and environmental implications of the system downsizing and increased reliance on electricity?

Microwave is one of the many possible alternative configurations that can be used to recover CO_2. Examples of other alternative designs include, but are not limited to, using humidity (Shi *et al* 2020) or pH swing (Jin *et al* 2020) in place of temperature and pressure gradient or assisting conventional regeneration with steam (Gebald *et al* 2019). Non-thermal plasma application is also demonstrated to desorb CO_2 from sorbents (Okubo *et al* 2017). TEA and LCA studies are gaining traction regarding DAC designs based on plant-level data published in 2018 and 2021 (Deutz and Bardow 2021, Terlouw *et al* 2021, Keith *et al* 2018, van der Giesen *et al* 2017). Expanding such studies to emerging DAC techniques would enable systematic comparison of available carbon removal options as well as provide further research directions.

6.2.3 Empirical validation and expanded analysis of CO_2 utilization in cement and concrete

Further empirical evidence can help reduce large uncertainties present in the current estimation of the potential scale of CO_2 reduction when CO_2 is utilized as an additive during the fabrication of concrete. The wide uncertainty range stems from the heterogeneity of the gathered data including, but not limited to, variations in material properties used and non-standardized CO_2

reaction procedures. Another recent study on CO_2 mitigation in concrete through utilizing CO_2 in its fabrication also found significant variations in results; in this case, over 60% of the studied cases resulted in a net increase in GHG emissions when CO_2 was added (Ravikumar *et al* 2021). This highlights the necessity of a follow-up study to reduce uncertainties and produce an improved carbon reduction estimation through CO_2 utilization.

While our systems-level comparison of the conventional and CO_2-added mixtures were based on 28-day compressive strength as a technical criterion, future investigation can expand the analysis to consider other properties of concrete such as durability. Concrete is characteristically brittle and has low tensile strength that makes it susceptible to failure under tension. For this reason, concrete is often supplemented with a rebar that provides tensile ductility and strength essential for structural applications. A past study finds that increased durability and service life of the structure can provide significant improvement in lifecycle GHG emissions of concrete (Keoleian *et al* 2005). Our work in Chapter 4, however, could not be expanded to assess tensile strength influence from CO_2 since the vast majority of the reviewed studies either lacked or omitted tensile strength information. Thus, understanding if the added CO_2 can further enhance the tensile strength of concrete, by how much, and under what condition remains an important research question.

CO_2 utilization and sequestration in cement and concrete are at their early stage of development, but they exhibit substantial potentials to reduce CO_2 emissions as shown in Chapter 4Chapter 5 of this work. While early works show promising results, products formulated with added CO_2 will ultimately need to be tested in the field for a prolonged duration to provide confidence in its long-term performance. Thus, prioritizing demonstration projects as well as fundamental research and development could help bridge the current knowledge gap in a timely manner.

6.2.4 Exploring the potential market for CO_2 removal and utilization

Successful deployment and scaling up of the carbon removal, utilization, and sequestration technology hinges on not only advancing research but also promoting appropriate *pull* from the demand side, including the creation of a long-term, robust market. However, an overwhelming proportion (>80%) of the existing literature on NET analyzed the supply side, such as research and development (Nemet *et al* 2018). In this context, recent heightened entrepreneurial interests in

carbon removal, utilization, and sequestration, as exemplified with the open solicitation by Microwave and Strip, provide invaluable opportunities to advance demand-pull. While the private sector is leading the development, the government can further accelerate the momentum by imposing appropriate policy measures that provide a long-term market for carbon offset and reductions. As highlighted in Chapter 4-Chapter 5 of this dissertation, the effective policy shall account for the gross CO_2 reduction made throughout the product/application lifecycle, not just the stored CO_2.

REFERENCES

Andrijevic M, Schleussner C-F, Gidden M J, McCollum D L and Rogelj J 2020 COVID-19 recovery funds dwarf clean energy investment needs *Science (80-.).* **370** 298–300 Online: https://www.sciencemag.org/lookup/doi/10.1126/science.abc9697

Cherbański R and Molga E 2009 Intensification of desorption processes by use of microwaves-An overview of possible applications and industrial perspectives *Chem. Eng. Process. Process Intensif.* **48** 48–58

Chronopoulos T, Fernandez-Diez Y, Maroto-Valer M M, Ocone R and Reay D A 2014 CO_2 desorption via microwave heating for post-combustion carbon capture *Microporous Mesoporous Mater.* **197** 288–90 Online: http://dx.doi.org/10.1016/j.micromeso.2014.06.032

Clean Air Task Force 2021 Scaling Up Climate Ambition: Carbon Capture, Removal, and Storage Priorities in the 117th Congress Online: https://www.catf.us/2021/05/scaling-up-climate-ambition-carbon-capture-removal-and-storage-priorities-in-the-117th-congress/

Coss P M and Cha C Y 2000 Microwave regeneration of activated carbon used for removal of solvents from vented air *J. Air Waste Manag. Assoc.* **50** 529–35

Deutz S and Bardow A 2021 Life-cycle assessment of an industrial direct air capture process based on temperature–vacuum swing adsorption *Nat. Energy* **6** 203–13 Online: http://www.nature.com/articles/s41560-020-00771-9

Falciglia P P, Roccaro P, Bonanno L, De Guidi G, Vagliasindi F G A and Romano S 2018 A review on the microwave heating as a sustainable technique for environmental remediation/detoxification applications *Renew. Sustain. Energy Rev.* **95** 147–70 Online: https://doi.org/10.1016/j.rser.2018.07.031

Friedlingstein P, O'Sullivan M, Jones M W, Andrew R M, Hauck J, Olsen A, Peters G P, Peters W, Pongratz J, Sitch S, Le Quéré C, Canadell J G, Ciais P, Jackson R B, Alin S, Aragão L E O C, Arneth A, Arora V, Bates N R, Becker M, Benoit-Cattin A, Bittig H C, Bopp L, Bultan S, Chandra N, Chevallier F, Chini L P, Evans W, Florentie L, Forster P M, Gasser T, Gehlen M, Gilfillan D, Gkritzalis T, Gregor L, Gruber N, Harris I, Hartung K, Haverd V, Houghton R A, Ilyina T, Jain A K, Joetzjer E, Kadono K, Kato E, Kitidis V, Korsbakken J I,

Landschützer P, Lefèvre N, Lenton A, Lienert S, Liu Z, Lombardozzi D, Marland G, Metzl N, Munro D R, Nabel J E M S, Nakaoka S I, Niwa Y, O'Brien K, Ono T, Palmer P I, Pierrot D, Poulter B, Resplandy L, Robertson E, Rödenbeck C, Schwinger J, Séférian R, Skjelvan I, Smith A J P, Sutton A J, Tanhua T, Tans P P, Tian H, Tilbrook B, Van Der Werf G, Vuichard N, Walker A P, Wanninkhof R, Watson A J, Willis D, Wiltshire A J, Yuan W, Yue X and Zaehle S 2020 Global Carbon Budget 2020 *Earth Syst. Sci. Data* **12** 3269–340

Gebald C, Repond N and Wurzbacher A 2019 Steam assisted vacuum desorption process for carbon dioxide capture

van der Giesen C, Meinrenken C J, Kleijn R, Sprecher B, Lackner K S and Kramer G J 2017 A Life Cycle Assessment Case Study of Coal-Fired Electricity Generation with Humidity Swing Direct Air Capture of CO_2 versus MEA-Based Postcombustion Capture *Environ. Sci. Technol.* **51** 1024–34 Online: http://pubs.acs.org/doi/abs/10.1021/acs.est.6b05028

Jin S, Wu M, Gordon R G, Aziz M J and Kwabi D G 2020 pH swing cycle for CO_2 capture electrochemically driven through proton-coupled electron transfer *Energy Environ. Sci.* **13** 3706–22 Online: http://xlink.rsc.org/?DOI=D0EE01834A

Jones A C and Sherlock M F 2020 *The Tax Credit for Carbon Sequestration (Section 45Q)* Online: https://crsreports.congress.gov

Joppa L, Luers A, Willmott E, Friedmann S J, Hamburg S P and Broze R 2021 Microsoft's million-tonne CO_2-removal purchase — lessons for net zero *Nature* **597** 629–32 Online: https://www.nature.com/articles/d41586-021-02606-3

Keith D W, Holmes G, St. Angelo D and Heidel K 2018 A Process for Capturing CO_2 from the Atmosphere *Joule* **2** 1–22 Online: https://linkinghub.elsevier.com/retrieve/pii/S2542435118302253

Keoleian G A, Kendall A, Dettling J E, Smith V M, Chandler R F, Lepech M D and Li V C 2005 Life Cycle Modeling of Concrete Bridge Design: Comparison of Engineered Cementitious Composite Link Slabs and Conventional Steel Expansion Joints *J. Infrastruct. Syst.* **11** 51–60 Online: http://ascelibrary.org/doi/10.1061/%28ASCE%291076-0342%282005%2911%3A1%2851%29

Matthews H D, Tokarska K B, Nicholls Z R J, Rogelj J, Canadell J G, Friedlingstein P, Frölicher T L, Forster P M, Gillett N P, Ilyina T, Jackson R B, Jones C D, Koven C, Knutti R, MacDougall A H, Meinshausen M, Mengis N, Séférian R and Zickfeld K 2020 Opportunities and challenges in using remaining carbon budgets to guide climate policy *Nat. Geosci.* **13** 769–79 Online: http://dx.doi.org/10.1038/s41561-020-00663-3

Meier M, Turner M, Vallee S, Conner W C, Lee K H and Yngvesson K S 2009 Microwave regeneration of zeolites in a 1 meter column *AIChE J.* **55** 1906–13

National Academies of Sciences Engineering and Medicine 2019 *Negative Emissions Technologies and Reliable Sequestration* (Washington, D.C.: National Academies Press) Online: https://www.nap.edu/catalog/25259

Nemet G F, Callaghan M W, Creutzig F, Fuss S, Hartmann J, Hilaire J, Lamb W F, Minx J C, Rogers S and Smith P 2018 Negative emissions - Part 3: Innovation and upscaling *Environ. Res. Lett.* **13**

Okubo M, Kuroki T, Yamada H, Yoshida K and Kuwahara T 2017 CO_2 Concentration Using Adsorption and Nonthermal Plasma Desorption *IEEE Trans. Ind. Appl.* **53** 2432–9

Polaert I, Estel L, Huyghe R and Thomas M 2010 Adsorbents regeneration under microwave irradiation for dehydration and volatile organic compounds gas treatment *Chem. Eng. J.* **162** 941–8 Online: http://dx.doi.org/10.1016/j.cej.2010.06.047

Ravikumar D, Zhang D, Keoleian G, Miller S, Sick V and Li V 2021 Carbon dioxide utilization in concrete curing or mixing might not produce a net climate benefit *Nat. Commun.* **12** 855 Online: http://dx.doi.org/10.1038/s41467-021-21148-w

Realmonte G, Drouet L, Gambhir A, Glynn J, Hawkes A, Köberle A C and Tavoni M 2019 An inter-model assessment of the role of direct air capture in deep mitigation pathways *Nat. Commun.* **10** 3277 Online: http://dx.doi.org/10.1038/s41467-019-10842-5

Robiou du Pont Y, Jeffery M L, Gütschow J, Christoff P and Meinshausen M 2016 National contributions for decarbonizing the world economy in line with the G7 agreement *Environ. Res. Lett.* **11** 054005 Online: https://iopscience.iop.org/article/10.1088/1748-9326/11/5/054005

Shi X, Xiao H, Kanamori K, Yonezu A, Lackner K S and Chen X 2020 Moisture-Driven CO_2 Sorbents *Joule* **4** 1823–37 Online: https://doi.org/10.1016/j.joule.2020.07.005

Terlouw T, Treyer K, Bauer C and Mazzotti M 2021 Life Cycle Assessment of Direct Air Carbon Capture and Storage with Low-Carbon Energy Sources *Environ. Sci. Technol.* **55** 11397–411 Online: https://pubs.acs.org/doi/10.1021/acs.est.1c03263

Turner M D, Laurence R L, Conner W C and Yngvesson K S 2000 Microwave radiation's influence on sorption and competitive sorption in zeolites *AIChE J.* **46** 758–68

University of Michigan Bendable Concrete Utilized on a Bridge Deck Online: https://www.urbanlab.umich.edu/project/bendable-concrete-utilized-on-a-bridge-deck-engineered-cementitious-composite-or-ecc/

Webley P A and Zhang J 2014 Microwave assisted vacuum regeneration for CO_2 capture from wet flue gas *Adsorption* **20** 201–10

Appendices

Appendix A

Supplementary Information for Chapter 2

A.1 Aqueous Kraft Process-based direct air capture configuration

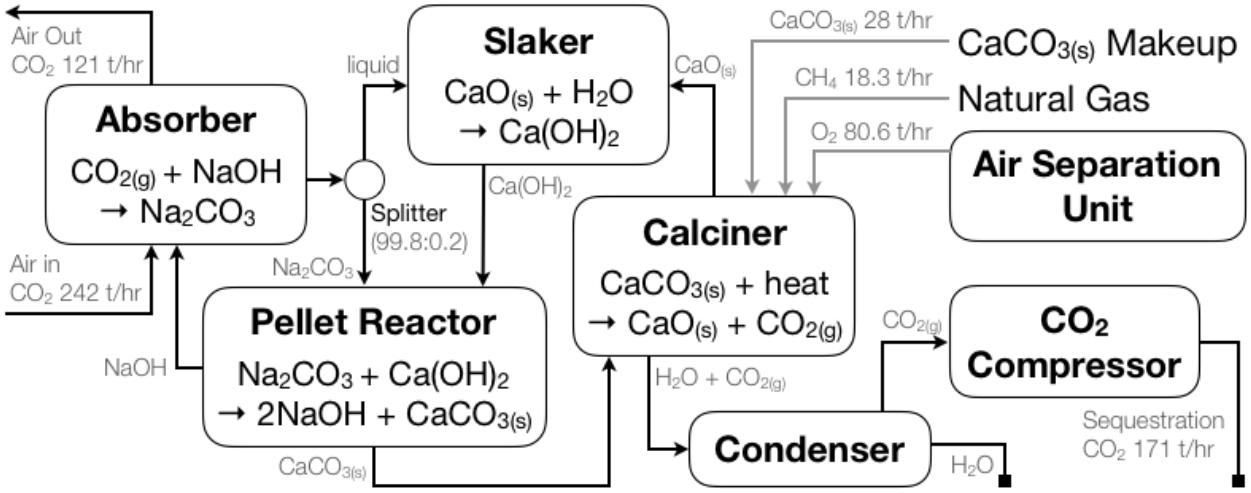

Figure A.1. Major processes and material flows of a direct air capture plant that annually captures 1.06 Mt of CO_2 from air. The CO_2 concentration in the air is assumed to be 500 ppm. This figure is adapted from (Socolow et al 2011) and (Baciocchi et al 2006).

The reference Kraft process-based direct air capture (DAC) plant (Figure A.1) is fundamentally based on the design adopted in the American Physical Society study (Socolow *et al* 2011). We update this reference DAC design based on recent publications, which are discussed in the next paragraph. (Socolow *et al* 2011) assumed 330 DAC units, each capturing 3.21 kt of CO_2 as investigated by Baciocchi et al. in 2006, collectively removing 1.06 Mt of CO_2 annually. Fans blow about 270 million m^3 of air per hour through plastic packing structure where strong alkaline solution selectively absorb half of the CO_2 from the air. The captured CO_2 is precipitated as $CaCO_3$ which is thermally decomposed to generate pure stream of CO_2. In the calciner, natural gas is combusted with pure oxygen produced on-site to provide 8.07 GJ of thermal energy needed to capture one tonne of CO_2 from air. This generates additional 0.413 tonnes of CO_2 per tonne of CO_2 captured from air, all of which is captured, compressed to 150 bar, and assumed to be permanently stored underground along with CO_2 captured from air. As a result, this 1 Mt-scale DAC plant captures roughly 1.5 Mt of CO_2 every year.

Updates to the process described in (Socolow *et al* 2011) include the following. First, we assume stainless steel packing material can be replaced with plastic packing to reduce the cost. This design modification help reduce the overall capital cost by 33% without sacrificing system performance (Zeman 2014, Holmes and Keith 2012). Second, we update the energy required to compress and store captured CO_2 using an 8-stage centrifugal, integral gear compressor and injecting CO_2 underground at 150 bar (National Energy Technology Laboratory 2018). The updated calculation also includes additional injection energy needed to replace ground water with injected CO_2, which is estimated to be around 1.5 kJ per mol CO_2 injected (House *et al* 2011). As a result, 0.588 GJ of energy is needed to compress and inject CO_2 underground for every tonne of CO_2 captured from air. Replacing the original compression energy calculated in the APS report with this value, and accounting for all the energy required to operate DAC, about 1.94 GJ of grid electricity is used to capture 1 tonne of CO_2 from air using the DAC plant. This total electricity requirement includes energy needed to run the fans in the absorbers, pump liquids, convey pellets, generate oxygen with air separation unit, and operate the compressor.

A.2 INPUT PARAMETERS, ASSUMPTIONS, LETSACT MODEL CODE, AND RESULT FILES

The following link (https://umich.box.com/s/fa6g7j3hy0sdo2pu1yqc8q3eay1e7hhb) provides access to the model input file, code, and result files generated for the analysis in this paper. This is a public link and does *not* require subscription or sign-in for Box. Table A.1 provides additional details about assumptions and data sources.

Table A.1. Input parameters and assumptions for EGUs and DAC plants in the U.S. electricity sector. This is an updated version of Table S4 from (Supekar and Skerlos 2017a).

Parameters	Values/Assumptions/Sources
Age-wise distribution of 2014 initial stock	Data of installed capacity, generation, and age of generators obtained from the NEEDS dataset; generation capacity older than 70 years, which comprised 3% of total capacity, is excluded (U.S. Environmental Protection Agency 2015, 2016, U.S. Energy Information Administration 2017b); DAC plants are assumed to be available starting 2015 and no initial fleet exists in 2014
Capacity discard probability	Assumed as a step function with discard probability = 0 until the expected service life of the technology, and = 1 beyond that.
Maximum service life	Assumed 60 years for PC, NGCC, PC-CCS, NGCC-CCS, N, and H; 40 years for NGGT, P, and G; 30 years for B, W, SPV, and STH; 25 years for DAC (Carbon Engineering n.d.)
Deployment & O&M costs, capacity factors	EGU costs are obtained from (Black & Veatch 2012, U.S. Energy Information Administration 2016, Lazard 2016). Cost assumptions for DAC are outlined in Table A**.4**. 90% of capacity factor is assumed for DAC in all uncertainty levels.
Capacity retirement cost	Retirement costs are comprised of the cost of any remaining capital liability assuming a financing period of 20 years, and a total interest rate of 20% comprised of 3% risk, 12% return on investment/equity, and 5% tax.

Heat rates	EGU heat rates are obtained from (Black & Veatch 2012, U.S. Energy Information Administration 2016, Lazard 2016). For DAC, heat rate is defined as the ratio of thermal energy demand with respect to electricity demand as shown in Table A.4.
Emission factors	Emission factors for EGUs are calculated based on heat rates and carbon content of fuels as specified in (U.S. Environmental Protection Agency 2014). Electricity demand of three 1 Mt-scale DAC plant designs used to calculate three uncertainty levels as shown in Table A.4
Fuel & electricity costs	Fuel prices and electricity costs are treated exogenously and obtained from the U.S. Annual Energy Outlook data for 2016 (U.S. Energy Information Administration 2017a).
Relative market penetration of different renewables	The relative capacity addition of new W, STH, SPV, and G plants follow a fixed proportion which reflect the resource availability and its distribution over the entire U.S.; The W:STH:SPV:G ratio is 1:0.1:0.1:0.03 for low case, 1:0.25:0.25:0.03 for nominal case, and 1:0.5:0.5:0.03 for high case (Jacobson and Delucchi 2011, MacDonald *et al* 2016)

A.3 SETUP OF UNCERTAINTY SCENARIOS FOR THE LETSACT MODEL

Input parameters with uncertainty ranges are grouped into 3 parameter sets as outlined in Table A.2. Each of these parameter sets are allowed for three uncertainty levels, which collectively define 27 uncertainty scenarios as listed in Table A.3. Then the LETSACT model generates unique set of optimized results using the diverse set of input parameters.

Table A.2. Three sets of input parameters that uniquely define 27 uncertainty scenarios. This is an updated table of Table 1 from (Supekar and Skerlos 2017a).

Parameter set	Input parameters included in a set
A) Costs	Power plant capital, O&M, retirement costs; fuel and electricity prices; revenues from electricity sales; capacity factors; relative capacity addition ratios between renewables
B) Emissions	Power plant thermal efficiency; decrease in efficiency with aging; carbon intensity of plants; upper limit for new capacity addition of pulverized coal plants
C) Demand	projected electricity demand

Table A.3. The uncertainty levels for each of the uncertainty categories (0 = Low, 1 = Nominal, 2 = High). This is an updated table of Table S4 from Supekar and Skerlos 2017.

Parameter Set \ Scenarios	1	2	3	4	5	6	7	8	9	10	11	12	13	14
A) Costs	0	1	2	0	1	2	0	1	2	0	1	2	0	1
B) Emissions	0	0	0	1	1	1	2	2	2	0	0	0	1	1
C) Demand	0	0	0	0	0	0	0	0	0	1	1	1	1	1

Parameter Set \ Scenarios	15	16	17	18	19	20	21	22	23	24	25	26	27
A) Costs	2	0	1	2	0	1	2	0	1	2	0	1	2
B) Emissions	1	2	2	2	0	0	0	1	1	1	2	2	2
C) Demand	1	1	1	1	2	2	2	2	2	2	2	2	2

A.4 UNCERTAINTY IN DAC CHARACTERISTICS AND CO_2 STORAGE POTENTIAL

A.4.1 DAC characteristics

Since direct air capture plants are still in their pilot stage, significant uncertainties exist in their cost and energy requirements based on variabilities in process design, financial assumptions, and other factors. DAC costs range from 35-1,000 $/tCO$_2$ captured (House *et al* 2011, Lackner *et al* 2012, Socolow *et al* 2011, Mazzotti *et al* 2013, Keith 2009, Lackner 2010, Zeman 2014, Keith *et al* 2006, Stolaroff *et al* 2008). One of the most commonly cited calculations is the APS study estimate, which concluded that DAC system will optimistically cost around 610 $/tCO$_2$. Subsequent studies (Zeman 2014, Holmes and Keith 2012) have pointed out that some of the design assumptions made in the APS study were not realistic and the cost can be reduced to 309-343 $/tCO$_2$ with different design choices. More recently, Carbon Engineering, a Canadian DAC startup developing similar Kraft process-based DAC, published their engineering calculation of 1Mt scale commercial DAC plant which shows lower energy requirement and cost compared to previous estimates (Keith *et al* 2018). On the other hand, House (2011) argue that overall cost of DAC will be much higher, on the order of 1,000 $/tCO$_2$, based on the trend of decreasing 2nd law efficiency with decreasing concentration as described by the Sherwood plot.

In this study, we develop three DAC plant designs and their corresponding energy, cost, and emissions estimates based on the ranges reported in the literature. These values are shown in Table A.4, and are incorporated into the uncertainty scenarios described in the main body of the paper. The nominal case is based on a modified optimistic case of APS study as outlined in the previous section. The unmodified optimistic case from APS study set the high sensitivity case. The low case reflects energy balance and cost calculation proposed by Carbon Engineering. The cost of transporting and storing captured CO$_2$ is obtained from National Energy Technology Laboratory (NETL) study (Grant *et al* 2017) where the cost uncertainty identified in the report for each of the four major storage basins in the U.S. is included in the analysis.

Table A.4. Energy, cost, and emission profiles of three DAC plant designs used to setup uncertainty range. Values under 'original DAC parameters' are used to generate variables listed under 'DAC parameters as 'reverse power plant'' that are used as inputs to the LETSACT model.

		DAC Sensitivity		
Original DAC Parameters	**Units[a]**	**Low**	**Nominal**	**High**
Representative Case		State-of-the-art design (Keith *et al* 2018) – Scenario C	Optimized design (Socolow *et al* 2011, Zeman 2014)	Non-optimized design (Socolow *et al* 2011) – Ideal case
Annual capture capacity	MtCO$_2$/year	0.98	1.06	1.06
DAC plant electricity use	GJ/tCO$_2$	1.32	1.94	1.94
DAC plant NG use	GJ/tCO$_2$	5.25	8.07	8.07
Derived 2nd law efficiency	%	11.8%	7.75%	7.75%

Capital cost	mil $	680	1,430	2,160
Fixed O&M cost[b]	mil $/year	26.5	55.8	84
Non-fuel Operating cost[c]	mil $/year	4	4	4
CO_2 transportation & storage cost[d]	$/t$CO_2$	36.7	42.7	126
DAC Parameters as "Reverse Power Plant"				
Nominal Capacity	MW	-40.9	-65.4	-65.4
Pseudo Heat Rate	Btu/kWh	-13,600	-14,200	-14,200
Carbon Intensity	tCO_2/MWh	2.73	1.85	1.85
Capital Cost	$/kW	16,600	21,900	33,000
Fixed O&M	$/kW-year	659	857	1,290
Variable O&M excluding purchased electricity[e]	$/MWh	47.6	50.1	133

[a] 'tCO_2' represents a tonne of CO_2 captured from air from DAC operation. All costs are based on 2015 US dollars

[b] Fixed O&M cost is assumed to be 3.9% of the capital cost, where maintenance costs 3% of the capital cost and labor costs 30% of the maintenance cost (Socolow *et al* 2011)

[c] The non-fuel operating cost includes cost of makeup water and chemicals during the operation of DAC

[d] Assumes average cost across four basins by weighting cost estimated for each basin with its storage capacity. Values assume viable CO_2 storage potential is 50 Gt. These costs include additional cost to transport and store CO_2 generated by on-site natural gas combustion.

[e] Variable O&M cost includes non-fuel operating cost and CO_2 transportation & storage cost.

A.4.2 CO_2 storage potential

(Grant et al 2017) estimate the total U.S. CO_2 storage potential to be between 413 – 448 Gt 97 corresponding to a minimum CO_2 storage value of 25 – 75 Gt at each of the four storage basins 98 listed above. This storage resource estimate from the NETL study is an order of magnitude larger 99 than the highest estimate for the amount of CO_2 storage from DAC plants as determined by the 100 LETSACT model in our analysis (about 25 GtCO_2 by 2050). It is therefore unlikely that CO_2 101 storage in a DAC-based CO_2 mitigation scenario would exceed the total CO_2 storage capacity. 102 However, this analysis does not include CO_2 storage that may be needed if other negative 103 emissions technologies (NETs) such as bioenergy with CCS are deployed at large scales. A 104 separate analysis that is outside the scope of this paper would be needed to ascertain whether the 105 strategic deployment of several NETs would run afoul of the CO_2 storage limits.

A.5 DETAILS OF DAC INTEGRATION INTO THE LETSACT MODEL

To integrate DAC plants into the LETSACT model, we model it with negative nominal capacity and heat rate. The negative nominal capacity indicates that DAC plants consume grid electricity to run fans, pumps, air separation units, compressors, and other auxiliary devices as

opposed to generating electricity. This concept is shown in Figure A.2, where DAC plants act as "reverse EGUs." The negative heat rate for DAC plants is expressed in equation (2.1), and it is the ratio of thermal energy demand ($\dot{Q}_{DAC}$) to electrical energy demand ($\dot{W}_{DAC}$) of a DAC plant. In the LETSACT model, this heat rate is used to estimate cost incurred from natural gas use in DAC plants, as shown in equation (A.2), by multiplying it with natural gas price.

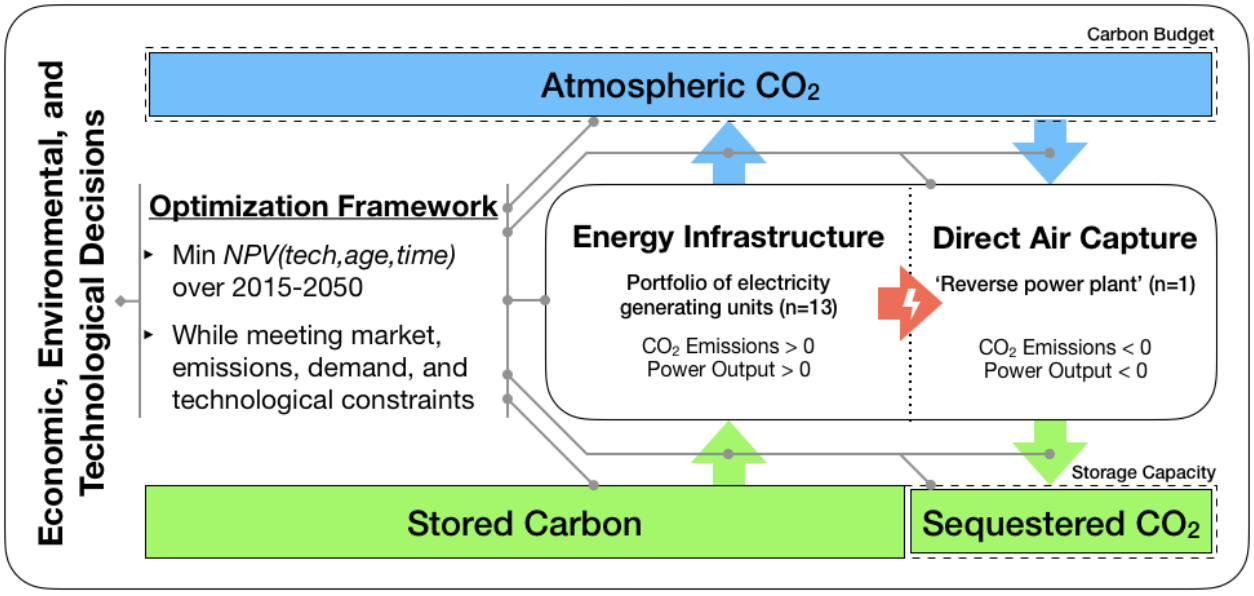

Figure A.2. Interactions between DAC plants and the existing electric infrastructure in the context of technological and environmental decision makings to achieve specific CO_2 mitigation targets in the LETSACT model.

$$HR_{DAC}\left(\frac{Btu}{kWh}\right) = -3412\left(\frac{Btu}{kWh}\right) \cdot \frac{\dot{Q}_{DAC}\left(\frac{GJ_{th}}{tCO_2}\right)}{\dot{W}_{DAC}\left(\frac{GJ_e}{tCO_2}\right)} \tag{A.1}$$

$$FuelCost_{DAC}\left(\frac{\$}{MWh}\right) = -1 \cdot NGprice\left(\frac{\$}{MMBtu}\right) \cdot \frac{HR_{DAC} \cdot 10^{-6}\left(\frac{MMBtu}{kWh}\right)}{10^{-3}\left(\frac{MWh}{kWh}\right)} \tag{A.2}$$

A.6 Energy and Carbon Balance of the Grid-Connected Direct Air Capture Plants

The net amount of CO_2 removed with DAC should account for the additional CO_2 emitted from its energy sources. In our DAC design, CO_2 generated from onsite natural gas combustion are captured and stored alongside air-captured CO_2 and does not contribute to additional emissions.

However, additional CO_2 is emitted remotely from operating grid to power DAC plants. As a result, the *net* CO_2 removal rate of a DAC plant decreases with increasing grid carbon intensity. Thus, a DAC plant needs to scale up to achieve the designed removal rate. But this ramp-up entails additional electricity use which only results in more emissions. This positive feedback is inherent to carbon capture facilities that operate on power sources that emit additional carbon emissions; the operation of CO_2 capture units result in additional emissions associated with the increased use of fuels (Supekar and Skerlos 2015, 2017b). Figure A.3 shows this feedback loop for DAC plants.

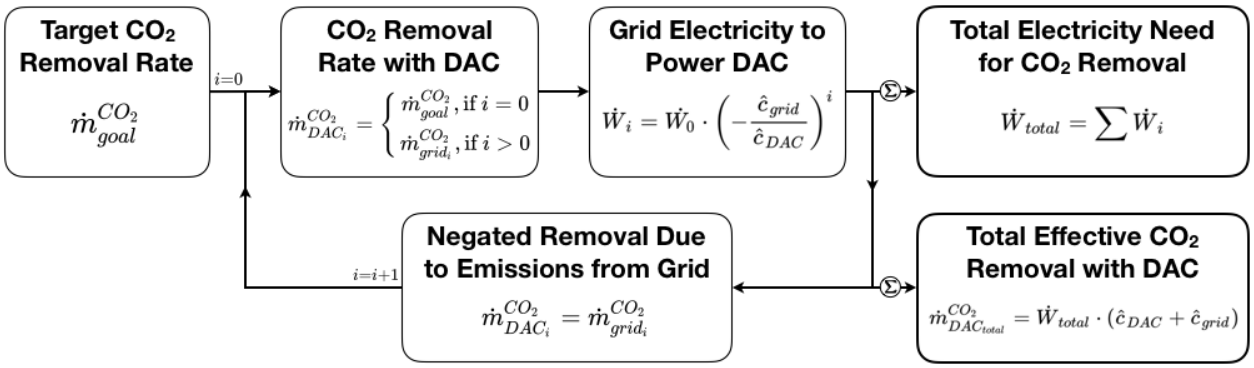

Figure A.3. Mass and energy feedback loop inherent to capturing CO_2 from the air with DAC plants powered by electric infrastructure. The total amount of electricity needed to achieve the target CO_2 removal rate can be calculated by summing incremental electricity needed to scale up DAC until the target removal rate is achieved.

Thus, the total amount of energy required to remove the desired amount of CO_2 from air can be calculated in a recursive fashion as shown in Figure A.3. We let $\dot{m}^{CO_2}$ be a mass flow of CO_2 where positive values represent emissions and negative values represent removal. We can also define $\hat{c}_{DAC}, \hat{c}_{grid}$ as carbon intensity of DAC and electric grid respectively, in terms of tonne of CO_2 removed/emitted per MWh of electricity use/generation. We let $\dot{W}_i$ be the electricity needed to operate a DAC plant at i^{th} recursion. At the initial iteration ($i = 0$), we assume that grid-emissions are zero and that we can remove the target amount of CO_2 through operating a DAC plant ($\dot{m}_{goal}^{CO_2} = \dot{m}_{DAC_0}^{CO_2}$). But considering non-zero emissions from grid, the net amount of removed CO_2 becomes $\dot{W}_0 \cdot (-\hat{c}_{DAC} + \hat{c}_{grid})$. To achieve the target removal rate, we need to scale up CO_2 removal rate with DAC to compensate for the additional emissions from grid, $\dot{W}_0 \hat{c}_{grid}$. The additional electricity requirement is $\dot{W}_1 = -W_0 \cdot \frac{\hat{c}_{grid}}{\hat{c}_{DAC}}$. But since this creates even further emissions from grid, the total amount of electricity required to meet the target removal rate can be

expressed as an infinite sum as seen in equation (A.3). This infinite sum converges only when $\left|\frac{\hat{c}_{grid}}{\hat{c}_{DAC}}\right| < 1$. We find that equation (A.3) converges in all of the three uncertainty cases of DAC.

$$\dot{W}_{total} = \lim_{n\to\infty} W_0 \cdot \left\{1 + \left(-\frac{\hat{c}_{grid}}{\hat{c}_{DAC}}\right) + \left(-\frac{\hat{c}_{grid}}{\hat{c}_{DAC}}\right)^2 + \cdots + \left(-\frac{\hat{c}_{grid}}{\hat{c}_{DAC}}\right)^n\right\} = W_0\left(\frac{\hat{c}_{DAC}}{\hat{c}_{DAC} + \hat{c}_{grid}}\right) \quad \text{(A.3)}$$

Figure A.4A shows how effective CO_2 removal linearly decreases with increasing carbon intensity of the grid powering the DAC plants. Figure A.4B shows how $\dot{W}_{total}$ increases nonlinearly with increasing carbon intensity of the grid to achieve a fixed amount of CO_2 removal. When the grid carbon intensity is 0.6 tCO_2/MWh, close to the current level of the U.S. power grid, 48% more electricity is needed to remove 1 Mt of CO_2 from air with DAC compared to operating DAC with a zero-emission grid. Thus, the deployment of DAC plants is delayed in LETSACT model as long as possible to minimize total mitigation cost. The thicker portions in Figure A.4 indicate the observed range of net CO_2 removal rate and net electricity demand of the DAC plants deployed in the LETSACT results. Typically, DAC plants deploy in LETSACT model when the additional electricity demand from positive emissions feedback fall below 6%.

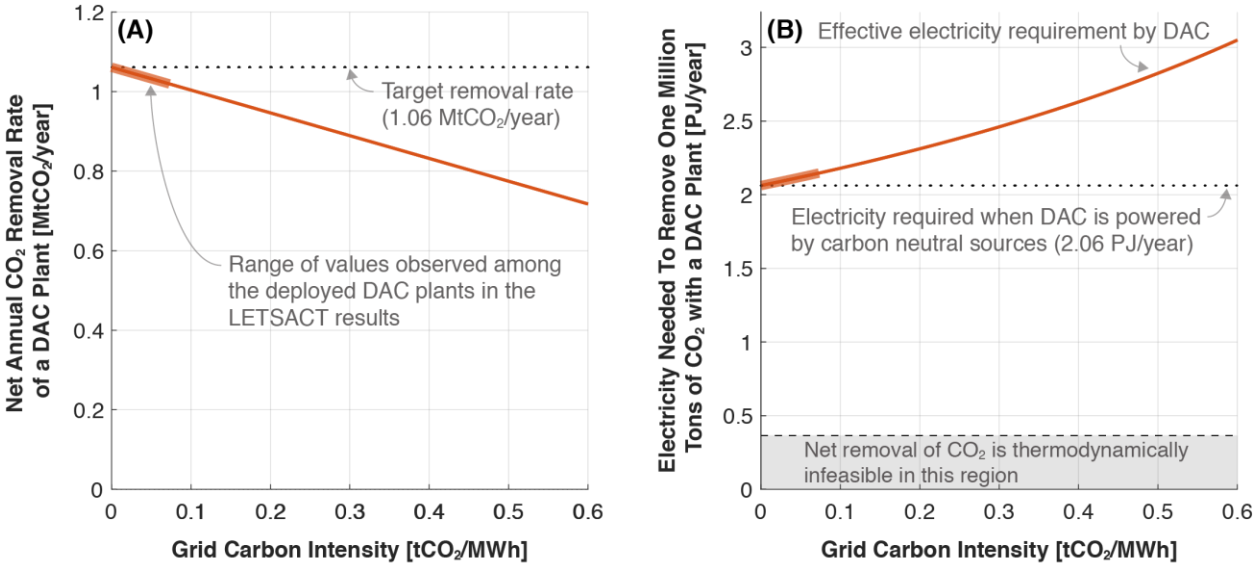

Figure A.4. (A) The net CO_2 removal rate of a DAC plant considering emissions from grid operation. (B) The effective electricity requirement by DAC to remove 1 Mt of CO_2 from air considering emission feedback from grid using equation (A.3).

A.7 CO_2 EMISSIONS CONSTRAINT SETUP

In the climate action cases, the LETSACT model runs with an additional CO_2 emissions constraint which limits cumulative CO_2 emissions between 2015 and 2050 below the target emission level. This cumulative emission constraint, or CO_2 emissions budget, is defined as an area under a piecewise function that linearly decreases from the emissions level in 2010 to the target emissions level in 2050 after which is kept constant for additional 60 years. The additional 60 years consider the service life of EGUs that are deployed in 2050 to ensure proper implementation of emissions constraint. Each point on the straight line represents an idealized annual CO_2 emission pathway of the U.S. electric sector. The actual emission trajectory may temporarily overshoot this ideal emission level as long as the excess emissions can be compensated later. Figure A.5 compares the idealized emission constraint curve with a business-as-usual (BAU) emissions trajectory generated by the LETSACT model. The emissions trajectory from 2010 to 2014 is based on historic emissions (U.S. Environmental Protection Agency 2018) and LETSACT model generates emission trajectories from 2015 to 2050. As shown in Figure A.5, the cumulative CO_2 emissions under BAU trajectory exceed carbon budget that reduced the annual emissions by 70% by 2050, as emission constraint is not imposed under BAU scenario.

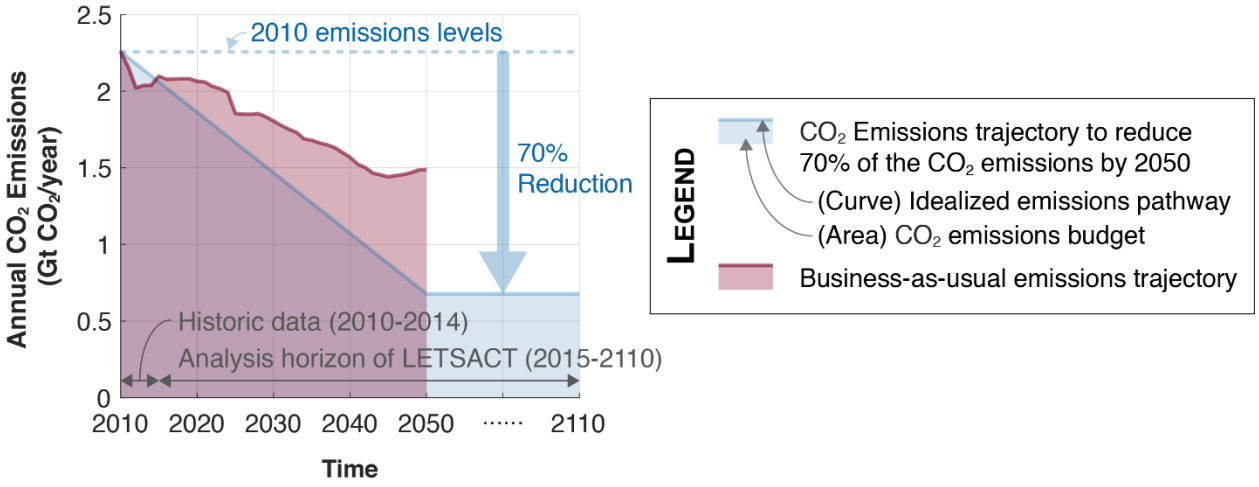

Figure A.5. CO_2 emissions constraint that reduces annual CO_2 emissions in 2050 to 70% below 2010 levels is compared to emissions trajectories generated with LETSACT model when no emissions constraint is imposed.

A.8 LIST OF TERMINOLOGIES

Table A.5. List of key terms used in this study and their descriptions.

Terms	Descriptions
Business-as-usual	Business-as-usual case refers to the LETSACT model runs with the constraints defined by equations 2–3 and a nation-wide implementation of Renewable Portfolio Standard, but *without* the 2050 CO_2 emissions constraint defined by

	equation 4. An example of emissions pathway under business-as-usual is shown in Figure A.6.
Climate action	Climate action cases refer to the results generated by running the LETSACT model with all constraints defined by equations 2–4, including the 2050 CO_2 emissions constraint and a nation-wide implementation or Renewable Portfolio standard. Figure A**.6** shows an example emissions pathway.
Climate action year	Climate action year is a year beyond which emissions constraint is activated. The LETSACT model runs without emissions constraint up to the year before climate action year, following a business-as-usual pathway until before that year. Thus, starting with the climate action year, the LETSACT model runs with the 2050 CO_2 emissions constraint. Figure A**.6** shows emissions pathway under climate action year = 2026.
Delayed climate action	Delayed climate action occurs when climate action initiates after 2015. In this case technology and emissions trajectory follows business-as-usual cases up until the year before climate action year.
Climate action timeframe	A collection of climate action years is called climate action timeframe.
Uncertainty scenarios	Three parameter categories, each with three possible values, collectively generate 27 unique parameter sets. Each uncertainty scenario is then defined by one of these parameter sets and corresponding LETSACT results created by running the model using the chosen parameter values. As a result, 27 uncertainty scenarios are generated.
Fleet turnover	Fleet turnover collectively represents new EGU additions, early EGU retirements decommission, and retirement of EGUs after their typical service life.
Emission trajectory	Emission trajectory denotes the annual trend in total CO_2 emissions generated from the U.S. electric sector as a result of running the LETSACT model. Example emission trajectories are shown in Figure A.6.
Technology trajectory	Technology trajectory collectively refers to the EGU stocks and flows over a certain period of time. An example of a technology trajectory is shown in Figure 2.4.
CO_2 budget	A sector-specific CO_2 budget used in this study refers to the amount of cumulative CO_2 emissions corresponding to the 70% emissions reduction in the U.S. electric sector by 2050 compared to 2010. The CO_2 budget is shown in Figure A.5 as a blue area below straight emission curve.

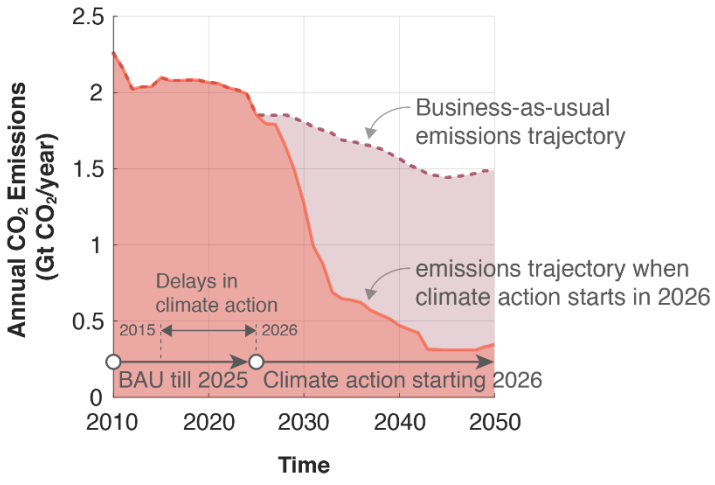

Figure A.6. Visual illustration of the terminologies listed in Table A.5. CAY denotes climate action year. Since climate action initiates beyond 2015, this example scenario describes a delayed climate action.

A.9 ADDITIONAL FIGURES ON TECHNOLOGY EVOLUTION AND FUEL USE

A.9.1 Retirement under DAC-based climate action versus preventive climate action

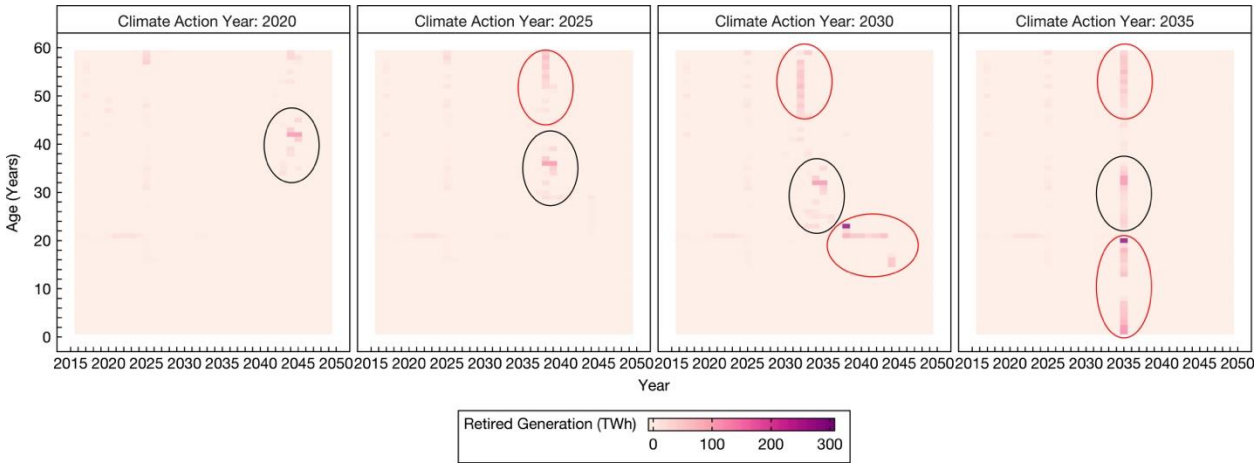

Figure A.7. Delayed climate action with DAC leads to the retirement of the same set of EGUs as in the case of preventive climate action without DAC, as marked in black. Delayed climate action leads to additional retirement of fossil fuel EGUs as marked in red, particular newer EGUs in the case of DAC-based delayed climate action.

A.9.2 Example technology trajectory with NGCC-CCS as a low-carbon EGU technology

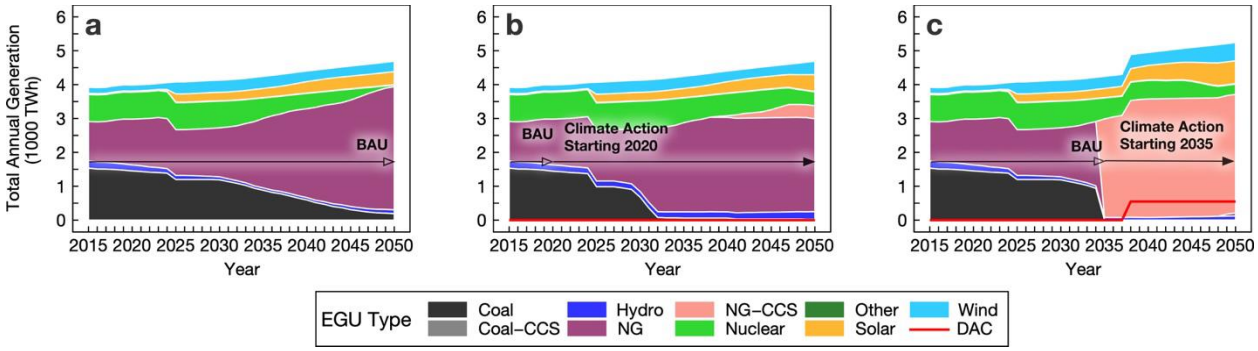

Figure A.8. Least-cost technology trajectories under a. BAU; b. climate action starting in 2020; and c. climate action starting in 2035 for a sample uncertainty scenario featuring natural gas combined cycle with CCS (NGCC-CCS) as a low-carbon EGU technology. Roughly 25% of all uncertainty scenarios rely on NGCC CCS along with renewables to meet 2050 emissions targets.

A.9.3 Changes in fuel use under climate action relative to business-as-usual

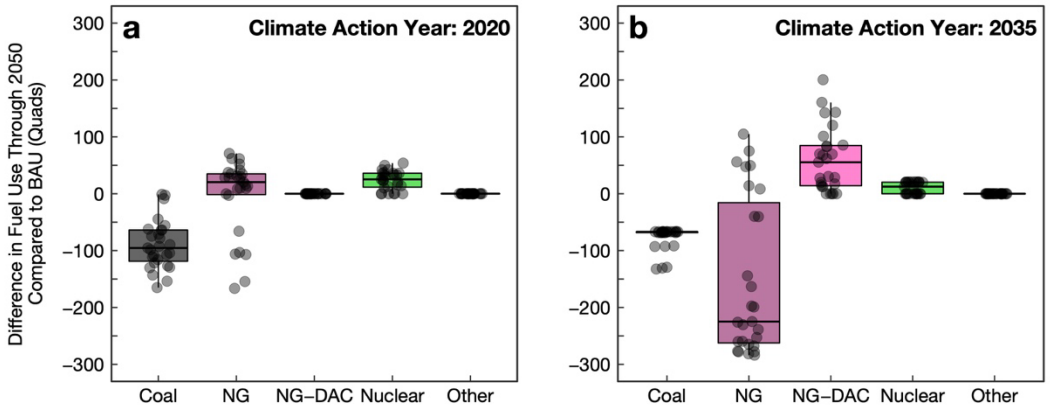

Figure A.9. Difference in total fuel use through 2050 relative to business-as-usual (BAU) for climate action year a. 2020 and b. 2035 expressed in quadrillion Btus (quads) for different uncertainty scenarios. Natural gas use in a. is slightly higher than BAU in some scenarios due to a higher penetration of NGCC (combined cycle) EGUs. Scenarios in b. showing increased non-DAC natural gas use rely on NGCC–CCS EGUs to supply low-carbon electricity in addition to renewables.

A.10 RESULTS FROM ADDITIONAL MODEL RUNS

A.10.1 4% and 10% discount rates

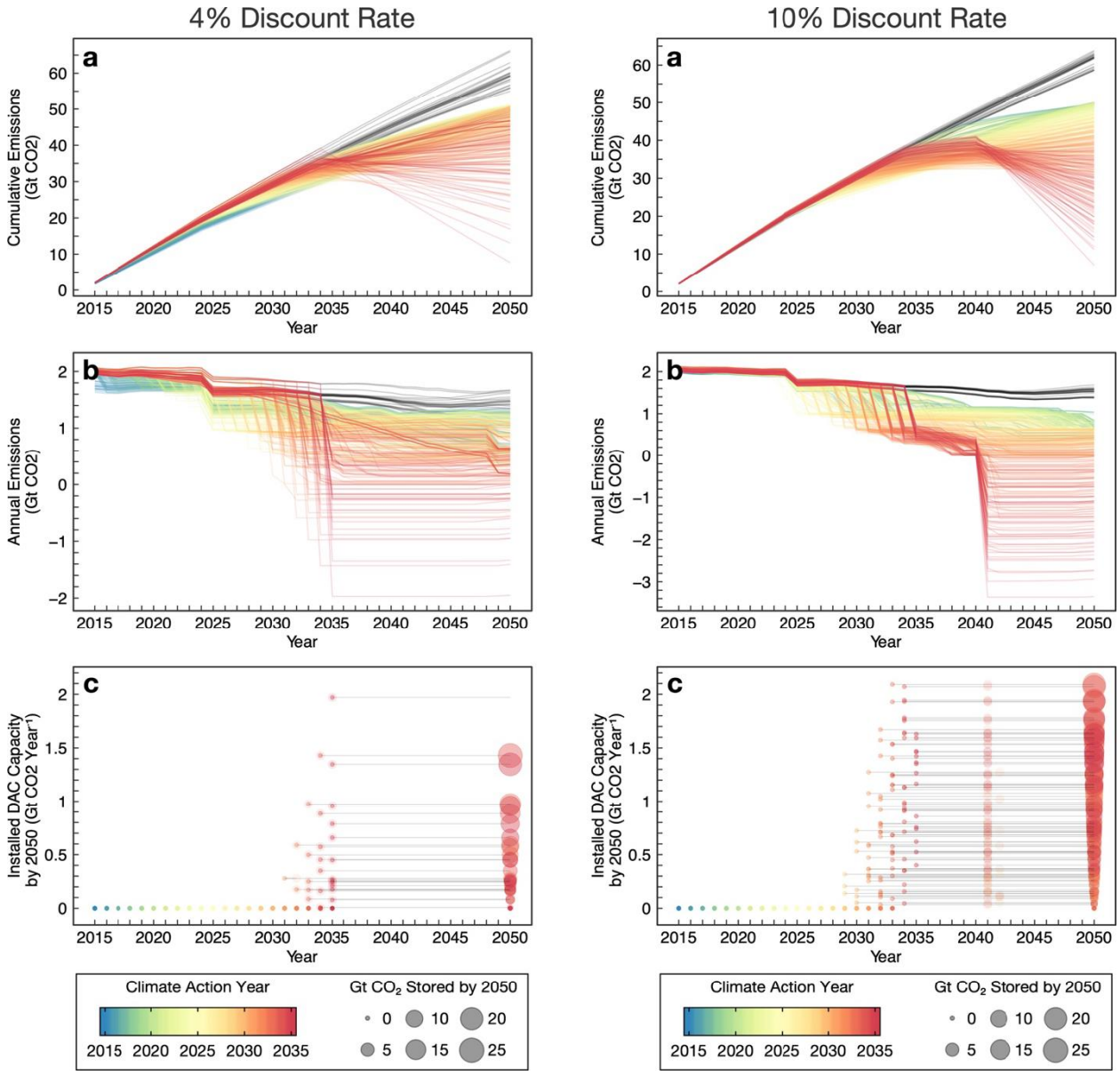

Figure A.10. a. Cumulative CO_2 emissions; b. annual CO_2 emissions; and c. DAC deployment under different climate action years with a 4% (a–c, left) and 10% (a–c, right) discount rate. Each individual curve or data point represents a single uncertainty scenario. Segments in c indicate the delay between start of climate action and actual deployment of DAC plants.

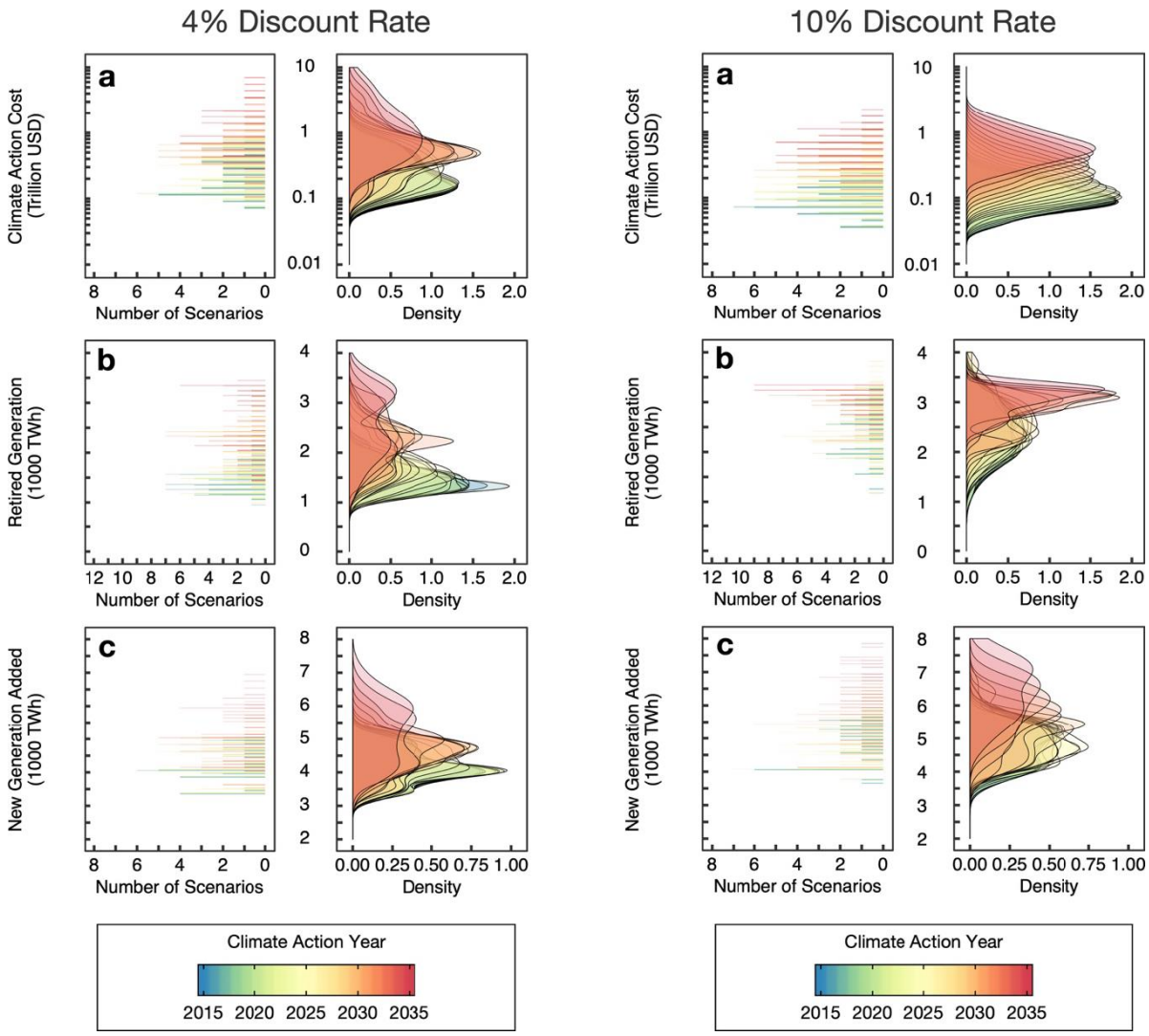

Figure A.11. a. Climate action cost; b. total generation retired early through 2050; and c. total new generation added through 2050 as a function of climate action year with a 4% (a–c, left) and 10% (a–c, right) discount rate. Approximated Gaussian density distribution for each quantity in the left panels in a – c is shown in their respective right panels.

A.10.2 60% and 80% emission reduction targets

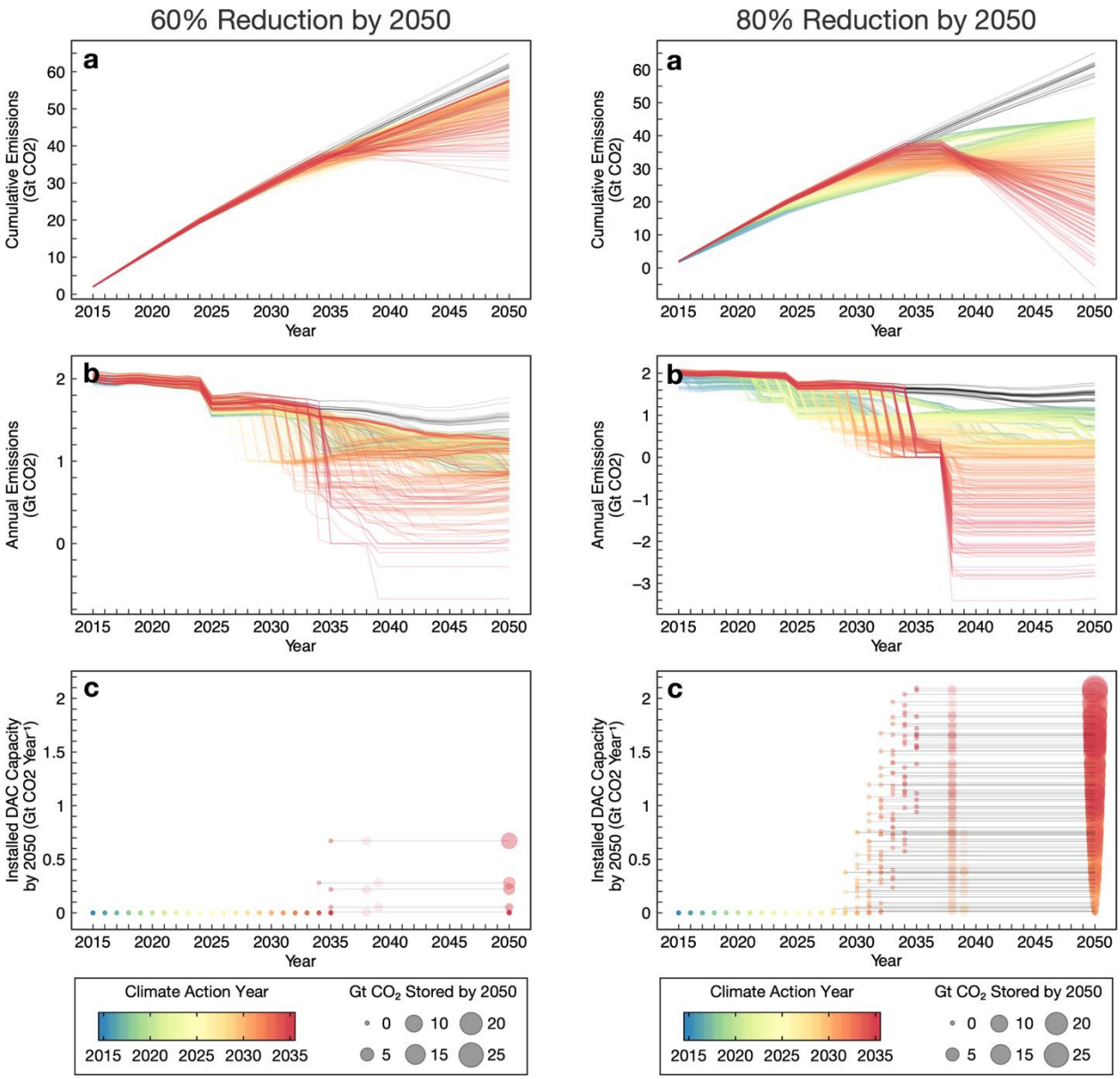

Figure A.12. a. Cumulative CO_2 emissions; b. annual CO_2 emissions; and c. DAC deployment under different climate action years for a 60% (a–c, left) and 80% (a–c, right) emissions reduction by 2050. Each individual curve or data point represents a single uncertainty scenario. Segments in c indicate the delay between start of climate action and actual deployment of DAC plants.

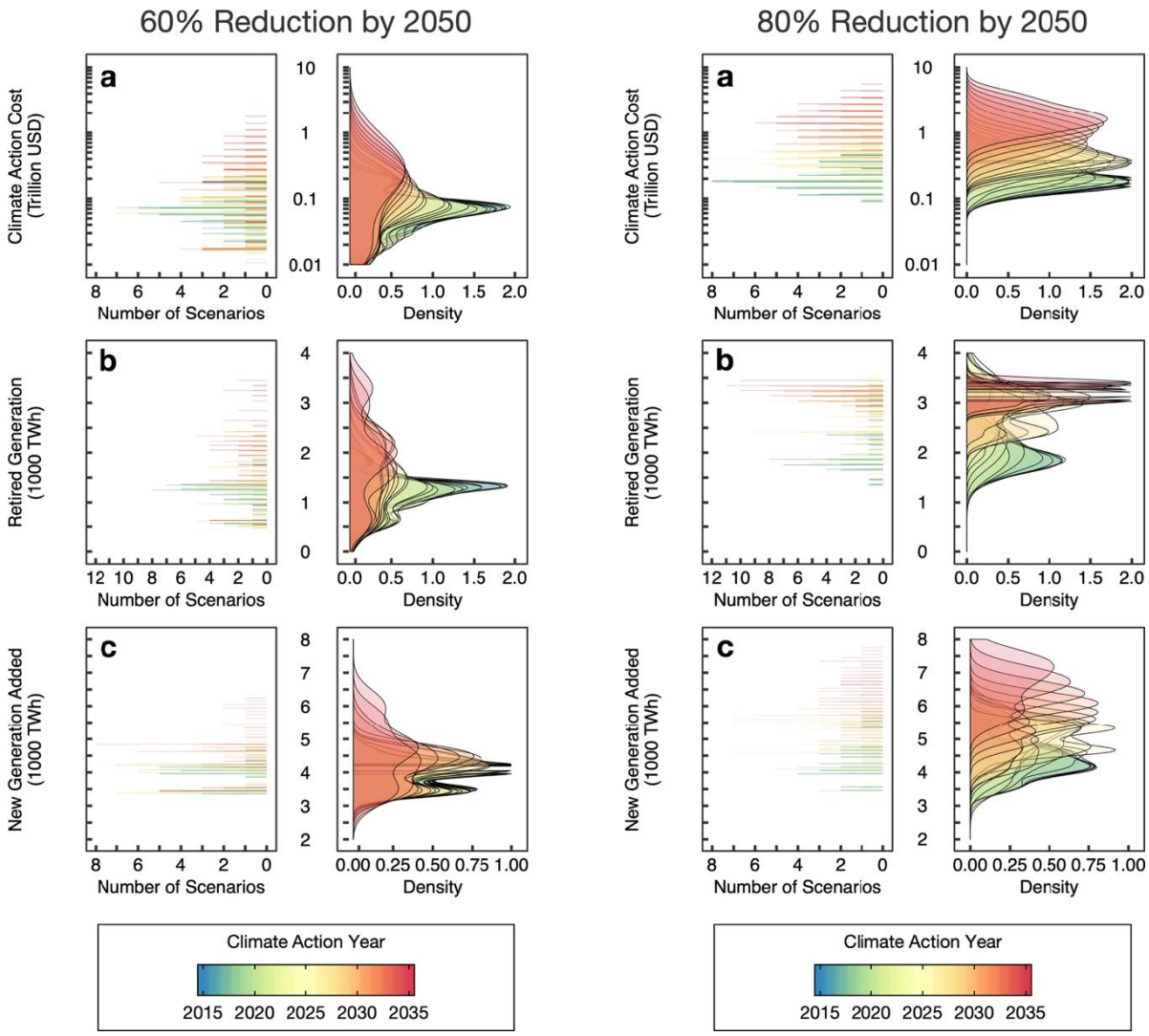

Figure A.13. a. Climate action cost; b. total generation retired early through 2050; and c. total new generation added through 2050 as a function of climate action year for a 60% (a–c, left) and 80% (a–c, right) emissions reduction by 2050. Approximated Gaussian density distribution for each quantity in the left panels in a – c is shown in their respective right panels.

REFERENCES

Baciocchi R, Storti G and Mazzotti M 2006 Process design and energy requirements for the capture of carbon dioxide from air *Chem. Eng. Process. Process Intensif.* **45** 1047–58

Black & Veatch 2012 *Cost Report Cost and Performance Data for Power Generation Technologies* Online: https://www.bv.com/docs/reports-studies/nrel-cost-report.pdf

Carbon Engineering Committee on Developing a Research Agenda for Carbon Dioxide Removal and Reliable Sequestration: Direct Air Capture Workshop Online: https://livestream.com/accounts/15221519/events/7703271/videos/164857832

Grant T, Morgan D and Kristin G 2017 *Carbon Dioxide Transport and Storage Costs in NETL Studies*

Holmes G and Keith D W 2012 An air-liquid contactor for large-scale capture of CO_2 from air *Philos. Trans. R. Soc. Math. Phys. Eng. Sci.* **370** 4380–403

House K Z, Baclig A C, Ranjan M, van Nierop E A, Wilcox J and Herzog H J 2011 Economic and energetic analysis of capturing CO_2 from ambient air *Proc. Natl. Acad. Sci.* **108** 20428–33

Jacobson M Z and Delucchi M A 2011 Providing all global energy with wind, water, and solar power, Part I: Technologies, energy resources, quantities and areas of infrastructure, and materials *Energy Policy* **39** 1154–69

Keith D W 2009 Why Capture CO_2 from the Atmosphere? *Science* **325** 1654–5

Keith D W, Ha-Duong M and Stolaroff J K 2006 Climate strategy with CO_2 capture from the air *Clim. Change* **74** 17–45

Keith D W, Holmes G, St. Angelo D and Heidel K 2018 A Process for Capturing CO_2 from the Atmosphere *Joule* **2** 1573–94

Lackner K S 2010 Washing carbon out of the air *Sci. Am.* **302** 66–71

Lackner K S, Brennan S, Matter J M, Park a.-H a., Wright a. and van der Zwaan B 2012 The urgency of the development of CO_2 capture from ambient air *Proc. Natl. Acad. Sci.* **109** 13156–62

Lazard 2016 *Lazard's Levelised Cost of Energy Analysis (version 10.0)* (New York, NY)

MacDonald A E, Clack C T M, Alexander A, Dunbar A, Wilczak J and Xie Y 2016 Future cost-competitive electricity systems and their impact on US CO_2 emissions *Nat. Clim. Change* **6** 526–31

Mazzotti M, Baciocchi R, Desmond M J and Socolow R H 2013 Direct air capture of CO_2 with chemicals: Optimization of a two-loop hydroxide carbonate system using a countercurrent air-liquid contactor *Clim. Change* **118** 119–35

National Energy Technology Laboratory 2018 *Carbon Capture Simulation Initiative (CCSI) Toolset* (Washington, DC) Online: https://github.com/CCSI-Toolset

Socolow R, Desmond M, Aines R, Blackstock J, Bolland O, Kaarsberg T, Lewis N, Mazzotti M, Pfeffer A, Sawyer K, Siirola J, Smit B and Wilcox J 2011 Direct Air Capture of CO_2 with Chemicals Panel on Public Affairs *Am. Phys. Soc. - Panel Public Aff.* 100

Stolaroff J K, Keith D W and Lowry G V. 2008 Carbon Dioxide Capture from Atmospheric Air Using Sodium Hydroxide Spray *Environ. Sci. Technol.* **42** 2728–35

Supekar S D and Skerlos S J 2017a Analysis of Costs and Time Frame for Reducing CO_2 Emissions by 70% in the U.S. Auto and Energy Sectors by 2050 *Environ. Sci. Technol.* **51** 10932–42

Supekar S D and Skerlos S J 2015 Reassessing the Efficiency Penalty from Carbon Capture in Coal-Fired Power Plants *Environ. Sci. Technol.* **49** 12576–84

Supekar S D and Skerlos S J 2017b Sourcing of Steam and Electricity for Carbon Capture Retrofits *Environ. Sci. Technol.* **51** 12908–17

U.S. Energy Information Administration 2017a *Annual Energy Outlook 2017 with Projections to 2050* (Washington, DC) Online: https://www.eia.gov/outlooks/aeo/pdf/0383%282017%29.pdf

U.S. Energy Information Administration 2016 *Capital Cost Estimates for Utility Scale Electricity Generating Plants* (Washington, DC) Online: https://www.eia.gov/analysis/studies/powerplants/capitalcost/pdf/capcost_assumption.pdf

U.S. Energy Information Administration 2017b *Electric Power Annual 2016* (Washington, DC: U.S. Department of Energy) Online: https://www.eia.gov/electricity/annual/pdf/epa.pdf

U.S. Environmental Protection Agency 2014 *Emission Factors for Greenhouse Gas Inventories* Online: https://www.epa.gov/sites/production/files/2015-07/documents/emission-factors_2014.pdf

U.S. Environmental Protection Agency 2016 *Inventory of U.S. Greenhouse Gas Emissions and Sinks 1990 – 2014* (Washington, DC) Online: https://www.epa.gov/ghgemissions/inventory-us-greenhouse-gas-emissions-and-sinks

U.S. Environmental Protection Agency 2018 Inventory of U.S. Greenhouse Gas Emissions and Sinks: 1990-2016 – Energy

U.S. Environmental Protection Agency 2015 *National Electric Energy Data System (NEEDS) v.5.14* (Washington, DC)

Zeman F 2014 Reducing the cost of ca-based direct air capture of CO_2 *Environ. Sci. Technol.* **48** 11730–5

Appendix B

Supplementary Information for Chapter 3

B.1 GAS TRANSPORT MODEL

B.1.1 Parameters used for gas transport and heat transfer models

Table B.1. Modeling parameters used for gas transport and heat transfer models

Parameter	Symbol	Value	Reference
Interior volume of the reaction chamber	V	6.9e-4 [m^3]	This study
Pumping speed	S_0	1.1 [m^3/hr]	This study
Effective pipe diameter	D	4.6 [mm]	This study
Effective pipe length	L	2 [m]	This study
Air leakage rate	$\frac{d\hat{y}_{CO_2}}{dt}$	2e-3 [Torr/s]	This study
Reference viscosity for CO_2	μ_{0,CO_2}	1.37e-4 [poise]	(COMSOL n.d.)
Reference viscosity for air	$\mu_{0,air}$	1.72e-4 [poise]	(COMSOL n.d.)
Reference viscosity for argon	$\mu_{0,Ar}$	2.13e-4 [poise]	(COMSOL n.d.)
Reference temperature for all gases	T_0	273.15 [K]	(COMSOL n.d.)
Sutherland's constant for CO_2	c_{CO_2}	222	(COMSOL n.d.)
Sutherland's constant for air	c_{air}	111	(COMSOL n.d.)
Sutherland's constant for argon	c_{Ar}	114	(COMSOL n.d.)
Gas-phase heat capacity (CO_2, argon)	$C_{p,CO_2}, C_{p,Ar}$	Temperature-dependent [J/mol-K]	Based on Shomate equation (National Institute of Standards and Technology n.d.)
Gas-phase heat capacity (air)	$C_{p,air}$	Temperature-dependent [J/mol-K]	(The Engineering ToolBox 2004)
Heat capacity of zeolite	$C_{p,z}$	1 [J/g-K]	(Lu *et al* 2020)
Heat capacity of mica	$C_{p,m}$	0.85 [J/g-K]	(The Gund Company n.d., S&R Optic GMbH n.d.)
Heat capacity of adsorbed CO_2	$C_{p,a}$	2 [J/g-K]	(Wurzbacher *et al* 2016)
Heat capacity of brass	$C_{p,w}$	0.377 [J/g-K]	(The Engineering ToolBox 2003)
Heat of CO_2 desorption	ΔH	35 [kJ/mol]	(Reynolds 2019, Son *et al* 2018)
Mass of zeolite	m_z	5 [g]	This study
Mass of Surfaguide	m_w	4,500 [g]	Typical value
Thermal conductivity of zeolite	k_z	0.1 [W/m-K]	Typical value
Thermal conductivity of mica	k_m	0.5 [W/m-K]	Typical value

Dielectric constant of zeolite	ε_r'	3.15	Typical value
Dielectric loss of zeolite	ε_r''	Temperature-dependent	This study
Emissivity of zeolite	$e_{m,z}$	0.8	Typical value
Emissivity of mica	$e_{m,m}$	0.75	Typical value
Vacuum pump efficiency	η	0.8	Typical value

B.1.2 CO_2 adsorption equilibrium of zeolite beads

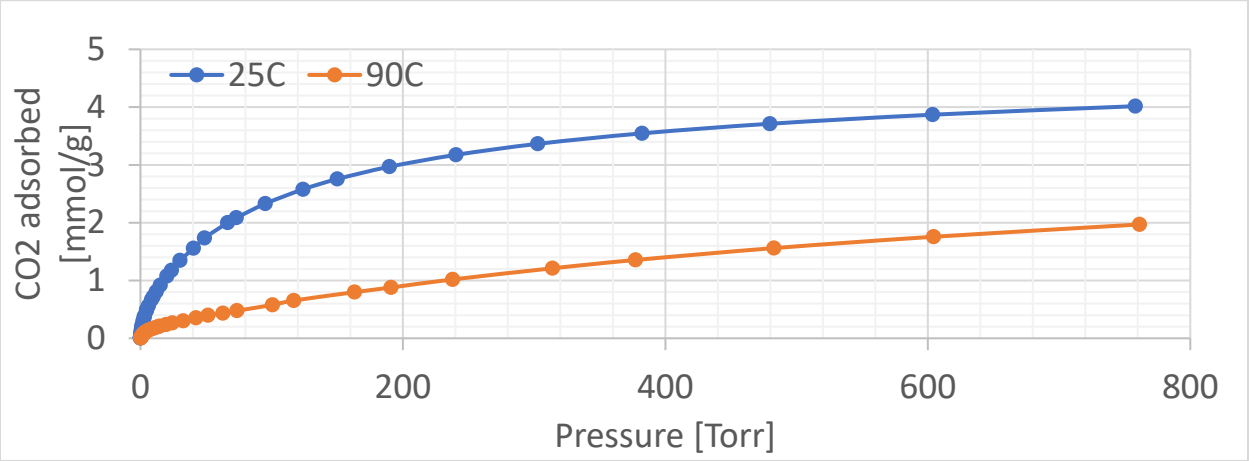

Figure B.1. Single-component CO_2 equilibrium adsorption isotherm of zeolite 13x bead is measured using a Micrometric ASAP 2050.

B.1.3 Estimating parameters from a pump-down curve

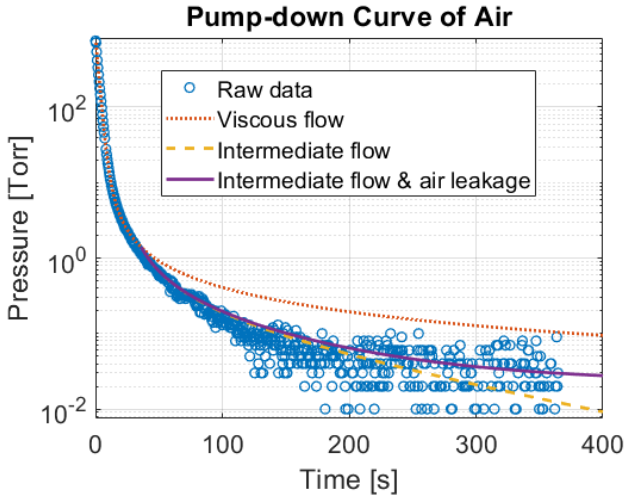

Figure B.2. Pump-down curve of air is used to adjust effective pumping speed and pipe dimensions. The calculated pressure evolution using fitted parameters show a good fit to the experimental data

Unlike the simplified geometry used to calculate gas-phase transport during experiments, the actual apparatus is constructed with a number of pipes with different inner diameters and tees. The vacuum pump is also connected to the system via pipes with a smaller diameter than the pump

inlet which limits its pumping speed. Thus, effective parameters – including pumping speed, pipe diameter, and length – that can be applied to the simplified geometry are derived from a pump-down curve of the empty reaction chamber from the ambient pressure. The reaction chamber filled with air at ambient pressure and temperature was evacuated by the vacuum pump until its pressure is reduced to below 0.5 Torr. As a result, 1.1 m^3/hour of pumping speed (55% of the maximum capacity), 0.18" of pipe diameter, and 2m of pipe lengths are determined as fitted values. The pump-down curve generated using the fitted parameters shows a good fit to the experimental data as shown in Figure B.2. The pump-down curve shows that the gas flow transition from viscous to intermediate when the total pressure decreases below 1 Torr, and that air leakage becomes important at low pressure. A constant air leakage rate of 8 Pa/s is assumed based on a separate measurement.

B.1.4 Quantifying CO_2 desorption rate using a mass transport model

The recorded pressure data primarily comprise partial pressure of air, argon, and CO_2, including residual CO_2 at the beginning of the measurement and CO_2 desorbed from zeolites during regeneration. The partial pressure of air and argon is computed using the effective parameters of the system identified through pump-down tests (B.1.3) and considering gas-specific viscosity and conductance using equation (3.2)-(3.9). The gas mixture inside the chamber before pump-down is assumed to be an isotropic mixture of air and argon with equal partial pressure contribution; the sorbent chamber is primarily filled with argon and the 6-way cross is mostly filled with air during the mass measurement of the sorbents prior to the onset of regeneration. Air leakage

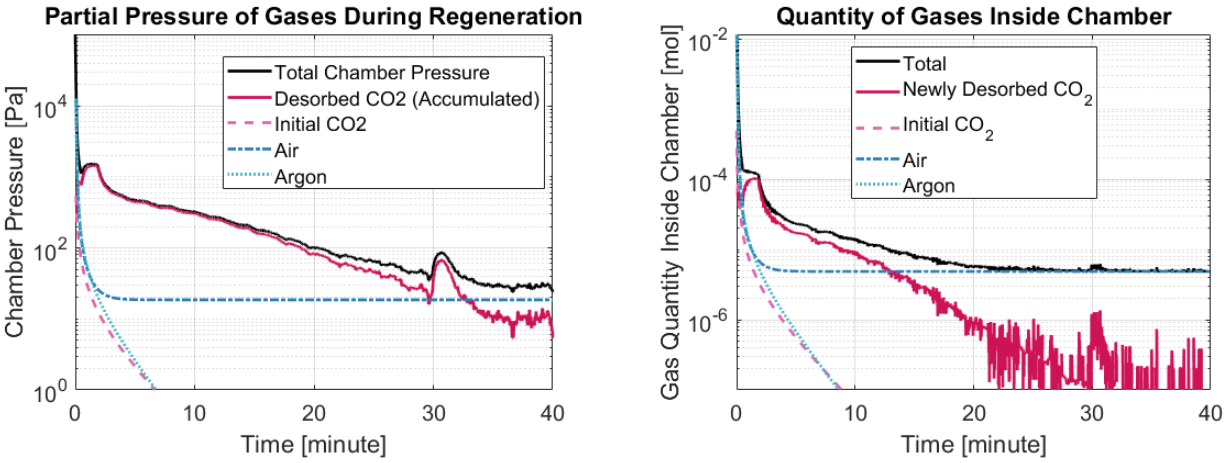

Figure B.3. (a) Estimated partial pressure of CO_2, air, and argon gas during CO_2 desorption measurement, (b) calculated mol quantity of the desorbed CO_2 after considering accumulation.

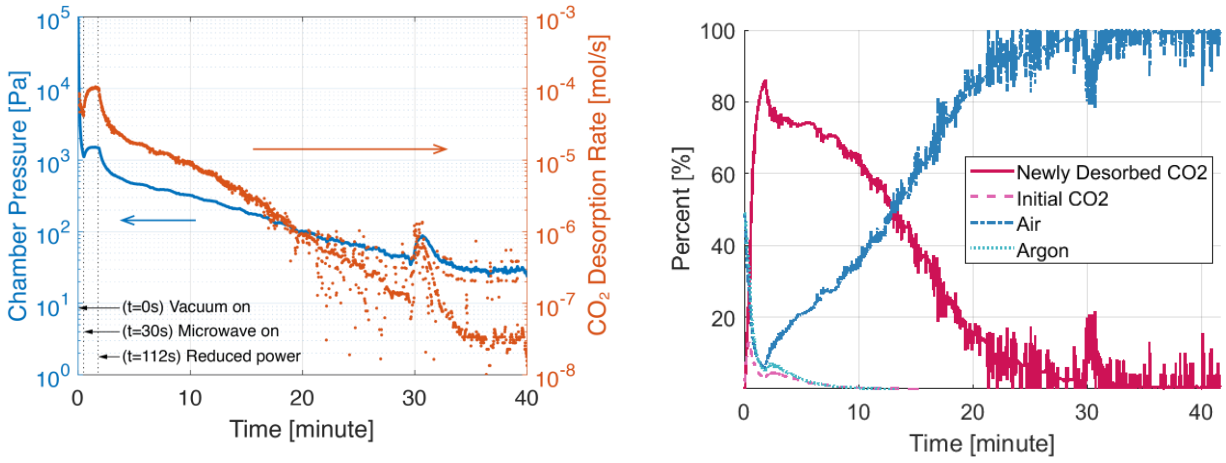

Figure B.4. (a) Measured chamber pressure and calculated CO_2 desorption rate, (b) Molar contribution of CO_2, air, and argon gases inside the chamber during sorbent regeneration

into the chamber with a constant rate is considered when estimating the partial pressure evolution of air. Then CO_2 partial pressure inside the chamber can be estimated by subtracting the partial pressure of air and argon from total pressure as shown in Figure B.3a.

The CO_2 partial pressure inside the chamber represents *accumulated* CO_2 at a given time, including newly recovered CO_2 and previously desorbed CO_2 that is yet to be evacuated from the chamber due to a limited pipe conductance. The partial pressure of the newly desorbed CO_2 can be estimated with equation (3.8) by considering dynamically changing conductance and total CO_2 partial pressure (Figure B.3b). Then, CO_2 desorption rate can be calculated using equation (3.9) as shown in Figure B.4a. The total quantity of the desorbed CO_2 estimated through this procedure should match the 1) measured mass change of the zeolite beads before and after the experiment and also 2) measured CO_2 adsorption capacity using sorption analyzer (Figure B.1), both of which indicate 4.1 mmol of CO_2 adsorption and desorption per gram of zeolite. Thus, temperature of the desorbed CO_2 gas is estimated to be between 45-55°C using equation (3.9) to find the value that yields 4.1 mmol/g of gross CO_2 desorption.

B.2 POWER DISSIPATION MODEL

B.2.1 COMSOL finite element model setup

The 3-D finite element model of the packed zeolites, mica cage, reaction chamber, Surfaguide, and Faraday cages was built with COMSOL Multiphysics packages utilizing RF and Heat Transfer modules. To reduce computational time, only the interior of the Surfaguide is modeled. Small dimensions, such as thin air between the reaction chamber and Faraday cage are omitted the completed FEM model of the packed sorbents and Surfaguide are shown in Figure B.5a. The system boundary of the system includes all components that contribute to the dielectric heating and thermal loss processes as shown in Figure 3.2b. Dimensions of the components are based on the experimental settings, with simplifications made to overcome computational challenges. Microwave (2.45 GHz) is incident from a rectangular port of the Surfaguide operating in the TE10 mode. Only the interior volume and boundaries of the Surfaguide are modeled to reduce computational time. The electric field distribution at the interior volume of the Surfaguide is determined by solving the Helmholtz equation (equation (B.1)). A portion of the input electromagnetic energy is dissipated as heat by zeolites according to equation (3.1). The scale of heat dissipation is proportional to the dielectric loss of the material which is a function of temperature (Figure B.7). The electromagnetic energy dissipated by zeolite becomes a source of heat of the system, increasing the temperature of the zeolites and surrounding environment through conductive (B.2) and radiative (B.3) heat transfer. Convective heat transfer is omitted as this is not expected to be a primary means of heat transfer under vacuum (<10 Torr).

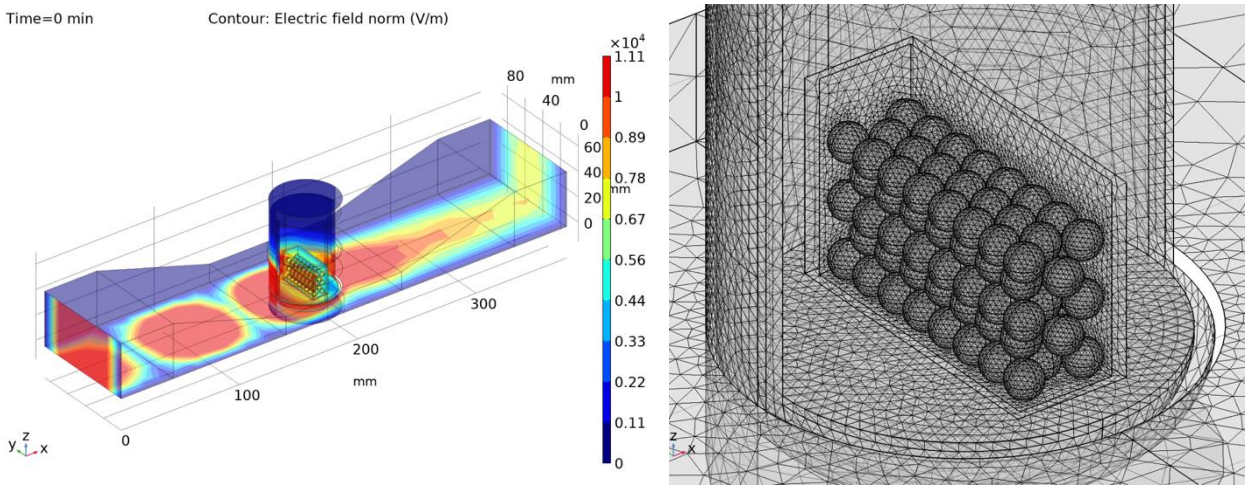

Figure B.5. (a) COMSOL simulation of electric field inside a simplified Surfaguide and packed sorbent structure, (b) packed sorbents are represented with close-packed 100 spheres

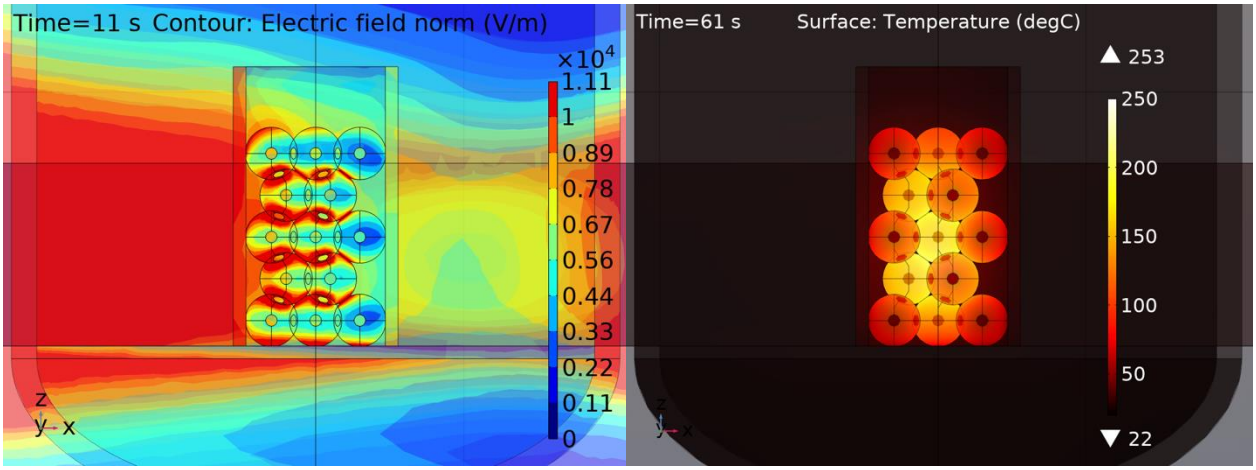

Figure B.6. (a) Electric field is concentrated inside the interior of the packed structure near contact points, (b) volumetric heating develops thermal gradient from interior core to the outer edge

$$\nabla \times \mu_r^{-1}\left(\nabla \times \vec{E}\right) - k_0^2\left(\varepsilon_r - \frac{j\sigma_e}{\omega\varepsilon_0}\right)\vec{E} = 0 \tag{B.1}$$

$$\rho C_p \frac{\partial T}{\partial t} - k\nabla^2 T = \dot{q}_d \tag{B.2}$$

$$\varepsilon A(G - n^2\sigma_{SB}T^4) = \dot{Q}_r \tag{B.3}$$

Packed zeolites were represented by hexagonally close-packed 100 equal spheres. The close-packed structure was first modeled with spheres of 4 mm in diameter. This created point contacts amongst the spheres and mica cage which requires extremely fine meshing and heavy computational resources. Thus, the diameter of the spheres is slightly enlarged after packing to allow partial overlapping amongst the beads and remove point contacts. This created a packed structure that has three beads across the direction of the microwave irradiation at the top as shown in Figure B.5b. To study geometry-related uncertainties, another packed structure was created with beads of approximately 3 mm in diameter following the same procedures. The resultant structure has four beads at the top across the direction of the microwave irradiation. These two packed configurations are denoted as ‘3 beads-thick’ and ‘4 beads-thick’ setup, respectively.

COMSOL simulation shows that the electric field is concentrated inside the interior of the packed volume near the contact points between the beads (Figure B.6a). This results in volumetric heating that heats zeolites from the inside out (Figure B.6b). These results are consistent with the heating profile observed with the IR thermometer.

B.2.2 Temperature-dependent dielectric loss of zeolite 13x

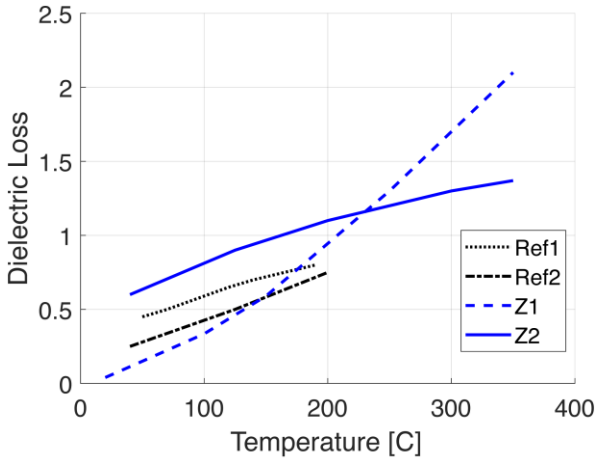

Figure B.7. Two temperature-dependent dielectric loss functions are used for the sensitivity. Reference data are based on (Polaert *et al* 2010)

Dielectric loss determines a material's ability to dissipate electromagnetic energy into heat based on equation (3.1). The dielectric loss of zeolite 13x monotonically increases with increasing temperature as measured by (Polaert *et al* 2010). In this study, dielectric loss of the zeolite is empirically determined by fitting the heating profile of the packed zeolite beads generated with the FEM to the surface temperature measurements. As a result, two dielectric loss functions are used to generate uncertainty ranges as shown in Figure B.7.

B.2.3 Observed surface zeolite temperature during dielectric heating

The heating profile of the packed zeolite structure with the application of microwave at a default mode as defined in B.3 is shown in Figure B.8. A 5g of packed zeolites are heated with

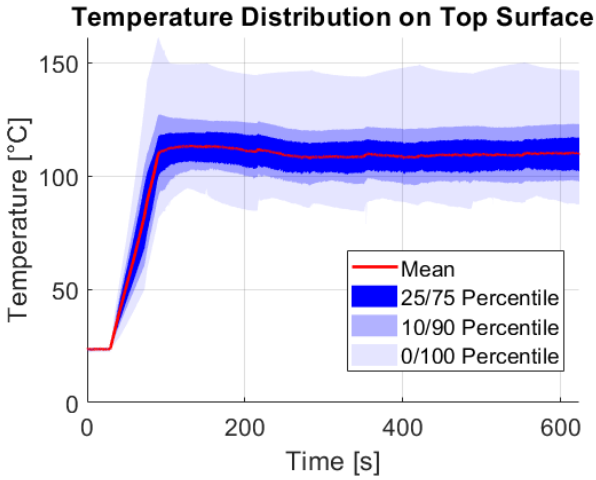

Figure B.8. Temperature profile of the packed zeolite beads measured at the top surface using IR thermometer

microwave from room temperature to 150°C (peak) in about one minute, after which microwave power is reduced to hold zeolite temperature near constant value. Zeolite beads are rotated 180 degrees every minute to promote even heating on both sides. As a result, average and peak temperature at the top surface was held at around 120°C and 150°C, respectively.

B.2.4 Estimating volumetric average zeolite temperature during dielectric heating

The dielectric heating results generated with the FEM is compared to the measured data shown in Figure B.8. A total of six uncertainty cases are simulated based on three zeolite geometries and two dielectric loss functions. The studied zeolite configurations include 3 or 4 beads-thick setups described in B.2.1 as well as a simple geometry that represents zeolites as a simple 'box' that entirely fill the mica cage. Dielectric loss functions are based on B.2.2.

The results show that the simplified packed-bead configurations reasonably replicate the observed temperature profile while the simple box geometry leads to an overestimation (Figure B.9). The assumptions on physical geometry can vary the simulation outcomes more than the assumptions on dielectric loss function. The 3 or 4 beads-thick setups used for the simulation assume packed structure entirely constructed with either 4 mm or 3mm beads, respectively. These simplified setups are expected to generate a reasonable uncertainty bounds as the actual size of the beads used for the experiments ranged between 2.4-4.8 mm. This is confirmed in Figure B.9 as the IR temperature measurements are bounded by the FEM results generated with 3 or 4 beads-thick configurations.

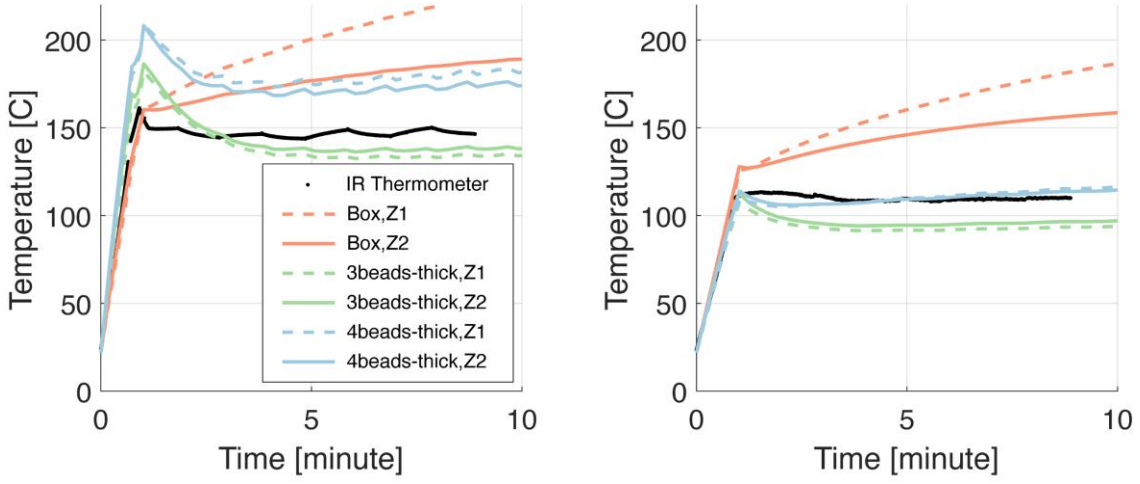

Figure B.9. Comparison of the observed surface temperature and FEM results during dielectric heating regarding (a) max and (b) average values

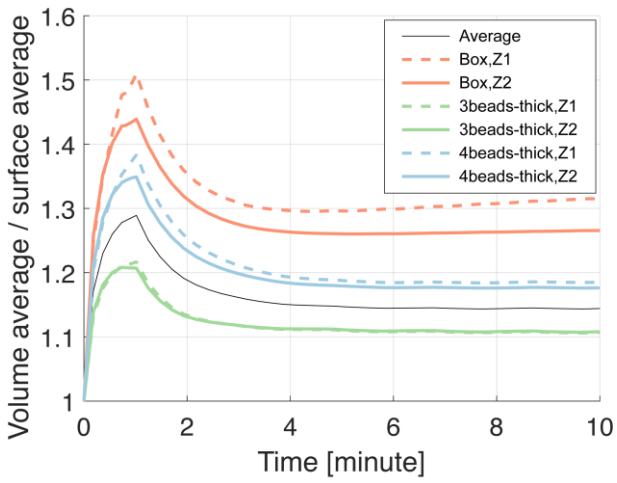

Figure B.10. Ratio of volumetric average and surface average temperature during dielectric heating as determined by FEM

Then, the volumetric temperature profile of zeolites during dielectric heating is estimated with the FEM as making such a measurement was not possible with the IR thermometer. The ratio of the volumetric average temperature of the zeolites relative to the average surface temperature at the top is shown in Figure B.**10**. Based on the range of results generated with FEM and the measured data (Figure B.**9**), the average values of the FEM results generated using 3 and 4 beads-thick configurations were used to estimate the volumetric heating of zeolites based on surface temperature measurement in equation (3.12). As a result, the average volumetric temperature of the zeolite beads during experiments is estimated to be nearly 135°C once the surface temperature is stabilized to around 120°C as shown in Figure B.8.

B.3 FINDING MODES OF MICROWAVE OPERATION THAT MINIMIZES ENERGY

The IR thermography confirms that packed zeolite 13x beads can be rapidly heated with microwave beyond 360°C, the measurement limit of the thermometer. Increasing incident power non-linearly increases both heating rate and ultimate temperature of zeolite, leading to a non-linear decrease in time to reach any target temperature (blue lines in Figure B.11a). However, increasing microwave power also non-linearly exacerbates heating uniformity – estimated with a standard deviation of temperature (σ) across the surface – due to positive feedback between enhanced microwave dissipation by the beads closer to the incident port and intensifying microwave absorption with increasing zeolite temperature (blue lines in Figure B.11b). The resultant cold spots can undermine the energy saved from rapid heating by requiring a prolonged microwave application.

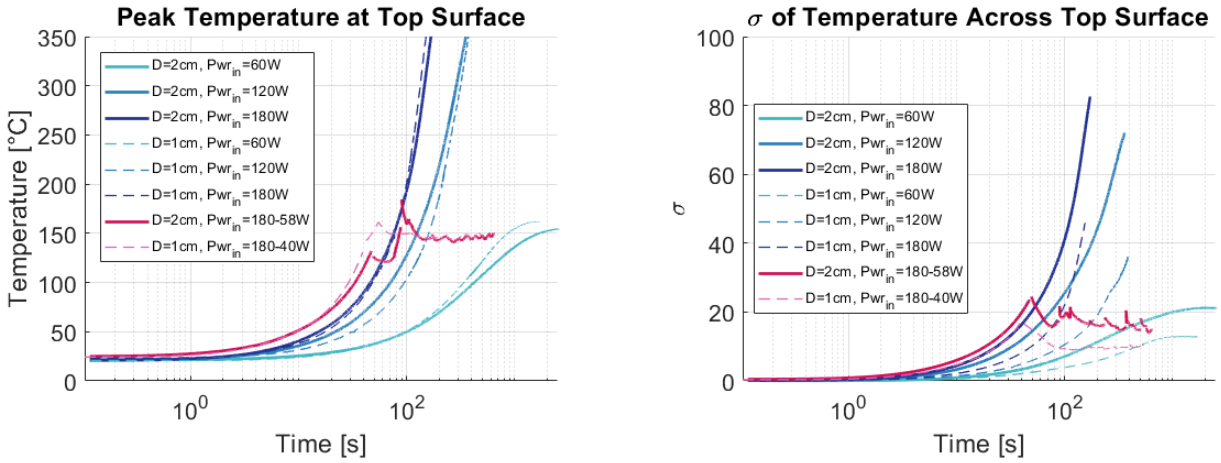

Figure B.11. (a) Peak temperature of the exposed top surface of the packed zeolite, (b) Standard deviation of temperature across top surface during dielectric heating.

We found that microwave energy needed to heat zeolite and regenerate CO_2 can be minimized by 1) dynamically adjusting microwave power from a higher to a lower value, and 2) by alternating the direction of microwave incidence simultaneously (red curves in Figure B.11). Power adjustment can minimize heating time while avoiding potential thermal degradation from overheating. Concurrent alternation of microwave irradiation helps lower σ. The combination of reduced heating time and decreased cold spots can lead to a minimized energy demand for CO_2 regeneration, as shown in Figure B.12 where 5g of packed zeolites were heated until its peak surface temperature reached 150°C. Using a constant microwave power, overall heating energy can be reduced by increasing power but at the expense of increasing σ (blues). Power adjustment and concomitant alternation of microwave incidence can evidently lower both heating energy and σ, resulting in a reduced overall microwave energy needed for regeneration (reds). Hence this

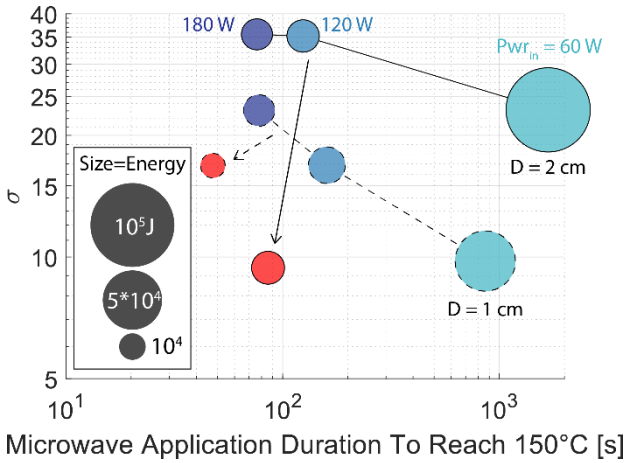

Figure B.12. Heating energy demand and σ can be lowered by using higher power and alternating the incidence direction. The initial high power needs to be tapered to a lower level to avoid overheating.

forms a default mode of microwave application for CO_2 regeneration in this study. Note that the actual scale of energy demand is lower considering electromagnetic leakage associated with the apparatus which is further discussed in the energy analysis.

REFERENCES

COMSOL The CFD Module User's Guide Online: https://doc.comsol.com/5.5/doc/com.comsol.help.cfd/cfd_ug_fluidflow_high_mach.08.27.html

Lu X, Wang Y, Estel L, Kumar N, Grénman H and Leveneur S 2020 Evolution of Specific Heat Capacity with Temperature for Typical Supports Used for Heterogeneous Catalysts *Processes* **8** 911 Online: https://www.mdpi.com/2227-9717/8/8/911

National Institute of Standards and Technology NIST Chemistry WebBook Online: https://webbook.nist.gov/chemistry/

Polaert I, Estel L, Huyghe R and Thomas M 2010 Adsorbents regeneration under microwave irradiation for dehydration and volatile organic compounds gas treatment *Chem. Eng. J.* **162** 941–8 Online: http://dx.doi.org/10.1016/j.cej.2010.06.047

Reynolds C 2019 *Decarbonizing Freight Transport: Mobile Carbon Capture from Heavy-Duty Vehicles* Online: http://hdl.handle.net/2027.42/151521

S&R Optic GMbH Properties of Mica Online: https://www.sr-optic.com/Materials/Mica/

Son K N, Cmarik G E, Knox J C, Weibel J A and Garimella S V. 2018 Measurement and Prediction of the Heat of Adsorption and Equilibrium Concentration of CO_2 on Zeolite 13X *J. Chem. Eng. Data* **63** 1663–74 Online: https://pubs.acs.org/doi/10.1021/acs.jced.8b00019

The Engineering ToolBox 2004 Air - Specific Heat at Constant Pressure and Varying Temperature Online: https://www.engineeringtoolbox.com/air-specific-heat-capacity-d_705.html

The Engineering ToolBox 2003 Metal Alloys - Specific Heats Online: https://www.engineeringtoolbox.com/specific-heat-metal-alloys-d_153.html

The Gund Company Material Data Sheet Online: https://thegundcompany.com/wp-content/uploads/2016/11/Mica-M-from-The-Gund-Co.pdf

Wurzbacher J A, Gebald C, Brunner S and Steinfeld A 2016 Heat and mass transfer of temperature–vacuum swing desorption for CO_2 capture from air *Chem. Eng. J.* **283** 1329–38 Online: http://dx.doi.org/10.1016/j.cej.2015.08.035

Appendix C

Supplementary Information for Chapter 4

C.1 CO_2 UTILIZATION TECHNOLOGIES AND INDUCED BOOST IN 28-DAY COMPRESSIVE STRENGTH

Past experiments show that compressive strength of concrete can increase when CO_2 is added during the formulation of concrete. These results are shown in Figure C.1. for compressive strength measured at 28 days after casting when CO_2 is added (a) during mixing (Monkman and MacDonald 2016, 2017, Monkman *et al* 2015, 2016a), (b) in RCA (Xuan *et al* 2016), or (c) while curing (Rostami *et al* 2012, Shi *et al* 2016, Zhang *et al* 2016) as a function of added CO_2 and substitution rate of natural coarse aggregate with recycled concrete aggregate (RCA). The added CO_2 enhances compressive strength through different mechanisms for each of the CO_2 utilization strategies as explained in the following paragraphs.

For carbonation during mixing, liquid CO_2 is injected directly into a mixer during batching and mixing. The injection timing of CO_2 is synchronized with the addition of ordinary Portland cement (OPC) and last a few minutes in adherence to the standard mixing time (Monkman and MacDonald 2016). The added CO_2 is converted into a mixture of CO_2 gas and solid CO_2 'snow' upon injection, forming nanoscale calcium carbonate that promotes hydration reactions and hence developing compressive strength (Monkman *et al* 2016b, 2018). As shown in Figure C.1 (A), compressive strength generally increases as more CO_2 is absorbed. If more than one percent of CO_2 is absorbed by the mass of cement, however, the boost in compressive strength can weaken. According to Monkman, the excess CO_2 may interfere with the subsequent hydration reaction (Monkman *et al* 2016b). Overall, compressive strength can increase by 3-30% depending on the amount of CO_2 reacted with the cement matrix. Results presented in Figure C.1 (A) include experiments performed on mixtures that use OPC as a primary binder and also mixtures that contain fly ash (FA) and ground granulated blast furnace slag (GGBS).

RCA is a repurposed waste concrete that can substitute natural aggregate (NA), both coarse and fine, but its use and application has been limited due to its poor quality (RILEM TC 121-DRG

1994, Behera *et al* 2014, Silva *et al* 2015, Goonan 2000). The use of fine RCA is tightly regulated or even banned in many countries for practical concerns and thus we only assess the use of coarse RCA to substitute coarse NA throughout this study (Evangelista and De Brito 2014, Thiery *et al* 2013). The carbonation process of RCA is nearly identical to that of carbonation curing (below); RCA is exposed to CO_2 enriched environment (0.1-5 bar of pure CO_2) in a sealed chamber typically for a few hours up to 24 hours (Zhan *et al* 2014, Xuan *et al* 2016). With proper pre- and post- carbonation treatment, CO_2 reacts with hydration products of residual cement in RCA to improve its mechanical properties – including density, flexural strength, and microhardness of interfacial transition zone – and thereby increase the compressive strength of concrete that incorporates it (Xuan *et al* 2016, Zhan *et al* 2014, Kou *et al* 2014, Zhan *et al* 2013, Zhang *et al* 2015). But substituting coarse NA with RCA alone also induces non-linear impact on compressive strength; compressive strength of concrete generally decreases with an increasing proportion of RCA (Behera *et al* 2014, Silva *et al* 2015) as shown in Figure C.1 (B). Considering both impacts from carbonation and RCA substitution, compressive strength of concrete can improve by 0.9-4.7% by substituting 20-40% of natural coarse aggregate with carbonated RCA, assuming about 0.74% of CO_2 by mass of RCA is absorbed in residual cement in RCA.

Lastly, fresh concrete products, within 24 hours after casting, can be cured with CO_2 in a controlled, CO_2 enriched environment. A recent review outlines the overall process of carbonation curing (Zhang *et al* 2017). First, excess water is removed from the surface of the freshly cast concrete product prior to carbonation treatment by exposing it to ambient environment (typically less than 20 hours). The conditioned concrete product is then exposed to a CO_2 enriched environment (1-5 bar of pure CO_2) where gaseous CO_2 diffuses and permeates through the surface of the concrete, dissolves into alkaline pore water, and reacts with both unhydrated and hydrated cement compounds to form binding matrix, improving compressive strength (Kashef-Haghighi *et al* 2015, Zhang *et al* 2017). Carbonation treatment may be employed for a few hours up to days but the rate of carbonation reaction decreases with prolonged duration. Upon reacting with CO_2, the concrete product is compensated for moisture to promote subsequent hydration reactions. As a result, 28 days compressive strength of concrete can be improved nearly 6-17% compared to the same samples prepared with conventional steam or moisture curing by absorbing about 7-17% of CO_2 by cement mass as shown in Figure C.1 (C) (Rostami *et al* 2012, Zhang and Shao 2016b, Zhang *et al* 2016). Between 12-20 hours or pre-carbonation air curing and 2-12 hours of

carbonation treatment with 1.5-5 bar of pure CO_2 were applied to a set of concrete mixtures that contain OPC and FA to generate these results. Thus, nearly an order of magnitude more CO_2 can be sequestered in concrete through curing than when CO_2 is added during mixing or in RCA.

Based on the literature review, we assumed in this study that compressive strength of concrete improves upon treatment with CO_2. While this assumption is generally validated, some studies found a decrease in compressive strength in certain occasions (El-Hassan *et al* 2013, Monkman and MacDonald 2017, Lee *et al* 2016): if essential procedures are omitted, when adequate degree of carbonation is not reached, or if additional factors negatively affect its development. For instance, adequate control of the surface water on concrete is essential to yield optimal results when CO_2 is applied through (Zhang *et al* 2017, Zhang and Shao 2016a). When the optimal water level was not maintained before, during, or after the curing process, hydration reactions were inhibited which led to a net loss in compressive strength (El-Hassan *et al* 2013, Lee *et al* 2016). When CO_2 was introduced during mixing, a decrease in compressive strength was observed when an excess amount of CO_2 was injected beyond the optimal dosage (Monkman *et al* 2016b). We assumed that CO_2 utilization would generally increase compressive strength when properly applied. When it does not contribute to increased strength, CO_2 utilization would not be used.

Also, it is important to note that this analysis is primarily based on compressive strength measured at 28 days after casting due to data availability. We expect consideration of compressive strength measured at longer age would not significantly affect the overall findings of this study since compressive strength of carbonated samples continue to develop beyond 28 days, and mostly show improved compressive strength compared to the uncarbonated counterpart, similar to the trend shown with 28 days compressive strength (Monkman *et al* 2016b, 2015, Monkman 2014).

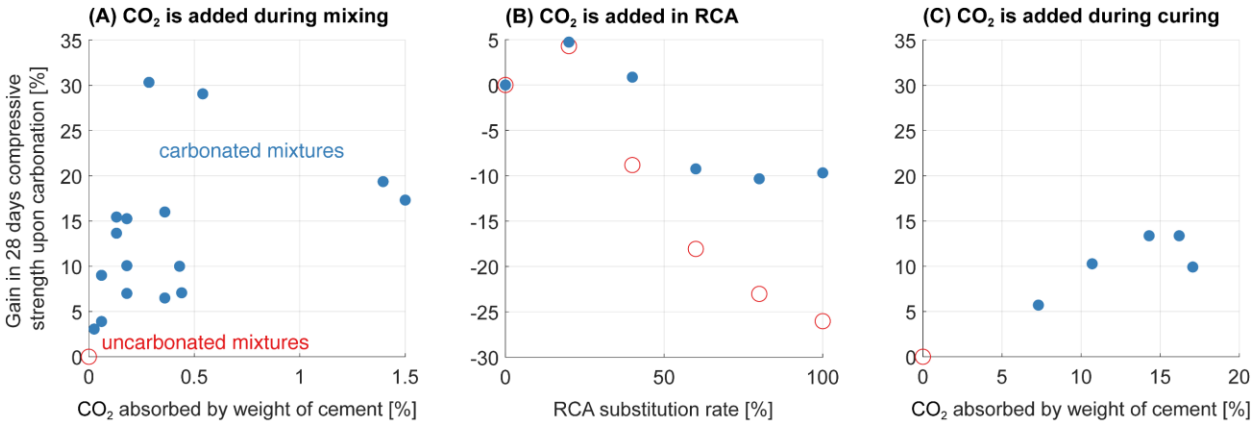

Figure C.1. Percentage gain in compressive strength when concrete is formulated with added CO_2 (A) during mixing, (B) in RCA, or (C) while curing.

However, precaution is needed when selecting alternative mixtures for specific applications especially when parameters not included in this analysis become important such as tradeoff between carbonation and pozzolanic reactions (Zhang *et al* 2016).

C.2 Step-wise derivation of CO_2-amended mixtures

The input files, codes, and the results generated for this analysis are available in the following link (https://umich.box.com/s/jpae59stixbjlkf6y2lqol4jpmshkd5d). The results are generated according to the step-wise calculations described below.

Step 1: Setup Cohort of Representative Mixtures. Since specific mixture designs for commercial concrete products are generally not available in the public domain, we compiled 696 validated concrete mixture designs found in 32 published reports and papers (see section C.12). Of the 696 mixtures, we use 48 regional benchmark mixtures (D_{Base}) created by the (National Ready Mixed Concrete Association 2016) to represent the diversity of mixtures currently employed in the U.S. The compressive strength of these 48 mixtures 28 days after casting ranges from 17 to 55 MPa. While higher strength beyond 55 MPa may be required for specific applications, these 48 mixtures collectively show comparable compressive strength distribution reported by the surveys made by NRMCA and European Ready Mixed Concrete Organization (National Ready Mixed Concrete Association 2016, European Ready Mixed Concrete Organization 2018). Hence, we assume that these 48 D_{Base} mixtures adequately represent the

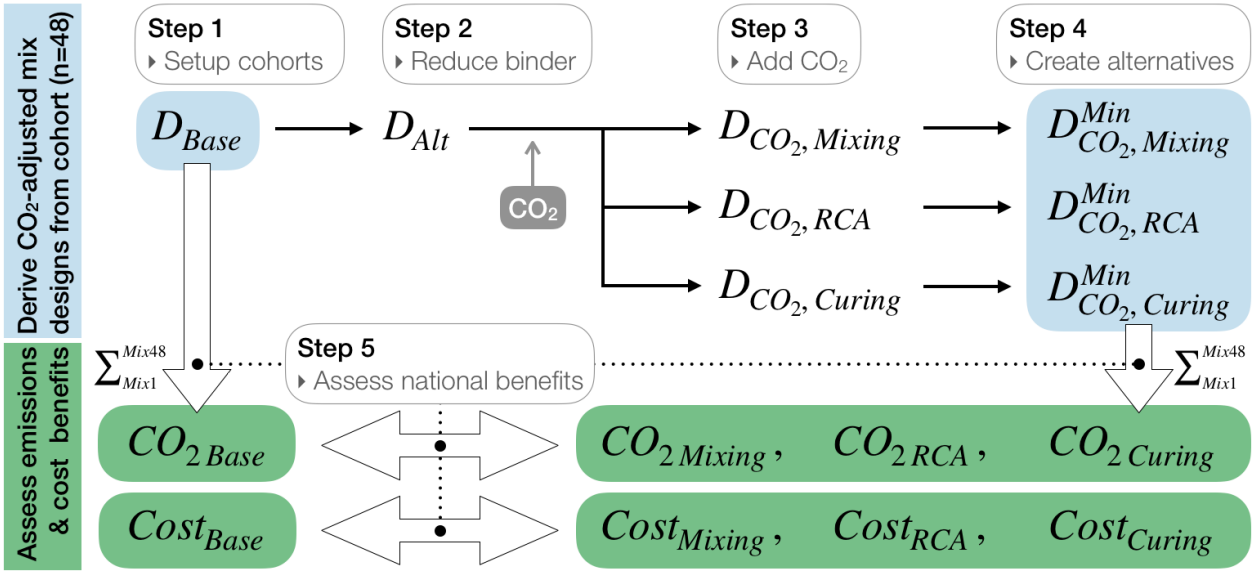

Figure C.2. Net CO_2 reductions and net material cost savings by transitioning to CO_2-amended formulations in the U.S. concrete industry are calculated by the difference between the total CO_2 emissions (CO_2) and material cost ($Cost$) of producing 48 $D_{CO_2}^{Min}$ mixtures with respect to 48 D_{Base} mixtures. Application of three CO_2 utilization strategy is independently assessed.

diversity of ready mixed concrete used in the U.S. Since ready-mixed concrete constitutes about 90% of the U.S. market, we further assume that these 48 D_{Base} mixtures can represent the entire U.S. market, including mixtures used for precast applications. Then, the national production volume of each D_{Base} mixture is derived from its relative representation in the simulated national population (National Ready Mixed Concrete Association 2016) and the national shipment data in 2015 (Van Oss 2018). Figure C.3 (1A-B) shows the distributions of the 696 compiled mixtures including 48 D_{Base}.

Step 2: Production of D_{Alt} Formulations. For each of the 48 D_{Base} mixtures, we formulate a collection of alternative designs, D_{Alt}, by looking at mixtures from the pool of 696 formulations and consider those with equal or less binder. A set of D_{Alt} mixtures for a sample D_{Base} mixture is located on or below the iso-binder curve of a sample D_{Base} as shown in Figure C.3 (2A). Some of these collected designs have a lower compressive strength than D_{Base} (Unsuitable Region) and some have a greater compressive strength (Suitable Region). For each D_{Base}, we assume that substituting with a formulation in the suitable region is infeasible as reducing binder cannot increase compressive strength. If the substitution with a mixture in the suitable region were possible or desirable, it would have happened already. In other words, we assume each D_{Base} to be an optimum based on local design constraints. Hence, we consider only the set of D_{Alt} mixtures in the unsuitable region possible for a sample D_{Base} mixture. This set of D_{Alt} mixtures includes the sample D_{Base} itself and other D_{Base} that are located in the suitable region.

Step 3: Production of D_{CO_2} Formulations. For each D_{Alt}, we produce a set of designs that incorporates CO_2 as part of its formulation (D_{CO_2}) by applying one of the CO_2 utilization strategies at a time. Experimental results show that compressive strength of concrete can increase when CO_2 is added during curing (Rostami *et al* 2012, El-Hassan and Shao 2014b, Zhang and Shao 2016b, Zhang *et al* 2016), mixing (Monkman and MacDonald 2016, 2017, Monkman *et al* 2015, 2016a), or in RCA (Xuan *et al* 2016). For each of the CO_2 utilization strategies, we compiled a range of data regarding the percent increase of compressive strength as a function of absorbed CO_2 in OPC or in RCA. When we add CO_2 using one of the utilization techniques, we apply the corresponding percent increase data to the compressive strength of D_{Alt} and generate a range of D_{CO_2} with increased compressive strength. Since binder content remains unchanged, D_{CO_2} mixtures follow the iso-binder line of D_{Alt} as shown in Figure C.3 (3A). We only consider D_{CO_2} mixtures in the suitable region that have compressive strength equal to or higher than D_{Base} to provide at least

the same level of material integrity as with the original D_{Base}. As a result, we create three sets of D_{CO_2} by adding CO_2 during curing, mixing, or in RCA as shown in Figure C.2. An example set of D_{CO_2} generated from a sample D_{Base} through employing carbonation curing is shown in Figure C.3 (3B).

As an example, properties of the sample D_{CO_2} mixtures shown in Figure C.3 (3A) are listed in Table C.2. The compiled percent increase data for compressive strength shown in Figure C.1 (C) are applied to the compressive strength of a sample D_{Alt} mixture to estimate the increased compressive strength of D_{CO_2}. Three sample D_{CO_2} mixtures fully recover the original compressive strength of D_{Base} after adding CO_2. The absorbed CO_2 is calculated by applying percent CO_2 absorption data points to the OPC content of D_{Alt}.

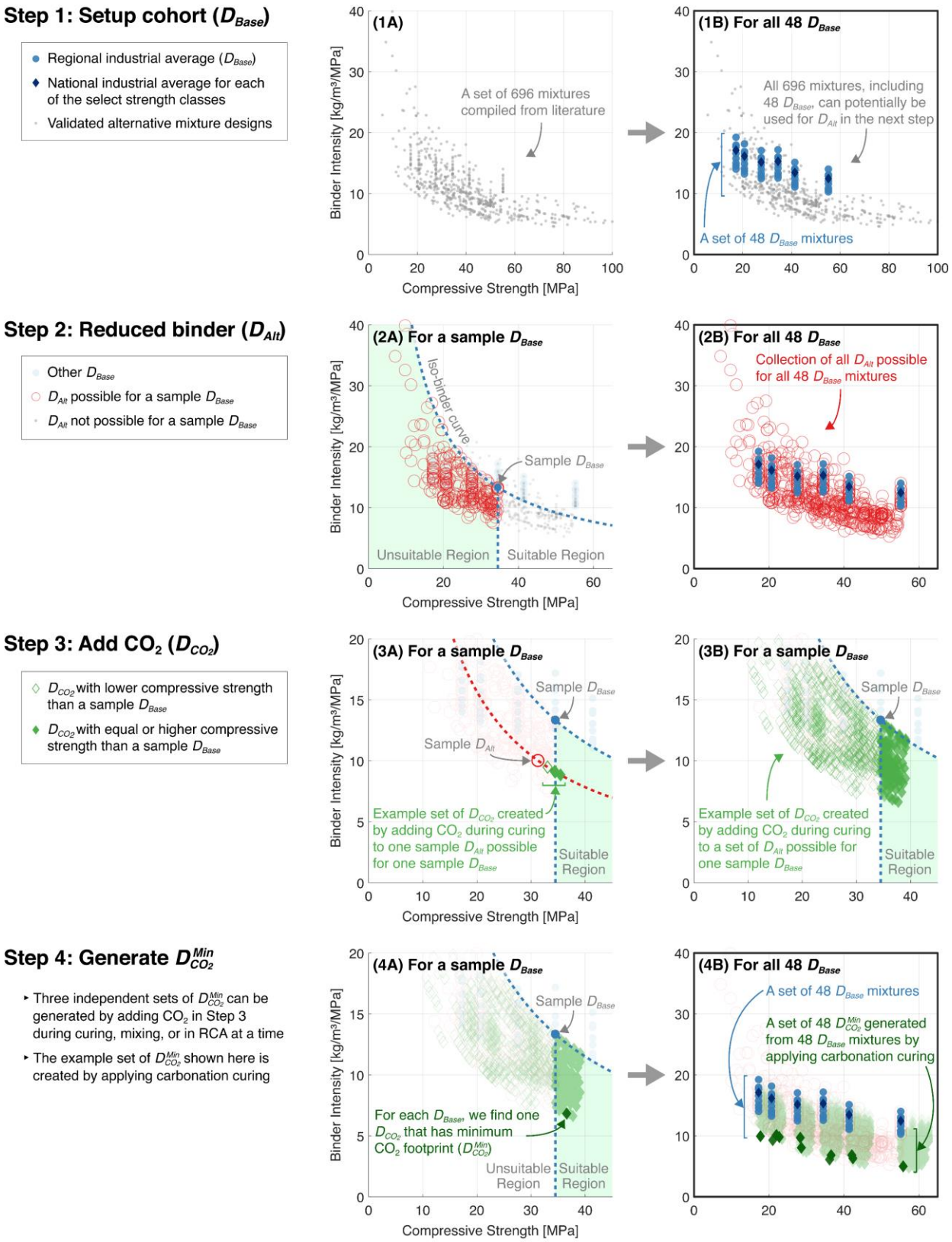

Figure C.3. Formulation of 48 $D_{CO_2}^{Min}$ mixtures from 48 D_{Base} mixtures according to the prescribed steps when carbonation curing is applied. Other sets of 48 $D_{CO_2}^{Min}$ mixtures generated when CO_2 is added during mixing or in RCA are not shown in this figure.

Table C.2. Sample calculations of D_{CO_2} mixtures from a sample D_{Base} by applying carbonation curing. The compiled data points shown in Figure C**.** are applied to a sample D_{Alt} to generate five sample D_{CO_2}. Three of these D_{CO_2} have compressive strength equal or greater than the original D_{Base}. Compressive strength is abbreviated as Comp.Str.

Sample Mixture Designs	OPC Content [kg/m^3]	Binder Content [kg/m^3]	Comp.Str. [MPa]	Binder intensity [kg/m^3/MPa]	CO_2 absorbed [kg/m^3]	Recovered original strength?	Effects of employing carbonation curing [%]	
							Increase in Comp.Str.	CO_2 absorbed
Sample D_{Base}	381.5	460.4	34.5	13.4		n/a		
Sample D_{Alt}	285.0	313.5	31.3	10.0		No		
Sample D_{CO_2} 1	285.0	313.5	33.0	9.5	20.8	No	5.7%	7.3%
Sample D_{CO_2} 2	285.0	313.5	35.4	8.8	40.8	Yes	13.4%	14.3%
Sample D_{CO_2} 3	285.0	313.5	34.4	9.1	48.6	No	9.9%	17.1%
Sample D_{CO_2} 4	285.0	313.5	35.4	8.8	46.2	Yes	13.4%	16.2%
Sample D_{CO_2} 5	285.0	313.5	34.5	9.1	30.5	Yes	10.3%	10.7%

Step 4: Construct Cohorts of Alternative Mixtures Formulated with CO_2 Among the set of D_{CO_2} mixtures available for each D_{Base} mixture, we select one D_{CO_2} that possesses the lowest CO_2 footprint ($D_{CO_2}^{Min}$) and substitute D_{Base} with it (Figure C.3 (4A)). As a result of this process, three sets of $D_{CO_2}^{Min}$, each containing 48 mixtures that replace 48 D_{Base} mixtures, are generated when CO_2 is added during mixing, curing, or during the recycling of concrete aggregate. Given the initial representation of the D_{Base}, it is reasonable to expect that the 48 $D_{CO_2}^{Min}$ mixtures in each set represent the diversity of CO_2-amended mixtures available to the U.S. concrete industry. Figure C.3 (4B) shows an example distribution of $D_{CO_2}^{Min}$ when CO_2 is applied during curing.

Step 5: Calculate Net CO_2 Reduction and Saved Cost by Formulating Concrete with CO_2 The CO_2 footprint of each of the D_{Base} mixtures can be calculated by summing the CO_2 footprint of its constituents and the CO_2 emitted during batching and mixing. The CO_2 footprint of $D_{CO_2}^{Min}$ mixtures additionally accounts for net CO_2 offset, which considers sequestered CO_2 in concrete and the additional CO_2 emitted while purifying byproduct CO_2 from industrial processes and transporting it to concrete plants (Supekar and Skerlos 2014). We assume industrial grade (purity ≥ 99.5%) byproduct CO_2 from ethanol, ammonia, or hydrogen plants would be used for CO_2 utilization processes. The net CO_2 reduction by formulating concrete with CO_2 in the U.S. can then be defined by the difference between the total CO_2 emissions generated by the 48 $D_{CO_2}^{Min}$ mixtures with respect to the 48 D_{Base} mixtures, with each mixture weighted by its national production volume. We assume that the $D_{CO_2}^{Min}$ formulations generated with carbonated RCA or with carbonation during mixing can be applied across the industry whereas $D_{CO_2}^{Min}$ prepared with carbonation curing can only be used in precast products.

Similarly, the material cost involved with fabricating each of the D_{Base} and $D_{CO_2}^{Min}$ mixtures can be calculated by adding the cost incurred from manufacturing each of its constituents. The net cost benefit of transitioning to CO_2-adjusted formulations is then defined by the change in total material cost incurred by producing 48 $D_{CO_2}^{Min}$ mixtures with respect to 48 D_{Base} mixtures, with each mixture weighted by its national production volume. The additional cost incurred by utilizing CO_2 includes the costs of recovering byproduct CO_2 and reacting CO_2 with constituents, which were estimated from published literature (El-Hassan and Shao 2014a, Shao 2014, Parsons Brinckerhoff and Global CCS Institute 2011). This additional cost of CO_2 utilization is compared to the saved material cost in the results to assess economic implication of CO_2 utilization. Data and equations used in this step are provided in section C.3-C.4.

C.3 CALCULATING THE RANGE OF MIXTURE-LEVEL CO_2 FOOTPRINT AND MATERIAL COST

C.3.1 Calculating the range of CO_2 footprint of a concrete mixture

The CO_2 generated by fabricating a cubic meter of concrete mixture is calculated by adding CO_2 footprint of its constituents and CO_2 emitted during batching and mixing operation using (A.3)-(C.3). When CO_2 is sequestered in concrete, we apply *net* CO_2 offset to its overall CO_2 footprint considering the mass of sequestered CO_2 and additional CO_2 generated during purifying byproduct CO_2 and transporting it to concrete plants. CO_2 footprint of each constituent accounts for greenhouse gases emitted while producing constituent and during transporting finished constituent to central mixing facilities as shown in (C.2).

$$c_{mixture} = \sum_i (m_i * c_i) + c_{B\&M} - m_{CO_2} \quad \text{(C.1)}$$

$$c_i = c_i^M + c_i^T = c_i^M + \sum_j (d_j^i * c_j) \quad \text{(C.2)}$$

$$m_{CO_2} = \begin{cases} m_{OPC} * wt\%_{absorption}^{OPC} \ (if\ CO_2\ is\ added\ during\ mixing\ or\ curing) \\ m_{RCA} * wt\%_{absorption}^{RCA} \ (if\ CO_2\ is\ added\ in\ RCA) \end{cases} \quad \text{(C.3)}$$

where $c_{mixture}$ stands for an overall carbon footprint of a concrete mixture ($kgCO_2e/m^3$) and m_i is a mass of constituent i (kg) – including OPC, FA, GGBS, silica fume (SF), metakaolin (Meta), natural pozzolan (Pozz), limestone (L), water, coarse natural aggregate (C.Agg.), RCA, fine natural aggregate (F.Agg.), and byproduced CO_2. c_i is a total carbon footprint of constituent i including its footprint from manufacturing (c_i^M) and transporting (c_i^T) it to concrete plants

(kgCO_2e/kg). d_j^i is an average distance travelled by constituent i from production site to concrete mixing plants via mode of transport j (km), including truck, rail, ocean, and barge. c_j is a carbon footprint of a mode of transport j (kgCO_2e/kg-km). $c_{B\&M}$ is a carbon footprint of batching and mixing operation at central concrete plants (kgCO_2e/m^3). m_{CO_2} represents an offset from absorbed CO_2 in concrete (kgCO_2e/m^3) as a result of adding CO_2 (step 3 in the section 2), where m_{OPC} and m_{RCA} are mass of OPC and RCA, respectively. $wt\%_{absorption}$ is a percent of CO_2 absorbed by mass of OPC or RCA whose value is determined according to the level of compressive strength increased when CO_2 is added (examples are provided in Table C.2). The *net* offset is then represented as $m_{CO_2} * (-1 + c_{CO_2})$, where c_{CO_2} is additional CO_2 emissions generated while recovering and purifying byproduct CO_2 and transporting it to concrete plants. m_{CO_2} is zero when no CO_2 is sequestered. Data compiled from cradle-to-gate life cycle emissions studies, environmental product declarations (EPD), and past literatures were used to form three levels of uncertainty range for each parameter as summarized in Table C.3 (World Business Council for Sustainable Development 2016, Marceau *et al* 2006, Portland Cement Association 2016c, 2016b, Van Oss 2018, Miller 2018, Heath *et al* 2014, Slag Cement Association 2015, Wernet *et al* 2016, Maddalena *et al* 2018, Jones *et al* 2011, Marceau *et al* 2007, McEwen 2017c, 2017b, 2017a, 2018, Griffiths-sattenspiel and Wilson n.d., National Ready Mixed Concrete Association 2016, Supekar and Skerlos 2014).

Chemical admixtures, such as plasticizer, superplasticizer, air-entraining agent, and set accelerator, are excluded from this analysis as their dosage rate is typically below one percent by mass of concrete in both benchmark and CO_2-amended mixtures and are not likely be a major source of emissions or cost. For instance, upon the joint employment of CO_2 utilization and binder reduction, our results show an increased average dosage rate of plasticizer and superplasticizer, from 0.12 kg/m3 up to 1.32 kg/m3, or from 0.038 % to 0.67 % by weight of OPC (median values). Using $10/kg as a cost of superplasticizer, the additional cost per cubic meter of concrete production from increased use of superplasticizer is $12 while the saved material cost from reduced OPC use is around $25 at the same time. The additional emissions from superplasticizer are up to 2.3 kgCO_2 while 190 kgCO_2 is avoided from reduced OPC use. The use of other admixtures decreases in CO_2-amended mixtures relative to the benchmark mixtures and thus their inclusion will further support our justification that the emission and cost incurred by admixtures do not

significantly alter the major findings of our study. Since data on admixtures are not as complete as other constituents, admixtures are not included in the final emission and cost calculations in this study. Researchers should be able to regenerate results with their own admixture data using the spreadsheet and codes that accompany this study.

The liquefied byproduct CO_2 recovered from ethanol, ammonia, and hydrogen plants is purified to industrial grade (≥99.5%). The range of CO_2 emitted during this recovery and purification process is based on literature (Supekar and Skerlos 2014). The processed byproduct CO_2 is typically transported via diesel powered tanker trailer that generates about 0.333 kg of CO_2 to move 1 tonne of CO_2 over 1 km (Supekar and Skerlos 2014). Based on spatial analysis (section C.5), we use one-way CO_2 delivery distance of 177.2, 177.4, and 177.8 km for low, nominal, and high uncertainty cases, respectively. This yields 0.059-0.0592 kg of additional CO_2 emissions from transporting 1 kg of liquefied byproduct CO_2 to concrete plants.

Some CO_2 footprint values were derived from multiple sources. The high carbon footprint value for OPC manufacturing represents a weighted average of regular Portland cement and blended cement with their relative production volume in the U.S. CO_2 footprint values of manufacturing coarse, fine, and recycled concrete aggregates are based on EPD reports published by four aggregate producers in the U.S. that collectively contain cradle-to-gate life cycle CO_2 emissions data of 88 aggregate products. Minimum, average, and maximum values for each aggregate type were used to set low, nominal, and high sensitivity values, respectively. The carbon footprint for batching and mixing operation is based on the average carbon footprint of the concrete plants used in ready-mixed and precast applications, weighted by OPC annually consumed in each application. The carbon footprint of each mode of transportation is based on the value found in Ecoinvent database version 3, using Tool for Reduction and Assessment of Chemicals and Other Environmental Impacts impact assessment method.

Table C.3. Carbon footprint of constituents and batching & mixing operation. These values are used to calculate carbon footprint of a cubic meter of concrete mixture using (A.3)-(C.3).

Sensitivity	Constituents i [kgCO_2e/kg]												[kgCO_2e/m^3]
Manufacturing	c_i^M	OPC	FA	GGBS	SF	Meta	Pozz	L	Water	C.Agg.	RCA	F.Agg.	CO_2	$c_{B\&M}$
	Low	0.757	0.029	0.085	0.015	0.236	4.00E-03	3.01E-3	5.14E-4	1.55E-3	3.12E-3	1.65E-3	0.122	2.98
	Nom	0.929	0.029	0.147	0.015	0.330	2.70E-02	3.01E-3	7.00E-4	3.93E-3	5.07E-3	4.02E-3	0.187	3.77
	High	1.037	0.029	0.280	0.015	0.423	3.20E-02	3.20E-2	7.00E-4	9.89E-3	6.87E-3	7.49E-3	0.251	4.83
Transport	c_i^T	OPC	FA	GGBS	SF	Meta	Pozz	L	Water	C.Agg.	RCA	F.Agg.	CO_2	$c_{B\&M}$
	Low	2.25E-2	2.83E-3	3.81E-3	3.11E-3	1.58E-4	1.58E-4	2.64E-5	0	2.98E-3	6.64E-5	3.64E-3	0.059	0

	Nom	2.74E-2	2.27E-2	1.25E-2	1.81E-2	9.19E-4	9.19E-4	1.05E-4	0	8.13E-3	2.05E-4	8.69E-3	0.059	0
	High	4.30E-2	5.32E-2	4.09E-2	6.29E-2	4.52E-3	4.52E-3	2.11E-4	0	1.16E-2	6.80E-4	1.10E-2	0.059	0
	c_i	OPC	FA	GGBS	SF	Meta	Pozz	L	Water	C.Agg.	RCA	F.Agg.	CO_2	$c_{B\&M}$
Overall	Low	0.780	0.032	0.089	0.018	0.236	4.16E-03	3.04E-3	5.14E-4	4.53E-3	3.19E-3	5.29E-3	0.181	2.98
	Nom	0.956	0.052	0.159	0.033	0.331	2.79E-02	3.12E-3	7.00E-4	1.21E-2	5.27E-3	1.27E-2	0.246	3.77
	High	1.080	0.082	0.321	0.078	0.428	3.65E-02	3.22E-2	5.00E-3	2.15E-2	7.55E-3	1.85E-2	0.311	4.83

C.3.2 Calculating the range of material cost of a concrete mixture

The material cost incurred by formulating a cubic meter of concrete can be calculated by adding cost of each constituent and transporting it to concrete mixing plants as shown in (C.4)-(C.5).

$$cost_{mixture} = \sum_i (m_i * cost_i) + cost_{B\&M} \quad \text{(C.4)}$$

$$cost_i = cost_i^M + cost_i^T = cost_i^M + \sum_j (d_j^i * cost_j) \quad \text{(C.5)}$$

where $cost_{mixture}$ is material cost of concrete mixture (\$/m^3), m_i is mass of constituent i (kg), $cost_i$ is a cost of constituent i (\$/kg), and $cost_{B\&M}$ is cost of batching and mixing operation at central concrete plants (\$/m^3). $cost_i^M$ and $cost_i^T$ are cost of manufacturing and transporting constituent i (\$/kg), respectively. d_j^i is an average distance travelled by constituent i from manufacturing site to concrete mixing plants via mode of transport j (km) and $cost_j$ is cost of a mode of transport j (\$/kg-km), including truck, rail, ocean, and barge. Cost of admixture is not considered in this calculation. Three levels of uncertainty cases were formed for each parameter as shown in Table C**.4** (Van Oss 2018, Shwekat and Wu 2018, Tolcin 2017a, 2017b, Black & Veatch 2016, Zayed and Nosair 2006, National Ready Mixed Concrete Association 2016, U.S. Department of Transportation Bureau of Transportation Statistics 2018, Organisation For Economic Co-operation and Development n.d., SEA-DISTANCES.ORG 2019).

The range of manufacturing cost for each constituent, with an exception of water, is based on the range found in USGS Minerals Yearbook Reports (Van Oss 2018, Shwekat and Wu 2018, Tolcin 2017a, 2017b). $cost_j$ for truck, rail, and barge transportation is represented by a national average value (U.S. Department of Transportation Bureau of Transportation Statistics 2018). For ocean transport costs of each constituent, we used average values calculated with the reported maritime transport cost between the U.S. and its major trading partners and approximated transport distance between them using an online tool (Organisation For Economic Co-operation and

Development n.d., SEA-DISTANCES.ORG 2019). The production cost of liquefied byproduct CO_2 is based on a bulk gaseous/supercritical CO_2 price available in a Global Carbon Capture and Storage Institute report (Parsons Brinckerhoff and Global CCS Institute 2011),and its transportation cost is based on the one-way delivery distance between 177.2-177.8 km derived in section C.5. The assumed CO_2 cost is reasonable given that CO_2 sourced from ethanol, ammonia, and hydrogen facilities constitutes a lower end of the CO_2 cost spectrum; CO_2 from ethanol plant ranges between \$6-\$12 per tonne and CO_2 captured during ammonia and hydrogen production is available at \$5-\$70 per tonne, while the national CO_2 cost in the U.S. is expected to be between \$22-\$55 per tonne (Bains *et al* 2017, Luckow *et al* 2016). Thus, CO_2 production cost between \$15 and \$50 per tonne reasonably represents liquefied byproduct CO_2 captured from ethanol, ammonia, and hydrogen plants including the possible additional cost from liquefaction.

Table C.4. Cost of each constituent and batching & mixing operation. These values are used to calculate material cost of formulating one cubic meter of concrete mixture using (C.4)-(C.5).

Sensitivity		Constituents i [\$/kg]												[\$/m^3]
Manufacturing	$cost_i^M$	OPC	FA	GGBS	SF	Meta	Pozz	L	Water	C.Agg.	RCA	F.Agg.	CO_2	$cost_{B\&M}$
	Low	89.7	50.0	78.1	380.0	380.0	50.0	2.0	0.4	10.8	4.6	9.0	15.0	14.9
	Nom	105.0	65.0	90.4	490.0	490.0	65.0	5.6	1.1	12.2	7.5	11.0	19.0	15.6
	High	150.3	80.0	110.2	600.0	600.0	80.0	14.3	2.5	14.2	19.1	12.0	50.0	17.3
Transport	$cost_i^T$	OPC	FA	GGBS	SF	Meta	Pozz	L	Water	C.Agg.	RCA	F.Agg.	CO_2	$cost_{B\&M}$
	Low	9.3	1.5	1.9	0.1	0.1	0.1	0.0	0.0	1.9	0.0	2.3	18.6	0
	Nom	15.1	12.9	6.7	10.0	0.6	0.6	0.1	0.0	4.3	0.1	5.4	18.7	0
	High	20.2	30.4	26.3	35.3	2.9	2.9	0.1	0.0	5.8	0.4	7.0	18.7	0
Overall	$cost_i$	OPC	FA	GGBS	SF	Meta	Pozz	L	Water	C.Agg.	RCA	F.Agg.	CO_2	$cost_{B\&M}$
	Low	99.0	51.5	80.0	380.1	380.1	50.1	2.0	0.4	12.7	4.6	11.3	33.6	14.9
	Nom	120.1	77.9	97.1	500.0	490.6	65.6	5.6	1.1	16.5	7.6	16.3	37.7	15.6
	High	170.5	110.4	136.5	635.3	602.9	82.9	14.5	2.5	20.0	19.5	19.0	68.7	17.3

C.3.3 Calculating the range of CO_2 utilization cost

The cost of CO_2 utilization includes the cost of recovered byproduct CO_2 and the cost of applying carbonation treatment. The cost of CO_2 utilization is separately calculated to contrast it with the saved material cost from switching to CO_2-adjusted designs.

The treatment cost of carbonation curing is estimated from two case studies when CO_2 is added in a sealed chamber to carbonate concrete blocks or concrete masonry units (El-Hassan and Shao 2014a, Shao 2014). Since steam curing is an industrial norm, the cost of carbonation curing treatment only considers additional costs incurred from switching from steam curing to

carbonation curing. The cost of RCA carbonation is derived from the cost of applying carbonation curing, assuming that the sealed chamber employed in carbonation curing is also used to carbonate RCA, and the volume of RCA carbonized in the chamber is equivalent to the volume of concrete products reacted with CO_2 during curing. The cost information of carbonation during mixing is not readily available in the public domain. A relevant startup company claims that adding CO_2 during mixing while reducing cement content by 5% can save roughly $5 per cubic yard of concrete treated (Anon n.d.). Since this produces cost bounds that span two orders of magnitude, we instead use orders of magnitude cost estimates between $10 and $1,000 per one tonne of CO_2 utilized. These estimated carbonation treatment costs are added with the cost of recovered byproduct CO_2 to calculate the total cost of CO_2 utilization as shown in Table C.5 (El-Hassan and Shao 2014a, Shao 2014, Parsons Brinckerhoff and Global CCS Institute 2011).

Table C.5. Cost estimates of the three CO_2 utilization technologies. The cost of CO_2 utilization is defined by adding the cost of recovered byproduct CO_2 and the cost of carbonation treatment.

Sensitivity	Cost of byproduct CO_2 [\$/tCO_2]	Cost of carbonation treatment [\$/tCO_2]			Total cost of CO_2 utilization [\$/tCO_2]		
		Mixing	RCA	Curing	Mixing	RCA	Curing
Low	33.6	10	10	0	44	44	34
Nom	37.7	100	500	100	138	538	138
High	68.7	1000	2000	600	1069	2069	669

C.4 CALCULATING THE RANGE OF NET CO_2 REDUCTION AND NET COST BENEFITS IN A NATIONAL LEVEL

C.4.1 Representing national concrete industry with a cohort of mixtures

The set of 48 D_{Base} mixtures and the set of 48 $D_{CO_2}^{Min}$ mixtures collectively represent the diversity of mixture designs found in the conventional and alternative U.S. concrete industry that employs CO_2 formulation, respectively. The national consumption level of each of these representative 48 mixture designs ($V_{concrete}^{x}$ (10^6 m^3/year)) can be calculated by applying its production-based weight (w^x) to the estimated national shipment volume of concrete in the U.S. ($V_{concrete}^{national}$ (10^6 m^3/year)) as shown in (C.6). Superscript x is a mixture index that has an integer value between 1 and 48; we assign the same mixture index x to a $D_{CO_2}^{Min}$ and its original counterpart D_{Base}. We assume CO_2 addition does not affect the relative production volume among mixture designs. Thus, a $D_{CO_2}^{Min}$ mixture and its original counterpart D_{Base} mixture have the same w^x and $V_{concrete}^{x}$. The w^x of a mixture is based on the relative production volume of a D_{Base} mixture among

the simulated national population (National Ready Mixed Concrete Association 2016). $V_{concrete}^{national}$ is estimated using the national OPC consumption rate in the U.S. (M_{OPC} (Mt/year)) as shown in (C.7). m_{OPC}^{x} is OPC contents in a cubic meter of concrete mixture x (kg/m^3). The uncertainty range of M_{OPC} is obtained from national OPC shipment data in 2015 (Van Oss 2018). The calculated range of $V_{concrete}$ for three uncertainty levels are shown in Table C.6.

$$V_{concrete}^{x} = w^{x} \cdot V_{concrete}^{national} \quad \text{(C.6)}$$

$$V_{concrete}^{national} = \frac{M_{OPC}}{\sum_{x=1}^{48}(m_{OPC}^{x} \cdot w^{x})} \quad \text{(C.7)}$$

The national material consumption level for other constituents can then be calculated by rearranging (C.7) as shown in (C.8).

$$M_i = \sum_{x=1}^{48}(m_i^{x} \cdot w^{x}) \cdot V_{concrete}^{national} \quad \text{(C.8)}$$

where M_i is a mass of constituent i consumed in the U.S. every year (Mt/year), and m_i^{x} is a content of constituent i in a cubic meter of concrete mixture x (kg/m^3). (C.9) can be used either with 48 D_{Base} mixtures or with 48 $D_{CO_2}^{Min}$ mixtures to calculate material consumptions in a conventional U.S. concrete industry or in an alternative U.S. concrete industry that employs CO_2 utilization, respectively. Example consumption estimates of FA and GGBS for conventional concrete industry is shown in Table C.6 (Van Oss 2018, American Coal Ash Association 2016, Portland Cement Association 2016a, European Ready Mixed Concrete Organization 2016, Miller *et al* 2016).

Table C.6. Comparison of the published material consumption rates in the U.S. concrete industry and the estimated values using (C.6)-(C.8).

Sensitivity	Annual Material Consumption Rates			
	OPC (M_{OPC}) [Mt/year]	FA [Mt/year]	GGBS [Mt/year]	Concrete ($V_{concrete}^{national}$) [mil m^3/year]
Low	69.3	13.2	3.06	217
Nom	71.8	13.6	3.17	225
High	75.7	14.4	3.34	237
U.S. (2015)	69-76	15.5-17.6	2.3-2.7	254-365

C.4.2 Estimating the range of national CO_2 emissions and material cost from U.S. concrete

We can calculate the national CO_2 emissions ($C^{national}$ (MtCO_2e/year)) and material cost ($COST^{national}$ (bil \$/year)) associated with manufacturing concrete in the U.S. by adding mixture-

level CO_2 footprint ($c^x_{mixture}$ (kgCO_2e/m^3)) and material cost ($cost^x_{mixture}$ (\$/m^3)) of 48 representative mixtures with each value multiplied with $V^x_{concrete}$ as shown in (C.9)-(C.10).

$$C^{national} = \sum_{x=1}^{48} (c^x_{mixture} \cdot V^x_{concrete})/1000 \quad \text{(C.9)}$$

$$COST^{national} = \sum_{x=1}^{48} (cost^x_{mixture} \cdot V^x_{concrete})/1000 \quad \text{(C.10)}$$

National CO_2 emissions and material cost associated with the conventional U.S. concrete industry can be assessed by using 48 D_{Base} mixtures in (C.9)-(C.10); Or 48 $D^{Min}_{CO_2}$ mixtures can be used to estimate co2 emissions and cost associated with the alternative concrete industry that incorporates CO_2.

A total of nine uncertainty cases are generated for each of $C^{national}$ and $COST^{national}$, considering three uncertainty levels for $V_{concrete}$ and three uncertainty levels for $c_{mixture}$ and $cost_{mixture}$. Table C.7 shows example estimations of the national CO_2 footprint and material cost for a conventional concrete industry using 48 D_{Base} mixtures (European Ready Mixed Concrete Organization 2016, Miller et al 2016, National Ready Mixed Concrete Association 2016, Ulama 2015, Ahmad 2015).

Table C.7. Comparison of the published national CO_2 emissions and cost associated with manufacturing conventional concrete in the U.S. and the estimated values using (C.9)-(C.10).

Material Uncertainty	CO_2 Emissions Uncertainty [MtCO_2e/year]			Material Cost Uncertainty [mil \$/year]		
	Low	Nom	High	Low	Nom	High
Low	57.2	72.9	85.5	15.5	19.2	24.9
Nom	59.3	75.5	88.6	16.1	19.9	25.8
High	62.4	79.6	93.4	17.0	21.0	27.2
U.S. (2015)	66-96			19-26*		

* Low end in the reference material cost (19 mil \$/year) is obtained from revenue spent on purchasing raw materials in ready-mixed and precast industry. High end (26 mil \$/year) is estimated by revenue spent on material purchases and others, which include freight expenses, repair and maintenance, etc.

C.4.3 Estimating maximum market penetration limit for each CO_2 utilization technology

The maximum market penetration limit for each CO_2 utilization technique is based on the market share of concrete applications that can potentially adopt the CO_2 utilization technology as shown in Table C.8 (Van Oss 2018). For this study, strategies of adding CO_2 during mixing or in RCA are assumed to be applicable to both ready-mixed and precast applications. We assumed that carbonation curing can only be used in precast application since curing process requires finished precast products be placed in a sealed carbonation chamber. Three uncertainty levels of maximum

market penetration limit for carbonation curing are set by the percentage of OPC used in precast industry (Van Oss 2018), assuming there are no meaningful differences in compositions between concrete used in precast and ready-mixed applications.

Table C.8. Uncertainty levels of maximum market penetration limit for each of the CO_2 utilization technologies.

Market Uncertainty	During Mixing	Carbonated RCA	Carbonation Curing*
Low	100%	100%	5.3%
Nom	100%	100%	8.7%
High	100%	100%	13.3%

***** Low uncertainty case of the carbonation curing is based on OPC classified for 'precast & prestressed' products by the U.S. Geological Survey. Nominal case additionally assumes that OPC used for 'other' products are included, and high case further includes OPC categorized for 'building material dealers' and 'government and others' in precast applications.

C.4.4 Estimating the net national CO_2 reduction and net cost savings

The net national CO_2 reductions ($\Delta C^{national}$ ($MtCO_2e$/year)) and net cost savings ($\Delta COST^{national}$ (bil \$/year)) by switching from conventional concrete formulations to CO_2-modified designs can be estimated using (C.11)-(C.12).

$$\Delta C^{national} = (C^{national}_{CO_2 Modified} - C^{national}_{Conventional}) \cdot Market_{Max} \quad \text{(C.11)}$$

$$\Delta COST^{national} = (COST^{national}_{CO_2 Modified} - COST^{national}_{Conventional}) \cdot Market_{Max} \quad \text{(C.12)}$$

The total CO_2 footprint and cost associated with the conventional U.S. concrete industry represented with 48 D_{Base} mixtures are denoted with the subscript $Conventional$; the total CO_2 footprint and cost associated with the alternative concrete industry that incorporates CO_2 represented with 48 $D^{Min}_{CO_2}$ mixtures are indicated with the subscript $CO_2 Modified$. $Market_{Max}$ is the maximal market penetration rate (%) for each CO_2 utilization technology defined in section C.4.3.

C.5 One-way CO_2 transport distance between industrial CO_2 sources to concrete plants

For each of the low, nominal, and high uncertainty cases, the average one-way transport distance of byproduct CO_2 is estimated with spatial analysis. The location of ethanol, ammonia, and hydrogen plants and their CO_2 supply capacity based on annual emissions are obtained from the Greenhouse Gas Reporting Program 2017 dataset (Figure C.4) (National Ready Mixed Concrete Association 2016, U.S. Environmental Protection Agency 2018).The location of concrete

plants is estimated by the zipcode of the concrete businesses in each county available in the U.S. Census County Business Patterns 2016 database (U.S. Census Bureau 2018). We use North American Industry Classification System (NAICS) code to identify ready-mixed and precast plants from the Census data – ready-mixed facilities are referenced with a NAICS code 327320 and precast plants are references with NAICS codes 327331, 327332, and 327390. As a result, 5,450 ready-mixed and 2,900 precast facilities are identified. Then the trucking distance from each of the concrete plants to closest industrial CO_2 sources are calculated using ArcGIS Pro spatial analysis software as shown in Figure C.5 and Figure C.6. The estimated distances are weighted with a region-based production volume from NRMCA report (National Ready Mixed Concrete Association 2016) and the relative market size between ready-mixed and precast applications (section C.4.3) to yield national average values; 177.2, 177.4, and 177.8 km for low, nominal, and high uncertainty cases, respectively.

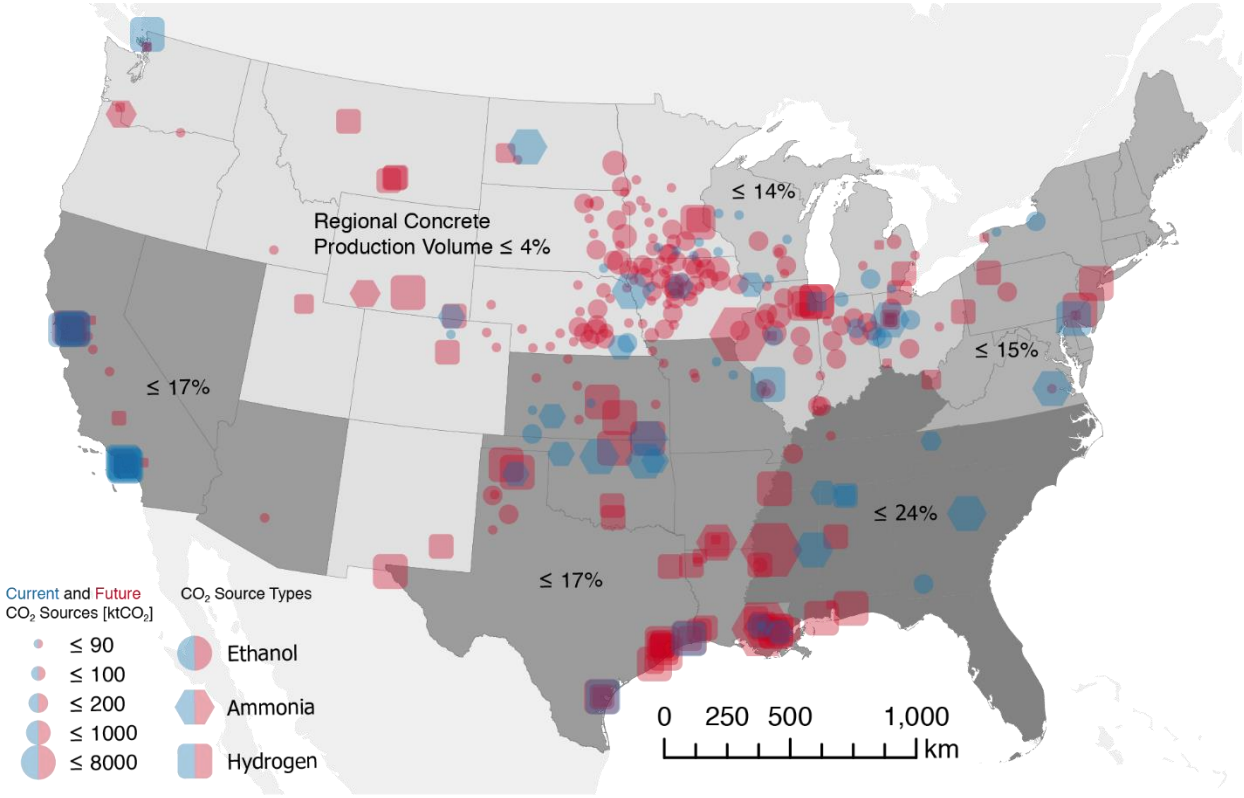

Figure C.4. Distribution of the CO_2 sources, including both current CO_2 suppliers (blue) and potential future suppliers (red). The shade of each group of states indicates regional concrete production volume.

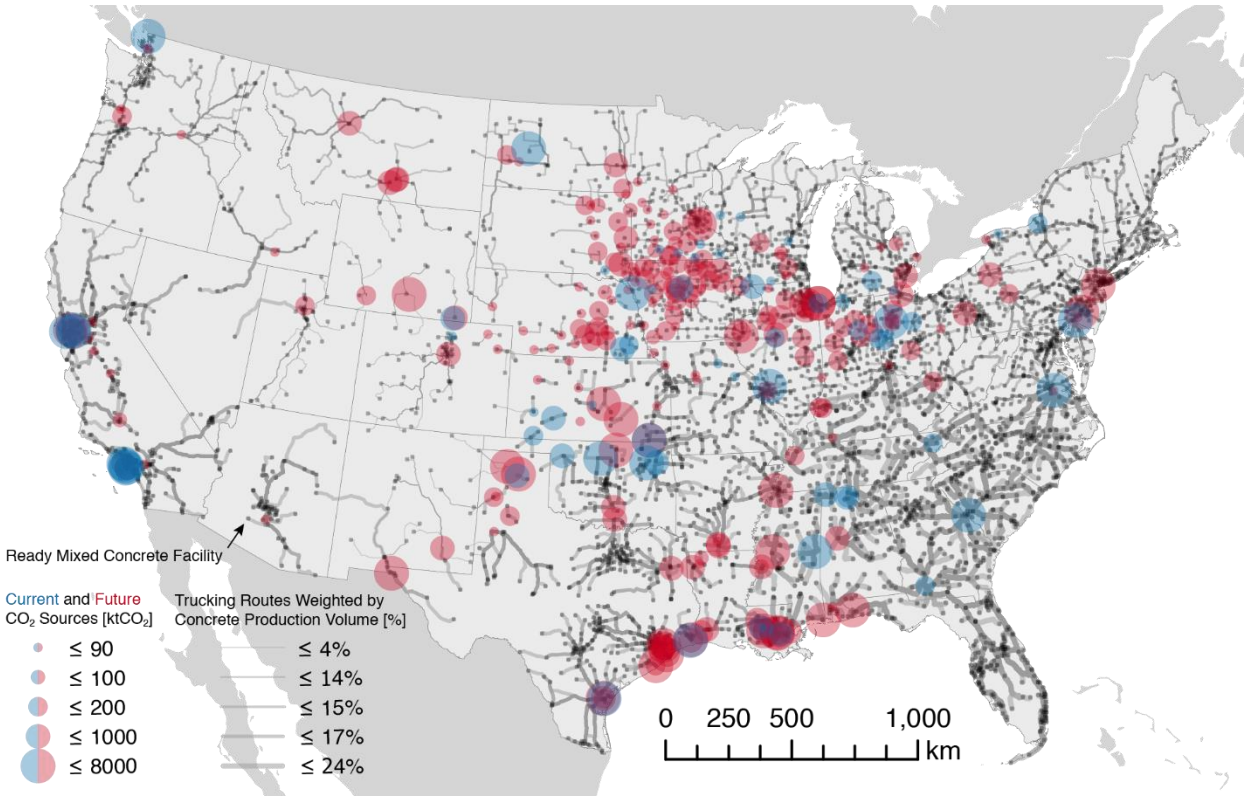

Figure C.5. Location of 5,450 ready-mixed facilities and trucking routes from the nearest CO_2 source

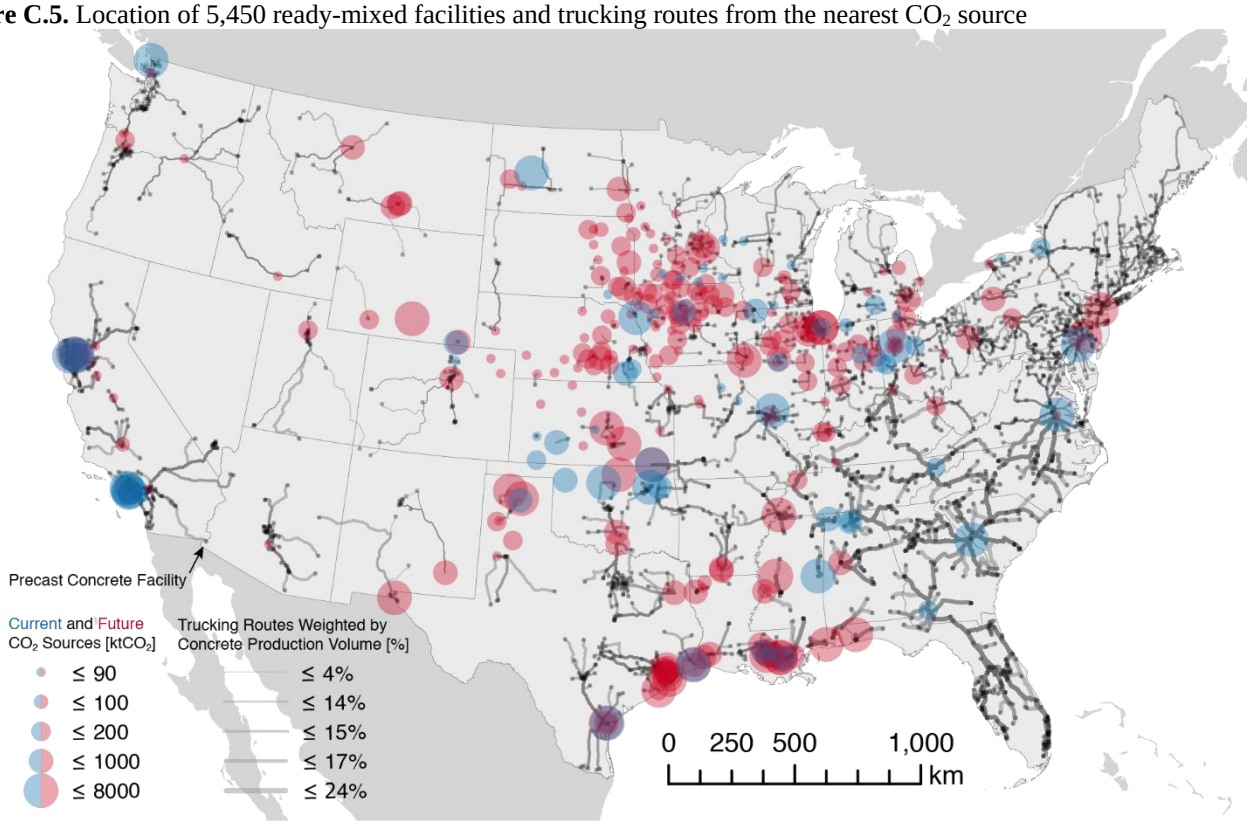

Figure C.6. Location of 2,900 precast facilities and trucking routes from the nearest CO_2 sources

C.6 MITIGATION POTENTIAL OF THE CO_2 UTILIZATION STRATEGIES CONSIDERING FULL 81 UNCERTAINTY CASES

Figure C.7 shows the overall CO_2 reduction achievable by implementing CO_2 utilization strategies coupled with binder reduction, considering a full range of uncertainties. A total of 81 uncertainty cases are generated for each of the CO_2 utilization strategies, by allowing three uncertainty levels for CO_2 emissions (section C.3.1) and cost (section C.3.2) of concrete constituents, annual concrete demand in the U.S. (section C.4.1), and maximum market penetration rate attainable for CO_2 utilization strategies (section C.4.3). The top three figures show percent CO_2 emission reductions in the U.S. concrete industry. The median values of these three figures constitute Figure 4.3 in the results section. The lower three figures show the same results in terms of Mt of CO_2 mitigation attainable in the U.S. concrete industry. The uncertainty bounds in the lower figures are wider due to the additional uncertainty in annual concrete consumption rate.

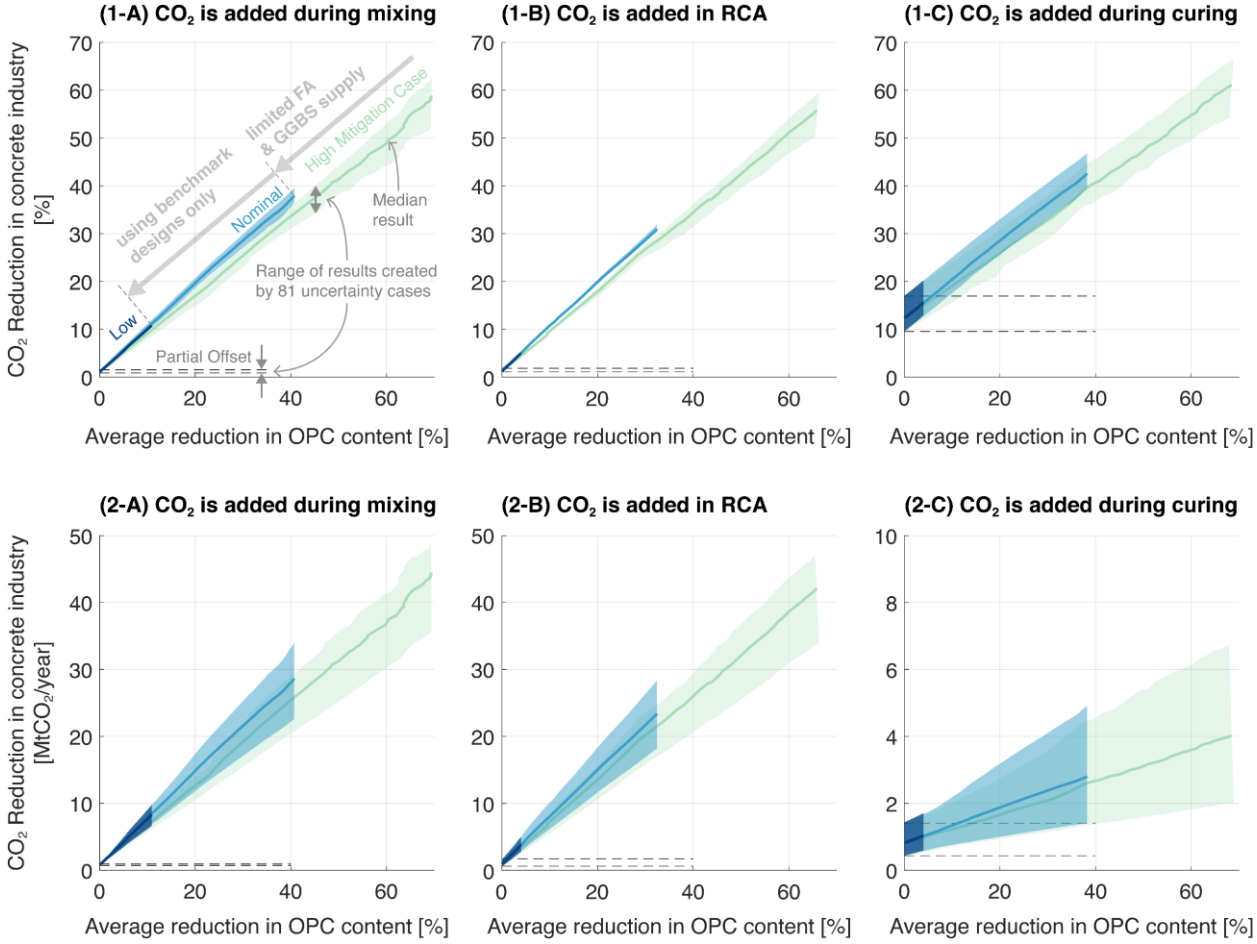

Figure C.7. Overall CO_2 mitigation potential by implementing combined strategy of reducing binder and adding CO_2 in concrete formulation, considering all 81 uncertainty cases.

C.7 MITIGATION IS PREDOMINANTLY GOVERNED BY AVOIDED CO_2 FROM REDUCED BINDER LOADING

Figure C.8 shows that the overall CO_2 reduction potential is predominantly governed by the avoided CO_2 from reduced binder use, regardless of the range of uncertainties considered and CO_2 utilization method used.

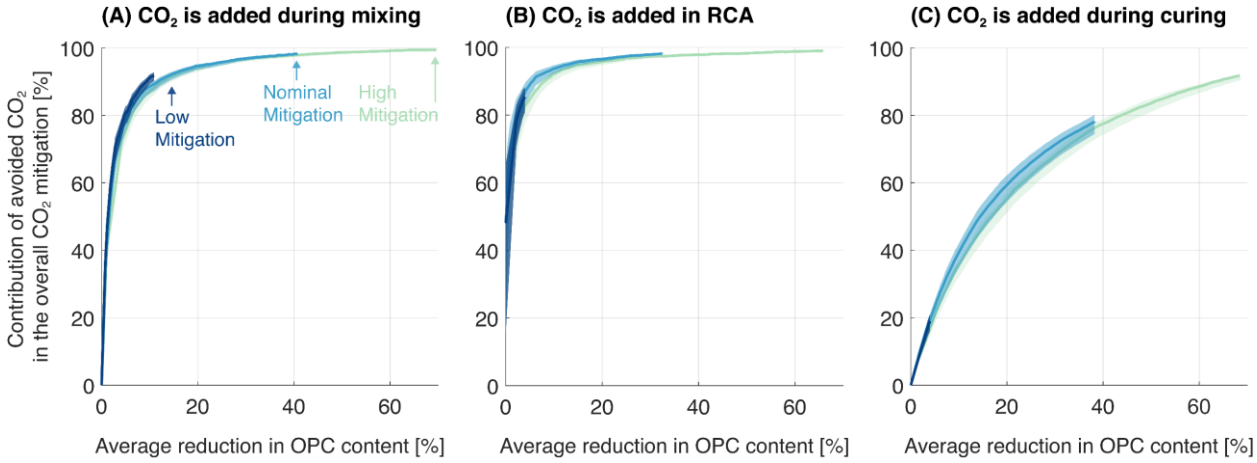

Figure C.8. Percent contribution of the avoided CO_2 from reduced binder use in the overall CO_2 mitigation when CO_2 is added (A) during mixing, (B) in RCA, or (c) through curing.

C.8 IMPACT OF THE CHOICE OF BASELINE MIXTURES ON THE FINAL RESULTS

The findings of this study that OPC reduction provides significant CO_2 reduction opportunity and that CO_2 utilization can catalyze additional OPC reduction are not particular to the U.S. industry but applicable to the global concrete industry. To assess the impact of the choice of D_{Base} on the final result, we regenerated the median results in the nominal mitigation case using 48 mixtures randomly selected from the database. Equal weight was given to each of the 48 randomly chosen mixtures. The distribution of 400 median results, each generated with a randomized set of 48 D_{Base}, clearly shows that our main findings are consistent regardless of the choice of D_{Base} (Figure C.9). This is understandable since the original 48 D_{Base} are selected for their statistical representation of the mixtures used in the U.S. and are indistinguishable from the other mixtures in the database in terms of their composition. Hence our findings would be valid for the global concrete industry. Note that the maximum scale of OPC reduction possible for 400 results generated with randomized set of D_{Base} is relatively lower than the results generated with the U.S. benchmark mixtures. This might imply that OPC usage in the U.S. is less optimized – hence more room for reduction.

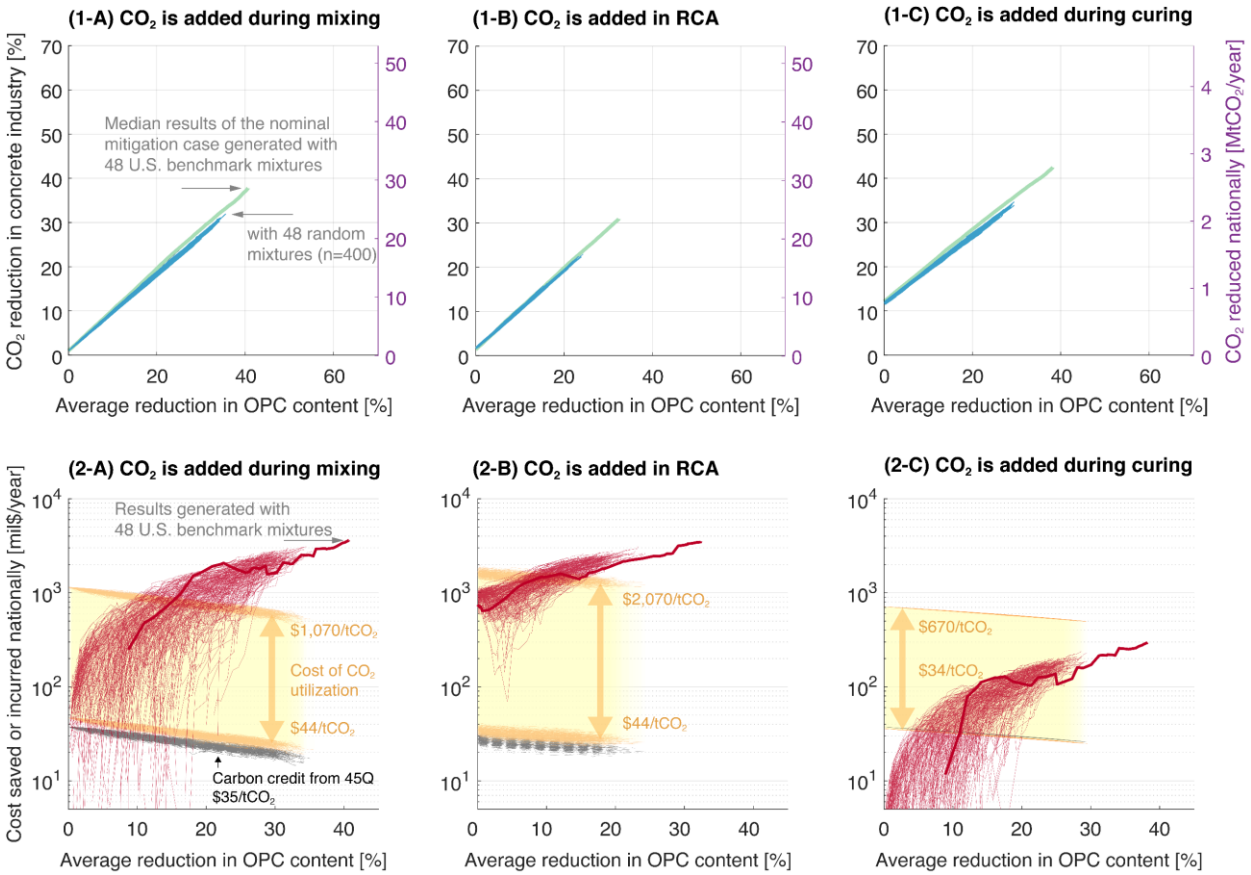

Figure C.9. Median results generated using 400 randomized sets of D_{Base} mixtures for nominal mitigation case.

C.9 COMPATIBILITY OF CO_2-AMENDED MIXTURES WITH STEEL REINFORCEMENT

Throughout our study, we assumed that the concrete formulated with added CO_2 would be compatible with steel reinforcement bars (rebar) that are commonly used in both ready-mixed and precast applications. To be compatible with rebar, concrete needs to maintain an alkaline environment (pH > 13) that provides chemical protection to rebar through passivation. Experiments on carbonation curing (Rostami *et al* 2011, Monkman and Shao 2010, Zhang and Shao 2016a, 2016b) and during mixing (Monkman *et al* 2015, 2018) found a negligible impact on pH from carbonation treatment. For carbonation curing, pH on the surface of concrete initially drops to nine upon reaction with CO_2 but subsequent hydration reactions that boost compressive strength also recover pH level above the corrosion threshold. When CO_2 is added during mixing, CO_2 reacts with freshly hydrating cement to form nano-scale calcium carbonate products and promote hydration reactions. The reaction pathways observed in both cases are distinct from weathering carbonation where CO_2 reacts with mature hydration products of concrete to weaken

its alkalinity. Here, it is important to note that the adequate pH value and thus compatibility with rebar may not be sustained if CO_2 is inadequately utilized in concrete. For instance, lack of water management during carbonation curing could hinder subsequent hydration reactions, compromising both compressive strength and alkalinity. Relevant studies on carbonated RCA are lacking. However, replacing chemically inert natural coarse aggregate with carbonated RCA is not anticipated to negatively affect pH at the core of concrete, as carbonated RCA will either be neutral or have slight alkalinity if residual cement is not fully carbonated. Further studies can help reduce uncertainties and help identify optimal CO_2 treatment strategy to use CO_2-treated concrete with rebar.

C.10 Impact of added CO_2 on long-term durability and lifecycle CO_2 storage potential

It is well understood that finished concrete products or structure progressively react with atmospheric CO_2. During this weathering carbonation, diffused CO_2 in concrete reacts with calcium hydroxide and lowers pH. The resulting deteriorated protective film of rebar against corrosion threatens the long-term durability of the reinforced concrete. While relevant literature on this issue is not available, the CO_2-amended mixtures produced with CO_2 addition during mixing and in RCA are likely to provide comparable level of passive protection to rebar against weathering carbonation relative to non-carbonated counterparts, as their pH levels are only affected by carbonation to a small extent. The amount of added CO_2 is only around 1% by mass of OPC for carbonation during mixing, leaving most binders available for further carbonation. For RCA carbonation, binders are left uncarbonated as with conventional mixtures. Studies on carbonation curing indicate that concrete cured with CO_2 could even have enhanced protection from weathering carbonation by developing protective surface layer that is less permeable, less absorptive, and have comparable pH and carbonation depth relative to conventional counterparts (Zhang and Shao 2016b, 2016a). But further studies would be needed to verify the impact of added CO_2 on weathering carbonation and long-term durability of concrete.

A significant amount of CO_2 can be sequestered in concrete during its use and demolition; CO_2 precipitates as calcium carbonate in concrete through weathering carbonation during use and by reacting with freshly exposed concrete after its demolition. One study estimates that close to 43% of the CO_2 emitted from calcination process during OPC production was sequestered back

into concrete in the last century (Xi *et al* 2016). It can be reasoned that CO_2-amended mixtures may sequester a comparable amount of CO_2 throughout its use and end-of-life phase relative to conventional counterparts given their similar pH levels. Further research would be needed to verify this hypothesis.

C.11 Impact of the compressive strength boost level on the overall CO_2 mitigation potential

The CO_2 reduction potential observed in this study is enabled by CO_2-induced increase in compressive strength. To analyze how the degree of increase in compressive strength impacts the overall CO_2 reduction potential, we perform a parametric uncertainty tests where we either raise or lower the degree of increase by an order of magnitude. Figure C.10 shows how the altered increase in compressive strength affects the mixture design choices when CO_2 is added during curing. The varied degree of increase either expands or shrinks the pool of D_{Alt} whose compressive strength can be recovered by adding CO_2, which influences the choice of $D_{CO_2}^{Min}$ and ultimately impacts the scale of achievable CO_2 reductions. Figure C.11 shows the impact on the overall CO_2 reduction potential of the nominal mitigation cases from altered degree of increase in compressive strength. When CO_2 is added in RCA, decrease in the overall CO_2 reduction by the lowered boost in strength is minimized since the RCA substitution itself can increases the compressive strength of concrete when its substitution rate is low (Figure C.7-B). Note that over 25% of CO_2 may be reduced even in the extreme case when compressive strength increase from CO_2 utilization is lowered by an order of magnitude, provided that binder use can be reduced.

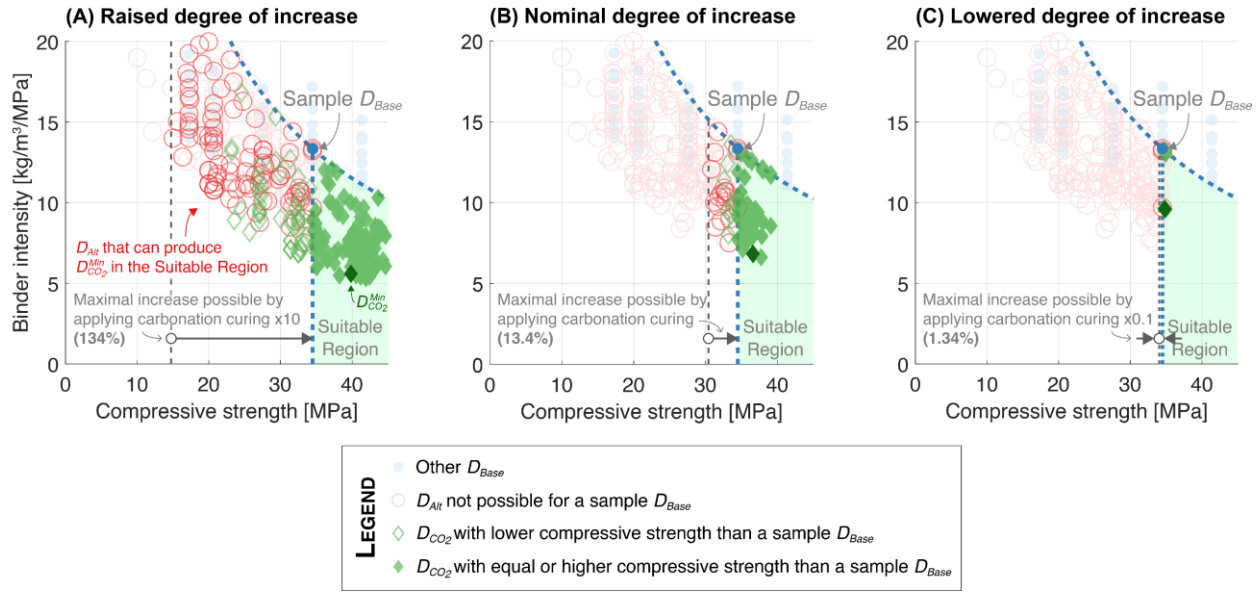

Figure C.10. Parametric tests show that different $D^{Min}_{CO_2}$ mixture is selected for a sample D_{Base} when the level of increase in strength from applying carbonation curing is either raised by an order of magnitude (A) or lowered by an order of magnitude (C) compared to the default level (B).

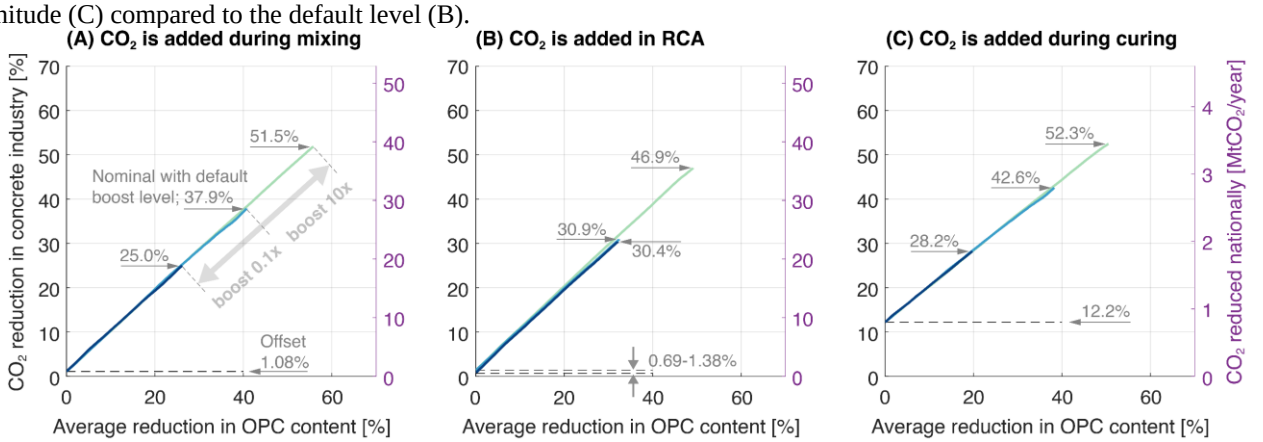

Figure C.11. Results of the parametric uncertainty analysis when the degree of CO_2-induced increase in compressive strength were raised or lowered by an order of magnitude. CO_2 is added (A) during mixing, (B) in RCA, or (c) through curing.

C.12 COMPILED CONCRETE MIXTURES USED IN THIS STUDY

The composition, 28-days compressive strength, CO_2 footprint, and material cost of a cubic meter of concrete mixtures used in this study are summarized in

Table C.9 (National Ready Mixed Concrete Association 2016, The Athena Sustainable Materials Institute 2016, Siddique 2004, Bouzoubaa *et al* 2001, Poon *et al* 2000, Liu *et al* 2012, Lam *et al* 1997, Celik *et al* 2015, Bilim *et al* 2009, Monteiro *et al* 1993, Felekoğlu *et al* 2007, Einsfeld and Velasco 2006, Vejmelková *et al* 2009, Haque and Kayali 1998, Wu *et al* 2001, Oner *et al* 2005, Oner and Akyuz 2007, Meddah *et al* 2014, Hedegaard and Hansen 1992, Han *et al* 2003, Moon *et al* 2017, Mohammadi and South 2016, Shannon *et al* 2017). The asterisk in mixture number indicates 48 mixtures used to form D_{Base}. The reported 28-days compressive strength of mixtures was converted to a corresponding value using a standard cylinder (Ø150mm x 300mm) according to Yi et al. if cylinder samples with different dimensions or cubic samples were used for measurements (Yi *et al* 2006). For each of the concrete mixtures, the calculated CO_2 footprint and material cost associated with manufacturing and transportation are displayed assuming nominal uncertainty cases.

Table C.9. Composition, 28-day compressive strength, CO_2 footprint, and material cost of a cubic meter of concrete mixtures compiled for this study. SP includes both plasticizer and superplasticizer. AE stands for air entraining agent.

Mix No.	Mixture Composition [kg/m^3]													Comp. Str. [MPa]	CO_2 Footprint [kgCO_2e/m^3]	Mat. Cost [$/m^3]	Ref.
	OPC	FA	GGBS	SF	Meta.	Pozz.	L	Water	C.Agg.	RCA	F.Agg.	SP	AE				
1	238	46	11	0	0	0	0	179	988	0	828	0.09	0.03	17.2	258	79	[(National Ready Mixed Concrete Association 2016)]
2	270	52	12	0	0	0	0	179	969	0	812	0.09	0.03	20.7	289	83	[(National Ready Mixed Concrete Association 2016)]
3	338	65	15	0	0	0	0	179	930	0	778	0.09	0.03	27.6	354	91	[(National Ready Mixed Concrete Association 2016)]
4	427	82	19	0	0	0	0	185	863	0	722	0.21	0.03	34.5	439	101	[(National Ready Mixed Concrete Association 2016)]
5	450	87	20	0	0	0	0	201	892	0	746	0.21	0.00	41.4	462	105	[(National Ready Mixed Concrete Association 2016)]
6	556	107	24	0	0	0	0	201	823	0	690	0.21	0.00	55.2	564	118	[(National Ready Mixed Concrete Association 2016)]
7	273	52	12	0	0	0	0	182	0	0	799	0.09	0.03	20.7	280	67	[(National Ready Mixed Concrete Association 2016)]
8	342	66	15	0	0	0	0	182	0	0	702	0.09	0.03	27.6	345	75	[(National Ready Mixed Concrete Association 2016)]
9	416	80	18	0	0	0	0	182	0	0	600	0.21	0.03	34.5	417	84	[(National Ready Mixed Concrete Association 2016)]
10*	246	26	37	0	0	0	0	188	991	0	850	0.09	0.03	17.2	269	81	[(National Ready Mixed Concrete Association 2016)]
11*	278	29	42	0	0	0	0	188	981	0	842	0.09	0.03	20.7	301	85	[(National Ready Mixed Concrete Association 2016)]
12*	349	37	53	0	0	0	0	188	962	0	825	0.09	0.03	27.6	370	95	[(National Ready Mixed Concrete Association 2016)]
13*	440	46	66	0	0	0	0	195	855	0	733	0.21	0.03	34.5	457	105	[(National Ready Mixed Concrete Association 2016)]
14*	464	49	71	0	0	0	0	211	884	0	758	0.21	0.00	41.4	482	109	[(National Ready Mixed Concrete Association 2016)]
15*	574	61	87	0	0	0	0	211	816	0	700	0.21	0.00	55.2	588	123	[(National Ready Mixed Concrete Association 2016)]
16	281	30	43	0	0	0	0	190	0	0	758	0.09	0.03	20.7	290	68	[(National Ready Mixed Concrete Association 2016)]
17	352	37	53	0	0	0	0	190	0	0	656	0.09	0.03	27.6	359	77	[(National Ready Mixed Concrete Association 2016)]
18	428	45	65	0	0	0	0	190	0	0	548	0.21	0.03	34.5	433	86	[(National Ready Mixed Concrete Association 2016)]
19*	214	37	8	0	0	0	0	157	1048	0	832	0.09	0.03	17.2	235	76	[(National Ready Mixed Concrete Association 2016)]
20*	242	42	8	0	0	0	0	157	1038	0	824	0.09	0.03	20.7	262	79	[(National Ready Mixed Concrete Association 2016)]
21*	303	52	11	0	0	0	0	157	1017	0	807	0.09	0.03	27.6	321	87	[(National Ready Mixed Concrete Association 2016)]
22*	381	66	13	0	0	0	0	163	946	0	751	0.21	0.03	34.5	395	96	[(National Ready Mixed Concrete Association 2016)]
23*	403	69	14	0	0	0	0	177	977	0	775	0.21	0.00	41.4	417	100	[(National Ready Mixed Concrete Association 2016)]
24*	498	85	17	0	0	0	0	177	916	0	727	0.21	0.00	55.2	507	111	[(National Ready Mixed Concrete Association 2016)]
25	246	42	8	0	0	0	0	160	0	0	826	0.09	0.03	20.7	253	63	[(National Ready Mixed Concrete Association 2016)]
26	309	53	11	0	0	0	0	160	0	0	740	0.09	0.03	27.6	313	70	[(National Ready Mixed Concrete Association 2016)]
27	376	65	13	0	0	0	0	160	0	0	648	0.21	0.03	34.5	377	78	[(National Ready Mixed Concrete Association 2016)]

Mix No.	Mixture Composition [kg/m^3]													Comp. Str. [MPa]	CO_2 Footprint [kgCO_2e/m^3]	Mat. Cost [$/m^3]	Ref.
	OPC	FA	GGBS	SF	Meta.	Pozz.	L	Water	C.Agg.	RCA	F.Agg.	SP	AE				
28*	201	37	4	0	0	0	0	146	1004	0	878	0.09	0.03	17.2	221	74	[(National Ready Mixed Concrete Association 2016)]
29*	227	42	4	0	0	0	0	146	985	0	861	0.09	0.03	20.7	247	77	[(National Ready Mixed Concrete Association 2016)]
30*	285	53	5	0	0	0	0	146	957	0	837	0.09	0.03	27.6	302	84	[(National Ready Mixed Concrete Association 2016)]
31*	360	67	6	0	0	0	0	151	909	0	794	0.21	0.03	34.5	374	93	[(National Ready Mixed Concrete Association 2016)]
32*	380	71	7	0	0	0	0	164	937	0	819	0.21	0.00	41.4	394	96	[(National Ready Mixed Concrete Association 2016)]
33*	471	88	8	0	0	0	0	164	890	0	778	0.21	0.00	55.2	481	107	[(National Ready Mixed Concrete Association 2016)]
34	230	43	4	0	0	0	0	148	0	0	876	0.09	0.03	20.7	238	61	[(National Ready Mixed Concrete Association 2016)]
35	289	54	5	0	0	0	0	148	0	0	797	0.09	0.03	27.6	294	68	[(National Ready Mixed Concrete Association 2016)]
36	352	66	6	0	0	0	0	148	0	0	702	0.21	0.03	34.5	354	75	[(National Ready Mixed Concrete Association 2016)]
37*	222	33	16	0	0	0	0	164	1046	0	873	0.09	0.03	17.2	245	78	[(National Ready Mixed Concrete Association 2016)]
38*	252	38	18	0	0	0	0	164	1026	0	857	0.09	0.03	20.7	273	82	[(National Ready Mixed Concrete Association 2016)]
39*	316	47	23	0	0	0	0	164	987	0	824	0.09	0.03	27.6	335	89	[(National Ready Mixed Concrete Association 2016)]
40*	399	60	29	0	0	0	0	170	928	0	774	0.21	0.03	34.5	414	99	[(National Ready Mixed Concrete Association 2016)]
41*	421	63	31	0	0	0	0	185	958	0	799	0.21	0.00	41.4	437	103	[(National Ready Mixed Concrete Association 2016)]
42*	522	79	39	0	0	0	0	185	898	0	750	0.21	0.00	55.2	534	115	[(National Ready Mixed Concrete Association 2016)]
43	266	20	24	0	0	0	0	166	0	0	793	0.09	0.03	20.7	274	65	[(National Ready Mixed Concrete Association 2016)]
44	334	24	30	0	0	0	0	166	0	0	704	0.09	0.03	27.6	338	72	[(National Ready Mixed Concrete Association 2016)]
45	407	30	37	0	0	0	0	166	0	0	599	0.21	0.03	34.5	408	80	[(National Ready Mixed Concrete Association 2016)]
46*	282	50	0	0	0	0	0	202	889	0	852	0.09	0.03	17.2	298	82	[(National Ready Mixed Concrete Association 2016)]
47*	319	56	0	0	0	0	0	202	872	0	835	0.09	0.03	20.7	333	87	[(National Ready Mixed Concrete Association 2016)]
48*	400	71	0	0	0	0	0	202	827	0	793	0.09	0.03	27.6	410	96	[(National Ready Mixed Concrete Association 2016)]
49*	504	89	0	0	0	0	0	209	756	0	724	0.21	0.03	34.5	508	108	[(National Ready Mixed Concrete Association 2016)]
50*	532	94	0	0	0	0	0	227	783	0	750	0.21	0.00	41.4	537	112	[(National Ready Mixed Concrete Association 2016)]
51*	657	116	0	0	0	0	0	227	712	0	682	0.21	0.00	55.2	656	127	[(National Ready Mixed Concrete Association 2016)]
52	322	57	0	0	0	0	0	204	0	0	771	0.09	0.03	20.7	325	71	[(National Ready Mixed Concrete Association 2016)]
53	403	71	0	0	0	0	0	204	0	0	664	0.09	0.03	27.6	402	81	[(National Ready Mixed Concrete Association 2016)]
54	491	87	0	0	0	0	0	204	0	0	550	0.21	0.03	34.5	485	90	[(National Ready Mixed Concrete Association 2016)]
55*	236	50	0	0	0	0	0	174	1018	0	817	0.09	0.03	17.2	255	78	[(National Ready Mixed Concrete Association 2016)]
56*	267	56	0	0	0	0	0	174	998	0	801	0.09	0.03	20.7	284	82	[(National Ready Mixed Concrete Association 2016)]

Mix No.	Mixture Composition [kg/m^3]													Comp. Str. [MPa]	CO_2 Footprint [kgCO_2e/m^3]	Mat. Cost [$/m^3]	Ref.
	OPC	FA	GGBS	SF	Meta.	Pozz.	L	Water	C.Agg.	RCA	F.Agg.	SP	AE				
57*	335	71	0	0	0	0	0	174	959	0	769	0.09	0.03	27.6	349	90	[(National Ready Mixed Concrete Association 2016)]
58*	422	89	0	0	0	0	0	180	889	0	713	0.21	0.03	34.5	432	100	[(National Ready Mixed Concrete Association 2016)]
59*	446	94	0	0	0	0	0	195	918	0	737	0.21	0.00	41.4	455	104	[(National Ready Mixed Concrete Association 2016)]
60*	551	116	0	0	0	0	0	195	858	0	689	0.21	0.00	55.2	555	116	[(National Ready Mixed Concrete Association 2016)]
61	271	57	0	0	0	0	0	176	0	0	809	0.09	0.03	20.7	276	66	[(National Ready Mixed Concrete Association 2016)]
62	339	71	0	0	0	0	0	176	0	0	714	0.09	0.03	27.6	341	74	[(National Ready Mixed Concrete Association 2016)]
63	414	87	0	0	0	0	0	176	0	0	613	0.21	0.03	34.5	412	82	[(National Ready Mixed Concrete Association 2016)]
64*	211	38	2	0	0	0	0	152	1003	0	836	0.09	0.03	17.2	231	74	[(National Ready Mixed Concrete Association 2016)]
65*	238	43	2	0	0	0	0	152	994	0	828	0.09	0.03	20.7	257	78	[(National Ready Mixed Concrete Association 2016)]
66*	299	54	2	0	0	0	0	152	954	0	795	0.09	0.03	27.6	315	85	[(National Ready Mixed Concrete Association 2016)]
67*	377	68	3	0	0	0	0	158	904	0	754	0.21	0.03	34.5	389	94	[(National Ready Mixed Concrete Association 2016)]
68*	398	72	4	0	0	0	0	171	934	0	779	0.21	0.00	41.4	410	98	[(National Ready Mixed Concrete Association 2016)]
69*	492	89	4	0	0	0	0	171	885	0	737	0.21	0.00	55.2	499	109	[(National Ready Mixed Concrete Association 2016)]
70	243	44	2	0	0	0	0	155	0	0	875	0.09	0.03	20.7	250	63	[(National Ready Mixed Concrete Association 2016)]
71	304	55	2	0	0	0	0	155	0	0	784	0.09	0.03	27.6	308	70	[(National Ready Mixed Concrete Association 2016)]
72	371	67	3	0	0	0	0	155	0	0	687	0.21	0.03	34.5	371	77	[(National Ready Mixed Concrete Association 2016)]
73*	228	65	11	0	0	0	0	185	982	0	803	0.09	0.03	17.2	249	79	[(National Ready Mixed Concrete Association 2016)]
74*	259	73	12	0	0	0	0	185	963	0	788	0.09	0.03	20.7	279	82	[(National Ready Mixed Concrete Association 2016)]
75*	325	92	16	0	0	0	0	185	915	0	749	0.09	0.03	27.6	342	91	[(National Ready Mixed Concrete Association 2016)]
76*	409	116	20	0	0	0	0	192	848	0	694	0.21	0.03	34.5	423	101	[(National Ready Mixed Concrete Association 2016)]
77*	432	122	21	0	0	0	0	208	876	0	717	0.21	0.00	41.4	446	105	[(National Ready Mixed Concrete Association 2016)]
78*	534	151	26	0	0	0	0	208	809	0	662	0.21	0.00	55.2	545	118	[(National Ready Mixed Concrete Association 2016)]
79	262	74	13	0	0	0	0	187	0	0	804	0.09	0.03	20.7	271	67	[(National Ready Mixed Concrete Association 2016)]
80	329	93	16	0	0	0	0	187	0	0	704	0.09	0.03	27.6	334	76	[(National Ready Mixed Concrete Association 2016)]
81	401	113	20	0	0	0	0	187	0	0	597	0.21	0.03	34.5	404	84	[(National Ready Mixed Concrete Association 2016)]
82	255	0	0	0	0	0	0	155	995	0	835	0.09	0.03	17.2	270	76	[(The Athena Sustainable Materials Institute 2016)]
83	214	53	0	0	0	0	0	155	995	0	793	0.09	0.03	17.2	234	75	[(The Athena Sustainable Materials Institute 2016)]
84	193	82	0	0	0	0	0	155	995	0	770	0.09	0.04	17.2	214	74	[(The Athena Sustainable Materials Institute 2016)]
85	170	113	0	0	0	0	0	155	995	0	746	0.09	0.04	17.2	193	74	[(The Athena Sustainable Materials Institute 2016)]

Mix No.	Mixture Composition [kg/m^3]													Comp. Str. [MPa]	CO_2 Footprint [kgCO_2e/m^3]	Mat. Cost [$/m^3]	Ref.
	OPC	FA	GGBS	SF	Meta.	Pozz.	L	Water	C.Agg.	RCA	F.Agg.	SP	AE				
86	178	0	77	0	0	0	0	155	995	0	829	0.09	0.03	17.2	209	75	[(The Athena Sustainable Materials Institute 2016)]
87	152	0	102	0	0	0	0	155	995	0	828	0.09	0.03	17.2	188	74	[(The Athena Sustainable Materials Institute 2016)]
88	128	0	128	0	0	0	0	155	995	0	826	0.09	0.03	17.2	169	73	[(The Athena Sustainable Materials Institute 2016)]
89	134	53	80	0	0	0	0	155	995	0	787	0.09	0.03	17.2	170	73	[(The Athena Sustainable Materials Institute 2016)]
90	288	0	0	0	0	0	0	155	995	0	807	0.09	0.03	20.7	302	80	[(The Athena Sustainable Materials Institute 2016)]
91	243	61	0	0	0	0	0	155	995	0	759	0.09	0.03	20.7	261	78	[(The Athena Sustainable Materials Institute 2016)]
92	218	94	0	0	0	0	0	155	995	0	733	0.09	0.04	20.7	239	78	[(The Athena Sustainable Materials Institute 2016)]
93	192	128	0	0	0	0	0	155	995	0	706	0.09	0.04	20.7	215	77	[(The Athena Sustainable Materials Institute 2016)]
94	202	0	87	0	0	0	0	155	995	0	801	0.09	0.03	20.7	233	78	[(The Athena Sustainable Materials Institute 2016)]
95	173	0	115	0	0	0	0	155	995	0	799	0.09	0.03	20.7	210	77	[(The Athena Sustainable Materials Institute 2016)]
96	144	0	144	0	0	0	0	155	995	0	797	0.09	0.03	20.7	187	76	[(The Athena Sustainable Materials Institute 2016)]
97	152	61	91	0	0	0	0	155	995	0	753	0.09	0.03	20.7	188	76	[(The Athena Sustainable Materials Institute 2016)]
98	365	0	0	0	0	0	0	155	995	0	744	0.09	0.03	27.6	375	88	[(The Athena Sustainable Materials Institute 2016)]
99	307	77	0	0	0	0	0	155	995	0	683	0.09	0.03	27.6	322	86	[(The Athena Sustainable Materials Institute 2016)]
100	276	119	0	0	0	0	0	155	995	0	650	0.09	0.04	27.6	295	85	[(The Athena Sustainable Materials Institute 2016)]
101	243	163	0	0	0	0	0	155	995	0	616	0.09	0.04	27.6	265	84	[(The Athena Sustainable Materials Institute 2016)]
102	256	0	110	0	0	0	0	155	995	0	736	0.09	0.03	27.6	287	86	[(The Athena Sustainable Materials Institute 2016)]
103	219	0	146	0	0	0	0	155	995	0	733	0.09	0.03	27.6	258	85	[(The Athena Sustainable Materials Institute 2016)]
104	183	0	183	0	0	0	0	155	995	0	731	0.09	0.03	27.6	229	84	[(The Athena Sustainable Materials Institute 2016)]
105	192	77	115	0	0	0	0	155	995	0	675	0.09	0.03	27.6	231	83	[(The Athena Sustainable Materials Institute 2016)]
106	456	0	0	0	0	0	0	160	913	0	750	0.21	0.03	34.5	460	98	[(The Athena Sustainable Materials Institute 2016)]
107	384	96	0	0	0	0	0	160	913	0	675	0.21	0.03	34.5	395	95	[(The Athena Sustainable Materials Institute 2016)]
108	345	148	0	0	0	0	0	160	913	0	634	0.21	0.04	34.5	360	94	[(The Athena Sustainable Materials Institute 2016)]
109	304	202	0	0	0	0	0	160	913	0	591	0.21	0.04	34.5	323	93	[(The Athena Sustainable Materials Institute 2016)]
110	319	0	136	0	0	0	0	160	913	0	740	0.21	0.03	34.5	351	94	[(The Athena Sustainable Materials Institute 2016)]
111	274	0	182	0	0	0	0	160	913	0	737	0.21	0.03	34.5	315	93	[(The Athena Sustainable Materials Institute 2016)]
112	228	0	228	0	0	0	0	160	913	0	734	0.21	0.03	34.5	278	92	[(The Athena Sustainable Materials Institute 2016)]
113	240	96	144	0	0	0	0	160	913	0	664	0.21	0.03	34.5	280	92	[(The Athena Sustainable Materials Institute 2016)]
114	481	0	0	0	0	0	0	174	913	0	772	0.21	0.00	41.4	485	101	[(The Athena Sustainable Materials Institute 2016)]

Mix No.	Mixture Composition [kg/m^3]													Comp. Str. [MPa]	CO_2 Footprint [kgCO_2e/m^3]	Mat. Cost [$/m^3]	Ref.
	OPC	FA	GGBS	SF	Meta.	Pozz.	L	Water	C.Agg.	RCA	F.Agg.	SP	AE				
115	405	101	0	0	0	0	0	174	913	0	692	0.21	0.00	41.4	416	99	[(The Athena Sustainable Materials Institute 2016)]
116	364	156	0	0	0	0	0	174	913	0	649	0.21	0.00	41.4	380	97	[(The Athena Sustainable Materials Institute 2016)]
117	321	214	0	0	0	0	0	174	913	0	604	0.21	0.00	41.4	341	96	[(The Athena Sustainable Materials Institute 2016)]
118	337	0	144	0	0	0	0	174	913	0	762	0.21	0.00	41.4	370	98	[(The Athena Sustainable Materials Institute 2016)]
119	289	0	192	0	0	0	0	174	913	0	759	0.21	0.00	41.4	331	97	[(The Athena Sustainable Materials Institute 2016)]
120	241	0	241	0	0	0	0	174	913	0	755	0.21	0.00	41.4	293	95	[(The Athena Sustainable Materials Institute 2016)]
121	253	101	152	0	0	0	0	174	913	0	682	0.21	0.00	41.4	295	95	[(The Athena Sustainable Materials Institute 2016)]
122	567	0	0	0	0	0	0	174	913	0	702	0.21	0.00	55.2	566	110	[(The Athena Sustainable Materials Institute 2016)]
123	477	119	0	0	0	0	0	174	913	0	608	0.21	0.00	55.2	485	107	[(The Athena Sustainable Materials Institute 2016)]
124	429	184	0	0	0	0	0	174	913	0	557	0.21	0.00	55.2	442	106	[(The Athena Sustainable Materials Institute 2016)]
125	378	252	0	0	0	0	0	174	913	0	503	0.21	0.00	55.2	396	104	[(The Athena Sustainable Materials Institute 2016)]
126	397	0	170	0	0	0	0	174	913	0	690	0.21	0.00	55.2	430	106	[(The Athena Sustainable Materials Institute 2016)]
127	340	0	227	0	0	0	0	174	913	0	686	0.21	0.00	55.2	385	105	[(The Athena Sustainable Materials Institute 2016)]
128	284	0	284	0	0	0	0	174	913	0	682	0.21	0.00	55.2	340	104	[(The Athena Sustainable Materials Institute 2016)]
129	298	119	179	0	0	0	0	174	913	0	595	0.21	0.00	55.2	342	103	[(The Athena Sustainable Materials Institute 2016)]
130	320	0	0	0	0	0	0	172	548	0	842	0.09	0.03	20.7	327	77	[(The Athena Sustainable Materials Institute 2016)]
131	269	68	0	0	0	0	0	172	473	0	910	0.09	0.03	20.7	282	76	[(The Athena Sustainable Materials Institute 2016)]
132	242	104	0	0	0	0	0	172	432	0	947	0.09	0.04	20.7	258	76	[(The Athena Sustainable Materials Institute 2016)]
133	213	142	0	0	0	0	0	172	403	0	963	0.09	0.04	20.7	232	75	[(The Athena Sustainable Materials Institute 2016)]
134	224	0	96	0	0	0	0	172	519	0	882	0.09	0.03	20.7	251	75	[(The Athena Sustainable Materials Institute 2016)]
135	192	0	128	0	0	0	0	172	519	0	879	0.09	0.03	20.7	226	74	[(The Athena Sustainable Materials Institute 2016)]
136	160	0	160	0	0	0	0	172	519	0	877	0.09	0.03	20.7	200	73	[(The Athena Sustainable Materials Institute 2016)]
137	168	68	101	0	0	0	0	172	462	0	922	0.09	0.03	20.7	202	74	[(The Athena Sustainable Materials Institute 2016)]
138	405	0	0	0	0	0	0	172	559	0	753	0.09	0.03	27.6	408	86	[(The Athena Sustainable Materials Institute 2016)]
139	341	85	0	0	0	0	0	172	490	0	798	0.09	0.03	27.6	351	84	[(The Athena Sustainable Materials Institute 2016)]
140	307	131	0	0	0	0	0	172	444	0	837	0.09	0.04	27.6	320	84	[(The Athena Sustainable Materials Institute 2016)]
141	270	180	0	0	0	0	0	172	409	0	854	0.09	0.04	27.6	287	83	[(The Athena Sustainable Materials Institute 2016)]
142	284	0	122	0	0	0	0	172	548	0	763	0.09	0.03	27.6	311	83	[(The Athena Sustainable Materials Institute 2016)]
143	243	0	162	0	0	0	0	172	548	0	760	0.09	0.03	27.6	279	82	[(The Athena Sustainable Materials Institute 2016)]

Mix No.	Mixture Composition [kg/m^3]													Comp. Str. [MPa]	CO_2 Footprint [kgCO_2e/m^3]	Mat. Cost [$/m^3]	Ref.
	OPC	FA	GGBS	SF	Meta.	Pozz.	L	Water	C.Agg.	RCA	F.Agg.	SP	AE				
144	202	0	202	0	0	0	0	172	536	0	776	0.09	0.03	27.6	246	81	[(The Athena Sustainable Materials Institute 2016)]
145	213	85	128	0	0	0	0	172	479	0	807	0.09	0.03	27.6	248	82	[(The Athena Sustainable Materials Institute 2016)]
146	463	0	0	0	0	0	0	163	606	0	653	0.21	0.03	34.5	463	92	[(The Athena Sustainable Materials Institute 2016)]
147	390	97	0	0	0	0	0	163	519	0	717	0.21	0.03	34.5	397	90	[(The Athena Sustainable Materials Institute 2016)]
148	351	150	0	0	0	0	0	163	462	0	769	0.21	0.04	34.5	362	90	[(The Athena Sustainable Materials Institute 2016)]
149	309	206	0	0	0	0	0	163	421	0	791	0.21	0.04	34.5	325	89	[(The Athena Sustainable Materials Institute 2016)]
150	324	0	139	0	0	0	0	163	577	0	691	0.21	0.03	34.5	351	89	[(The Athena Sustainable Materials Institute 2016)]
151	278	0	185	0	0	0	0	163	577	0	687	0.21	0.03	34.5	315	88	[(The Athena Sustainable Materials Institute 2016)]
152	231	0	231	0	0	0	0	163	559	0	712	0.21	0.03	34.5	278	87	[(The Athena Sustainable Materials Institute 2016)]
153	244	97	146	0	0	0	0	163	496	0	744	0.21	0.03	34.5	281	87	[(The Athena Sustainable Materials Institute 2016)]
154	335	0	0	0	0	0	0	141	1187	0	712	0.00	0.00	35.0	348	87	[(Marceau *et al* 2007)]
155	279	0	0	0	0	0	0	141	1187	0	771	0.00	0.00	25.0	295	81	[(Marceau *et al* 2007)]
156	223	0	0	0	0	0	0	141	1127	0	831	0.00	0.00	20.0	241	75	[(Marceau *et al* 2007)]
157	179	44	0	0	0	0	0	141	1127	0	831	0.00	0.00	20.0	201	73	[(Marceau *et al* 2007)]
158	167	56	0	0	0	0	0	141	1127	0	831	0.00	0.00	20.0	191	72	[(Marceau *et al* 2007)]
159	145	0	78	0	0	0	0	141	1127	0	831	0.00	0.00	20.0	179	73	[(Marceau *et al* 2007)]
160	112	0	112	0	0	0	0	141	1127	0	831	0.00	0.00	20.0	153	72	[(Marceau *et al* 2007)]
161	504	0	0	0	0	0	0	178	1050	0	555	0.00	0.00	50.0	506	103	[(Marceau *et al* 2007)]
162	445	0	0	56	0	0	0	136	1112	0	611	0.00	0.00	70.0	452	125	[(Marceau *et al* 2007)]
163	223	0	0	0	0	0	0	141	1127	0	831	0.00	0.00	20.0	241	75	[(Marceau *et al* 2007)]
164	300	100	0	0	0	0	0	160	1020	0	668	1.81	0.00	35.0	317	87	[(Bushi and Meil 2014)]
165	206	69	0	0	0	0	0	123	1100	0	910	1.81	0.28	25.0	229	79	[(Bushi and Meil 2014)]
166	204	36	0	0	0	0	0	160	1009	0	925	0.00	0.00	20.0	225	75	[(Athena 2005)]
167	297	53	0	0	0	0	0	160	1092	0	722	0.00	0.00	30.0	313	85	[(Athena 2005)]
168	352	0	0	33	0	0	0	165	1088	0	748	0.00	0.00	60.0	364	105	[(Athena 2005)]
169	191	19	0	0	0	0	0	160	970	0	963	0.00	0.00	15.0	211	72	[(Athena 2005)]
170	218	22	0	0	0	0	0	160	1009	0	925	0.00	0.00	20.0	237	75	[(Athena 2005)]
171	319	31	0	0	0	0	0	160	1092	0	722	0.00	0.00	30.0	333	86	[(Athena 2005)]
172	209	71	0	0	0	0	0	142	1116	0	890	0.00	0.00	21.0	232	79	[(Zachar and Naik n.d.)]

Mix No.	Mixture Composition [kg/m^3]													Comp. Str. [MPa]	CO_2 Footprint [kgCO_2e/m^3]	Mat. Cost [$/m^3]	Ref.
	OPC	FA	GGBS	SF	Meta.	Pozz.	L	Water	C.Agg.	RCA	F.Agg.	SP	AE				
173	71	119	0	0	0	0	0	152	1127	0	801	0.00	0.00	10.0	102	65	[(Zachar and Naik n.d.)]
174	251	59	0	0	0	0	0	142	1068	0	914	0.00	0.00	27.5	271	83	[(Zachar and Naik n.d.)]
175	307	71	0	0	0	0	0	142	1127	0	801	0.00	0.00	34.0	325	90	[(Zachar and Naik n.d.)]
176	349	71	0	0	0	0	0	152	1068	0	777	0.00	0.00	42.0	364	93	[(Zachar and Naik n.d.)]
177	564	44	0	0	0	0	0	204	1068	0	504	0.00	0.00	69.0	565	113	[(Zachar and Naik n.d.)]
178	223	0	0	0	0	0	0	141	1127	0	831	0.00	0.00	21.0	241	75	[(Marceau *et al* 2002)]
179	335	0	0	0	0	0	0	141	1187	0	712	0.00	0.00	34.5	347	87	[(Nisbet *et al* 2000)]
180	279	0	0	0	0	0	0	141	1187	0	771	0.00	0.00	27.6	295	81	[(Nisbet *et al* 2000)]
181	223	0	0	0	0	0	0	141	1127	0	831	0.00	0.00	20.7	241	75	[(Nisbet *et al* 2000)]
182	190	33	0	0	0	0	0	141	1127	0	831	0.00	0.00	20.7	211	73	[(Nisbet *et al* 2000)]
183	179	44	0	0	0	0	0	141	1127	0	831	0.00	0.00	20.7	201	73	[(Nisbet *et al* 2000)]
184	504	0	0	0	0	0	0	178	1050	0	555	0.00	0.00	51.7	506	103	[(Nisbet *et al* 2000)]
185	445	56	0	0	0	0	0	136	1112	0	611	0.00	0.00	68.9	453	102	[(Nisbet *et al* 2000)]
186	500	60	0	0	0	0	0	178	1068	0	608	0.00	0.00	65.0	506	108	[(Mehta and Aïtcin 1990)]
187	390	100	0	0	0	0	0	161	1141	0	575	0.00	0.00	65.0	403	99	[(Mehta and Aïtcin 1990)]
188	360	150	0	0	0	0	0	148	1157	0	603	3.00	0.00	80.0	377	100	[(Mehta and Aïtcin 1990)]
189	315	0	135	36	0	0	0	145	1130	0	745	6.00	0.00	82.0	351	115	[(Mehta and Aïtcin 1990)]
190	500	0	0	30	0	0	0	135	1100	0	700	15.00	0.00	90.0	505	120	[(Mehta and Aïtcin 1990)]
191	485	0	0	0	0	0	0	130	1143	0	762	3.40	0.00	70.0	491	105	[(Mehta and Aïtcin 1990)]
192	317	0	167	0	0	0	0	133	1145	0	749	7.00	0.00	72.0	357	101	[(Mehta and Aïtcin 1990)]
193	315	0	155	35	0	0	0	143	1142	0	744	7.50	0.00	80.0	354	117	[(Mehta and Aïtcin 1990)]
194	449	0	0	39	0	0	0	130	1149	0	758	11.00	0.00	82.0	458	120	[(Mehta and Aïtcin 1990)]
195	427	0	0	59	0	0	0	132	1139	0	754	14.90	0.00	91.0	437	128	[(Mehta and Aïtcin 1990)]
196	450	0	0	50	0	0	0	140	1108	0	687	17.00	0.00	93.0	458	124	[(Mehta and Aïtcin 1990)]
197	500	0	0	42	0	0	0	138	1130	0	675	10.00	0.00	97.0	506	126	[(Mehta and Aïtcin 1990)]
198	486	0	0	54	0	0	0	135	1112	0	661	20.00	0.00	100.0	492	130	[(Mehta and Aïtcin 1990)]
199	580	0	0	70	0	0	0	140	1025	0	620	12.00	0.00	103.0	581	147	[(Mehta and Aïtcin 1990)]
200	517	0	0	58	0	0	0	126	1126	0	641	25.00	0.00	107.0	522	136	[(Mehta and Aïtcin 1990)]
201	180	0	120	0	0	0	0	120	1271	0	821	0.64	0.00	57.2	221	83	[(Obla *et al* 2017)]

Mix No.	Mixture Composition [kg/m^3]													Comp. Str. [MPa]	CO_2 Footprint [kgCO_2e/m^3]	Mat. Cost [$/m^3]	Ref.
	OPC	FA	GGBS	SF	Meta.	Pozz.	L	Water	C.Agg.	RCA	F.Agg.	SP	AE				
202	198	0	132	0	0	0	0	132	1250	0	807	0.42	0.00	58.8	240	86	[(Obla *et al* 2017)]
203	223	0	149	0	0	0	0	149	1203	0	777	0.08	0.00	58.6	265	90	[(Obla *et al* 2017)]
204	256	0	171	0	0	0	0	171	1133	0	731	0.00	0.00	54.1	299	94	[(Obla *et al* 2017)]
205	291	0	0	0	0	0	0	116	1229	0	813	0.96	0.00	44.7	307	84	[(Obla *et al* 2017)]
206	322	0	0	0	0	0	0	129	1206	0	798	0.46	0.00	49.7	337	87	[(Obla *et al* 2017)]
207	206	69	0	0	0	0	0	110	1226	0	811	0.56	0.00	41.8	230	79	[(Obla *et al* 2017)]
208	236	79	0	0	0	0	0	126	1235	0	818	0.34	0.00	45.4	259	84	[(Obla *et al* 2017)]
209	133	0	88	0	0	0	0	104	1227	0	812	0.05	0.05	26.4	170	74	[(Obla *et al* 2017)]
210	153	0	101	0	0	0	0	120	1236	0	818	0.05	0.05	32.8	192	78	[(Obla *et al* 2017)]
211	166	0	110	0	0	0	0	129	1281	0	827	0.38	0.00	52.1	206	81	[(Obla *et al* 2017)]
212	175	0	116	0	0	0	0	138	1181	0	781	0.12	0.12	32.1	214	80	[(Obla *et al* 2017)]
213	180	0	120	0	0	0	0	141	1247	0	805	0.15	0.00	49.9	221	83	[(Obla *et al* 2017)]
214	203	0	135	0	0	0	0	159	1201	0	775	0.00	0.00	47.9	244	86	[(Obla *et al* 2017)]
215	207	0	138	0	0	0	0	163	1122	0	742	0.10	0.10	32.6	247	85	[(Obla *et al* 2017)]
216	233	0	155	0	0	0	0	183	1130	0	730	0.00	0.00	45.7	274	89	[(Obla *et al* 2017)]
217	279	0	0	0	0	0	0	131	1281	0	828	1.21	0.00	47.9	297	84	[(Obla *et al* 2017)]
218	304	0	0	0	0	0	0	142	1244	0	803	0.43	0.00	43.5	320	86	[(Obla *et al* 2017)]
219	345	0	0	0	0	0	0	162	1207	0	780	0.00	0.00	47.8	358	90	[(Obla *et al* 2017)]
220	397	0	0	0	0	0	0	187	1141	0	737	0.00	0.00	45.5	407	94	[(Obla *et al* 2017)]
221	201	67	0	0	0	0	0	126	1284	0	829	0.62	0.00	37.4	225	80	[(Obla *et al* 2017)]
222	218	73	0	0	0	0	0	137	1251	0	808	0.38	0.00	39.4	242	81	[(Obla *et al* 2017)]
223	246	82	0	0	0	0	0	154	1203	0	777	0.00	0.00	37.6	268	84	[(Obla *et al* 2017)]
224	285	95	0	0	0	0	0	179	1145	0	739	0.00	0.00	36.5	305	88	[(Obla *et al* 2017)]
225	148	0	99	0	0	0	0	136	1267	0	818	0.34	0.00	40.1	187	77	[(Obla *et al* 2017)]
226	163	0	109	0	0	0	0	150	1243	0	803	0.00	0.00	36.4	202	80	[(Obla *et al* 2017)]
227	184	0	123	0	0	0	0	168	1195	0	772	0.00	0.00	38.1	224	82	[(Obla *et al* 2017)]
228	214	0	143	0	0	0	0	196	1144	0	739	0.00	0.00	42.1	255	86	[(Obla *et al* 2017)]
229	238	0	0	0	0	0	0	132	1224	0	810	0.34	0.00	27.1	256	78	[(Obla *et al* 2017)]
230	266	0	0	0	0	0	0	147	1202	0	796	0.26	0.00	31.4	283	81	[(Obla *et al* 2017)]

Mix No.	Mixture Composition [kg/m^3]													Comp. Str. [MPa]	CO_2 Footprint [kgCO_2e/m^3]	Mat. Cost [$/m^3]	Ref.
	OPC	FA	GGBS	SF	Meta.	Pozz.	L	Water	C.Agg.	RCA	F.Agg.	SP	AE				
231	176	59	0	0	0	0	0	129	1252	0	828	0.26	0.00	22.9	200	76	[(Obla *et al* 2017)]
232	194	65	0	0	0	0	0	143	1221	0	807	0.15	0.00	23.9	218	77	[(Obla *et al* 2017)]
233	400	0	0	0	0	0	0	164	1228	0	616	2.20	0.00	34.8	409	94	[(Siddique 2004)]
234	240	160	0	0	0	0	0	160	1224	0	614	2.50	0.00	25.0	264	87	[(Siddique 2004)]
235	220	180	0	0	0	0	0	164	1226	0	610	2.60	0.00	23.1	246	86	[(Siddique 2004)]
236	200	200	0	0	0	0	0	160	1225	0	616	2.70	0.00	21.6	228	86	[(Siddique 2004)]
237	168	206	0	0	0	0	0	120	1052	0	701	3.03	0.49	23.3	197	81	[(Bouzoubaa *et al* 2001)]
238	391	0	0	0	0	0	0	125	1111	0	740	4.36	0.51	42.5	401	93	[(Bouzoubaa *et al* 2001)]
239	385	0	0	0	0	0	0	154	1094	0	729	1.21	0.12	37.4	394	92	[(Bouzoubaa *et al* 2001)]
240	389	0	0	0	0	0	0	164	1093	0	729	2.66	0.17	44.9	398	92	[(Bouzoubaa *et al* 2001)]
241	170	209	0	0	0	0	0	122	1066	0	710	3.03	0.31	29.6	199	82	[(Bouzoubaa *et al* 2001)]
242	391	0	0	0	0	0	0	125	1111	0	740	4.36	0.51	42.0	401	93	[(Bouzoubaa *et al* 2001)]
243	385	0	0	0	0	0	0	154	1094	0	729	1.09	0.11	37.6	394	92	[(Bouzoubaa *et al* 2001)]
244	384	0	0	0	0	0	0	162	1081	0	720	1.69	0.17	40.8	393	91	[(Bouzoubaa *et al* 2001)]
245	637	0	0	0	0	0	0	150	936	0	711	18.40	0.00	84.6	633	119	[(Poon *et al* 2000)]
246	475	158	0	0	0	0	0	150	924	0	681	18.30	0.00	92.0	486	111	[(Poon *et al* 2000)]
247	347	283	0	0	0	0	0	148	920	0	639	23.70	0.00	77.6	370	105	[(Poon *et al* 2000)]
248	702	0	0	0	0	0	0	135	949	0	641	35.10	0.00	84.1	695	126	[(Poon *et al* 2000)]
249	512	173	0	0	0	0	0	133	932	0	620	34.70	0.00	88.8	522	116	[(Poon *et al* 2000)]
250	372	305	0	0	0	0	0	130	927	0	608	33.80	0.00	76.9	394	109	[(Poon *et al* 2000)]
251	320	57	0	0	0	0	0	151	1032	0	711	1.25	0.10	41.7	334	87	[(Liu *et al* 2012)]
252	219	146	0	0	0	0	0	146	1032	0	720	0.47	0.10	29.4	242	82	[(Liu *et al* 2012)]
253	274	117	0	0	0	0	0	157	1032	0	674	0.44	0.10	29.9	293	86	[(Liu *et al* 2012)]
254	219	146	0	0	0	0	0	146	1032	0	720	0.47	0.10	31.7	242	82	[(Liu *et al* 2012)]
255	237	101	0	0	0	0	0	135	1032	0	777	1.14	0.10	40.1	258	82	[(Liu *et al* 2012)]
256	219	146	0	0	0	0	0	146	1032	0	720	0.47	0.10	34.3	242	82	[(Liu *et al* 2012)]
257	196	196	0	0	0	0	0	157	1032	0	662	0.00	0.10	28.7	222	82	[(Liu *et al* 2012)]
258	169	169	0	0	0	0	0	135	1032	0	767	0.51	0.10	31.0	196	79	[(Liu *et al* 2012)]
259	167	251	0	0	0	0	0	167	1032	0	603	0.00	0.10	24.1	197	82	[(Liu *et al* 2012)]

Mix No.	Mixture Composition [kg/m^3]													Comp. Str. [MPa]	CO_2 Footprint [kgCO_2e/m^3]	Mat. Cost [$/m^3]	Ref.
	OPC	FA	GGBS	SF	Meta.	Pozz.	L	Water	C.Agg.	RCA	F.Agg.	SP	AE				
260	500	0	0	0	0	0	0	150	1086	0	724	7.50	0.00	79.9	504	106	[(Lam *et al* 1997)]
261	425	75	0	0	0	0	0	150	1086	0	700	7.50	0.00	75.4	436	102	[(Lam *et al* 1997)]
262	375	125	0	0	0	0	0	150	1086	0	683	9.25	0.00	76.6	391	100	[(Lam *et al* 1997)]
263	275	225	0	0	0	0	0	150	1086	0	650	10.50	0.00	62.0	300	95	[(Lam *et al* 1997)]
264	225	275	0	0	0	0	0	150	1086	0	634	13.00	0.00	55.3	254	92	[(Lam *et al* 1997)]
265	475	0	0	25	0	0	0	150	1086	0	719	8.00	0.00	84.9	481	115	[(Lam *et al* 1997)]
266	375	100	0	25	0	0	0	150	1086	0	686	9.25	0.00	81.5	390	110	[(Lam *et al* 1997)]
267	275	200	0	25	0	0	0	150	1086	0	654	11.00	0.00	69.3	299	105	[(Lam *et al* 1997)]
268	400	0	0	0	0	0	0	160	1157	0	710	4.00	0.00	54.0	409	94	[(Lam *et al* 1997)]
269	340	60	0	0	0	0	0	160	1157	0	690	4.40	0.00	43.4	355	92	[(Lam *et al* 1997)]
270	300	100	0	0	0	0	0	160	1157	0	660	4.80	0.00	42.7	318	89	[(Lam *et al* 1997)]
271	220	180	0	0	0	0	0	160	1157	0	634	5.20	0.00	31.7	246	86	[(Lam *et al* 1997)]
272	180	220	0	0	0	0	0	160	1157	0	621	6.40	0.00	31.4	209	84	[(Lam *et al* 1997)]
273	380	0	0	20	0	0	0	160	1157	0	688	5.50	0.00	62.8	391	102	[(Lam *et al* 1997)]
274	300	80	0	20	0	0	0	160	1157	0	662	5.50	0.00	54.4	318	98	[(Lam *et al* 1997)]
275	220	160	0	20	0	0	0	160	1157	0	636	6.00	0.00	39.2	245	94	[(Lam *et al* 1997)]
276	410	0	0	0	0	0	0	205	1132	0	609	0.00	0.00	41.3	417	94	[(Lam *et al* 1997)]
277	349	62	0	0	0	0	0	205	1132	0	589	0.00	0.00	36.9	361	91	[(Lam *et al* 1997)]
278	308	103	0	0	0	0	0	205	1132	0	576	0.00	0.00	34.1	324	89	[(Lam *et al* 1997)]
279	226	185	0	0	0	0	0	205	1132	0	549	0.00	0.00	29.4	250	85	[(Lam *et al* 1997)]
280	185	226	0	0	0	0	0	205	1132	0	536	0.00	0.00	25.1	212	83	[(Lam *et al* 1997)]
281	390	0	0	21	0	0	0	205	1132	0	605	0.00	0.00	45.3	398	101	[(Lam *et al* 1997)]
282	308	82	0	21	0	0	0	205	1132	0	578	0.00	0.00	45.3	324	97	[(Lam *et al* 1997)]
283	226	164	0	21	0	0	0	205	1132	0	552	0.00	0.00	32.2	249	94	[(Lam *et al* 1997)]
284	461	0	0	0	0	0	0	161	922	0	922	6.59	0.00	50.9	468	101	[(Celik *et al* 2015)]
285	389	0	0	69	0	0	0	160	915	0	915	5.56	0.00	40.8	401	127	[(Celik *et al* 2015)]
286	342	0	0	114	0	0	0	160	912	0	912	4.51	0.00	31.7	357	144	[(Celik *et al* 2015)]
287	317	136	0	0	0	0	0	159	906	0	906	4.41	0.00	48.2	336	94	[(Celik *et al* 2015)]
288	224	225	0	0	0	0	0	157	897	0	897	2.55	0.00	39.3	252	90	[(Celik *et al* 2015)]

Mix No.	Mixture Composition [kg/m^3]													Comp. Str. [MPa]	CO_2 Footprint [kgCO_2e/m^3]	Mat. Cost [$/m^3]	Ref.
	OPC	FA	GGBS	SF	Meta.	Pozz.	L	Water	C.Agg.	RCA	F.Agg.	SP	AE				
289	248	135	0	68	0	0	0	158	902	0	902	2.83	0.00	35.4	273	120	[(Celik *et al* 2015)]
290	202	179	0	67	0	0	0	157	897	0	897	2.08	0.00	32.0	231	117	[(Celik *et al* 2015)]
291	156	223	0	67	0	0	0	156	892	0	892	1.56	0.00	24.6	189	115	[(Celik *et al* 2015)]
292	111	266	0	67	0	0	0	155	888	0	888	1.11	0.00	19.5	148	112	[(Celik *et al* 2015)]
293	248	90	0	113	0	0	0	158	902	0	902	3.32	0.00	34.3	272	139	[(Celik *et al* 2015)]
294	202	135	0	112	0	0	0	157	898	0	898	2.30	0.00	29.8	230	136	[(Celik *et al* 2015)]
295	156	179	0	112	0	0	0	156	893	0	893	1.78	0.00	27.3	188	134	[(Celik *et al* 2015)]
296	111	223	0	111	0	0	0	156	890	0	890	1.27	0.00	19.5	147	131	[(Celik *et al* 2015)]
297	350	0	0	0	0	0	0	105	1198	0	832	12.25	0.00	70.9	364	91	[(Bilim *et al* 2009)]
298	280	0	70	0	0	0	0	105	1195	0	830	11.55	0.00	76.1	308	89	[(Bilim *et al* 2009)]
299	210	0	140	0	0	0	0	105	1189	0	826	8.75	0.00	75.7	252	88	[(Bilim *et al* 2009)]
300	140	0	210	0	0	0	0	105	1186	0	824	7.00	0.00	68.5	196	86	[(Bilim *et al* 2009)]
301	70	0	280	0	0	0	0	105	1180	0	820	5.60	0.00	58.6	140	84	[(Bilim *et al* 2009)]
302	350	0	0	0	0	0	0	140	1145	0	795	5.25	0.00	59.7	362	90	[(Bilim *et al* 2009)]
303	280	0	70	0	0	0	0	140	1139	0	791	4.20	0.00	61.5	307	88	[(Bilim *et al* 2009)]
304	210	0	140	0	0	0	0	140	1136	0	789	3.50	0.00	62.8	251	86	[(Bilim *et al* 2009)]
305	140	0	210	0	0	0	0	140	1130	0	785	1.75	0.00	57.8	195	84	[(Bilim *et al* 2009)]
306	70	0	280	0	0	0	0	140	1127	0	783	2.80	0.00	47.1	139	83	[(Bilim *et al* 2009)]
307	350	0	0	0	0	0	0	175	1089	0	757	0.70	0.00	50.1	361	88	[(Bilim *et al* 2009)]
308	280	0	70	0	0	0	0	175	1086	0	754	0.00	0.00	53.3	305	86	[(Bilim *et al* 2009)]
309	210	0	140	0	0	0	0	175	1080	0	750	0.00	0.00	52.3	250	85	[(Bilim *et al* 2009)]
310	140	0	210	0	0	0	0	175	1077	0	748	0.00	0.00	42.2	194	83	[(Bilim *et al* 2009)]
311	70	0	280	0	0	0	0	175	1071	0	744	0.00	0.00	28.0	138	81	[(Bilim *et al* 2009)]
312	400	0	0	0	0	0	0	120	1151	0	800	16.00	0.00	75.4	410	96	[(Bilim *et al* 2009)]
313	320	0	80	0	0	0	0	120	1145	0	795	14.00	0.00	76.1	346	94	[(Bilim *et al* 2009)]
314	240	0	160	0	0	0	0	120	1142	0	793	9.60	0.00	76.7	283	92	[(Bilim *et al* 2009)]
315	160	0	240	0	0	0	0	120	1136	0	789	6.00	0.00	72.7	219	90	[(Bilim *et al* 2009)]
316	80	0	320	0	0	0	0	120	1130	0	785	4.80	0.00	63.3	155	88	[(Bilim *et al* 2009)]
317	400	0	0	0	0	0	0	160	1089	0	757	6.00	0.00	59.7	409	94	[(Bilim *et al* 2009)]

Mix No.	Mixture Composition [kg/m^3]													Comp. Str. [MPa]	CO_2 Footprint [kgCO_2e/m^3]	Mat. Cost [$/m^3]	Ref.
	OPC	FA	GGBS	SF	Meta.	Pozz.	L	Water	C.Agg.	RCA	F.Agg.	SP	AE				
318	320	0	80	0	0	0	0	160	1083	0	752	4.00	0.00	61.7	345	92	[(Bilim *et al* 2009)]
319	240	0	160	0	0	0	0	160	1077	0	748	4.00	0.00	62.5	281	90	[(Bilim *et al* 2009)]
320	160	0	240	0	0	0	0	160	1074	0	746	2.40	0.00	57.1	217	88	[(Bilim *et al* 2009)]
321	80	0	320	0	0	0	0	160	1068	0	742	3.60	0.00	49.6	154	86	[(Bilim *et al* 2009)]
322	400	0	0	0	0	0	0	200	1024	0	711	0.40	0.00	48.1	408	92	[(Bilim *et al* 2009)]
323	320	0	80	0	0	0	0	200	1021	0	709	0.00	0.00	49.2	344	90	[(Bilim *et al* 2009)]
324	240	0	160	0	0	0	0	200	1015	0	705	0.00	0.00	48.2	280	88	[(Bilim *et al* 2009)]
325	160	0	240	0	0	0	0	200	1009	0	701	0.00	0.00	37.5	216	86	[(Bilim *et al* 2009)]
326	80	0	320	0	0	0	0	200	1006	0	699	0.00	0.00	23.7	152	84	[(Bilim *et al* 2009)]
327	450	0	0	0	0	0	0	135	1100	0	765	18.00	0.00	75.1	457	100	[(Bilim *et al* 2009)]
328	360	0	90	0	0	0	0	135	1097	0	763	14.40	0.00	76.5	385	98	[(Bilim *et al* 2009)]
329	270	0	180	0	0	0	0	135	1092	0	759	11.70	0.00	78.3	313	96	[(Bilim *et al* 2009)]
330	180	0	270	0	0	0	0	135	1086	0	754	9.00	0.00	75.3	242	94	[(Bilim *et al* 2009)]
331	90	0	360	0	0	0	0	135	1080	0	750	8.10	0.00	62.0	170	92	[(Bilim *et al* 2009)]
332	450	0	0	0	0	0	0	180	1033	0	718	4.50	0.00	60.1	456	99	[(Bilim *et al* 2009)]
333	360	0	90	0	0	0	0	180	1027	0	713	3.60	0.00	68.7	384	96	[(Bilim *et al* 2009)]
334	270	0	180	0	0	0	0	180	1021	0	709	2.25	0.00	62.1	312	94	[(Bilim *et al* 2009)]
335	180	0	270	0	0	0	0	180	1015	0	705	2.25	0.00	57.8	240	92	[(Bilim *et al* 2009)]
336	90	0	360	0	0	0	0	180	1009	0	701	1.35	0.00	43.8	168	90	[(Bilim *et al* 2009)]
337	450	0	0	0	0	0	0	225	962	0	668	0.00	0.00	45.5	454	97	[(Bilim *et al* 2009)]
338	360	0	90	0	0	0	0	225	956	0	664	0.00	0.00	47.1	382	94	[(Bilim *et al* 2009)]
339	270	0	180	0	0	0	0	225	950	0	660	0.00	0.00	46.1	311	92	[(Bilim *et al* 2009)]
340	180	0	270	0	0	0	0	225	944	0	656	0.00	0.00	36.9	239	90	[(Bilim *et al* 2009)]
341	90	0	360	0	0	0	0	225	938	0	652	0.00	0.00	25.9	167	88	[(Bilim *et al* 2009)]
342	478	0	0	0	0	0	0	196	902	0	765	0.00	0.00	51.3	482	101	[(Monteiro *et al* 1993)]
343	398	0	0	0	0	0	0	199	920	0	866	0.00	0.00	46.2	407	93	[(Monteiro *et al* 1993)]
344	329	0	0	0	0	0	0	198	914	0	929	0.00	0.00	35.6	341	86	[(Monteiro *et al* 1993)]
345	282	0	0	0	0	0	0	198	911	0	976	0.00	0.00	25.4	297	81	[(Monteiro *et al* 1993)]
346	306	0	0	0	0	0	0	153	961	0	1023	0.00	0.00	46.9	321	85	[(Monteiro *et al* 1993)]

Mix No.	Mixture Composition [kg/m^3]													Comp. Str. [MPa]	CO_2 Footprint [kgCO_2e/m^3]	Mat. Cost [$/m^3]	Ref.
	OPC	FA	GGBS	SF	Meta.	Pozz.	L	Water	C.Agg.	RCA	F.Agg.	SP	AE				
347	484	0	0	0	0	0	0	242	875	0	721	0.00	0.00	45.2	486	100	[(Monteiro *et al* 1993)]
348	377	0	0	0	0	0	0	227	562	0	861	3.70	0.00	54.3	382	84	[(Felekoğlu *et al* 2007)]
349	376	0	0	0	0	0	0	203	577	0	886	6.50	0.00	48.1	382	85	[(Felekoğlu *et al* 2007)]
350	377	0	0	0	0	0	0	181	593	0	898	7.90	0.00	45.3	383	85	[(Felekoğlu *et al* 2007)]
351	376	0	0	0	0	0	0	158	609	0	932	9.00	0.00	41.4	383	86	[(Felekoğlu *et al* 2007)]
352	377	0	0	0	0	0	0	140	630	0	963	13.00	0.00	35.2	384	87	[(Felekoğlu *et al* 2007)]
353	420	0	0	47	0	0	0	147	992	0	860	11.50	0.00	62.9	430	120	[(Einsfeld and Velasco 2006)]
354	457	0	0	50	0	0	0	153	992	0	814	12.40	0.00	82.3	465	125	[(Einsfeld and Velasco 2006)]
355	540	0	0	60	0	0	0	151	992	0	724	14.80	0.00	85.2	543	139	[(Einsfeld and Velasco 2006)]
356	457	0	0	50	0	0	0	153	992	0	814	12.40	0.00	81.3	465	125	[(Einsfeld and Velasco 2006)]
357	457	0	0	50	0	0	0	153	992	0	814	12.40	0.00	79.4	465	125	[(Einsfeld and Velasco 2006)]
358	484	0	0	0	0	0	0	188	910	0	812	5.67	0.00	72.4	488	102	[(Vejmelková *et al* 2009)]
359	440	0	44	0	0	0	0	188	910	0	812	5.67	0.00	70.1	453	101	[(Vejmelková *et al* 2009)]
360	400	0	0	0	0	0	0	146	1113	0	761	6.00	0.00	67.3	409	95	[(Haque and Kayali 1998)]
361	360	40	0	0	0	0	0	137	1084	0	741	6.00	0.00	81.6	373	92	[(Haque and Kayali 1998)]
362	340	60	0	0	0	0	0	151	1069	0	731	6.00	0.00	63.8	354	91	[(Haque and Kayali 1998)]
363	500	0	0	0	0	0	0	178	1012	0	692	7.50	0.00	80.3	503	104	[(Haque and Kayali 1998)]
364	450	50	0	0	0	0	0	115	876	0	667	7.50	0.00	96.4	456	99	[(Haque and Kayali 1998)]
365	425	75	0	0	0	0	0	134	958	0	655	7.50	0.00	88.6	434	99	[(Haque and Kayali 1998)]
366	472	0	202	0	0	0	0	175	950	0	634	8.43	0.00	85.3	507	118	[(Wu *et al* 2001)]
367	472	0	202	0	0	0	0	175	950	0	634	8.43	0.00	86.1	507	118	[(Wu *et al* 2001)]
368	472	0	202	0	0	0	0	175	950	0	634	8.43	0.00	72.4	507	118	[(Wu *et al* 2001)]
369	472	0	202	0	0	0	0	175	950	0	634	8.43	0.00	69.3	507	118	[(Wu *et al* 2001)]
370	267	0	115	0	0	0	0	168	1112	0	741	4.78	0.00	61.1	301	89	[(Wu *et al* 2001)]
371	267	0	115	0	0	0	0	168	1112	0	741	4.78	0.00	57.1	301	89	[(Wu *et al* 2001)]
372	267	0	115	0	0	0	0	168	1112	0	741	4.78	0.00	52.5	301	89	[(Wu *et al* 2001)]
373	267	0	115	0	0	0	0	168	1112	0	741	4.78	0.00	53.9	301	89	[(Wu *et al* 2001)]
374	238	0	102	0	0	0	0	187	1020	0	680	1.70	0.00	38.9	269	82	[(Wu *et al* 2001)]
375	238	0	102	0	0	0	0	187	1020	0	680	1.70	0.00	37.5	269	82	[(Wu *et al* 2001)]

Mix No.	Mixture Composition [kg/m^3]													Comp. Str. [MPa]	CO_2 Footprint [kgCO_2e/m^3]	Mat. Cost [$/m^3]	Ref.
	OPC	FA	GGBS	SF	Meta.	Pozz.	L	Water	C.Agg.	RCA	F.Agg.	SP	AE				
376	238	0	102	0	0	0	0	187	1020	0	680	1.70	0.00	14.4	269	82	[(Wu *et al* 2001)]
377	238	0	102	0	0	0	0	187	1020	0	680	1.70	0.00	39.1	269	82	[(Wu *et al* 2001)]
378	200	30	0	0	0	0	0	216	558	0	1293	0.00	0.00	20.9	220	72	[(Oner *et al* 2005)]
379	200	65	0	0	0	0	0	221	538	0	1246	0.00	0.00	21.4	221	74	[(Oner *et al* 2005)]
380	200	100	0	0	0	0	0	229	519	0	1203	0.00	0.00	21.2	222	76	[(Oner *et al* 2005)]
381	240	35	0	0	0	0	0	223	540	0	1251	0.00	0.00	20.0	258	77	[(Oner *et al* 2005)]
382	240	80	0	0	0	0	0	228	516	0	1195	0.00	0.00	21.6	259	79	[(Oner *et al* 2005)]
383	240	120	0	0	0	0	0	236	495	0	1146	0.00	0.00	19.9	260	81	[(Oner *et al* 2005)]
384	280	40	0	0	0	0	0	230	522	0	1208	0.00	0.00	27.3	295	81	[(Oner *et al* 2005)]
385	280	95	0	0	0	0	0	236	493	0	1142	0.00	0.00	27.7	297	84	[(Oner *et al* 2005)]
386	280	140	0	0	0	0	0	245	470	0	1088	0.00	0.00	27.9	298	86	[(Oner *et al* 2005)]
387	320	50	0	0	0	0	0	237	501	0	1159	0.00	0.00	18.7	333	85	[(Oner *et al* 2005)]
388	320	105	0	0	0	0	0	243	473	0	1096	0.00	0.00	27.6	335	88	[(Oner *et al* 2005)]
389	320	160	0	0	0	0	0	251	446	0	1032	0.00	0.00	25.3	337	91	[(Oner *et al* 2005)]
390	250	0	0	0	0	0	0	218	555	0	1285	0.00	0.00	26.6	266	76	[(Oner *et al* 2005)]
391	200	50	0	0	0	0	0	219	547	0	1266	0.00	0.00	33.3	220	73	[(Oner *et al* 2005)]
392	200	85	0	0	0	0	0	224	529	0	1225	0.00	0.00	33.8	222	75	[(Oner *et al* 2005)]
393	200	115	0	0	0	0	0	232	511	0	1184	0.00	0.00	34.1	222	77	[(Oner *et al* 2005)]
394	300	0	0	0	0	0	0	225	536	0	1242	0.00	0.00	25.1	313	81	[(Oner *et al* 2005)]
395	240	60	0	0	0	0	0	225	527	0	1221	0.00	0.00	33.4	258	78	[(Oner *et al* 2005)]
396	240	100	0	0	0	0	0	231	508	0	1176	0.00	0.00	30.8	260	80	[(Oner *et al* 2005)]
397	240	140	0	0	0	0	0	240	484	0	1122	0.00	0.00	33.2	261	82	[(Oner *et al* 2005)]
398	350	0	0	0	0	0	0	232	517	0	1197	0.00	0.00	39.7	360	86	[(Oner *et al* 2005)]
399	280	70	0	0	0	0	0	232	507	0	1174	0.00	0.00	39.9	296	82	[(Oner *et al* 2005)]
400	280	120	0	0	0	0	0	240	481	0	1114	0.00	0.00	31.4	298	85	[(Oner *et al* 2005)]
401	280	165	0	0	0	0	0	249	457	0	1058	0.00	0.00	38.8	299	87	[(Oner *et al* 2005)]
402	400	0	0	0	0	0	0	239	498	0	1154	0.00	0.00	36.7	407	91	[(Oner *et al* 2005)]
403	320	80	0	0	0	0	0	240	484	0	1122	0.00	0.00	38.7	334	87	[(Oner *et al* 2005)]
404	320	135	0	0	0	0	0	247	458	0	1062	0.00	0.00	38.5	336	90	[(Oner *et al* 2005)]

Mix No.	Mixture Composition [kg/m^3]													Comp. Str. [MPa]	CO_2 Footprint [kgCO_2e/m^3]	Mat. Cost [$/m^3]	Ref.
	OPC	FA	GGBS	SF	Meta.	Pozz.	L	Water	C.Agg.	RCA	F.Agg.	SP	AE				
405	320	185	0	0	0	0	0	225	436	0	1009	0.00	0.00	36.9	338	92	[(Oner *et al* 2005)]
406	280	0	440	0	0	0	0	295	723	0	477	0.00	0.00	39.9	357	112	[(Oner and Akyuz 2007)]
407	245	0	385	0	0	0	0	279	799	0	526	0.00	0.00	35.1	316	104	[(Oner and Akyuz 2007)]
408	210	0	330	0	0	0	0	261	877	0	578	0.00	0.00	29.7	275	97	[(Oner and Akyuz 2007)]
409	175	0	275	0	0	0	0	248	948	0	624	0.00	0.00	23.5	234	89	[(Oner and Akyuz 2007)]
410	280	0	360	0	0	0	0	278	796	0	525	0.00	0.00	43.9	345	106	[(Oner and Akyuz 2007)]
411	245	0	315	0	0	0	0	263	864	0	569	0.00	0.00	38.8	306	99	[(Oner and Akyuz 2007)]
412	210	0	270	0	0	0	0	251	927	0	611	0.00	0.00	32.3	267	93	[(Oner and Akyuz 2007)]
413	175	0	225	0	0	0	0	238	991	0	654	0.00	0.00	25.4	227	86	[(Oner and Akyuz 2007)]
414	280	0	280	0	0	0	0	263	866	0	570	0.00	0.00	45.2	334	100	[(Oner and Akyuz 2007)]
415	245	0	245	0	0	0	0	250	924	0	609	0.00	0.00	39.5	296	94	[(Oner and Akyuz 2007)]
416	210	0	210	0	0	0	0	240	979	0	645	0.00	0.00	32.6	258	88	[(Oner and Akyuz 2007)]
417	175	0	175	0	0	0	0	230	1033	0	681	0.00	0.00	26.0	220	82	[(Oner and Akyuz 2007)]
418	280	0	200	0	0	0	0	247	936	0	617	0.00	0.00	44.4	323	94	[(Oner and Akyuz 2007)]
419	245	0	175	0	0	0	0	239	982	0	647	0.00	0.00	38.7	286	89	[(Oner and Akyuz 2007)]
420	210	0	150	0	0	0	0	231	1027	0	677	0.00	0.00	31.8	250	84	[(Oner and Akyuz 2007)]
421	175	0	125	0	0	0	0	223	1073	0	707	0.00	0.00	25.2	213	78	[(Oner and Akyuz 2007)]
422	280	0	120	0	0	0	0	236	999	0	659	0.00	0.00	39.1	311	88	[(Oner and Akyuz 2007)]
423	245	0	105	0	0	0	0	230	1036	0	683	0.00	0.00	33.7	276	84	[(Oner and Akyuz 2007)]
424	210	0	90	0	0	0	0	224	1072	0	707	0.00	0.00	28.0	241	79	[(Oner and Akyuz 2007)]
425	175	0	75	0	0	0	0	218	1109	0	731	0.00	0.00	22.0	206	74	[(Oner and Akyuz 2007)]
426	280	0	60	0	0	0	0	231	1041	0	686	0.00	0.00	31.5	302	84	[(Oner and Akyuz 2007)]
427	245	0	53	0	0	0	0	225	1073	0	708	0.00	0.00	27.1	268	80	[(Oner and Akyuz 2007)]
428	210	0	45	0	0	0	0	219	1106	0	729	0.00	0.00	22.1	234	76	[(Oner and Akyuz 2007)]
429	175	0	38	0	0	0	0	215	1135	0	748	0.00	0.00	16.9	200	71	[(Oner and Akyuz 2007)]
430	250	0	0	0	0	0	0	219	1111	0	732	0.00	0.00	21.2	266	76	[(Oner and Akyuz 2007)]
431	175	0	0	0	0	0	0	209	1166	0	768	0.00	0.00	12.2	195	69	[(Oner and Akyuz 2007)]
432	300	0	0	0	0	0	0	225	1075	0	708	0.00	0.00	27.0	313	81	[(Oner and Akyuz 2007)]
433	210	0	0	0	0	0	0	214	1140	0	751	0.00	0.00	16.4	228	72	[(Oner and Akyuz 2007)]

Mix No.	Mixture Composition [kg/m^3]													Comp. Str. [MPa]	CO_2 Footprint [kgCO_2e/m^3]	Mat. Cost [$/m^3]	Ref.
	OPC	FA	GGBS	SF	Meta.	Pozz.	L	Water	C.Agg.	RCA	F.Agg.	SP	AE				
434	350	0	0	0	0	0	0	232	1037	0	684	0.00	0.00	32.7	360	86	[(Oner and Akyuz 2007)]
435	245	0	0	0	0	0	0	218	1114	0	735	0.00	0.00	21.1	261	76	[(Oner and Akyuz 2007)]
436	400	0	0	0	0	0	0	239	999	0	659	0.00	0.00	37.8	407	91	[(Oner and Akyuz 2007)]
437	280	0	0	0	0	0	0	224	1087	0	716	0.00	0.00	25.7	294	79	[(Oner and Akyuz 2007)]
438	235	0	0	0	0	0	0	185	1200	0	700	0.71	0.00	23.9	252	75	[(Meddah *et al* 2014)]
439	200	0	0	0	0	0	35	185	1200	0	700	0.71	0.00	20.8	218	71	[(Meddah *et al* 2014)]
440	176	0	0	0	0	0	59	185	1200	0	700	0.71	0.00	15.6	196	69	[(Meddah *et al* 2014)]
441	153	0	0	0	0	0	82	185	1200	0	700	0.71	0.00	11.3	174	66	[(Meddah *et al* 2014)]
442	129	0	0	0	0	0	106	185	1200	0	700	0.71	0.00	5.6	151	63	[(Meddah *et al* 2014)]
443	285	0	0	0	0	0	0	185	1200	0	730	0.68	0.00	32.1	300	82	[(Meddah *et al* 2014)]
444	242	0	0	0	0	0	43	185	1200	0	730	0.68	0.00	28.2	259	77	[(Meddah *et al* 2014)]
445	214	0	0	0	0	0	71	185	1200	0	730	0.68	0.00	23.0	232	74	[(Meddah *et al* 2014)]
446	185	0	0	0	0	0	100	185	1200	0	730	0.68	0.00	17.4	205	70	[(Meddah *et al* 2014)]
447	157	0	0	0	0	0	128	185	1200	0	730	0.68	0.00	12.2	178	67	[(Meddah *et al* 2014)]
448	285	0	0	0	0	0	0	185	1200	0	710	0.40	0.00	35.6	300	81	[(Meddah *et al* 2014)]
449	264	0	0	0	0	0	47	185	1200	0	710	0.40	0.00	31.7	280	79	[(Meddah *et al* 2014)]
450	233	0	0	0	0	0	78	185	1200	0	710	0.40	0.00	26.5	250	76	[(Meddah *et al* 2014)]
451	202	0	0	0	0	0	109	185	1200	0	710	0.40	0.00	20.4	220	72	[(Meddah *et al* 2014)]
452	171	0	0	0	0	0	140	185	1200	0	710	0.40	0.00	14.8	191	68	[(Meddah *et al* 2014)]
453	310	0	0	0	0	0	0	185	1200	0	670	0.39	0.00	43.4	323	84	[(Meddah *et al* 2014)]
454	302	0	0	0	0	0	53	185	1200	0	670	0.39	0.00	39.5	316	83	[(Meddah *et al* 2014)]
455	266	0	0	0	0	0	89	185	1200	0	670	0.39	0.00	32.6	282	79	[(Meddah *et al* 2014)]
456	231	0	0	0	0	0	124	185	1200	0	670	0.39	0.00	26.1	248	75	[(Meddah *et al* 2014)]
457	195	0	0	0	0	0	160	185	1200	0	670	0.39	0.00	19.1	214	71	[(Meddah *et al* 2014)]
458	355	0	0	0	0	0	0	185	1200	0	625	0.86	0.00	51.2	366	88	[(Meddah *et al* 2014)]
459	349	0	0	0	0	0	62	185	1200	0	625	0.86	0.00	46.5	360	88	[(Meddah *et al* 2014)]
460	308	0	0	0	0	0	103	185	1200	0	625	0.86	0.00	39.1	321	83	[(Meddah *et al* 2014)]
461	267	0	0	0	0	0	144	185	1200	0	625	0.86	0.00	31.3	282	79	[(Meddah *et al* 2014)]
462	226	0	0	0	0	0	185	185	1200	0	625	0.86	0.00	23.4	243	74	[(Meddah *et al* 2014)]

Mix No.	Mixture Composition [kg/m^3]													Comp. Str. [MPa]	CO_2 Footprint [kgCO_2e/m^3]	Mat. Cost [$/m^3]	Ref.
	OPC	FA	GGBS	SF	Meta.	Pozz.	L	Water	C.Agg.	RCA	F.Agg.	SP	AE				
463	118	49	68	0	0	0	0	185	1200	0	700	0.54	0.00	17.8	153	72	[(Meddah *et al* 2014)]
464	118	47	59	12	0	0	0	185	1200	0	700	0.71	0.00	20.0	152	76	[(Meddah *et al* 2014)]
465	118	47	59	0	12	0	0	185	1200	0	700	0.61	0.00	18.7	155	76	[(Meddah *et al* 2014)]
466	112	59	59	0	0	0	6	185	1200	0	700	0.56	0.00	16.1	146	71	[(Meddah *et al* 2014)]
467	143	60	83	0	0	0	0	185	1200	0	730	0.48	0.00	25.2	180	77	[(Meddah *et al* 2014)]
468	143	57	71	14	0	0	0	185	1200	0	730	0.66	0.00	28.2	179	83	[(Meddah *et al* 2014)]
469	143	57	71	0	14	0	0	185	1200	0	730	0.51	0.00	26.9	183	83	[(Meddah *et al* 2014)]
470	135	71	71	0	0	0	7	185	1200	0	730	0.46	0.00	23.4	172	76	[(Meddah *et al* 2014)]
471	155	65	90	0	0	0	0	185	1200	0	710	0.31	0.00	28.7	193	80	[(Meddah *et al* 2014)]
472	155	62	78	15	0	0	0	185	1200	0	710	0.40	0.00	32.1	192	86	[(Meddah *et al* 2014)]
473	155	62	78	0	15	0	0	185	1200	0	710	0.34	0.00	30.4	196	86	[(Meddah *et al* 2014)]
474	147	78	78	0	0	0	8	185	1200	0	710	0.25	0.00	26.1	185	78	[(Meddah *et al* 2014)]
475	178	75	103	0	0	0	0	185	1200	0	670	0.25	0.00	35.2	217	84	[(Meddah *et al* 2014)]
476	178	71	89	17	0	0	0	185	1200	0	670	0.36	0.00	39.1	215	91	[(Meddah *et al* 2014)]
477	178	71	89	0	17	0	0	185	1200	0	670	0.28	0.00	37.3	221	91	[(Meddah *et al* 2014)]
478	169	89	89	0	0	0	9	185	1200	0	670	0.21	0.00	32.1	207	82	[(Meddah *et al* 2014)]
479	205	86	119	0	0	0	0	185	1200	0	625	0.62	0.00	41.3	246	89	[(Meddah *et al* 2014)]
480	205	82	103	20	0	0	0	185	1200	0	625	0.70	0.00	46.9	244	97	[(Meddah *et al* 2014)]
481	205	82	103	0	20	0	0	185	1200	0	625	0.66	0.00	44.7	250	97	[(Meddah *et al* 2014)]
482	195	103	103	0	0	0	10	185	1200	0	625	0.57	0.00	37.8	234	87	[(Meddah *et al* 2014)]
483	235	0	0	0	0	35	0	185	1200	0	700	0.71	0.00	19.1	252	75	[(Seddik Meddah 2015)]
484	235	0	0	0	0	71	0	185	1200	0	700	1.18	0.00	14.8	252	75	[(Seddik Meddah 2015)]
485	235	0	0	0	0	106	0	185	1200	0	700	1.81	0.00	11.3	252	75	[(Seddik Meddah 2015)]
486	285	0	0	0	0	43	0	185	1200	0	730	0.68	0.00	25.6	300	82	[(Seddik Meddah 2015)]
487	285	0	0	0	0	86	0	185	1200	0	730	1.37	0.00	21.7	300	82	[(Seddik Meddah 2015)]
488	285	0	0	0	0	128	0	185	1200	0	730	2.05	0.00	15.6	300	82	[(Seddik Meddah 2015)]
489	310	0	0	0	0	47	0	185	1200	0	710	0.40	0.00	28.7	324	84	[(Seddik Meddah 2015)]
490	310	0	0	0	0	93	0	185	1200	0	710	1.09	0.00	24.8	324	84	[(Seddik Meddah 2015)]
491	310	0	0	0	0	140	0	185	1200	0	710	1.61	0.00	18.7	324	84	[(Seddik Meddah 2015)]

Mix No.	Mixture Composition [kg/m^3]													Comp. Str. [MPa]	CO_2 Footprint [kgCO_2e/m^3]	Mat. Cost [$/m^3]	Ref.
	OPC	FA	GGBS	SF	Meta.	Pozz.	L	Water	C.Agg.	RCA	F.Agg.	SP	AE				
492	355	0	0	0	0	53	0	185	1200	0	670	0.39	0.00	36.0	366	89	[(Seddik Meddah 2015)]
493	355	0	0	0	0	107	0	185	1200	0	670	1.17	0.00	32.1	366	89	[(Seddik Meddah 2015)]
494	355	0	0	0	0	160	0	185	1200	0	670	2.34	0.00	24.8	366	89	[(Seddik Meddah 2015)]
495	410	0	0	0	0	62	0	185	1200	0	625	0.86	0.00	44.7	418	95	[(Seddik Meddah 2015)]
496	410	0	0	0	0	123	0	185	1200	0	625	2.05	0.00	39.1	418	95	[(Seddik Meddah 2015)]
497	410	0	0	0	0	185	0	185	1200	0	625	3.12	0.00	32.1	419	95	[(Seddik Meddah 2015)]
498	235	0	0	0	0	24	0	185	1200	0	700	1.01	0.00	23.0	252	75	[(Seddik Meddah 2015)]
499	235	0	0	0	0	47	0	185	1200	0	700	1.62	0.00	20.0	252	75	[(Seddik Meddah 2015)]
500	235	0	0	0	0	71	0	185	1200	0	700	2.42	0.00	16.9	252	75	[(Seddik Meddah 2015)]
501	235	0	0	0	0	94	0	185	1200	0	700	3.43	0.00	13.9	252	75	[(Seddik Meddah 2015)]
502	285	0	0	0	0	29	0	185	1200	0	730	1.08	0.00	31.3	300	82	[(Seddik Meddah 2015)]
503	285	0	0	0	0	57	0	185	1200	0	730	1.77	0.00	27.8	300	82	[(Seddik Meddah 2015)]
504	285	0	0	0	0	86	0	185	1200	0	730	2.99	0.00	23.4	300	82	[(Seddik Meddah 2015)]
505	285	0	0	0	0	114	0	185	1200	0	730	4.08	0.00	20.0	300	82	[(Seddik Meddah 2015)]
506	310	0	0	0	0	31	0	185	1200	0	710	1.09	0.00	34.7	324	84	[(Seddik Meddah 2015)]
507	310	0	0	0	0	62	0	185	1200	0	710	2.14	0.00	30.8	324	84	[(Seddik Meddah 2015)]
508	310	0	0	0	0	93	0	185	1200	0	710	2.95	0.00	26.5	324	84	[(Seddik Meddah 2015)]
509	310	0	0	0	0	124	0	185	1200	0	710	4.03	0.00	23.0	324	84	[(Seddik Meddah 2015)]
510	355	0	0	0	0	36	0	185	1200	0	670	1.38	0.00	42.6	366	89	[(Seddik Meddah 2015)]
511	355	0	0	0	0	71	0	185	1200	0	670	2.41	0.00	38.6	366	89	[(Seddik Meddah 2015)]
512	355	0	0	0	0	107	0	185	1200	0	670	4.47	0.00	33.4	366	89	[(Seddik Meddah 2015)]
513	355	0	0	0	0	142	0	185	1200	0	670	5.08	0.00	29.1	366	89	[(Seddik Meddah 2015)]
514	410	0	0	0	0	41	0	185	1200	0	625	1.72	0.00	49.9	418	95	[(Seddik Meddah 2015)]
515	410	0	0	0	0	82	0	185	1200	0	625	2.91	0.00	46.5	418	95	[(Seddik Meddah 2015)]
516	410	0	0	0	0	123	0	185	1200	0	625	5.17	0.00	40.8	418	95	[(Seddik Meddah 2015)]
517	410	0	0	0	0	164	0	185	1200	0	625	6.56	0.00	35.6	419	95	[(Seddik Meddah 2015)]
518	200	0	0	0	0	0	0	200	1060	0	846	0.00	0.00	11.3	219	71	[(Hedegaard and Hansen 1992)]
519	273	0	0	0	0	0	0	195	1116	0	732	0.00	0.00	22.9	288	79	[(Hedegaard and Hansen 1992)]
520	351	0	0	0	0	0	0	195	1147	0	670	0.00	0.00	32.9	362	88	[(Hedegaard and Hansen 1992)]

Mix No.	Mixture Composition [kg/m^3]													Comp. Str. [MPa]	CO_2 Footprint [kgCO_2e/m^3]	Mat. Cost [$/m^3]	Ref.
	OPC	FA	GGBS	SF	Meta.	Pozz.	L	Water	C.Agg.	RCA	F.Agg.	SP	AE				
521	425	0	0	0	0	0	0	193	1122	0	607	0.00	0.00	41.7	432	95	[(Hedegaard and Hansen 1992)]
522	507	0	0	0	0	0	0	195	1096	0	565	0.00	0.00	52.3	509	104	[(Hedegaard and Hansen 1992)]
523	35	282	0	0	0	0	0	176	1160	0	606	1.33	0.00	1.3	74	71	[(Hedegaard and Hansen 1992)]
524	36	360	0	0	0	0	0	180	1115	0	547	1.35	0.00	2.2	77	75	[(Hedegaard and Hansen 1992)]
525	106	141	0	0	0	0	0	176	1180	0	696	0.00	0.00	7.1	136	70	[(Hedegaard and Hansen 1992)]
526	106	211	0	0	0	0	0	176	1168	0	624	0.00	0.00	7.8	138	74	[(Hedegaard and Hansen 1992)]
527	108	288	0	0	0	0	0	180	1126	0	562	1.27	0.00	10.3	143	79	[(Hedegaard and Hansen 1992)]
528	106	352	0	0	0	0	0	176	1099	0	524	3.34	0.00	8.6	143	83	[(Hedegaard and Hansen 1992)]
529	180	72	0	0	0	0	0	180	1166	0	721	0.00	0.00	14.7	203	74	[(Hedegaard and Hansen 1992)]
530	176	141	0	0	0	0	0	176	1191	0	650	0.00	0.00	20.4	202	78	[(Hedegaard and Hansen 1992)]
531	180	216	0	0	0	0	0	180	1136	0	577	0.00	0.00	21.6	208	82	[(Hedegaard and Hansen 1992)]
532	180	288	0	0	0	0	0	180	1097	0	531	2.11	0.00	20.2	211	87	[(Hedegaard and Hansen 1992)]
533	180	360	0	0	0	0	0	180	1052	0	490	3.83	0.00	23.6	214	91	[(Hedegaard and Hansen 1992)]
534	246	70	0	0	0	0	0	176	1174	0	660	0.00	0.00	27.8	265	81	[(Hedegaard and Hansen 1992)]
535	252	144	0	0	0	0	0	180	1147	0	593	0.00	0.00	27.1	274	86	[(Hedegaard and Hansen 1992)]
536	252	216	0	0	0	0	0	180	1110	0	544	1.68	0.00	30.0	276	90	[(Hedegaard and Hansen 1992)]
537	246	282	0	0	0	0	0	176	1082	0	509	4.17	0.00	26.2	273	93	[(Hedegaard and Hansen 1992)]
538	252	360	0	0	0	0	0	180	1017	0	465	7.16	0.00	37.6	282	98	[(Hedegaard and Hansen 1992)]
539	324	72	0	0	0	0	0	180	1155	0	611	0.99	0.00	40.8	339	89	[(Hedegaard and Hansen 1992)]
540	324	144	0	0	0	0	0	180	1122	0	558	2.06	0.00	38.3	342	94	[(Hedegaard and Hansen 1992)]
541	317	211	0	0	0	0	0	176	1096	0	520	3.64	0.00	50.0	338	97	[(Hedegaard and Hansen 1992)]
542	317	282	0	0	0	0	0	176	1048	0	484	7.97	0.00	43.1	340	101	[(Hedegaard and Hansen 1992)]
543	396	72	0	0	0	0	0	180	1135	0	572	2.62	0.00	45.3	407	97	[(Hedegaard and Hansen 1992)]
544	387	141	0	0	0	0	0	176	1108	0	534	3.85	0.00	45.7	401	100	[(Hedegaard and Hansen 1992)]
545	34	270	0	0	0	0	0	169	1189	0	621	0.00	0.00	3.3	73	71	[(Hedegaard and Hansen 1992)]
546	33	330	0	0	0	0	0	165	1170	0	579	0.00	0.00	2.3	74	74	[(Hedegaard and Hansen 1992)]
547	108	144	0	0	0	0	0	180	1169	0	696	0.00	0.00	12.4	138	71	[(Hedegaard and Hansen 1992)]
548	106	211	0	0	0	0	0	176	1171	0	628	0.00	0.00	9.7	138	75	[(Hedegaard and Hansen 1992)]
549	106	282	0	0	0	0	0	176	1143	0	573	0.50	0.00	9.7	141	79	[(Hedegaard and Hansen 1992)]

Mix No.	Mixture Composition [kg/m^3]													Comp. Str. [MPa]	CO_2 Footprint [kgCO_2e/m^3]	Mat. Cost [$/m^3]	Ref.
	OPC	FA	GGBS	SF	Meta.	Pozz.	L	Water	C.Agg.	RCA	F.Agg.	SP	AE				
550	106	352	0	0	0	0	0	176	1416	0	679	2.89	0.00	6.4	149	90	[(Hedegaard and Hansen 1992)]
551	176	70	0	0	0	0	0	176	1169	0	725	0.00	0.00	22.5	199	73	[(Hedegaard and Hansen 1992)]
552	176	141	0	0	0	0	0	176	1177	0	645	0.00	0.00	21.6	202	78	[(Hedegaard and Hansen 1992)]
553	180	216	0	0	0	0	0	180	1139	0	582	0.00	0.00	20.8	208	83	[(Hedegaard and Hansen 1992)]
554	176	282	0	0	0	0	0	176	1116	0	542	0.92	0.00	16.9	207	86	[(Hedegaard and Hansen 1992)]
555	176	352	0	0	0	0	0	176	1073	0	503	2.32	0.00	19.2	210	90	[(Hedegaard and Hansen 1992)]
556	252	72	0	0	0	0	0	180	1170	0	658	0.00	0.00	34.7	271	82	[(Hedegaard and Hansen 1992)]
557	246	141	0	0	0	0	0	176	1160	0	603	0.00	0.00	31.6	268	85	[(Hedegaard and Hansen 1992)]
558	246	211	0	0	0	0	0	176	1128	0	553	1.28	0.00	31.3	271	89	[(Hedegaard and Hansen 1992)]
559	246	282	0	0	0	0	0	176	1086	0	513	2.69	0.00	27.7	273	94	[(Hedegaard and Hansen 1992)]
560	246	352	0	0	0	0	0	176	1040	0	478	4.43	0.00	28.8	276	98	[(Hedegaard and Hansen 1992)]
561	317	70	0	0	0	0	0	176	1168	0	618	0.54	0.00	47.0	333	89	[(Hedegaard and Hansen 1992)]
562	317	141	0	0	0	0	0	176	1133	0	563	2.02	0.00	42.1	335	93	[(Hedegaard and Hansen 1992)]
563	317	211	0	0	0	0	0	176	1099	0	524	3.22	0.00	39.2	338	97	[(Hedegaard and Hansen 1992)]
564	317	282	0	0	0	0	0	176	1054	0	487	6.65	0.00	36.9	340	101	[(Hedegaard and Hansen 1992)]
565	387	70	0	0	0	0	0	176	1147	0	581	2.15	0.00	45.0	399	96	[(Hedegaard and Hansen 1992)]
566	387	141	0	0	0	0	0	176	1111	0	535	2.32	0.00	45.0	401	100	[(Hedegaard and Hansen 1992)]
567	330	0	0	0	0	0	0	198	963	0	788	0.00	0.00	31.9	341	84	[(Han *et al* 2003)]
568	297	33	0	0	0	0	0	198	955	0	781	0.00	0.00	32.7	311	83	[(Han *et al* 2003)]
569	264	66	0	0	0	0	0	198	947	0	775	0.00	0.00	27.1	281	81	[(Han *et al* 2003)]
570	231	99	0	0	0	0	0	198	938	0	768	0.00	0.00	24.2	251	79	[(Han *et al* 2003)]
571	350	0	0	0	0	0	0	193	962	0	787	0.00	0.00	35.0	360	87	[(Han *et al* 2003)]
572	315	35	0	0	0	0	0	193	953	0	780	0.00	0.00	37.1	328	85	[(Han *et al* 2003)]
573	280	70	0	0	0	0	0	193	945	0	773	0.00	0.00	32.7	296	83	[(Han *et al* 2003)]
574	254	100	0	0	0	0	0	193	936	0	766	0.00	0.00	29.9	273	82	[(Han *et al* 2003)]
575	420	0	0	0	0	0	0	168	1054	0	703	5.04	0.00	48.1	427	95	[(Han *et al* 2003)]
576	378	42	0	0	0	0	0	168	1044	0	696	5.04	0.00	48.7	389	93	[(Han *et al* 2003)]
577	336	84	0	0	0	0	0	168	1032	0	688	6.30	0.00	46.5	351	91	[(Han *et al* 2003)]
578	294	126	0	0	0	0	0	168	1020	0	680	7.14	0.00	41.4	312	89	[(Han *et al* 2003)]

Mix No.	Mixture Composition [kg/m^3]													Comp. Str. [MPa]	CO_2 Footprint [kgCO_2e/m^3]	Mat. Cost [$/m^3]	Ref.
	OPC	FA	GGBS	SF	Meta.	Pozz.	L	Water	C.Agg.	RCA	F.Agg.	SP	AE				
579	480	0	0	0	0	0	0	168	1025	0	683	7.20	0.00	54.5	484	101	[(Han *et al* 2003)]
580	432	48	0	0	0	0	0	168	1012	0	675	7.20	0.00	53.9	440	99	[(Han *et al* 2003)]
581	384	96	0	0	0	0	0	168	999	0	666	7.20	0.00	54.2	397	97	[(Han *et al* 2003)]
582	336	144	0	0	0	0	0	168	986	0	657	8.64	0.00	50.2	353	94	[(Han *et al* 2003)]
583	520	0	0	0	0	0	0	166	1042	0	638	9.36	0.00	60.1	522	106	[(Han *et al* 2003)]
584	468	52	0	0	0	0	0	166	1027	0	629	9.36	0.00	59.8	474	103	[(Han *et al* 2003)]
585	416	104	0	0	0	0	0	166	1013	0	621	10.40	0.00	56.8	427	101	[(Han *et al* 2003)]
586	364	156	0	0	0	0	0	166	998	0	612	11.96	0.00	42.8	380	98	[(Han *et al* 2003)]
587	600	0	0	0	0	0	0	162	1056	0	569	12.00	0.00	69.5	598	115	[(Han *et al* 2003)]
588	540	60	0	0	0	0	0	162	1039	0	560	12.00	0.00	65.6	543	112	[(Han *et al* 2003)]
589	480	120	0	0	0	0	0	162	1022	0	550	13.80	0.00	62.9	488	109	[(Han *et al* 2003)]
590	420	180	0	0	0	0	0	162	1005	0	541	18.00	0.00	50.3	434	106	[(Han *et al* 2003)]
591	289	0	0	0	0	0	32	124	1053	0	818	0.00	0.00	48.4	303	81	[(Shannon *et al* 2017)]
592	294	0	0	0	0	0	27	126	1053	0	814	0.00	0.00	52.8	308	82	[(Shannon *et al* 2017)]
593	288	0	0	0	0	0	33	124	1053	0	814	0.00	0.00	38.3	302	81	[(Shannon *et al* 2017)]
594	279	0	0	0	0	0	42	120	1053	0	814	0.00	0.00	46.2	294	80	[(Shannon *et al* 2017)]
595	86	32	192	0	0	0	10	133	1112	0	732	0.00	0.00	38.7	141	78	[(Shannon *et al* 2017)]
596	88	32	192	0	0	0	8	134	1112	0	730	0.00	0.00	27.8	143	78	[(Shannon *et al* 2017)]
597	86	32	192	0	0	0	10	133	1112	0	730	0.00	0.00	39.6	141	78	[(Shannon *et al* 2017)]
598	84	32	192	0	0	0	12	132	1112	0	730	0.00	0.00	41.5	139	77	[(Shannon *et al* 2017)]
599	86	64	160	0	0	0	10	133	1112	0	729	0.00	0.00	42.6	138	77	[(Shannon *et al* 2017)]
600	88	64	160	0	0	0	8	134	1112	0	727	0.00	0.00	33.5	139	77	[(Shannon *et al* 2017)]
601	86	64	160	0	0	0	10	133	1112	0	727	0.00	0.00	30.4	138	77	[(Shannon *et al* 2017)]
602	84	64	160	0	0	0	12	132	1112	0	728	0.00	0.00	41.5	135	77	[(Shannon *et al* 2017)]
603	86	96	128	0	0	0	10	143	1112	0	706	0.00	0.00	28.0	134	76	[(Shannon *et al* 2017)]
604	88	96	128	0	0	0	8	143	1112	0	705	0.00	0.00	26.9	136	76	[(Shannon *et al* 2017)]
605	86	96	128	0	0	0	10	143	1112	0	705	0.00	0.00	23.6	134	76	[(Shannon *et al* 2017)]
606	84	96	128	0	0	0	12	141	1112	0	705	0.00	0.00	30.0	131	76	[(Shannon *et al* 2017)]
607	144	32	128	0	0	0	16	131	1053	0	803	0.00	0.00	37.6	187	79	[(Shannon *et al* 2017)]

Mix No.	Mixture Composition [kg/m^3]													Comp. Str. [MPa]	CO_2 Footprint [kgCO_2e/m^3]	Mat. Cost [$/m^3]	Ref.
	OPC	FA	GGBS	SF	Meta.	Pozz.	L	Water	C.Agg.	RCA	F.Agg.	SP	AE				
608	146	32	128	0	0	0	14	132	1053	0	802	0.00	0.00	49.1	189	79	[(Shannon *et al* 2017)]
609	144	32	128	0	0	0	16	131	1053	0	802	0.00	0.00	46.9	186	78	[(Shannon *et al* 2017)]
610	139	32	128	0	0	0	21	129	1053	0	802	0.00	0.00	42.9	182	78	[(Shannon *et al* 2017)]
611	144	64	96	0	0	0	16	131	1053	0	801	0.00	0.00	32.8	183	78	[(Shannon *et al* 2017)]
612	146	64	96	0	0	0	14	132	1053	0	799	0.00	0.00	49.7	185	78	[(Shannon *et al* 2017)]
613	144	64	96	0	0	0	16	131	1053	0	799	0.00	0.00	46.0	183	78	[(Shannon *et al* 2017)]
614	139	64	96	0	0	0	21	129	1053	0	752	0.00	0.00	45.1	178	77	[(Shannon *et al* 2017)]
615	144	80	80	0	0	0	16	131	1053	0	800	0.00	0.00	30.6	181	78	[(Shannon *et al* 2017)]
616	146	80	80	0	0	0	14	132	1053	0	797	0.00	0.00	48.2	184	78	[(Shannon *et al* 2017)]
617	144	80	80	0	0	0	16	131	1053	0	797	0.00	0.00	40.9	181	77	[(Shannon *et al* 2017)]
618	139	80	80	0	0	0	21	129	1053	0	797	0.00	0.00	40.3	177	77	[(Shannon *et al* 2017)]
619	115	64	128	0	0	0	13	132	1053	0	799	0.00	0.00	33.9	161	77	[(Shannon *et al* 2017)]
620	117	64	128	0	0	0	11	133	1053	0	797	0.00	0.00	40.0	162	78	[(Shannon *et al* 2017)]
621	115	96	96	0	0	0	13	132	1053	0	796	0.00	0.00	32.8	157	77	[(Shannon *et al* 2017)]
622	117	96	96	0	0	0	11	133	1053	0	794	0.00	0.00	33.5	159	77	[(Shannon *et al* 2017)]
623	115	32	160	0	0	0	13	132	1053	0	801	0.00	0.00	32.4	164	78	[(Shannon *et al* 2017)]
624	117	32	160	0	0	0	11	133	1053	0	799	0.00	0.00	42.0	166	78	[(Shannon *et al* 2017)]
625	289	0	0	0	0	0	32	124	1098	0	860	0.00	0.00	47.4	304	83	[(Shannon *et al* 2017)]
626	294	0	0	0	0	0	27	126	1098	0	856	0.00	0.00	45.3	309	83	[(Shannon *et al* 2017)]
627	279	0	0	0	0	0	42	120	1098	0	856	0.00	0.00	49.2	295	82	[(Shannon *et al* 2017)]
628	86	64	160	0	0	0	10	133	1112	0	818	0.00	0.00	37.7	139	78	[(Shannon *et al* 2017)]
629	88	64	160	0	0	0	8	134	1112	0	817	0.00	0.00	46.0	140	79	[(Shannon *et al* 2017)]
630	84	64	160	0	0	0	12	132	1112	0	817	0.00	0.00	47.1	136	78	[(Shannon *et al* 2017)]
631	144	64	96	0	0	0	16	131	1098	0	843	0.00	0.00	42.4	184	79	[(Shannon *et al* 2017)]
632	146	64	96	0	0	0	14	132	1098	0	841	0.00	0.00	53.5	186	80	[(Shannon *et al* 2017)]
633	139	64	96	0	0	0	21	129	1098	0	841	0.00	0.00	49.2	180	79	[(Shannon *et al* 2017)]
634	340	0	0	0	0	0	0	160	1702	0	798	0.00	0.00	34.9	360	98	[(Moon *et al* 2017)]
635	288	0	0	0	0	0	52	160	1702	0	798	0.00	0.00	36.1	310	92	[(Moon *et al* 2017)]
636	255	0	0	0	0	0	85	160	1702	0	798	0.00	0.00	32.2	279	88	[(Moon *et al* 2017)]

Mix No.	Mixture Composition [kg/m^3]													Comp. Str. [MPa]	CO_2 Footprint [kgCO_2e/m^3]	Mat. Cost [$/m^3]	Ref.
	OPC	FA	GGBS	SF	Meta.	Pozz.	L	Water	C.Agg.	RCA	F.Agg.	SP	AE				
637	221	0	0	0	0	0	119	160	1702	0	798	0.00	0.00	29.7	246	84	[(Moon *et al* 2017)]
638	288	0	0	0	0	0	52	160	1702	0	798	0.00	0.00	36.6	310	92	[(Moon *et al* 2017)]
639	221	0	0	0	0	0	119	160	1702	0	798	0.00	0.00	32.9	246	84	[(Moon *et al* 2017)]
640	288	0	0	0	0	0	52	160	1702	0	798	0.00	0.00	41.7	310	92	[(Moon *et al* 2017)]
641	221	0	0	0	0	0	119	160	1702	0	798	0.00	0.00	34.6	246	84	[(Moon *et al* 2017)]
642	303	106	0	0	0	0	16	170	1050	0	760	0.00	0.00	50.0	322	90	[(Mohammadi and South 2016)]
643	303	106	0	0	0	0	16	170	1050	0	760	0.00	0.00	50.0	322	90	[(Mohammadi and South 2016)]
644	318	112	0	0	0	0	17	178	1039	0	687	0.00	0.00	50.0	335	91	[(Mohammadi and South 2016)]
645	318	112	0	0	0	0	17	178	1039	0	687	0.00	0.00	50.0	335	91	[(Mohammadi and South 2016)]
646	295	106	0	0	0	0	24	170	1050	0	760	0.00	0.00	51.2	314	89	[(Mohammadi and South 2016)]
647	295	106	0	0	0	0	24	170	1050	0	760	0.00	0.00	51.2	314	89	[(Mohammadi and South 2016)]
648	310	112	0	0	0	0	25	178	1039	0	687	0.00	0.00	51.2	327	90	[(Mohammadi and South 2016)]
649	310	112	0	0	0	0	25	178	1039	0	687	0.00	0.00	51.2	327	90	[(Mohammadi and South 2016)]
650	287	106	0	0	0	0	32	170	1050	0	760	0.00	0.00	48.9	306	88	[(Mohammadi and South 2016)]
651	287	106	0	0	0	0	32	170	1050	0	760	0.00	0.00	48.9	306	88	[(Mohammadi and South 2016)]
652	302	112	0	0	0	0	34	178	1039	0	687	0.00	0.00	48.9	319	89	[(Mohammadi and South 2016)]
653	302	112	0	0	0	0	34	178	1039	0	687	0.00	0.00	48.9	319	89	[(Mohammadi and South 2016)]
654	281	106	0	0	0	0	38	170	1050	0	760	0.00	0.00	45.9	300	88	[(Mohammadi and South 2016)]
655	281	106	0	0	0	0	38	170	1050	0	760	0.00	0.00	45.9	300	88	[(Mohammadi and South 2016)]
656	295	112	0	0	0	0	40	178	1039	0	687	0.00	0.00	45.9	313	88	[(Mohammadi and South 2016)]
657	295	112	0	0	0	0	40	178	1039	0	687	0.00	0.00	45.9	313	88	[(Mohammadi and South 2016)]
658	222	106	85	0	0	0	12	170	1050	0	760	0.00	0.00	50.0	258	89	[(Mohammadi and South 2016)]
659	222	106	85	0	0	0	12	170	1050	0	760	0.00	0.00	40.0	258	89	[(Mohammadi and South 2016)]
660	215	90	135	0	0	0	11	177	1033	0	683	0.00	0.00	50.0	256	90	[(Mohammadi and South 2016)]
661	215	90	135	0	0	0	11	177	1033	0	683	0.00	0.00	50.0	256	90	[(Mohammadi and South 2016)]
662	216	106	85	0	0	0	18	170	1050	0	760	0.00	0.00	50.3	252	88	[(Mohammadi and South 2016)]
663	216	106	85	0	0	0	18	170	1050	0	760	0.00	0.00	40.2	252	88	[(Mohammadi and South 2016)]
664	209	90	135	0	0	0	17	177	1033	0	683	0.00	0.00	50.3	251	89	[(Mohammadi and South 2016)]
665	209	90	135	0	0	0	17	177	1033	0	683	0.00	0.00	50.3	251	89	[(Mohammadi and South 2016)]

Mix No.	Mixture Composition [kg/m^3]													Comp. Str. [MPa]	CO_2 Footprint [kgCO_2e/m^3]	Mat. Cost [$/m^3]	Ref.
	OPC	FA	GGBS	SF	Meta.	Pozz.	L	Water	C.Agg.	RCA	F.Agg.	SP	AE				
666	211	106	85	0	0	0	23	170	1050	0	760	0.00	0.00	50.1	247	87	[(Mohammadi and South 2016)]
667	211	106	85	0	0	0	23	170	1050	0	760	0.00	0.00	40.1	247	87	[(Mohammadi and South 2016)]
668	203	90	135	0	0	0	23	177	1033	0	683	0.00	0.00	50.1	246	89	[(Mohammadi and South 2016)]
669	203	90	135	0	0	0	23	177	1033	0	683	0.00	0.00	50.1	246	89	[(Mohammadi and South 2016)]
670	206	106	85	0	0	0	28	170	1050	0	760	0.00	0.00	48.0	242	87	[(Mohammadi and South 2016)]
671	206	106	85	0	0	0	28	170	1050	0	760	0.00	0.00	38.4	242	87	[(Mohammadi and South 2016)]
672	199	90	135	0	0	0	27	177	1033	0	683	0.00	0.00	48.0	241	88	[(Mohammadi and South 2016)]
673	199	90	135	0	0	0	27	177	1033	0	683	0.00	0.00	48.0	241	88	[(Mohammadi and South 2016)]
674	150	0	295	0	0	0	8	178	1036	0	704	0.00	0.00	50.0	216	91	[(Mohammadi and South 2016)]
675	150	0	295	0	0	0	8	178	1036	0	704	0.00	0.00	50.0	216	91	[(Mohammadi and South 2016)]
676	142	0	295	0	0	0	16	178	1036	0	704	0.00	0.00	51.9	208	90	[(Mohammadi and South 2016)]
677	142	0	295	0	0	0	16	178	1036	0	704	0.00	0.00	51.9	208	90	[(Mohammadi and South 2016)]
678	139	0	295	0	0	0	19	178	1036	0	704	0.00	0.00	50.6	205	90	[(Mohammadi and South 2016)]
679	139	0	295	0	0	0	19	178	1036	0	704	0.00	0.00	50.6	205	90	[(Mohammadi and South 2016)]
680	291	106	0	0	0	0	15	170	1050	0	760	0.00	0.00	50.0	310	89	[(Mohammadi and South 2016)]
681	291	106	0	0	0	0	15	170	1050	0	760	0.00	0.00	50.0	310	89	[(Mohammadi and South 2016)]
682	283	106	0	0	0	0	23	170	1050	0	760	0.00	0.00	47.2	302	88	[(Mohammadi and South 2016)]
683	283	106	0	0	0	0	23	170	1050	0	760	0.00	0.00	47.2	302	88	[(Mohammadi and South 2016)]
684	275	106	0	0	0	0	31	170	1050	0	760	0.00	0.00	45.5	295	87	[(Mohammadi and South 2016)]
685	275	106	0	0	0	0	31	170	1050	0	760	0.00	0.00	45.5	295	87	[(Mohammadi and South 2016)]
686	269	106	0	0	0	0	37	170	1050	0	760	0.00	0.00	45.2	289	86	[(Mohammadi and South 2016)]
687	269	106	0	0	0	0	37	170	1050	0	760	0.00	0.00	45.2	289	86	[(Mohammadi and South 2016)]
688	311	91	0	0	0	0	16	179	1040	0	681	0.00	0.00	40.0	327	89	[(Mohammadi and South 2016)]
689	311	91	0	0	0	0	16	179	1040	0	681	0.00	0.00	65.0	327	89	[(Mohammadi and South 2016)]
690	311	91	0	0	0	0	16	179	1040	0	681	0.00	0.00	65.0	327	89	[(Mohammadi and South 2016)]
691	294	91	0	0	0	0	33	179	1040	0	681	0.00	0.00	38.1	311	87	[(Mohammadi and South 2016)]
692	294	91	0	0	0	0	33	179	1040	0	681	0.00	0.00	40.2	311	87	[(Mohammadi and South 2016)]
693	294	91	0	0	0	0	33	179	1040	0	681	0.00	0.00	61.9	311	87	[(Mohammadi and South 2016)]
694	288	91	0	0	0	0	39	179	1040	0	681	0.00	0.00	65.4	305	86	[(Mohammadi and South 2016)]

Mix No.	Mixture Composition [kg/m^3]													Comp. Str. [MPa]	CO_2 Footprint [kgCO_2e/m^3]	Mat. Cost [$/m^3]	Ref.
	OPC	FA	GGBS	SF	Meta.	Pozz.	L	Water	C.Agg.	RCA	F.Agg.	SP	AE				
695	288	91	0	0	0	0	39	179	1040	0	681	0.00	0.00	61.9	305	86	[(Mohammadi and South 2016)]
696	288	91	0	0	0	0	39	179	1040	0	681	0.00	0.00	65.4	305	86	[(Mohammadi and South 2016)]

REFERENCES

Ahmad A 2015 IBISWorld Industry Report 32739 Precast Concrete Manufacturing in the US

American Coal Ash Association 2016 Coal Ash Recycling Reaches Record 56 Percent Amid Shifting Production and Use Patterns Online: https://www.acaa-usa.org/Portals/9/Files/PDFs/2016-Survey-Results.pdf

Anon CarbonCure Online: https://www.carboncure.com/

Athena 2005 Cement and Structural Concrete Products: Life Cycle Inventory Update #2 Online: https://calculatelca.com/wp-content/themes/athenasmisoftware/images/LCA Reports/Cement_And_Structural_Concrete.pdf

Bains P, Psarras P and Wilcox J 2017 CO_2 capture from the industry sector Prog. Energy Combust. Sci. **63** 146–72

Behera M, Bhattacharyya S K, Minocha A K, Deoliya R and Maiti S 2014 Recycled aggregate from C&D waste & its use in concrete – A breakthrough towards sustainability in construction sector: A review Constr. Build. Mater. **68** 501–16 Online: http://dx.doi.org/10.1016/j.conbuildmat.2014.07.003

Bilim C, Atiş C D, Tanyildizi H and Karahan O 2009 Predicting the compressive strength of ground granulated blast furnace slag concrete using artificial neural network Adv. Eng. Softw. **40** 334–40

Black & Veatch 2016 Largest cities rate survey 2016 Online: https://www.financingsustainablewater.org/resource-search/50-largest-cities-rate-survey-2016

Bouzoubaa N, Zhang M H and Malhotra V M 2001 Mechanical properties and durability of concrete made with high-volume fly ash blended cements using a coarse fly ash Cem. Concr. Res. **31** 1393–402 Online: http://www.sciencedirect.com/science/article/B6TWG-445GDD3-2/2/08625b87cca89be3f1658eae31460569

Bushi L and Meil J 2014 An Environmental Life Cycle Assessment of Portland Limestone and Ordinary Portland Cements in Concrete J. Clean. Prod. **73** 1–10 Online: 10.1016/j.jclepro.2013.10.044%5Cnhttp://search.ebscohost.com/login.aspx?direct=true&db=bth&AN=96186882&site=ehost-live

Celik K, Meral C, Petek Gursel A, Mehta P K, Horvath A and Monteiro P J M 2015 Mechanical properties, durability, and life-cycle assessment of self-consolidating concrete mixtures made with blended portland cements containing fly ash and limestone powder Cem. Concr. Compos. **56** 59–72 Online: http://dx.doi.org/10.1016/j.cemconcomp.2014.11.003

Einsfeld R A and Velasco M S L 2006 Fracture parameters for high-performance concrete Cem. Concr. Res. **36** 576–83

El-Hassan H and Shao Y 2014a Carbon Storage through Concrete Block Carbonation J. Clean Energy Technol. **2** 287–91 Online: http://www.jocet.org/index.php?m=content&c=index&a=show&catid=34&id=414

El-Hassan H and Shao Y 2014b Dynamic carbonation curing of fresh lightweight concrete Mag. Concr. Res. **66** 708–18 Online: http://www.icevirtuallibrary.com/doi/10.1680/macr.13.00222

El-Hassan H, Shao Y and Ghouleh Z 2013 Reaction Products in Carbonation-Cured Lightweight Concrete J. Mater. Civ. Eng. **25** 799–809 Online: http://ascelibrary.org/doi/10.1061/%28ASCE%29MT.1943-5533.0000638

European Ready Mixed Concrete Organization 2016 Ready-mixed concrete industry statistics year 2015

European Ready Mixed Concrete Organization 2018 Ready-mixed concrete industry statistics Year 2017 Online: https://mediatheque.snbpe.org/userfiles/file/ERMCO Statistics 2017 V3 19_07_18.pdf

Evangelista L and De Brito J 2014 Concrete with fine recycled aggregates: A review Eur. J. Environ. Civ. Eng. **18** 129–72

Felekoğlu B, Türkel S and Baradan B 2007 Effect of water/cement ratio on the fresh and hardened properties of self-compacting concrete Build. Environ. **42** 1795–802

Goonan T G 2000 Recycled Aggregates — Profitable Resource Conservation. U.S. Geological Survey Circular Online: https://pubs.usgs.gov/fs/fs-0181-99/fs-0181-99so.pdf

Griffiths-sattenspiel B and Wilson W The Carbon Footprint of Water | River Network Online: http://www.rivernetwork.org/resource-library/carbon-footprint-water

Han S H, Kim J K and Park Y D 2003 Prediction of compressive strength of fly ash concrete by new apparent activation energy function Cem. Concr. Res. **33** 965–71

Haque M N and Kayali O 1998 Properties of High-Strength Concrete Using a Fine Fly Ash Cem. Concr. Res. **28** 1445–52

Heath A, Paine K and McManus M 2014 Minimising the global warming potential of clay based geopolymers J. Clean. Prod. **78** 75–83 Online: http://dx.doi.org/10.1016/j.jclepro.2014.04.046

Hedegaard S E and Hansen T C 1992 Modified water/cement ratio law for compressive strength of fly ash concretes Mater. Struct. **25** 273–83

Jones R, Mccarthy M and Newlands M 2011 Fly Ash Route to Low Embodied CO_2 and Implications for Concrete Construction World Coal Ash Conf.

Kashef-Haghighi S, Shao Y and Ghoshal S 2015 Mathematical modeling of CO_2 uptake by concrete during accelerated carbonation curing Cem. Concr. Res. **67** 1–10 Online: http://dx.doi.org/10.1016/j.cemconres.2014.07.020

Kou S C, Zhan B J and Poon C S 2014 Use of a CO_2 curing step to improve the properties of concrete prepared with recycled aggregates Cem. Concr. Compos. **45** 22–8 Online: http://dx.doi.org/10.1016/j.cemconcomp.2013.09.008

Lam L, Wong Y L and Poon C S 1997 Effect of Fly Ash and Silica Fume On Compressive and Fracture Behaviors of Concrete Cem. Concr. Res. **28** 271–83

Lee J, Song H, Kim B, Song T and Seo C 2016 The application of CO_2 in the curing process of cement brick products J. Ceram. Process. Res. **17** 17–25 Online: http://jcpr.kbs-lab.co.kr/file/JCPR_vol.17_2016/JCPR17-1/04.2015-030_17-25.pdf

Liu R, Durham S A, Rens K L and Ramaswami A 2012 Optimization of Cementitious Material Content for Sustainable Concrete Mixtures J. Mater. Civ. Eng. **24** 745–53 Online: http://ascelibrary.org/doi/10.1061/%28ASCE%29MT.1943-5533.0000444

Luckow P, Stanton E A, Fields S, Ong W, Biewald B, Jackson S and Fisher J 2016 Spring 2016 National Carbon Dioxide Price Forecast Synap. Energy Econ. 1–35 Online: http://www.synapse-energy.com/sites/default/files/2016-Synapse-CO_2-Price-Forecast-66-008.pdf

Maddalena R, Roberts J J and Hamilton A 2018 Can Portland cement be replaced by low-carbon alternative materials? A study on the thermal properties and carbon emissions of innovative cements J. Clean. Prod. **186** 933–42 Online: https://doi.org/10.1016/j.jclepro.2018.02.138

Marceau M L, Gajda J, Vangeem M G and Nisbet M A 2002 Partial Environmental Life Cycle Inventory of an Insulating Concrete Form House Compared to a Wood Frame House Online: https://www.nrmca.org/taskforce/Item_2_TalkingPoints/Sustainability/Sustainability/SN2464.pdf

Marceau M L, Nisbet M a and Vangeem M G 2006 Life Cycle Inventory of Portland Cement Concrete Manufacture Online: https://www.nrmca.org/taskforce/Item_2_TalkingPoints/Sustainability/Sustainability/SN2095b - Cement LCI 2006.pdf

Marceau M L, Nisbet M A and Vangeem M G 2007 Life Cycle Inventory of Portland Cement Concrete

McEwen L 2018 Environmental Product Declaration-KANGLEY ROCK & RECYCLING Online: https://www.astm.org/CERTIFICATION/DOCS/384.EPD_Kangley_Rock__Recycling_final_-Feb-21-2018.pdf

McEwen L 2017a Environmental product declaration-Martin Marietta Online: https://www.astm.org/CERTIFICATION/DOCS/359.EPD_for_Martin_Marietta_EPD_final.pdf

McEwen L 2017b Environmental Product Declaration-Polaris Materials Corporation Online: https://www.astm.org/CERTIFICATION/DOCS/344.EPD_Polaris_Materials_final.pdf

McEwen L 2017c Environmental Product Declaration-Vulcan Materials Company Online: https://www.vulcanmaterials.com/docs/default-source/default-document-library/pleasanton-epd_final

Meddah M S, Lmbachiya M C and Dhir R K 2014 Potential use of binary and composite limestone cements in concrete production Constr. Build. Mater. **58** 193–205 Online: http://dx.doi.org/10.1016/j.conbuildmat.2013.12.012

Mehta P and Aïtcin P C 1990 Principles Underlying Production of High-Performance Concrete Cem. Concr. Aggregates **12** 70

Miller S A 2018 Supplementary cementitious materials to mitigate greenhouse gas emissions from concrete: can there be too much of a good thing? J. Clean. Prod. **178** 587–98 Online: https://doi.org/10.1016/j.jclepro.2018.01.008

Miller S A, Horvath A and Monteiro P J M 2016 Readily implementable techniques can cut annual CO_2 emissions from the production of concrete by over 20% Environ. Res. Lett. **11** 074029 Online: https://iopscience.iop.org/article/10.1088/1748-9326/11/7/074029

Mohammadi J and South W 2016 Effect of up to 12% substitution of clinker with limestone on commercial grade concrete containing supplementary cementitious materials Constr. Build. Mater. **115** 555–64 Online: http://dx.doi.org/10.1016/j.conbuildmat.2016.04.071

Monkman S 2014 Carbon Dioxide Utilization in Fresh Industrially Produced Ready Mixed Concrete NRMCA 2014 International Concrete Sustainability Conference Online: http://www.nrmcaevents.org/?nav=download&file=653

Monkman S, Kenward P A, Dipple G, MacDonald M and Raudsepp M 2018 Activation of cement hydration with carbon dioxide J. Sustain. Cem. Mater. **7** 160–81 Online: https://www.tandfonline.com/doi/full/10.1080/21650373.2018.1443854

Monkman S and MacDonald M 2016 Carbon dioxide upcycling into industrially produced concrete blocks Constr. Build. Mater. **124** 127–32 Online: http://dx.doi.org/10.1016/j.conbuildmat.2016.07.046

Monkman S and MacDonald M 2017 On carbon dioxide utilization as a means to improve the sustainability of ready-mixed concrete J. Clean. Prod. **167** 365–75 Online: http://dx.doi.org/10.1016/j.jclepro.2017.08.194

Monkman S, Macdonald M and Hooton D 2016a Using CO_2 to reduce the carbon footprint of concrete 1st International Conference on Grand Challenges in Construction Materials pp 1–8 Online: http://www.igcmat.com/papers/Monkman_igcmat_2016.pdf

Monkman S, MacDonald M and Hooton D 2015 Using Carbon Dioxide as a Beneficial Admixture in Ready-Mixed Concrete NRMCA 2015 International Concrete Sustainability Conference Online: https://www.emcoblock.com/pdf/divisions/bay-ready-mix/SMonkman-NRMCA-ICSC-2015-draft-150414.pdf

Monkman S, MacDonald M, Hooton R D and Sandberg P 2016b Properties and durability of concrete produced using CO_2 as an accelerating admixture Cem. Concr. Compos. **74** 218–24 Online: http://dx.doi.org/10.1016/j.cemconcomp.2016.10.007

Monkman S and Shao Y 2010 Carbonation Curing of Slag-Cement Concrete for Binding CO_2 and Improving Performance J. Mater. Civ. Eng. **22** 296–304 Online: http://ascelibrary.org/doi/10.1061/%28ASCE%29MT.1943-5533.0000018

Monteiro P J M, Helene P R L and Kang S H 1993 Designing concrete mixtures for strength, elastic modulus and fracture energy Mater. Struct. **26** 443–52

Moon G D, Oh S, Jung S H and Choi Y C 2017 Effects of the fineness of limestone powder and cement on the hydration and strength development of PLC concrete Constr. Build. Mater. **135** 129–36 Online: http://dx.doi.org/10.1016/j.conbuildmat.2016.12.189

National Ready Mixed Concrete Association 2016 NRMCA Member National and Regional Life Cycle Assessment Benchmark (Industry Average) Report – Version 2 . 0 Online: https://www.nrmca.org/sustainability/EPDProgram/Downloads/NRMCA_Benchmark_Report_-_October_14_2014_web.pdf

Nisbet M a, VanGeem M G, Gajda J and Marceau M L 2000 Environmental Life Cycle Inventory of Portland Cement Concrete Online: http://www.nrmca.org/taskforce/item_2_talkingpoints/sustainability/sustainability/sn2137.pdf

Obla K H, Hong R, Lobo C L and Kim H 2017 Should Minimum Cementitious Contents for Concrete Be Specified? Transp. Res. Rec. J. Transp. Res. Board **2629** 1–8 Online: http://trrjournalonline.trb.org/doi/10.3141/2629-01

Oner A and Akyuz S 2007 An experimental study on optimum usage of GGBS for the compressive strength of concrete Cem. Concr. Compos. **29** 505–14

Oner A, Akyuz S and Yildiz R 2005 An experimental study on strength development of concrete containing fly ash and optimum usage of fly ash in concrete Cem. Concr. Res. **35** 1165–71

Organisation For Economic Co-operation and Development Maritime Transport Costs Online: https://stats.oecd.org/Index.aspx?DataSetCode=MTC

Van Oss H G 2018 2015 Minerals Yearbook - Cement Online: https://prd-wret.s3-us-west-2.amazonaws.com/assets/palladium/production/atoms/files/myb1-2015-cemen.pdf

Parsons Brinckerhoff and Global CCS Institute 2011 Accelerating the update of CCS: Industrial Use of Captured Carbon Dioxide Online: https://www.globalccsinstitute.com/archive/hub/publications/14026/accelerating-uptake-ccs-industrial-use-captured-carbon-dioxide.pdf

Poon C S, Lam L and Wong Y L 2000 Study on high strength concrete prepared with large volumes of low calcium fly ash Cem. Concr. Res. **30** 447–55

Portland Cement Association 2016a 2016 U.S . Cement Industry Annual Yearbook Online: http://www2.cement.org/econ/pdf/Yearbook2016_2sided.pdf

Portland Cement Association 2016b Environmental Product Declaration - Blended Cement Online: https://www.astm.org/CERTIFICATION/DOCS/293.EPD_for_Blended_Cements_-_Industry_Wide_EPD.pdf

Portland Cement Association 2016c Environmental Product Declaration - Portland Cement Online: https://www.cement.org/docs/default-source/sustainabilty2/pca-portland-cement-epd-062716.pdf?sfvrsn=2

RILEM TC 121-DRG 1994 Specifications for concrete with recycled aggregates Mater. Struct. **27** 557–9 Online: http://www.springerlink.com/index/10.1007/BF02473217

Rostami V, Shao Y and Boyd A J 2011 Durability of concrete pipes subjected to combined steam and carbonation curing Constr. Build. Mater. **25** 3345–55 Online: http://dx.doi.org/10.1016/j.conbuildmat.2011.03.025

Rostami V, Shao Y, Boyd A J and He Z 2012 Microstructure of cement paste subject to early carbonation curing Cem. Concr. Res. **42** 186–93 Online: http://dx.doi.org/10.1016/j.cemconres.2011.09.010

SEA-DISTANCES.ORG 2019 Sea Distances / Port Distances Online: https://sea-distances.org/

Seddik Meddah M 2015 Durability performance and engineering properties of shale and volcanic ashes concretes Constr. Build. Mater. **79** 73–82 Online: http://dx.doi.org/10.1016/j.conbuildmat.2015.01.020

Shannon J, Howard I L and Tim Cost V 2017 Potential of Portland-Limestone Cement to Improve Performance of Concrete Made With High Slag Cement and Fly Ash Replacement Rates J. Test. Eval. **45** 20150306 Online: http://www.astm.org/doiLink.cgi?JTE20150306

Shao Y 2014 Beneficial Use of Carbon Dioxide in Precast Concrete Production Online: https://www.osti.gov/servlets/purl/1155035

Shi C, Li Y, Zhang J, Li W, Chong L and Xie Z 2016 Performance enhancement of recycled concrete aggregate – A review J. Clean. Prod. **112** 466–72 Online: http://dx.doi.org/10.1016/j.jclepro.2015.08.057

Shwekat K and Wu H-C 2018 Benefit-cost analysis model of using class F fly ash-based green cement in masonry units J. Clean. Prod. **198** 443–51 Online: https://linkinghub.elsevier.com/retrieve/pii/S0959652618318857

Siddique R 2004 Performance characteristics of high-volume Class F fly ash concrete Cem. Concr. Res. **34** 487–93

Silva R V., De Brito J and Dhir R K 2015 The influence of the use of recycled aggregates on the compressive strength of concrete: A review Eur. J. Environ. Civ. Eng. **19** 825–49 Online: http://dx.doi.org/10.1080/19648189.2014.974831

Slag Cement Association 2015 Environmental product declaration-slag cement

Supekar S D and Skerlos S J 2014 Market-Driven Emissions from Recovery of Carbon Dioxide Gas Environ. Sci. Technol. **48** 14615–23 Online: https://pubs.acs.org/sharingguidelines

The Athena Sustainable Materials Institute 2016 A Cradle-to-Gate Life Cycle Assessment of Ready-Mixed Concrete Manufactured by NRMCA Members Online: https://www.nrmca.org/sustainability/EPDProgram/Downloads/NRMCA_LCA_ProjectReportV2_20161006.pdf

Thiery M, Dangla P, Belin P, Habert G and Roussel N 2013 Carbonation kinetics of a bed of recycled concrete aggregates: A laboratory study on model materials Cem. Concr. Res. **46** 50–65 Online: http://dx.doi.org/10.1016/j.cemconres.2013.01.005

Tolcin A C 2017a 2015 Minerals Yearbook: Slag-Iron and Steel U.S. Geol. Surv. Online: https://minerals.usgs.gov/minerals/pubs/commodity/indium/myb1-2015-indiu.pdf%0Ahttps://minerals.usgs.gov/minerals/pubs/commodity/lithium/myb1-2015-lithi.pdf

Tolcin A C 2017b 2015 Minerals Yearbook: Stone, Crushed U.S. Geol. Surv. Online: https://minerals.usgs.gov/minerals/pubs/commodity/indium/myb1-2015-indiu.pdf%0Ahttps://minerals.usgs.gov/minerals/pubs/commodity/lithium/myb1-2015-lithi.pdf

U.S. Census Bureau 2018 County Business Patterns: 2016 Online: https://www.census.gov/data/datasets/2016/econ/cbp/2016-cbp.html

U.S. Department of Transportation Bureau of Transportation Statistics 2018 National Transportation Statistics Online: http://www.bts.gov/publications/national_transportation_statistics/

U.S. Environmental Protection Agency 2018 Greenhouse gas reporting program Online: https://www.epa.gov/ghgreporting/ghg-reporting-program-data-sets

Ulama D 2015 IBISWorld Industry Report 32732 Ready-Mix Concrete Manufacturing in the US

Vejmelková E, Pavlíková M, Keršner Z, Rovnaníková P, Ondráček M, Sedlmajer M and Černý R 2009 High performance concrete containing lower slag amount: A complex view of mechanical and durability properties Constr. Build. Mater. **23** 2237–45

Wernet G, Bauer C, Steubing B, Reinhard J, Moreno-Ruiz E and Weidema B 2016 The ecoinvent database version 3 (part I): overview and methodology Int. J. Life Cycle Assess. **21** 1218–30 Online: http://link.springer.com/10.1007/s11367-016-1087-8

World Business Council for Sustainable Development 2016 “Getting the Numbers Right” (GNR) Database Online: http://www.wbcsdcement.org/index.php/key-issues/climate-protection/gnr-database

Wu K-R, Chen B, Yao W and Zhang D 2001 Effect of coarse aggregate type on mechanical properties of high-performance concrete Cem. Concr. Res. **31** 1421–5 Online: https://linkinghub.elsevier.com/retrieve/pii/S0008884601005889

Xi F, Davis S J, Ciais P, Crawford-Brown D, Guan D, Pade C, Shi T, Syddall M, Lv J, Ji L, Bing L, Wang J, Wei W, Yang K-H, Lagerblad B, Galan I, Andrade C, Zhang Y and Liu Z 2016 Substantial global carbon uptake by cement carbonation Nat. Geosci. **9** 880–3 Online: http://www.nature.com/articles/ngeo2840

Xuan D, Zhan B and Poon C S 2016 Assessment of mechanical properties of concrete incorporating carbonated recycled concrete aggregates Cem. Concr. Compos. **65** 67–74 Online: http://dx.doi.org/10.1016/j.cemconcomp.2015.10.018

Yi S T, Yang E I and Choi J C 2006 Effect of specimen sizes, specimen shapes, and placement directions on compressive strength of concrete Nucl. Eng. Des. **236** 115–27

Zachar J and Naik T R More Sustainable and Economical Concrete Using Fly Ash, Used Foundry Sand, and Other Residuals Online: https://www4.uwm.edu/cbu/Presentations/Ancona/Ancona-FdrySD-Zachar&Naik.pdf

Zayed T M and Nosair I A 2006 Cost management for concrete batch plant using stochastic mathematical models Can. J. Civ. Eng. **33** 1065–74 Online: http://www.nrcresearchpress.com/doi/10.1139/l06-051

Zhan B, Poon C S, Liu Q, Kou S and Shi C 2014 Experimental study on CO_2 curing for enhancement of recycled aggregate properties Constr. Build. Mater. **67** 3–7 Online: http://dx.doi.org/10.1016/j.conbuildmat.2013.09.008

Zhan B, Poon C and Shi C 2013 CO_2 curing for improving the properties of concrete blocks containing recycled aggregates Cem. Concr. Compos. **42** 1–8 Online: http://dx.doi.org/10.1016/j.cemconcomp.2013.04.013

Zhang D, Cai X and Shao Y 2016 Carbonation Curing of Precast Fly Ash Concrete J. Mater. Civ. Eng. **28** 04016127 Online: http://ascelibrary.org/doi/10.1061/%28ASCE%29MT.1943-5533.0001649

Zhang D, Ghouleh Z and Shao Y 2017 Review on carbonation curing of cement-based materials J. CO_2 Util. **21** 119–31 Online: https://doi.org/10.1016/j.jcou.2017.07.003

Zhang D and Shao Y 2016a Early age carbonation curing for precast reinforced concretes Constr. Build. Mater. **113** 134–43 Online: http://dx.doi.org/10.1016/j.conbuildmat.2016.03.048

Zhang D and Shao Y 2016b Effect of early carbonation curing on chloride penetration and weathering carbonation in concrete Constr. Build. Mater. **123** 516–26 Online: http://dx.doi.org/10.1016/j.conbuildmat.2016.07.041

Zhang J, Shi C, Li Y, Pan X, Poon C S and Xie Z 2015 Influence of carbonated recycled concrete aggregate on properties of cement mortar Constr. Build. Mater. **98** 1–7 Online: http://dx.doi.org/10.1016/j.conbuildmat.2015.08.087

Appendix D

Supplementary Information for Chapter 5

D.1 Economic parameters used for manufacturing analysis

Table D.1. Economic parameters used to analyze manufacturing of concrete and ECC ties

Parameters	Unit	Value	Reference
Cost of capital	%	5%	(Damodaran 2021)
Maintenance	%	4%	(Towler and Sinnott 2013)
Insurance	%	2%	(Towler and Sinnott 2013)
Offsite/Outside Battery Limits	%	55%	(Towler and Sinnott 2013)
Engineering	%	20%	(Towler and Sinnott 2013)
Contingency	%	10%	(Towler and Sinnott 2013)
Years to recover equipment investment	year	10	Typical value used
Years to recover factory investment	year	30	Typical value used
Factory floor space cost	$/m2	161	(Buildingsguide 2021)
Storage floor cost	$/m2	32	20% of the factory floor space cost
Scaling exponent for floor space	1	0.67	Typical value used
Equipment occupancy markup	%	50%	Typical value used
Electricity	$/kWh	0.07	(EIA 2021a)
Natural Gas	$/Mcf	3.9	(EIA 2021b)
Wages	$/person-hour	45.5	(Engineering News-Record 2021)

D.2 Environmental impact associated with manufacturing and disposing of ties

Table D.2. Environmental impact associated with manufacturing and disposal of concrete and ECC ties

[Concrete Tie]		GWP $kgCO_2eq$	ODP kgCFC-11eq	AP $kgSO_2eq$	EP kgNeq
Raw Materials	*Materials Total*	*7.0E+01*	*2.1E-06*	*1.5E-01*	*7.0E-02*
	Portland cement	6.1E+01	1.4E-06	1.2E-01	6.7E-02
	Fly ash	2.0E-04	3.8E-11	6.3E-07	8.0E-08
	Coarse aggregate	3.2E+00	4.7E-07	2.0E-02	1.6E-03
	Sand	1.5E+00	2.3E-07	8.0E-03	6.8E-04
	Water reducer	9.3E-01	1.1E-10	1.4E-03	5.1E-04
	Air entraining admixture	2.7E-02	3.9E-12	6.6E-05	7.3E-06
	PVA fiber	0.0E+00	0.0E+00	0.0E+00	0.0E+00
	Water	1.7E-02	8.0E-10	8.2E-05	2.7E-06
	Prestressing wire	3.4E+00	1.2E-11	6.9E-03	3.2E-04

	CO_2	-	-	-	-
Manufacturing	*Manufacturing Total*	*2E+00*	*9E-08*	*8E-02*	*5E-04*
Wire Tensioning	Electricity	5E-01	2E-08	2E-03	3E-05
Curing	*Curing Total*	1E+00	6E-08	8E-02	5E-04
Boiler	Electricity	3E-01	1E-08	1E-03	2E-05
	Natural Gas	1E+00	5E-08	8E-02	4E-04
End of Life	*End of Life Total*	*3.7E+00*	*7.5E-07*	*1.8E-02*	*2.4E-03*
TOTAL		7.5E+01	2.9E-06	2.5E-01	7.3E-02

[ECC Tie]		GWP $kgCO_2eq$	ODP kgCFC-11eq	AP $kgSO_2eq$	EP kgNeq
Raw Materials	*Materials Total*	*1.2E+02*	*2.8E-06*	*7.5E-01*	*1.3E-01*
	Portland cement	1.1E+02	2.5E-06	2.1E-01	1.2E-01
	Fly ash	1.4E-03	2.8E-10	4.6E-06	5.8E-07
	Coarse aggregate	0.0E+00	0.0E+00	0.0E+00	0.0E+00
	Sand	1.6E+00	2.5E-07	8.6E-03	7.4E-04
	Water reducer	1.9E-01	2.3E-11	2.9E-04	1.0E-04
	Air entraining admixture	0.0E+00	0.0E+00	0.0E+00	0.0E+00
	PVA fiber	1.9E+00	6.3E-08	7.3E-03	2.8E-04
	Water	4.8E-03	2.3E-10	2.3E-05	7.7E-07
	Prestressing wire	0.0E+00	0.0E+00	0.0E+00	0.0E+00
	CO_2	1.76E+00	0.00E+00	5.28E-01	5.66E-03
Manufacturing	*Manufacturing Total*	*3E+00*	*2E-07*	*1E-02*	*2E-04*
Curing	*Curing Total*	3E+00	2E-07	1E-02	2E-04
Drying	Electricity	3.50	0.00	0.01	0.00
End of Life	*End of Life Total*	*2.3*	*5.25E-07*	*0.01*	*0.00122*
TOTAL		1.2E+02	3.5E-06	7.8E-01	1.3E-01

D.3 ENVIRONMENTAL IMPACT OF THE PURCHASED CO_2

Table D.3. Environmental impact associated with purchased CO_2 from ammonia or ethanol plants or from DAC

[per $kgCO_2$]	GWP $kgCO_2eq$	ODP kgCFC-11eq	AP $kgSO_2eq$	EP kgNeq	Source
Ammonia/Ethanol	1.5E-01		4.4E-02	4.7E-04	(Supekar and Skerlos 2014)
DAC-Current	-4.1E-01	8.2E-10	8.0E-04	3.2E-04	(Deutz and Bardow 2021)
DAC-100% wind	-9.5E-01	8.2E-10	1.5E-04	7.3E-05	(Deutz and Bardow 2021)

D.4 UNCERTAINTY PARAMETERS FOR THE USE-PHASE STOCHASTIC MODEL

Table D.4. life of parameters and their ranges used to assess tie replacements and train delays during use-phase

	Units	Low	Nom	High	Descriptions & Reference
Service Life & Durability of Ties					
Concrete					
Average Service Life (μ)	[year]	40	45	60	

Weibull shape parameter (k)	[1]	2.8	4.6	6.4	± 40% of (MacLEAN 1957)
Weibull scaling parameter (λ)	[1]	1.07	1.01	0.99	Determined by k
Cost of TLS	[$/tie]	400	700	1000	(Northeast Corridor Commission 2018, 2019, Amtrak 2020, Northeast Corridor Commission 2021, 2020)
Cost of Spot Treatment	[$/tie]	1000	2000	3000	(Northeast Corridor Commission 2018, 2019, Amtrak 2020, Northeast Corridor Commission 2021, 2020)
ECC					
Average Service Life (μ)	[year]	40	70	100	
Weibull shape parameter (k)	[1]	2.8	4.6	6.4	± 40% of (MacLEAN 1957)
Weibull scaling parameter (λ)	[1]	1.07	1.01	0.99	Determined by k
Cost of TLS	[$/tie]	500	875	1250	Considers cost premium of ECC ties
Cost of Spot Treatment	[$/tie]	1035	2065	3100	Considers cost premium of ECC ties
Train Operation					
Intercity Passenger					
Train Length	[m]	161	201	241	
Daily Transit	[#/day]	20	25	30	± 20% of 25 trips/day
Delay Cost	[$/hr]	4005	5007	6008	
Maximum Electricity Consumption Rate	[kW]	4500	4750	5000	L: -10% of H H: Max power output from (Siemens 2014)
Tie Replacement					
TLS Threshold	[1]	0	-	1	
Replacement Capacity - TLS	[#/km-month]	19.7	39.4	59.1	± 50% of (Amtrak 2019)
Replacement Capacity - Spot Treatment	[#/km-month]	3.2	6.5	9.7	± 50% of (Amtrak 2019)
Diesel consumption - TLS	[l/tie]	0.2	0.3	0.4	(Federal Railroad Administration 1980)
Diesel consumption - Spot	[l/tie]	0.5	1.4	5.7	(Federal Railroad Administration 1980)
Minimum application length of TLS	[km]	0.16	0.80	1.61	L: 0.1 mile (Lovett *et al* 2015); H: L*10

REFERENCES

Amtrak 2020 Five-Year Plans - Service and Asset Line Plans | FY 2021-2026

Amtrak 2019 Infrastructure Asset Line Plan FY20-24 Online: https://www.amtrak.com/content/dam/projects/dotcom/english/public/documents/corporate/businessplanning/Amtrak-Infrastructure-Asset-Line-Plan-FY20-24.pdf

Buildingsguide 2021 Cost to build a warehouse Online: https://www.buildingsguide.com/blog/planning-steel-warehouse-building/

Damodaran A 2021 Cost of Capital by Sector (US) Online: http://pages.stern.nyu.edu/~adamodar/New_Home_Page/datafile/wacc.html

Deutz S and Bardow A 2021 Life-cycle assessment of an industrial direct air capture process based on temperature–vacuum swing adsorption Nat. Energy **6** 203–13 Online: http://www.nature.com/articles/s41560-020-00771-9

EIA 2021a Electric Power Annual 2020 Online: https://www.eia.gov/electricity/annual/

EIA 2021b Natural Gas Prices Online: https://www.eia.gov/dnav/ng/ng_pri_sum_dcu_nus_a.htm

Engineering News-Record 2021 Construction Economics Online: https://www.enr.com/economics

Federal Railroad Administration 1980 Track Renewal System And Wood Tie Reuse Analysis

Lovett A H, Dick C T, Ruppert C and Barkan C P L 2015 Cost and Delay of Railroad Timber and Concrete Crosstie Maintenance and Replacement Transp. Res. Rec. J. Transp. Res. Board **2476** 37–44 Online: http://journals.sagepub.com/doi/10.3141/2476-06

MacLEAN J D 1957 Percentage Renewals and Average Life of Railway Ties

Northeast Corridor Commission 2020 Northeast Corridor Annual Report : Operations and Infrastructure Fiscal Year 2019

Northeast Corridor Commission 2021 Northeast Corridor Annual Report : Operations and Infrastructure Fiscal Year 2020

Northeast Corridor Commission 2018 Northeast Corridor One-Year Implementation Plan Fiscal Year 2018

Northeast Corridor Commission 2019 Northeast Corridor One-Year Implementation Plan Fiscal Year 2019

Siemens 2014 Amtrak Cities Sprinter ACS-64 Electric Locomotive Online: http://www.mobility.siemens.com/mobility/global/SiteCollectionDocuments/en/rail-solutions/locomotives/customspecific-solutions/amtrak-acs64-en.pdf

Supekar S D and Skerlos S J 2014 Market-Driven Emissions from Recovery of Carbon Dioxide Gas Environ. Sci. Technol. **48** 14615–23 Online: https://pubs.acs.org/sharingguidelines

Towler G and Sinnott R 2013 Chemical Engineering Design (Elsevier) Online: https://linkinghub.elsevier.com/retrieve/pii/C20090612162